Dissertation

submitted to the
Combined Faculties for the Natural Sciences and for Mathematics
of the Ruperto-Carola University of Heidelberg, Germany
for the degree of
Doctor of Natural Sciences

presented by

M.Sc. Jana Zimmer
born in: Speyer
Oral-examination: 27.06.2017

The role of SOCS1 in the cell nucleus - Regulation of local immunity in the lung?

Referees:

Prof. Dr. Ralf Bartenschlager
Prof. Dr. Alexander Dalpke

Abbreviations

A

Actb	ActinB
ad	Aqua destillata
AEC's	Airway epithelial cells
ALI	Air-liquid interface
APC	Antigen presenting cell
ATM	Ataxia Telangiectasia Mutated
ATP	Adenosine triphosphate
ATR	Ataxia Telangiectasia And Rad3-Related Protein

B

B cell	B lymphocyte
BAC	Bacterial artificial chromosome
BAL	Bronchoalveolar lavage
BMM	Bone marrow-derived macrophage
bp	Base pairs
BSA	Bovine serum albumin

C

C	Celsius
CCL26	CC-chemokine ligand-26, Eotaxin
CD	Cluster of differentiation
cDNA	Complementary DNA
CFSE	Carboxyfluoresceindiacetate N-succinimidylester
CLR	C-type lectin
cm	Centimeter
C_t	Treshold cycle

D

DC	Dendritic cell
ddH_2O	Double destilled water
DMEM	Dulbecco's modified eagle medium
DMSO	Dimethylsulfoxide
DNA	Deoxyribonucleid acid
DNase	Deoxyribonuclease
dNTP	Deoxynucleosid triphosphate
ds	double stranded
DTT	Dithiotreitol

E

ECL	Enhanced chemiluminescence
EDTA	Ethylenediaminetetraacetic acid
EGTA	Triethyleneglycoldiaminetetraacetic acid
ELISA	Enzyme-linked immunoabsorbent assay
ESS	Extended SH2 subdomain

F

FACS	Fluorescence activated cell sorting
FCS	Fetal calf serum
FITC	Fluoresceinisothiocyanat

Fig.	Figure
Foxp3	Forkhead Box P3
fw	Forward
G	
GAS	Gamma interferon activated sequences
GATA3	GATA Binding Protein 3
GM-CSF	Granulocyte-macrophage-colony stimulating factor
H	
h	Human
h	Hour
HDM	House dust mite
HRP	Horseradish peroxidase
I	
ICAM-1	Intercellular adhesion molecule-1
IF	Immunofluorescence
IFN	Interferon
IFNGR	Interferonγ receptor
IHC	Immunohistochemistry
IκB	Inhibitor of NFκB
IKK	Inhibitor of kappa B kinase
IL	Interleukin
Indo	Indoleamine 2,3-Dioxygenase 1, IDO
IPTG	Isopropyl βD-thiogalactopyranoside
IRF	Interferon response factor
ISRE	Interferon-stimulated response element
J	
JAK	Janus kinase
K	
kDa	Kilodalton
KIR	Kinase inhibitory region
L	
LPS	Lipopolysaccharide
LRR	Leucine-rich repeat
M	
M	Molar
MAP, MAPK	Mitogen-activated protein, -kinase
MAVS	Mitochondrial anti-viral signaling protein
MCh	methacholine
MGL	Transgene containing <u>m</u>utated Socs1, e<u>G</u>FP and <u>L</u>uciferase
MHC	Major Histocompatibility Complex
min	Minute
ml	Milliliter
mM	Milimolar
mRNA	Messenger RNA
MyD88	Myeloid differentiation primary response 88
N	
NaCl	Sodiumchloride
NFκB	Nuclear factor kappa B
ng	Nanogram
NLR	NOD-like receptor
NLS	Nuclear localization sequence
nm	Nanometer

nt	Nucleotides
O	
OVA	Ovalbumin
P	
P/S	Penicillin/ Streptomycin
PAGE	Polyacrylamide gel electrophoresis
PAMP	Pathogen-associated molecular pattern
PBS	Phosphate buffered saline
PCR	Polymerase chain reaction
PFA	Paraformaldehyde
pg	Picogram
PGE_2	Prostaglandin E2
pH	Potential hydrogen
PI	Propidium iodide
PIAS	protein inhibitors of activated STATs
pI:C	Polyinosinic-polycytidylic acid
pmTEC	primary murine trachea epithelial cell
PRR	Pattern recognition receptor
PTPs	Protein tyrosine phosphatases
pY-STAT1	STAT1 phosphorylated at tyrosine 701
Q	
qRT-PCR	Quantitative real-time polymerase chain reaction
R	
rE	Relative expression
RIG-I	Retinoic acid inducible gene I
RLR	RIG-I-like receptor
RLU	Relative luminescence unit
RNA	Ribonucleic acid
RNase	Ribonuclease
Rorc	RAR Related Orphan Receptor C
ROS	Reactive oxygen species
rpm	Revolutions per minute
RPMI	Roswell Park Memorial Institute
RT	Room temperature
rv	Reverse
S	
sec	Second
SD	Standard deviation
SDS	Sodiumdodecyl sulfate
SH2	Src-homology 2
SOCS	Suppressor of Cytokine Signaling
ss	Single-stranded
STAT	Signal transducers and activators of transcription
T	
T cell	T lymphocyte
TAE	Tris acetate EDTA
T-bet	T-box transcription factor TBX21
TBS	Tris buffered saline
TCR	T cell receptor
TEMED	Tetramethylethylendiamine
Th	T-helper
tg	Transgenic

TIR	Toll/Interleukin 1 receptor
TIRAP	TIR domain-containing adaptor protein
TLR	Toll-like receptor
TNFα	Tumor necrosis factor alpha
TRAF	TNF receptor-associated factor
TRAM	TRIF-related adaptor molecule
TRIF	TIR domain-containing protein inducing IFNβ
Treg	Regulatory T-cell
Tris	Tris(hydroxymethyl)aminomethan
U	
U	Unit
U-STAT	Unphosphorylated STAT1
UTR	Untranslated region
V	
v/v	Volume per volume
W	
WB	Western Blot
w/v	Weight per volume
wt	Wild type

List of Figures

List of Tables

Contents

Contents

Contents

1. Abstract

Suppressor of Cytokine Signaling 1 (SOCS1) is a negative feedback inhibitor of cytoplasmic Janus kinase (JAK) and signal transducer and activator of transcription (STAT) signaling pathways. In 2008, it has been shown that SOCS1 contains a nuclear localization sequence (NLS) resulting in translocation of the protein into the cell nucleus. The exact function of SOCS1 in the cell nucleus remains largely unknown. To study the role of SOCS1 in the cell nucleus *in vivo*, a transgenic mouse model was established using a bacterial artificial chromosome (BAC) containing a $\underline{m}$utated *Socs1* locus with non-nuclear *Socs1∆NLS*, $\underline{G}$FP and *firefly $\underline{L}$uciferase*, termed MGL. C57BL/6 mice expressing only non-nuclear Socs1∆NLS were bred by back-crossing Socs1MGL^{tg} mice on a SOCS1 deficient background and named Socs1$^{-/-}$MGL^{tg} mice. Non-nuclear Socs1∆NLS was shown to rescue those mice from the early lethal phenotype observed in Socs1$^{-/-}$ mice. Interferon gamma (IFNγ) signaling was analyzed by Western Blot, flow cytometry, quantitative real-time PCR and whole-genome expression analysis. Socs1$^{-/-}$MGL^{tg} mice showed functional regulation of canonical IFNγ signaling – a function classically attributed to cytoplasmic SOCS1. Only a small subset of non-canonical, IFNγ dependent genes was differentially regulated. In contrast, Socs1$^{-/-}$MGL^{tg} mice showed altered cell cycle regulation as well as sustained NFκB signaling - two functions suggested to be dependent on SOCS1 in the cell nucleus. Socs1$^{-/-}$MGL^{tg} mice spontaneously developed a Th2 prone low-grade inflammation in the lung including elevated serum IgE levels and low-grade airway eosinophilia. Influx of eosinophils could be enhanced both in an experimental asthma model using ovalbumin and upon IL-13 instillation. Bone-marrow transplantation experiments indicated an important role for radiation-resistant cells in the development of the allergic phenotype in Socs1$^{-/-}$MGL^{tg} mice. Therefore, epithelial cells were investigated in more detail. Reduced epithelial cell barrier integrity was observed both *in vivo* by the detection of albumin in BAL and *in vitro* using primary murine trachea epithelial cells (pmTECs). In summary, Socs1$^{-/-}$MGL^{tg} mice were used to study the role of nuclear SOCS1. Nuclear SOCS1 was shown to be an important regulator of local immunity in the lung and to exert a so-far unrecognized function in epithelial cells.

2. Zusammenfassung

SOCS1 ("Suppressor of Cytokine Signaling 1") ist induzierbarer feedback Inhibitor für JAK/ STAT (Janus kinase/ signal transducer and activator of transcription) Signalwege. Es wurde gezeigt, dass SOCS1 eine nukleäre Kernlokalisationssequenz ("nuclear localization sequence", NLS) besitzt, die dazu führt, dass das Protein in den Zellkern transloziert. Um die Funktion von SOCS1 im Zellkern *in vivo* zu untersuchen, wurde eine transgene Maus mit Hilfe eines bakteriellen artifiziellen Chromosomes (BACs) generiert. Diese Maus enthält neben einem mutierten SOCS1 Lokus, in dem SOCS1 durch nicht kerngängiges SOCS1ΔNLS ersetzt wurde, die Reporter eGFP und Luciferase, und wird MGL^{tg} bezeichnet. C57BL/6 MGL transgene Mäuse wurden auf einen SOCS1 defizienten Hintergrund gezüchtet, sodass diese Tieren kein SOCS1 im Kern exprimieren. Diese Mäuse wurden Socs1$^{-/-}$MGL^{tg} genannt. Nicht kerngängiges SOCS1ΔNLS war in der Lage den Interferonγ Signalweg zu regulieren, wie es für SOCS1 im Zytoplasma beschrieben ist. Somit konnten Socs1$^{-/-}$MGL^{tg} Mäuse vor dem lethalen Phänotyp SOCS1 defizienter Mäuse gerettet werden. Die funktionelle Regulation des Interferonγ Signalweges wurde anhand von phosphorylierten STAT1, klassischen Interferonγ induzierten Zielgenen und genom-umfassender Expressionsanalysen untersucht. Ein Teil der nicht-klassischen Interferonγ abhängigen Gene war jedoch in Socs1$^{-/-}$MGL^{tg} Mäusen unterschiedlich reguliert. Socs1$^{-/-}$MGL^{tg} Mäuse zeigten weiterhin Unterschiede im Zellzyklus sowie NFκB Signalweg, dessen negative Regulation durch SOCS1 im Kern beschrieben ist. Daher liegt die Vermutung nahe, dass Socs1$^{-/-}$MGL^{tg} Mäuse kein funktionelles SOCS1 im Kern exprimieren und verwendet werden können, um die *in vivo* Relevanz von SOCS1 im Kern zu untersuchen. Interessanter Weise zeigten Socs1$^{-/-}$MGL^{tg} Mäuse eine spontane leicht-gradige Entzündung in der Lunge. Genauere Analysen zeigten, dass es sich um eine Th2 abhängige Eosinophilie handelt. Erhöhte Serum IgE Werte weisen auf eine allergische Atemwegserkrankung hin. Die Eosinophilie konnte in einem klassischen Asthma Modell durch Ovalbumin sowie durch Gabe von IL-13 - einem klassischen Th2 Zytokin- noch verstärkt werden. Um herauszufinden welcher Zelltyp für den Lungenphänotyp verantwortlich ist, wurde eine Knochenmarktransplantation durchgeführt. Ergebnisse bestätigten eine wichtige Rolle der strahlungsresistenten Zellen wie zum Beispiel Epithelzellen an der Entstehung der Th2 abhängigen Atemwegserkrankung. Daher wurden Epithelzellen genauer untersucht und eine erhöhte Durchlässigkeit sowohl in primären Trachea-Epithelzellen *in vitro*, als erhöhte Albumin Werte in der BAL *in vivo* festgestellt. Zusammenfassend konnten Socs1$^{-/-}$MGL^{tg} Mäuse genutzt werden, um die bislang unterschätzte Funktion von SOCS1 im Kern zu untersuchen und dessen Rolle bei der Entstehung von Th2 bedingten Atemwegserkrankungen wie Asthma genauer zu untersuchen.

3. Introduction

3.1. Cytokine receptors

Cytokines represent a diverse group of small soluble proteins that can act upon secretion in an autocrine or paracrine fashion. Cytokine receptors are cell-surface glycoproteins that bind specifically to cytokines and initiate signaling cascades. There are different receptor classes: type I cytokine receptors, type II cytokine receptors, tumor necrosis factor (TNF) receptor family, IL-1 receptors, tyrosine kinase receptors and chemokine receptors. Type I cytokine receptors as well as type II cytokine receptors signal via the Janus kinase (JAK)/ signal transducers and activators of transcription (STAT) signaling pathway [255, 43, 155, 110, 209]. The JAK/ STAT pathway was originally discovered through the study of interferon induced intracellular signal transduction. Meanwhile, a large number of cytokines, hormones and growth factors have been found to activate JAK/ STAT signaling such as interleukins or hematopoietic growth factors. A well known example for JAK/ STAT signaling is signal transduction upon IFNγ (see Fig. 1). Upon binding of IFNγ to its receptor, the receptor subunits (IFNγ receptor chains 1 and 2; IFNGR1 and IFNGR2) dimerize leading to autophosphorylation and activation of associated JAKs [21]. There are four members of the JAK family: JAK1, JAK2, JAK3 and Tyk2. To enable diversity of immune responses, activation of different combinations of JAKs by different cytokine receptors is possible. Both receptor chains of the IFNγ receptor are associated with JAKs [124]: IFNGR1 with JAKl and IFNGR2 with JAK2 [123]. Once in close proximity to each other, JAKs activate each other by phosphorylation, and then phosphorylate the IFNGR1 chain on tyrosine 440 [88] to create docking sites for STAT1. Members of the STAT family of proteins contain a SH2 domain and are therefore major substrates of JAKs [118, 156]. There are seven mammalian STATs: STAT1, STAT2, STAT3, STAT4, STAT5A, STAT5B and STAT6 [42]. Upon receptor phosphorylation, STAT1 binds through its SH2 domain and gets phosphorylated by JAKs on tyrosine 701 (pY-STAT1) [225]. Phosphorylated STAT1 proteins form homodimers through mutual SH2-phosphotyrosine (pY) interactions and translocate into the nucleus. Rapid accumulation of pY-STATs in the nucleus in turn activate transcription of certain target genes by binding to specific IFNγ-activated sequences (GAS) in the promoter region. Type I interferon signaling additionally leads to an activation of interferon-stimulated response elements (ISREs). Besides tyrosine phosphorylation of STAT1 leading to its activation, serine phosphorylation of STATs occurs leading to increased activity and specificity [48, 147]. In contrast to tyrosine phosphorylation, it is not substantial for signaling.

There is emerging evidence of non-canonical JAK/ STAT activity. Stat1$^{-/-}$ mice infected with Sendai virus, MCMV, or DENV developed some level of resistance against these pathogens, showing that STAT1-independent responses to IFNs exist [76, 245, 80]. STAT-independent pathways include the PI3K/AKT pathway or the mitogen activated protein kinase (MAPK) pathway [131]. It has been shown that IFNAR1, TYK2 and unphosphorylated STAT1 translocate into the nucleus as well [3, 152]. Non-canonical JAK/ STAT activity can be achieved by tyrosine kinase-independent action of JAKs, transcriptional complexes other than ISGF3 and GAF, and pathways building on U-STATs that are not phosphorylated on tyrosine [48]. Mice with a kinase-dead TYK2 showed a rescue in natural killer cell maturation and tumor killing as compared to TYK2$^{-/-}$ mice [221], arguing for a tyrosine kinase-independent action. Similar data was shown for JAK2. JAK2 kinase-dead mutants revealed a kinase-independent scaffolding function of JAK2 for the IFNγ receptor complex [137]. In addition, classical interferon signaling leads not only to accumulation of pY-STAT1 in the cell nucleus, but also unphosphorylated
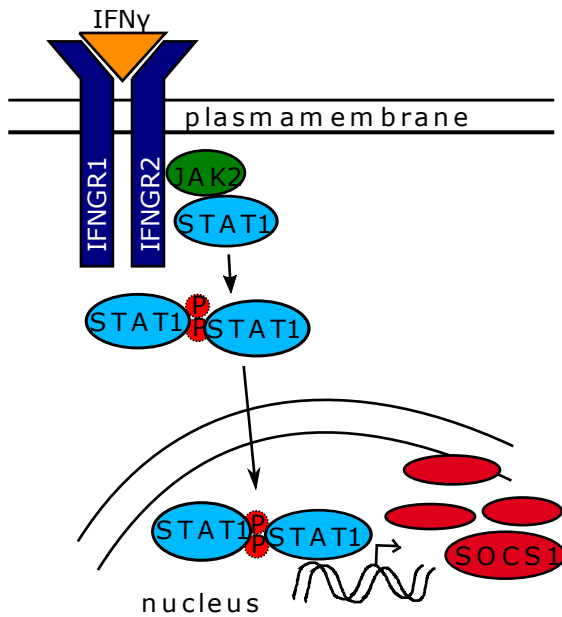
Figure 1.: JAK/ STAT signaling pathway. Upon binding of IFNγ (orange triangle) to its receptor (dark blue), receptor subunits IFNGR1 and IFNGR2 dimerize leading to autophosphorylation and activation of associated JAKs. This creates docking sites for cytoplasmic STAT1 proteins that get phosphorylated. Phosphorylated STAT1s dimerize and translocate into the nucleus to activate gene transcription by binding to IFNγ-activated sequences in promoter regions for their target genes. One target is SOCS1 that negatively regulates the signaling pathway in the cytosol. Figure adapted from Samuel, 2001 [234].

STAT1 (U-STAT1) [182, 30]. pY-STATs and U-STATs shuttle via different pathways into the nucleus where they lead to activation of a distinct set of genes. U-STAT1 dependent genes such as IFI24, IFI44, OAS or BST2 are induced upon stimulation with IFNβ or IFNγ especially at low doses and expression of those genes increased even after 48 to 72 h unlike pY-STAT1 dependent genes that are usually early-induced [220]. Besides classical interferon signaling via STAT1, there has been evidence of STAT1-independent pathways [80, 226, 182].

There are three types of IFNγ induced genes:

1st genes dependent on pY-STAT1 activation such as IRF1, IP-10, MIG or SOCS1. Those genes need binding of pY-STAT1 dimers to GAS elements.

2nd genes that can be induced in both a pY-STAT1 dependent and independent manner such as MCP1, GGR1 or SOCS2 and SOCS3

3rd genes that are induced independently of pY-STAT1 such as IL-1β, c-myc or c-jun [226, 80]

To ensure for effective pathogen clearance on the one hand and to avoid excessive immune signaling and autoimmunity on the other hand, duration and intensity of the signaling need to be tightly regulated. Regulation can occur at various levels: abundance of ligand for the receptor, expression or stability of the receptor or expression or stability of internal components of the signaling cascade [132, 87, 246]. There are different kinds of negative regulators: SOCS (Suppressor of Cytokine Signaling) proteins [257, 194, 62], PIAS (protein inhibitors of activated STATs), CD45 and PTPs (protein tyrosine phosphatases) [249]. SOCS proteins negatively regulate JAK/ STAT signaling by acting as negative feedback inhibitors upon interferon stimulation, whereas negative regulators such as PIAS terminate STAT action by promoting degradation of receptors and pathway components.

3.2. Suppressor of Cytokine Signaling (SOCS) proteins

3.2.1. Structure and Regulation of SOCS1 proteins

Structure of SOCS1 proteins

The Suppressor of Cytokine Signaling (SOCS) family is important for negative feedback inhibition of Janus kinases (JAK) and signal transducer and activator of transcription (STAT) signaling. SOCS proteins get induced upon type I and II cytokine receptor signaling and in turn regulate the signaling as inducible negative feedback inhibitors. The family contains eight members, namely SOCS1 – 7 and CIS. All SOCS family members share key structural elements (see Fig. 2) such as the central cytokine-inducible Src-homology 2 (SH2) domain, which together with the extended SH2 subdomain (ESS) allows binding to phosphorylated tyrosine [290]. Negative regulation of cytokine signaling by SOCS proteins can be performed by either direct binding to receptors or JAKs [290] or by competing with STATs for binding sites [224]. Therefore, the SH2 domain is substantial and determines substrate specificity. SOCS2 binds to phosphorylated tyrosine on cytokine receptors, whereas SOCS3 preferably binds to gp130-like receptors and SOCS1 to interferon receptors and JAKs. In addition, all SOCS proteins contain the common C-terminal SOCS-box, a 40 amino acid long motive giving the family its name [5, 87, 115]. The SOCS-box interacts with Elongin B, C and other proteins to build a E3-ubiquitin ligase leading to degradation of associated proteins via the proteasome. The N-terminal region of SOCS proteins is of varying length and amino acid composition. The two closely related proteins SOCS1 and SOCS3 additionally contain a kinase inhibitory region (KIR) through which they can act as a pseudosubstrate for Janus kinases [81]. SOCS1 is the only SOCS family member known to contain a bipartite NLS located between the SH2 domain and the SOCS-box.
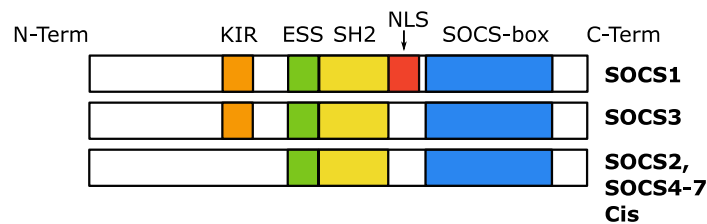
Figure 2.: Structure of SOCS proteins.
Schematic structure of SOCS family members. All SOCS family members contain a central cytokine-inducible Src-homology 2 (SH2) domain (yellow) together with an extended SH2 subdomain (ESS, green), an amino-terminal (N-term) domain of variable length and divergent sequence, and a carboxy-terminal 40-amino-acid long SOCS-box (blue). SOCS1 and SOCS3 additionally contain a kinase-inhibitory region (KIR, orange). SOCS1 is the only family member containing a nuclear localization sequence (NLS, red) located between the SH2 domain and the SOCS-box. Not to scale. Figure adapted from Alexander, 2002 [5].

Regulation of SOCS1 proteins

Upon activation of JAK/ STAT signaling, transcriptional and translational induction of SOCS proteins follows. SOCS proteins in turn inhibit ongoing receptor activation in a negative feedback loop. There are STAT1, 3 and 6 binding site through ISRE and GAS elements in the SOCS1 5' flanking region [194, 233, 237]. Although constant expression of SOCS1 is rather low and is sometimes difficult to detect, it can be strongly and rapidly induced [257, 194, 62]. Moreover, there is data indicating that certain SOCS proteins are unstable [295, 136] and that their half-life is influenced by binding of Elongins B and C to their SOCS box [295, 136]. By interacting with the SOCS box, the Elongin B/C complex increases expression of SOCS1 by inhibiting its degradation [136]. SOCS1 can be regulated by translational repression [89, 237]. Structure-

function analyses indicated that this effect is mediated by the 5' untranslated region (UTR) and that it relates to the presence of two upstream AUGs in this region [89]. This translational repression is responsible for low endogenous concentration of SOCS in resting cells. Further studies revealed that translation of SOCS1 is cap-dependent and modulated by eIF4E-binding proteins [89].

3.2.2. Inhibition of JAK/ STAT signaling pathway by SOCS1

SOCS1 has first been described in 1997 as a negative feedback inhibitor of cytoplasmic JAK/ STAT signaling (see Fig. 1) [62, 194, 257]. Firstly, by the means of the ESS and the KIR domains, SOCS1 can directly bind to JAK2 and inhibit its catalytic activity. [290]. Therefore, the SH2 domain of SOCS1 binds to Y1009 within the activated domain in JAK2 and the KIR acts as a pseudosubstrate. Secondly, SOCS1 has been shown to bind to interferon receptor domains occupying binding sites for STATs [68, 224]. Finally, due to the SOCS box, SOCS1 acts as an ubiquitin E3 ligase that targets JAK cytokine receptor complexes for proteasomal degradation [281, 295]. In particular, the SOCS-box interacts with Elongins B and C leading to recruitment of an E3-ubiquitin ligase complex consisting of Elongin B/C, Cullin-2 /Cullin-5, SOCS1 and the ring-finger protein Rbx1 or Rbx2 [138, 135]. In presence of an E1 activating enzyme and an E2 conjugating enzyme, this E3-ubiquitin ligase complex transfers polyubiquitin chains on the substrate that is bound to SOCS1 leading to its proteasomal degradation.
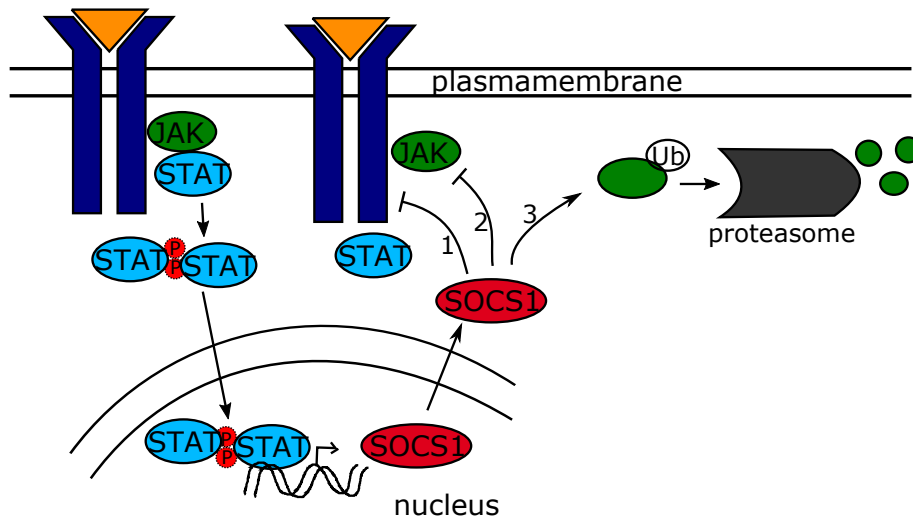
Figure 3.: Negative feedback inhibition of the JAK/ STAT signaling pathway by SOCS1. Activation of the receptor (dark blue) by binding of a ligand (orange triangle) leads to phosphorylation of the associated Janus kinases (JAKs) and phosphorylation of STATs. Phosphorylated STATs dimerize and translocate into the nucleus to activate gene transcription. One target is SOCS1 (red) that negatively regulates the signaling pathway in the cytosol. Inhibition of JAK/ STAT signaling is achieved by (1) competing with STAT binding sites, (2) direct binding to JAK or by (3) degradation of JAK cytokine receptor complexes via the proteasome. Figure adapted from Shuai and Liu, 2003 [246].

3.2.3. Additional functions of SOCS1

Besides negative regulation of JAK/ STAT signaling, SOCS1 has been shown to act as a crosstalk inhibitor for TLR signaling pathways [41, 40, 258, 196]. Macrophages lacking SOCS1 are hypersensitive to LPS as shown by increased production of pro-inflammatory cytokines [139, 196]. In addition, LPS-induced NO synthesis, TNFα production and both IκB and p38 phosphorylation were elevated in SOCS1 deficient macrophages [139]. Indirect paracrine inhibition of TLR

signaling was shown by IFNβ leading to the activation of secondary genes [11]. In addition to indirect regulation of TLR signaling, SOCS1 contributes to direct regulation of the pathway by interacting with components of the TLR signaling pathway [171, 196]. It has been shown that after TLR2 and TLR4 stimulation, the MyD88 adapter like (MAL) protein interacts with SOCS1 leading to its phosphorylation, polyubiquitination and subsequent degradation [171]. SOCS1 has also been shown to be involved in maturation and differentiation of DCs. Immature DCs show constitutive activation of STAT6. During maturation, STAT6 signal diminishes leading to a strong induction of SOCS1 together with SOCS2, SOCS3 and CIS accompanied with the predominant use of STAT1 signals in mature DCs [129].

In 2008, a nuclear localization sequence (NLS) was identified for SOCS1, resulting in translocation of the protein into the cell nucleus [12, 143]. SOCS1 directly interacts with the tumor suppressor p53 in the cell nucleus leading to activation of p53 via phosphorylation of serine 15 by forming a ternary complex with ATR or ATM [169]. Activation of the p53 pathway by SOCS1 can establish an anti-proliferative program in cells exposed to sustained or aberrant cytokine stimulation. p53 activation results in G1 arrest and apoptosis by synthesis of inhibitors of cyclin-dependent kinases, such as p21/WAF1 [1, 242]. Therefore, an anti-proliferative role for SOCS1 is suggested [134, 169]. Moreover, SOCS1 induces proteasomal degradation of NFκB [168, 230, 232]. NFκB proteins function as dimeric transcription factors and consist of the subunits NFκB1 (p105/p50), NFκB2 (p100/p52), c-Rel, RelA (p65) or RelB. In the canonical pathway, NFκB proteins are bound and inhibited by IκB inhibitors. Activation of the IKK complex (IKKα, IKKβ, and NEMO) phosphorylated IκB proteins leading to their ubiquitination and proteasomal degradation and the release of NFκB complexes. Active NFκB complexes translocate into the nucleus where they induce expression of pro-inflammatory cytokines such as IL-1, IL-6, IL-8, or TNFα. In particular, SOCS1 interacts with the NFκB subunit p65 in the cell nucleus, thereby limiting induction of a subset of NFκB dependent genes [260]. Interaction with p65 has been shown for SOCS1, but no additional SOCS family member. The N-terminal part of the SH2 domain contributes to p65 binding, whereas the SOCS box mediates E3 ubiquitin ligase activity. Therefore, a mutant lacking the SOCS-box is ineffective in p65 ubiquitination [260]. SOCS1 is also involved in degradation of tyrosine phosphorylated ASK1 in response to growth factors. In SOCS1 deficient mice, ASK1 expression and activity are upregulated, resulting in enhanced TNF-induced activation of JNK, expression of pro-inflammatory molecules and apoptotic responses [106]. SOCS1 additionally interacts with HPV (human papilloma virus) E7 protein and induces ubiquitination and degradation of E7 [134].

3.2.4. SOCS1 in T cell differentiation

CD4$^+$ T cells are activated by foreign antigens presented on APC's via MHC class II and induced depending on the surrounding cytokine milieu into different Th cell subtypes. IL-12 and IFNγ lead to activation of the transcription factor Tbet via STAT4 and differentiation of naïve CD4$^+$ T cell into Th1 cells [261]. Those cells are produced against intracellular viral and bacterial pathogens. In contrast, Th2 cells play a major role in protection against large extracellular pathogens and during allergic responses. Th2 cells are characterized by the expression of Gata3 via STAT6 in an IL-4 and IL-10 dominant milieu [8]. Another Th cell subset is the Th17 cell that is important for mucosal immunity and autoimmune disorders. TGFβ and IL-6 favour the differentiation of Th17 cells that are expressing Rorc via STAT3 [288]. Regulatory T cells (Tregs) maintain immune homeostasis. Those cells are induced in a TGFβ and IL-10 dominant milieu and are characterized by the expression of Foxp3 [298]. Overexpression of SOCS1 in T cells results in disturbed thymocyte development with an increasing number of CD4$^+$ thymocytes and spontaneous activation of lymphocytes in the periphery [72]. Altered thymic T cell development and aberrant T cell activation has been shown for SOCS1 deficient mice [173, 272]. T cells from SOCS1 deficient mice proliferate spontaneously in the presence of IL-2 without the need for a T cell receptor signal [173]. This data suggest that SOCS1 can regulate T cell differentiation.

Indeed, SOCS1 is differentially expressed both in Th1 and Th2 cells. The lack of SOCS1 leads to elevated IFNγ or IL-4 levels in response to classical Th1 or Th2 model organisms (*Listeria monocytogenes* or *Nippostrongylus brasiliensis*) [72], respectively. Differentiation into Th1 or Th2 phenotype is accompanied by preferential expression of distinct SOCS mRNA transcripts and proteins. SOCS1 expression is 5-fold higher in Th1 as compared to Th2 cells. In contrast, Th2 cells contain 23-fold higher levels of SOCS3 [61]. There is conflicting data regarding which cell fate SOCS1 drives differentiation towards. On the one hand, SOCS1 blocks Th1 development via inhibition of IFNγ signaling favouring Th2 differentiation [264, 54]. Tanaka et al. showed in 2008 that most SOCS1 deficient naïve CD4$^+$ T cells differentiate into Th1 cells, even under Th2 or Th17 skewing conditions [264]. In line with this, SOCS1-deficient mice develop autoimmune inflammatory diseases with age [274] and are sensitive to dextran sulfate sodium induced colitis [117], but resistant to experimental autoimmune encephalomyelitis, a typical Th17 type disease [264]. Th1 skewing in SOCS1 deficient animals is achieved by high levels of IFNγ [264].

On the other hand, SOCS1 negatively regulates Th2-dependent pathways by inhibition of pSTAT6 [73]. Administration of IL-13 induces SOCS1 expression at the inflammatory site that in turn suppresses IL-13–dependent STAT6 activation. Thereby, Eotaxin expression can be downregulated leading to reduced airway inflammation [73]. In addition, serum IgE levels and infiltrating eosinophils are considerably increased in the lungs of OVA-treated Socs1$^{-/-}$IFN$\gamma^{-/-}$ mice as compared to IFN$\gamma^{-/-}$ mice [153]. Those mice show increased expression of the Th2 cytokines, IL-4, IL-5 and IL-13 in CD4$^+$ cells of the lung [153]. In line with this, *Socs1* gene expression is significantly lower in the airways of severe asthmatics compared with mild/moderate asthmatics, and inversely correlates with airway eosinophilia [57, 73]. Data suggest that the absence of SOCS1 leads to Th2 bias. In addition, SOCS1 is necessary for Th17 differentiation [58]. Th17 suppression by SOCS1 deficiency is probably due to the excessive IFNγ signaling [61]. SOCS1 also plays an important role in the regulation of Tregs. Higher numbers of Tregs are observed in the thymus and spleen of T cell-specific SOCS1 deficient mice [161], probably due to increased IL-2 levels. It has been shown that SOCS1 deletion in Tregs induces the development of spontaneous dermatitis, splenomegaly, and lymphadenopathy, suggesting a defective Treg function in these mice [160].

3.2.5. Physiological Relevance of SOCS1

SOCS1 proteins are ubiquitously expressed, however with predominant expression in the lung, spleen [194], thymus [257] and liver [173]. SOCS1 has been shown to have an essential role in immune regulation. SOCS1 deficient mice develop a fatal neonatal disease that results in death by three weeks of age due to unlimited IFNγ signaling leading to multiorgan inflammation [173, 256, 193] (see Table 1). Those mice are characterized by neonatal death, fatty liver degeneration, hematopoietic infiltrations in various organs as well as accelerated apoptosis and aberrant T cell activation [173, 256, 193]. This phenotype is highly dependent on IFNγ hypersensitivity as Socs1$^{-/-}$IFN$\gamma^{-/-}$ mice show reduced pathology, however, these mice develop polycystic kidneys as well as chronic inflammation [181, 6]. Deletion of the SOCS box of SOCS1 delays the onset of the disease [296], but still leads to increased responsiveness to IFNγ and the development of chronic inflammatory lesions. Marine et al. characterized the phenotype of the Socs1$^{-/-}$ mice further, showing perturbed thymic T cell development and activation in Socs1 deficient mice [173]. T cell-specific Socs1$^{-/-}$ mice do not develop the lethal multiorgan inflammation, but rather specific lymphoid deficiencies through defective T cell development and proliferation [72, 272]. In addition, Socs1$^{-/-}$ mice can be rescued by back-crossing to either STAT4$^{-/-}$ or STAT6$^{-/-}$ mice [64, 193], supporting the important role for SOCS1 in T cells. Consistent with this, Socs1$^{-/-}$ mice that additionally lack Rag2 (recombination activating gene, a key gene in lymphoid maturation), survive the early lethal phenotype of Socs1$^{-/-}$ mice and exhibit normal levels of IFNγ. However, Socs1$^{-/-}$Rag2$^{-/-}$ mice show increased CD8$^+$ T cell differentiation, splenomegaly, and lymphadenopathy [173, 264]. They show accumulation of DCs in the thymus and spleen,

Table 1.: Effects of SOCS1 manipulation in mice.

Mouse model	Phenotype	Described by
Socs1$^{-/-}$	Neonatal death, Lymphopenia, Fatty liver degeneration	[257, 194, 173]
Socs1$^{-/-}$IFN$\gamma^{-/-}$	Polycystic kidneys, Inflammatory lesions	[296]
Socs1$^{-/-}$Rag2$^{-/-}$	Increased CD8$^+$ differentiation, Splenomegaly	[173, 264]
Socs1$^{\text{SOCS-box del}}$	Increased responsiveness to IFNγ, Inflammatory lesions	[296]
Socs1$^{-/-}$CD28$^{-/-}$	Aberrant expansion of CD8$^+$ DCs, Autoimmunity	[274, 100]
Socs1$^{-/-}$TCR$\alpha^{-/-}$	Aberrant expansion of CD8$^+$ DCs, Autoimmunity	[274]
Socs1$^{-/-}$TCR$^{\text{tg}}$	Inflammatory lesions, Aberrant T cell activation	[37]

which are hyperresponsive to both IFNγ and IL-4. Socs1$^{-/-}$TCR$\alpha^{-/-}$ or Socs1$^{-/-}$CD28$^{-/-}$ mice are rescued from early lethality of Socs1$^{-/-}$ mice as well [274, 100]. However, the CD8$^+$ DC subset is increased, resulting in enhanced secretion of IFNγ and IL-12p40 [274]. Therefore, those mice show DC mediated systemic autoimmunity at an old age [100, 274]. Socs1$^{-/-}$TCR$^{\text{tg}}$ mice (expressing a transgenic TCR detecting only exogenous antigen) have an increased lifespan as compared to Socs1$^{-/-}$ mice [37]. However, TCR transgenic SOCS1 deficient mice still die as young adults with inflammatory infiltrations and aberrant T cell activation [37], suggesting both antigen-dependent and -independent mechanisms to be responsible for the inflammatory disease in SOCS1 deficient mice.

SOCS1 expression has been linked to several diseases. The anti-proliferative role of SOCS1 is circumvented by aberrant methylation resulting in silencing of SOCS1 transcription in hepato-cellular cancers [293]. In a murine arthritis model, the extent of joint destruction and synovial inflammation is exacerbated in Socs1$^{-/-}$ mice [60]. In addition, SOCS1 expression has been shown to correlate inversely with the severity of disease in idiopathic pulmonary fibrosis patients [197]. However, SOCS1 does not always confer protection against immune diseases. Thus, transgenic mice expressing high levels of SOCS1 in lymphocytes spontaneously develop colitis [126]. In addition, SOCS1 plays a role in allergic diseases including psoriasis and allergic contact dermatitis [67], where it is highly expressed in keratinocytes. SOCS1 was also shown to protect β-cells from cytotoxic T cells in a murine type 1 diabetes model [15]. Furthermore, increased expression of SOCS1 was observed in livers of obese insulin-resistant mice [276]. Furthermore, SOCS1 plays an important role in the pathogenesis of asthma which has been shown both in a mouse model using SOCS1$^{-/-}$IFN$\gamma^{-/-}$ mice [153] and in asthmatic patients [101, 79, 57]. There is a significant association between an SOCS1 promoter polymorphism (-1478CA >del) and adult asthma [101]. Severe asthmatic patients with persistent airway eosinophilia have reduced airway epithelial SOCS1 expression [57]. Data shows the involvement of SOCS1 in many inflammatory diseases and therefore SOCS1 is a potential target for drug development. SOCS mimetics are peptides corresponding to functional domains of SOCS1 coupled to protein translocation domains that facilitate cell entry. Peptides resembling the KIR region are potent therapeutics in experimental allergic encephalomyelitis mouse model of multiple sclerosis [190] and show promising results in a psoriasis model [148] and diabetes-associated cardiovascular diseases [227].

3.3. Immunerecognition in the lung

Immune reactions in primary "sterile" organs such as spleen or blood differ from immune reactions in organs where commensal microbes are found such as the the respiratory tract or the gastrointestinal tract. The respiratory tract displays a large surface of the body that is crucial for gas exchange. It is in constant contact with the outside environment. Whereas the pharyngeal mucosa is colonized by microbes, the lower respiratory tract is considered to be colonized by only few usually nonpathogenic microbes [102]. Pathogenic microbes that migrate into the

respiratory tract represent a serious threat that requires immediate immune responses. On the other hand, constant immune responses against nonpathogenic microbes need to be prevented to avoid chronic infections and autoimmunity. Therefore, tolerance mechanisms are necessary to assure tissue homeostasis and host protection. Alveolar and airway epithelial cells serve distinct roles in the innate defense of the lungs and therefore differ in their cellular composition. The alveolar epithelium consists of two main populations: alveolar type I and type II epithelial cells. The predominant cell by number is the alveolar type I epithelial cell, covering 95% of the epithelial cell [259]. Alveolar type II epithelial cells express chemokines and cytokines, synthesize and secrete pulmonary surfactants and participate in the innate immune response of the lung [175]. Gas exchange is mediated by the close apposition of type I and type II epithelial cells to the endothelial cells of pulmonary capillaries, creating an extensive surface area. In contrast, the airways (trachea, bronchi and bronchioles) show of a pseudostratified epithelium consisting of mainly ciliated cells and a small number of secretory cells including serous, club, neuroendocrine and goblet cells. In the airways of mouse and other rodents, secretory cells are more abundant [285]. Airway epithelial cells (AECs) prevent colonization by inhaled bacteria in four ways [174, 50]:

- AECs built a physical barrier between the outside environment and immune cells through cell-cell contacts.

- AECs physically remove pathogens by ciliary clearance.

- AECs produce a broad-spectrum of antimicrobials (such as defensins, LL-37, lysozyme or secretory leukocyte proteinase inhibitor) and secrete them in the mucus [14, 240].

- AECs recruit phagocytic cells and orchestrate inflammatory responses.

To recognize pathogenic microorganisms, airway epithelial cells are equipped with pattern recognition receptors (PRRs) such as TLRs (Toll-like receptors), RLRs (RIG-I (retinoic acid inducible gene I)-like receptors) and NLRs (NOD (nucleotide-binding oligomerization domain)-like receptors) [178, 189, 217, 241, 9, 86, 206, 149, 275]. TLRs are classically found either on the cell surface (TLR1, 2, 4, 5, 6, 10) or in the endosome (TLR3, 7, 8, 9, 11, 13) [2, 109, 176]. They recognize a variety of PAMPs such as peptidoglycan or lipoproteins (recognized by TLR1, 2, 6) [262], double-stranded RNA or the mimetic pI:C (recognized by TLR3) [7], LPS (lipopolysaccharide, recognized by TLR4) [218], flagellin (recognized by TLR5) [4], single-stranded RNA (recognized by TLR7, 8) [94, 170] or unmethylated CpG-rich DNA (recognized by TLR9) [33]. Signaling through TLRs induces a signaling cascade leading to production of pro-inflammatory molecules and recruitment of phagocytic cells and APCs to the site of pathogen invasion. To induce tolerance and prevent from constant activation, morphology and differentiation of epithelial cells is critical. Primary airway epithelial cells cultured under air-liquid interface (ALI) differentiate into ciliated cells that are more resistant to virus infection and show weaker inflammatory responses [159] as compared to undifferentiated cells. Importantly, multiple receptors have a polarized distribution in epithelial cells such as the IFNα/β receptor (IFNAR) that is exclusively expressed on the basolateral surface [32]. Another example is basolateral localization of TLR2 and 6 or intracellular localization of TLR4 that prevents the interaction between PAMPs located in the airway lumen and their respective receptors unless the integrity of the epithelial barrier is compromised [127, 95]. Endogenous low expression of receptors and upregulation only upon stimulation is another important mechanism to prevent from constant signaling. It has been shown that TLR3 expression can be induced by the influenza A virus and by dsRNA in alveolar and bronchial epithelial cells [95]. In addition, mucins are exclusively expressed on the apical surfaces of differentiated epithelial cells and negatively regulate TLR signaling [277]. Another important mechanism to induce tolerance by epithelial cells is the secretion of prostaglandins. Prostaglandin E2 (PGE$_2$) for example as a key regulator of DC functions, alters MHC class II surface expression and cytokine production [278, 279].

3.4. Scientific question

Since its discovery as a classical feedback inhibitor for JAK/ STAT signaling, there has been emerging evidence that there are additional functions for SOCS1 except for regulation of JAK/ STAT signaling. In 2008, a nuclear localization sequence (NLS) has been identified for SOCS1, resulting in translocation of the protein into the cell nucleus [12, 143]. To date, some functions for nuclear SOCS1 have been described, however, the physiological relevance has not been addressed so far. To study the function of SOCS1 in the cell nucleus in more detail in an *in vivo* system, a transgenic mouse model was established using a bacterial artificial chromosome (BAC) containing a $\underline{m}$utated *Socs1* locus with non-nuclear *Socs1*Δ*NLS*, $\underline{G}FP$ and *firefly* $\underline{L}$*uciferase*, termed MGL. MGL transgenic mice should be characterized to ensure for successful integration and regulation of the BAC. Afterwards, mice expressing only non-nuclear *Socs1* (thereafter referred to as Socs1$^{-/-}$MGL^{tg} mice) were analyzed for disease symptoms. Socs1$^{-/-}$MGL^{tg} mice were rescued from early-lethal phenotype as compared to mice deficient for SOCS1. Since this phenotype is known to be highly dependent on IFNγ, IFNγ signaling should be analyzed in Socs1$^{-/-}$MGL^{tg} mice. Unlike IFNγ signaling that is known to be regulated by SOCS1 in the cytoplasm, NFκB signaling is described as a classical function for SOCS1 in the cell nucleus and should therefore be used to answer the question whether Socs1$^{-/-}$MGL^{tg} mice lack nuclear SOCS1. Socs1$^{-/-}$MGL^{tg} mice should be further characterized with respect to their pathophysiology, focusing on lung pathology. The aim of this study is to establish a mouse model that allows investigating the physiological relevance of nuclear SOCS1.

4. Materials and Methods

4.1. Materials

4.1.1. Devices

Instrument	Company
AutoMACS	Miltenyi Biotec, Bergisch-Gladbach
Bioanalyzer	Agilent Technologies GmbH, Berlin
Blotting chambers	Biometra, Jena
Centrifuges	Heraeus Instruments, Hanau (Multi 3 SR)
	Sigma 2K15/ B. Braun, Melsungen (Multi 3 SR+)
Counting chamber	Neubauer 0.00025mm^2/0.1 mm/ Brand GmbH, Schwerin
Cytospin	Cytospin 4/A. Dervos – G. Dimitrakopoulos and Co S. A., Athen, Greece
COULTER Ac-T	Hematology Analyzer, Beckmann Coulter, Brea, CA, USA
ELISA reader	Sunrise/ Tecan, Crailsheim
FACS	FACSCanto/ Becton Dickinson, Heidelberg
Gel Documentation	Peqlab, Erlangen
Heating blocks	AccuBlock, digital dry bath/ Eppendorf, Hamburg
Incubators	BBD6220i/ Heraeus Instruments, Hanau
Luminometer	LUMIstar OPTIMA system, BMG LABTECH, Offenburg
Magnetic stirrer	Ikamag Reo stirrer/ Roth, Karlsruhe
Micro-CT SKYSCAN 1276	Burker, Billerica, MA, USA
Microscope	Leica DM-LS/ Leica GmbH, Wetzlar
	Leica DMI 6000B, Leica Microsystems GmbH, Wetzlar
PCR-Thermocycler	Primus 96 advanced/ Peqlab Biotechnology GmBH, Erlangen
	Primus 25 advanced
pH-Meter	Seven Easy/ Mettler-Toledo, Giessen
Photometer	NanoDrop ND-1000/ Peqlab Biotechnology GmBH, Erlangen
Power supply	Power Pac HC/ BioRad, München
	Consort E835/ Sigma-Aldrich, Steinheim
Real time PCR cycler	StepOne Real-time PCR/ Applied Biosystems, Foster City, USA
Scales	Sartorius Basic Feinwaage Sartorius TE 2101
Shaker	Heidolph 1010/ Hilab, Karlsruhe
Sterile bench	Hera Safe KS 12/ Heraeus Instruments, Hanau
TER system	Millicell electrical resistance system (ERS), Millipore, Darmstadt
Vortexer	Heidolph Reax 2000/ Hilab, Karlsruhe
Tissueruptor	Quiagen, Hilden

4.1.2. Software

Software	Description
Bio-Capt	For visualizing gels, Vilber Lourmat GmbH
FACSDiva	BD Bioscience, San Diego
FCS Express	Demo version 5, DeNOVO Software, Glendale, CA, USA
GraphPad Prism	Version 6.05, GraphPad Software, Inc. San Diego, USA
ImageJ	1.46r developed at the National Institutes of Health, USA
Inkscape	0.92.0 r15299, licensed GPLv2
LAS AF	2.6.0.7266, Leica Microsystems, Solms
LeicaLS Lite	Leica Microsystems, Solms
Magellan V	For protein determination and ELISA, Tecan, Grödig, Austria
NanoDrop	3.0.1, Nanodrop Technologies, Rockland, USA
OPTIMA	For Luciferase assay, BMG Labtech, Allmendgrün
Tierbase	Version 4D v14 SQL Release 8, University Heidelberg

4.1.3. Consumables

Consumable	Company
Blotting membrane	Immobilon-P Transfer/ MilliporeBillerica, USA
Blotting paper	Whatman GB003/ Whatman GmbH, Dassel
Eppendorf tubes	0.5 ml, 1.5 ml or 2 ml, Eppendorf AG, Hamburg
Cell culture bottles	Cellstar, Greiner Bio-One GmbH, Frickenhausen
Cell culture plates	6-/12-/24-/96-well or 10 cm plates, Cellstar, Greiner Bio-One GmbH, Frickenhausen
Culture plates for microscopy	1. glass bottom dish (35 mm) ibidi GmbH, Martinsried 2. μ-Slide 8 well glass bottom (175 μm) ibidi GmbH, Martinsried
Cell scraper	Greiner Bio-One GmbH, Frickenhausen
ELISA plates	96 well, Greiner Bio-One GmbH, Frickenhausen
Luminometer plates	LUMI TRAC 200, USA Sceintific, Ocala, FL, USA
Needles	22G, 27G or 29G, BD Biosciences, Heidelberg
Pipette tips	0.1-100 μl, 1-200 μl or 100-1000 μl, Corning, New York, USA
qRT-PCR plates	MicroAmp, Fast 96-well reaction plate (0.1 ml)/ AppliedBiosystems, UK
Syringes	2 ml or 10 ml, BD Discardit/ BD Biosciences, Heidelberg 1 ml, Braun, Melsungen
Transwell plate	12 mm insert, 0.4 μm polyester membrane insert (#CLS3470-48EA) Corning Costar, Sigma, MO, USA
Tubes	Cellstar Tubes (50 ml, 15 ml), Greiner Bio-One, Frickenhausen

4.1.4. Chemicals and Reagents

Chemical/ Reagent	Company
Acetic acid (100%)	Riedel-de Haën AG, Seelze
Acrylamid, stock solution	Carl Roth GmbH, Karlsruhe
Agarose	Eurobio, Courtaboeuf, France
Ampicillin (Sodium salt)	Sigma-Aldrich, Taufkirchen
Alcian Blue Solution	Sigma-Aldrich, Taufkirchen
Aluminum hydroxide	Thermo, Rockford, IL, USA
Aprotinin	Sigma-Aldrich, Taufkirchen
APS (Ammonium persulphate)	Sigma-Aldrich, Taufkirchen
Aqua dest	Braun, Melsungen
Arginine	Carl Roth GmbH, Karlsruhe
Bacto-Agar	BD, Biosciences, Heidelberg
BamH1 (10 U/μl, #ER0051)	ThermoFisher Scientific, Waltham, MA, USA
Bromphenol blue	Sigma-Aldrich, Taufkirchen
BSA (Bovine serum albumin)	Carl Roth GmbH, Karlsruhe
anti-CD3/CD28-coated beads	ThermoFisher Scientific, Waltham, MA, USA
CFSE	Sigma Aldrich, Taufkrichen
Collagen-IV, human placenta #C7521	Sigma, MO, USA
Cycloheximide	Merck Millipore, Massachusetts, US
DiffQuick stain	Medion Diagnostics, Duedingen, Switzerland
DMEM (Dulbecco's Modified Eagle Medium)	Biochrom AG, Berlin
DMSO (Dimethylsulfoxide)	Sigma-Aldrich, Taufkirchen
DMEM:Ham's F12 1:1 Mix	GibcoTM/Invitrogen, Karlsruhe
DMSO (Dimethyl sulfoxide)	SERVA Electrophoresis GmbH, Heidelberg
DNase I #11284932001	Roche, Mannheim
DTT (Dithiothreitol)	Sigma-Aldrich, Taufkirchen
ECL-Reagent	PerkinElmer, Rodgau
EcoRI (10 U/μl, #ER0271)	ThermoFisher Scientific, Waltham, MA, USA
EDTA	AppliChem GmbH, Darmstadt
EGTA	Carl Roth GmbH, Karlsruhe
Ethanol	Sigma Aldrich, Taufkirchen
Eukitt mounting medium	Sigma-Aldrich, Taufkirchen
FCS (Fetal calf serum)	1 Biowest, Nuaillé, Frankreich
	2 GibcoTM/Invitrogen, Karlsruhe
Fe(NO$_3$)$_3$ (Ferric nitrate)	Sigma-Aldrich, Taufkirchen
FITC–dextran	Sigma-Aldrich, Taufkirchen
Giemsa staining solution	Merck, Darmstadt
Glutamaic acid	Carl Roth GmbH, Karlsruhe
HCl (Hydrochloric acid)	Merck, Darmstadt
Heparin solution	StemCell Technologies, Köln
Hoechst 34580 (Trihydrochloride salt)	Sigma Aldrich, Taufkirchen
Insulin, recombinant #12585014	ThermoFisher Scientific, Waltham, MA, USA
Imidazole	Merck, Darmstadt
IPTG #R1171	ThermoFisher Scientific, Waltham, MA, USA
Jet Prime Transfection Reagent	Polyplus-transfection SA, Illkirch, France
Kanamycine	AppliChem GmbH, Darmstadt
Latex beads	#L1030, Sigma Aldrich, Taufkirchen
LB Broth	AppliChem GmbH, Darmstadt
Leupeptin (-hydrochloride)	Sigma-Aldrich, Taufkirchen

Chemical/ Reagent	Company
Liberase #5401119001	Roche, Mannheim
Lysozyme	Sigma-Aldrich, Taufkirchen
May-Grünwald staining solution	Merck, Darmstadt
β-Mercaptoethanol	Sigma-Aldrich, Taufkirchen
NaCl (Sodiumchloride)	AppliChem GmbH, Darmstadt
NaH_2PO_4 (Sodiumdihydrogenphosphate)	AppliChem GmbH, Darmstadt
Na_3PO_4 (Sodiumphosphate)	Merck, Darmstadt
$Na_2S_2O_5$ (Sodiummetabisulfite)	Sigma-Aldrich, Taufkirchen
Na_3VO_4 (Sodium orthovanadate)	Sigma Aldrich, Taufkirchen
Ovalbumin (EndoGrade)	Hyglos GmbH, Regensburg
PFA (Paraformaldehyde)	Merck, Darmstadt
PBS (1x) with or without $Ca2^+/Mg^{2+}$	PAA Laboratories, Pasching, Austria
Penicillin/Streptomyin (100x)	Sigma-Aldrich, Taufkirchen
Pepstatin A	Sigma-Aldrich, Taufkirchen
PeqFect	Peqlab, Erlangen
Periodic acid	10%, Sigma-Aldrich, Taufkirchen
Phusion Taq Polymerase (2000 U/ml, #M0530S)	New England Biolabs (NEB), Ipswich, MA, USA
Propidium iodide # 25535-16-4	Sigma-Aldrich, Taufkirchen
Pronase E #P5147	Sigma, MO, USA
Protease inhibitors	Roche, Mannheim
Proteinase K #03115836001	Roche, Mannheim
Red blood cell lysis buffer	eBioscience, CA, USA
Roticlear	Carl Roth GmbH, Karslruhe
Rotiquant	Carl Roth GmbH, Karslruhe
RPMI 1640 Medium (1x)	Biochrome AG, Berlin
Saponin	Carl Roth GmbH, Karslruhe
Schiff's Reagent	Sigma-Aldrich, Taufkirchen
SDS (Sodiumdodecylsulphate)	AppliChem GmbH, Darmstadt
SYBR Green PCR Master Mix Fast	Applied Biosystems, Foster City, USA
T4 Ligase (ExpressLink #A13726)	Invitrogen, Karlsruhe
Taq DNA Polymerase (5 U/μl, #EP0402)	ThermoFisher Scientific, Vilnius, Lithuania
TEMED (Tetramethylethylendiamin)	Sigma-Aldrich, Taufkirchen
Thrombin	Sigma-Aldrich, Taufkirchen
Tris Base	AppliChem GmbH, Darmstadt
Triton X-100	Merck, Darmstadt
Trypan blue	Sigma-Aldrich, Taufkirchen
Trypsin/EDTA (10x)	PAA Laboratories, Pasching, Austria
Tween 20	Sigma-Aldrich, Taufkirchen
Ultroser G #15950–017	Pall Corporation, Dreieich, Germany
Urea	Sigma Aldrich, Taufkirchen
XhoI (10 U/μl, #ER0691)	ThermoFisher Scientific, Waltham, MA, USA
Xylene	Sigma-Aldrich, Taufkirchen

4.1.5. Kits

Kit	Company
OptEIA Mouse IL-6 ELISA	#555240, BD Biosciences, Heidelberg
OptEIA Mouse TNFα ELISA	#560478, BD Biosciences, Heidelberg
OptEIA Mouse IL-12p40 ELISA	#555165, BD Biosciences, Heidelberg
Mouse IL-33 ELISA	#DY3626-05, R&D systems, Minneapolis, MN, USA
Albumin ELISA	#108791, abcam, Cambridge, UK
TransAM Kit	#43296, Active Motif, Carlsbad, CA, USA
IL-4, IL-5 and IL-13 CBA Flex Set	#558298, 55832, 558349, BD Biosciences, Franklin Lakes, NJ, USA
Monoclonal anti-IgE	clone R35-72, BD Biosciences, Heidelberg
Anti-IgE conjugated with HRP	clone 23G3, Southern Biotech, Birmingham, AL, USA
High Capacity cDNA Reverse Transcription	Applied Biosystems, Life Technologies, Darmstadt
HotStartTaq DNA Polymerase	Qiagen, Hilden
IHC Detection	Mouse and Rabbit Specific HRP/DAB (ABC) Detection, #ab64264, abcam, Cambridge, UK
PeqGold DNase I Digest Kit	Peqlab Biotechnology GmBH, Erlangen
PeqGold Total RNA Kit	Peqlab Biotechnology GmBH, Erlangen
RNeasy Total RNA Kit	Quiagen, Hilden
CD4$^+$ negative selection Kit	#130-104-454, Miltenyi Biotec, Bergisch Gladbach
CD11c$^+$ positive selection Kit	#130-052-001, Miltenyi Biotec, Bergisch Gladbach

4.1.6. Buffers

Buffer	Ingredients
PBS	80 mM disodiumhydrogenphosphate, 20 mM sodium dihydrogenphosphate 1.4 M sodium chloride, pH 7.4
Penicillin/Streptomycin, 100x	10,000 U/ml penicillin G, 10 mg/ml streptomycin, 0.9% (w/v) NaCl
Trypan blue solution	2 mg/ml trypan blue in 1x PBS
Trypsin solution	0.05% trypsin, 0.02% EDTA in 1x PBS
Buffer for agarose gels	
TAE buffer	2M Tris-Base, 1M conc. acetic acid, 0.05 M EDTA, pH 8.0
Buffers for ELISA	
Coating buffer	0.1 M Na$_2$CO$_3$, pH 9.5
Wash buffer	0.05% Tween 20 in PBS (v/v)
Blockbuffer	PBS/10% FCS (v/v)
Buffers for Westen Blot	
Lamelli buffer, 4x	200 mM Tris-HCl, 0.4% (w/v) bromophenolblue, 40% (w/v) glycerol, 8% (w/v) SDS, 400 mM (v/v) β-mercaptoethanol, pH 8.8
Separating gel buffer	1.5 M Tris-HCl, 0.4% (w/v) SDS, pH 8.8
Stacking gel buffer	1 M Tris-HCl, 0.8% (w/v) SDS, pH 6.8
SDS Page running buffer	25 mM TRIS-OH, 192 mM Glycin, 10% (v/v) Methanol, pH 8.3
Semidry blotting buffer	25 mM Tris-OH, 192 mM Glycin, 10% (v/v) Methanol, pH 8.3
Blocking buffer	5% BSA solution in 1x TBS, 0.05% (v/v) Tween-20
Wash buffer (TBST)	1x TBS, 0.05% (v/v) Tween-20

Buffer	Ingredients
10x TBS	100 mM Tris-HCl, pH 8.0; 1.5 M NaCl
Buffers for IHC	
EDTA buffer	1 mM EDTA, pH 8.0
Citrate buffer	10 mM Citric Acid, 0.05% Tween-20, pH 6.0
Wash buffer	1x PBS, 0.05% (v/v) Tween-20
Buffer for FACS	
FACS buffer	1x PBS, 2% (v/v) FCS
Buffers for Luciferase Assay	
Luciferase lysis buffer	1% (v/v) Triton X-100, 25 mM Glycyl-Glycine (pH 7.8), 15 mM $MgSO_4$, 4 mM EGTA and 1 mM DTT
Luciferase assay buffer	100 mM K_3PO_4, 100 mM $MgSO_4$, 200 mM EGTA, H_2O, pH 7.8, before use: 2 mM ATP, 1 MM DTT, 25 mM GlyGly (D-luciferine)
Buffers for protein expression	
Lysis buffer	50 mM NaH_2PO_4, 300 mM NaCl, 50 mM Imidazole, 0.5% Triton X-100, before use: 2 mg/ml lysozyme
Wash buffer	50 mM Tris-HCl, pH 7.5, 100 mM NaCl, 1% Triton X-100
Dialysis buffer	20 mM Na_3PO_4, 20 mM NaCl, 50 mM arginine, 50 mM glutamate, 2 mM DTT, 1 mM EDTA, pH 6.5
Extraction buffer	50 mM Tris-HCl, pH 7.5, 8 M urea, 1 mM DTT, before use: add Proteinase inhibitors
Buffers for H&E staining	
Haematoxylin solution	50 g/l aluminium ammonium sulphate, 5 g/l haematoxylin (CI 75290), 1% ethanol, 1 g/l sodium iodate, 2% acetic acid, 30% glycerol
Acid alcohol	0.3% HCl, 70% ethanol
Scott's tap water substitute	2 g/l sodium hydrogen carbonate, 20 g/l magnesium sulphate
Eosin solution	1% eosin (CI 45380), 1% phloxine (CI 45405), 95% alcohol and 4% acetic acid

4.1.7. Media

Media	Description
DMEM Culture Medium	10% (v/v) heat-inactivated FCS, penicillin G (100 IU/ml), streptomycin sulfate (100 μg/ml), Biochrom, Berlin
DMEM for differentiation of BMMs	10% (v/v) heat-inactivated FCS, penicillin G (100 IU/ml), streptomycin sulfate (100 μg/ml); 30% of M-CSF containing supernatant, Biochrom, Berlin
DMEM / Ham's F12 culture medium	DMEM/ Ham's F12 1:1 medium mix, 5% (v/v) heatinactivated FCS, penicillin G (100 IU/ml), streptomycin sulfate (100 μg/ml), 120 IU/l human insulin, Biochrom, Berlin
RPMI Culture Medium	10% (v/v) heat-inactivated FCS, penicillin G (100 IU/ml), streptomycin sulfate (100 μg/ml), Biochrom, Berlin
UltroserG Medium	DMEM/Ham's F12 1:1 medium mix, penicillin G (100 IU/ml), streptomycin sulfate (100 μg/ml) and 2% UltroserG serum complement, Biochrom, Berlin

4.1.8. Markers and Stains

Marker	Company
6x Loading Dye	Thermo Fisher Scientific, Waltham, USA
GeneRuler DNA Ladder Mix	Fermentas, St.Leon-Rot
PageRule Plus Protein ladder	Fermentas, St.Leon-Rot
peqGREEN DNA/RNA Dye	Peqlab, Erlangen
CellMask Membrane Stain	ThermoFisher Scientific, Waltham, MA, USA
Hoechst	final concentration $1\mu g/ml$, Sigma Aldrich, Taufkirchen

4.1.9. Antibodies

Antigen	Dilution	Company
SOCS1 (Hybridoma supernatant)	1:20	newly generated by immunizing mice against the peptide RRITRASALLDA, Abmart, Shanghai
SOCS1 (Charles River)	1:50-2000	Newly generated polyclonal antibody against recombinant murine SOCS1, Charles River, Chatillon-sur-Chalaronne, Ecully, France
SOCS1 (CST)	1:50-2000	#3950, Cell Signaling Biotechnology, Frankfurt
SOCS1 (Abcam)	1:50-2000	#ab-9870, Abcam, Cambridge, UK
SOCS1 (SC)	1:50-2000	#sc-9021, Santa Cruz Biotechnology, Heidelberg
β-Actin	1:4000	#4970, Cell Signaling Biotechnology, Frankfurt
IκBα	1:1000	#9242, Cell Signaling Biotechnology, Frankfurt
pSTAT1 (Tyr701)	1:1000	#9167, Cell Signaling Biotechnology, Frankfurt
STAT1	1:1000	#9172, Cell Signaling Biotechnology, Frankfurt
Histon3 (H3)	1:1000	#9715, Cell Signaling Biotechnology, Frankfurt
E-Cadherin	1:1000	#3195, Cell Signaling Biotechnology, Frankfurt
Occludin	1:1000	#168986, Abcam, Cambridge, UK
Anti-Rabbit IgG HRP-linked	1:4000	#7074, Cell Signaling Biotechnology, Frankfurt
Anti-Mouse IgG HRP-linked	1:4000	#7076, Cell Signaling Biotechnology, Frankfurt
AlexaFluor 647 Anti-STAT1 (pY701)	1:50	#612597, BD Biosciences, Heidelberg
PE Anti-Mouse CD11c	1:50	#553802, BD Biosciences, Heidelberg
FITC Anti-Mouse CD4	1:100	#561828, BD Biosciences, Heidelberg
FITC Anti-Mouse CD3	1:50	#559975, BD Biosciences, Heidelberg
APC anti-Mouse CD45.2	1:200	#558702, BD Biosciences, Heidelberg
FITC Anti-Mouse CD45.1	1:200	#561871, BD Biosciences, Heidelberg
PE Anti-Mouse F4/80	1:50	#56541, BD Biosciences, Heidelberg
APC-Cy7 Anti-Mouse CD11b	1:50	#557657, BD Biosciences, Heidelberg
FITC Anti-Mouse MHCII	1:50	#553623, BD Biosciences, Heidelberg

4.1.10. Stimuli

Stimuli	Description
Poly(I:C), pIC	Invivogen, Toulouse, France
S-LPS	from Salmonella minnesota, smooth-LPS, Ulrich Seydel, Forschungszentrum Borstel
CpG	phosphorothioate-modified CpG-oligonucleotide 1668 from TIB Molbiol, Berlin
IFNγ	#315-05, Peprotech, Hamburg
IL-13	#210-13, Peprotech, Hamburg
OVA	Ovalbumin grade VI #A2512; Sigma-Aldrich, Deisenhofen Ovalbumin grade V #A5503; Sigma-Aldrich, Deisenhofen
IL-2	#402-ML-020, R&D Systems, Minneapolis, MN, USA
IL-4	#214-14, Peprotech, Hamburg, Germany
anti-IFNγ	#517903, BioLegend, San Diego, CA, USA
anti-IL-12	#505203, BioLegend, San Diego, CA, USA
T-cell stimulation	containing PMA and ionomycin, #00-4970, eBioscience, CA, USA
Dynabeads®	Mouse T-Activator CD3/CD28 for T-Cell Expansion and Activationm #11456D, ThermoFisher Scientific, Waltham, MA, USA

4.1.11. Anesthetic solution

Anesthetic	Description
Xylazine and Ketamine	1.2 ml ketamine (10%), 8 ml NaCl, 0.8 ml xylazine (2%), 100 μl/ 10 g bodyweight i.p.
Isofluorane	4% isofluorane, 500 ml/min O$_2$, inhaled for max. 45 sec.
Pentobarbital	Narcoren 16 g / 100 ml solution, 25 μl / 10 g bodyweight i.p.

4.1.12. Vectors and plasmids

Vector	Description
eGFP-C1	Enhanced GFP. CMV promotor and cloning sites for BamHI and XhoI. Kanamycine resistance.
eGFP-mSocs1	Murine Socs1 cloned into eGFP-C1 backbone via BamHI and XhoI generating a fusionprotein. Kanamycin resistance.
eGFP-mSocs1ΔNLS	Murine Socs1ΔNLS cloned into eGFP-C1 backbone via BamHI and XhoI. In Socs1ΔNLS, the NLS is replaced by the sequence GCT GGT ACT GAG CCG ACC TCT CTC CTC CAA CGT GGC CAC CCT from Socs3. Kanamycine resistance.
pGex-mSocs1	Vector for protein expression with a tac promoter that is induced by IPTG. Murine Socs1 cloned into pGex using BamHI and EcoRI. Generates GST-tagged protein. Thrombin protease sites for cleavage of the GST taq. Ampicillin resistance.
PA-GFP-C1	photoactivatable GFP, pPAGFP-C1 was a gift from Jennifer Lippincott-Schwartz (Addgene plasmid #11910) [213]. CMV promotor and cloning sites for BamHI and XhoI. Kanamycine resistance.
PA-GFP-mSocs1	Murine Socs1 cloned into PA-GFP-C1 backbone via BamHI and XhoI. Kanamycine resistance.

4.1.13. Primers

Target	Forward sequence 5'-3'	Reverse sequence 5'-3'
Socs1ΔNLS	CAC CTT CTT GGT GCG CG	GAG GAG AGA GGT CGG CTC AGT AC
Socs1	CAC CTT CTT GGT GCG CG	CCC CCA ACA TGC GGC GCG
Socs1WT	FAM-ATGTTGGGGGCCCCGCTGCG-BHQ2	
Actb	CCC TGT GCT TGG CTT CAC CGA	ACA GTG TGG GTG ACC CCG TTC
GFP	CAA CAG CCA CGT CTA TAT CAT	ATG TTG TGG CGG ATC TTG AAG
Luciferase	TAA ACG GCC ACA AGT TCA GC	TTC ATG TGG TCG GGG TAG C
TNFα	AAA ATT CGA GTG ACA AGC CTG TAG	CCC TTG AAG AGA ACC TGG GAG TAG
IL-6	CCG GAG AGG AGA CTT CAC AG	TTC TGC AAG TGC ATC ATC GT
IL-12p40	AAG AAG GAA AAT GGA ATT TGG TCC	ATG TCA CTG CCC GAG AGT CAG
iNOS	CAG CTG GGC TGT ACA AAC CTT	CAT GGG AAG TGA AGC GTT TCG
Irf9	GCC GAG TGG TGG GTA AGA C	GCA AAG GCG CTG AAC AAA GAG
Icam1	GGC ATT GTT CTC TAA TGT CTC CG	TGT CGA GCT TTG GGA TGG TAC
Gdf3	ATG CAG CCT TAT CAA CGG CTT	AGG CGC TTT CTC TAA TCC CAG
Sla	ATG GGG AAT AGC ATG AAA TCC AC	GGA GAT GGG TAG TCA GTC AGC
Sell	TAC ATT GCC CAA AAG CCC TTA	CAT CGT TCC ATT CCC AGA GT C
Indo	GCT TTG CTC TAC CAC ATC CAC	CAG GCG CTG TAA CCT GTG T
IL-4	GGT CTC AAC CCC CAG CTA GT	GCC GAT GAT CTC TCT CAA GTG AT
IL-5	CTC TGT TGA CAA GAC CTG	TCT TCA GTA TGT CTA GCC CCT G
IL-13	CCT GGC TCT TGC TTG CCT T	GGT CTT GTG TGA TGT TGC TCA
IL-25	ACA GGG ACT TGA ATC GGG TC	TGG TAA AGT GGG ACG AGG TTG
IL-33	TCC AAC TCC AAG ATT TCC CCG	CAT GCA GTA GAC ATG GCA GAA
Tslp	ACG GAT GGG GCT AAC TTA CAA	AGT CCT CGA TTT GCT CGA ACT
CCL26	TTC TTC GAT TTG GGT CTC CTT G	GTG CAG CTC TTG TCG GTG AA

4.1.14. Primer for genotyping

Target	Forward sequence 5'-3'	Reverse sequence 5'-3'	Annealing
Socs1WT	GCA TCC CTC TTA ACC CGG TAC	AAA TGA AGC CAG AGA CCC TCC	59 °C
Socs1KO	CCT CCA GCT GGC CCC TCG AGT AGG ATG	CAT CGC CAT TCC AGG CTG CGC AAC TGT T	59 °C
Socs1MGL	TAA ACG GCC ACA AGT TCA GC	TTC ATG TGG TCG GGG TAG C	59 °C
β2M	CAC CGG AGA ATG GGA AGC CGA A	TCC ACA CAG ATG GAG CGT CCA G	59 °C

4.1.15. Organisms

Mice

C57BL/6 mice were purchased from Charles River Laboratories. Breeding occurred under specific pathogen free conditions in the animal facility (IBF, Heidelberg, Germany). Breeding and monthly control for infections were performed according to the GV-SOLAS, 1995. Transgenic mice were generated by pronucleus injection using a BAC containing a part of chromosome #16 (10.78 – 10.80 Mb) including a _m_utated Socs1 locus with non-nuclear Socs1ΔNLS, e_G_FP (codon optimized for mouse and human) and _L_uciferaseCBG99 (Click Beetle Green from Pyrophorus plagiophalam), termed MGL (RP23-360O7). The BAC (generated by Arnold Küblbeck, DKFZ) consist of the sequence for *Socs1ΔNLS* (red indicating the exchanged NLS corresponding region), GFP (green), Luciferase and 2 A sequences in between the three coding regions (blue):

ATG GTA GCA CGC AAC CAG GTG GCA GCC GAC AAT GCG ATC TCC CCG GCA GCA GAG CCC
CGA CGG CGG TCA GAG CCC TCC TCG TCC TCG TCT TCG TCC TCG CCA GCG GCC CCC GTG
CGT CCC CGG CCC TGC CCG GCG GTC CCA GCC CCA GCC CCT GGC GAC ACT CAC TTC CGC
ACC TTC CGC TCC CAC TCC GAT TAC CGG CGC ATC ACG CGG ACC AGC GCG CTC CTG GAC
GCC TGC GGC TTC TAT TGG GGA CCC CTG AGC GTG CAC GGG GCG CAC GAG CGG CTG CGT
GCC GAG CCC GTG GGC ACC TTC TTG GTG CGC GAC AGT CGC CAA CGG AAC TGC TTC TTC
GCG CTC AGC GTG AAG ATG GCT TCG GGC CCC ACG AGC ATC CGC GTG CAC TTC CAG GCC
GGC CGC TTC CAC TTG GAC GGC AGC CGC GAG ACC TTC GAC TGC CTT TTC GAG CTG CTG
GAG CAC TAC GTG GCG GCG CC G CTG GTA CTG AGC CGA CCT CTC TCC TCC AAC GTG GCC
ACC CT G CAG GAG CTG TGT CGC CAG CGC ATC GTG GCC GCC GTG GGT CGC GAG AAC CTG
GCG CGC ATC CCT CTT AAC CCG GTA CTC CGT GAC TAC CTG AGT TCC TTC CCC TTC CAG ATC
GGT TCC GGA GCC ACG AAC TTC TCT CTT TTA AAG CAA GCA GGA GAC GTG GAA GAA AAC
CCC GGT CCC ATG GTG AGC AAG GGC GAG GAG CTG TTC ACC GGG GTG GTG CCC ATC CTG
GTC GAG CTG GAC GGC GAC GTA AAC GGC CAC AAG TTC AGC GTG TCC GGC GAG GGC GAG
GGC GAT GCC ACC TAC GGC AAG CTG ACC CTG AAG TTC ATC TGC ACC ACC GGC AAG CTG
CCC GTG CCC TGG CCC ACC CTC GTG ACC ACC CTG ACC TAC GGC GTG CAG TGC TTC AGC
CGC TAC CCC GAC CAC ATG AAG CAG CAC GAC TTC TTC AAG TCC GCC ATG CCC GAA GGC TAC
GTC CAG GAG CGC ACC ATC TTC TTC AAG GAC GAC GGC AAC TAC AAG ACC CGC GCC GAG
GTG AAG TTC GAG GGC GAC ACC CTG GTG AAC CGC ATC GAG CTG AAG GGC ATC GAC TTC
AAG GAG GAC GGC AAC ATC CTG GGG CAC AAG CTG GAG TAC AAC TAC AAC AGC CAC AAC
GTC TAT ATC ATG GCC GAC AAG CAG AAG AAC GGC ATC AAG GTG AAC TTC AAG ATC CGC
CAC AAC ATC GAG GAC GGC AGC GTG CAG CTC GCC GAC CAC TAC CAG CAG AAC ACC CCC
ATC GGC GAC GGC CCC GTG CTG CTG CCC GAC AAC CAC TAC CTG AGC ACC CAG TCC GCC
CTG AGC AAA GAC CCC AAC GAG AAG CGC GAT CAC ATG GTC CTG CTG GAG TTC GTG ACC
GCC GCC GGG ATC ACT CTC GGC ATG GAC GAG CTG TAC AAG GGT TCC GGA GCC ACG AAC
TTC TCT CTT TTA AAG CAA GCA GGA GAC GTG GAA GAA AAC CCC GGT CCC 5' ATG GTG AAG
CGT GAG AAA AAT GTC ATC TAT GGC CCT GAG CCT CTC CAT CCT TTG GAG GAT TTG ACT GCC
GGC GAA ATG CTG TTT CGT GCT CTC CGC AAG CAC TCT CAT TTG CCT CAA GCC TTG GTC
GAT GTG GTC GGC GAT GAA TCT TTG AGC TAC AAG GAG TTT TTT GAG GCA ACC GTC TTG
CTG GCT CAG TCC CTC CAC AAT TGT GGC TAC AAG ATG AAC GAC GTC GTT AGT ATC TGT
GCT GAA AAC AAT ACC CGT TTC TTC ATT CCA GTC ATC GCC GCA TGG TAT ATC GGT ATG ATC
GTG GCT CCA GTC AAC GAG AGC TAC ATT CCC GAC GAA CTG TGT AAA GTC ATG GGT ATC
TCT AAG CCA CAG ATT GTC TTC ACC ACT AAG AAT ATT CTG AAC AAA GTC CTG GAA GTC
CAA AGC CGC ACC AAC TTT ATT AAG CGT ATC ATC ATC TTG GAC ACT GTG GAG AAT ATT CAC
GGT TGC GAA TCT TTG CCT AAT TTC ATC TCT CGC TAT TCA GAC GGC AAC ATC GCA AAC TTT
AAA CCA CTC CAC TTC GAC CCT GTG GAA CAA GTT GCA GCC ATT CTG TGT AGC AGC GGT
ACT ACT GGA CTC CCA AAG GGA GTC ATG CAG ACC CAT CAA AAC ATT GCG TGC GTG CTG
ATC CAT GCT CTC GAT CCA CGC GTG GGC ACT CAG CTG ATT CCT GGT GTC ACC GTC TTG
GTC TAC TTG CCT TTC TTC CAT GCT TTC GGC TTT AGC ATT ACT TTG GGT TAC TTT ATG GTC

GGT CTC CGC GTG ATT ATG TTC CGC CGT TTT GAT CAG GAG GCT TTC TTG AAA GCC ATC
CAA GAT TAT GAA GTC CGC AGT GTC ATC AAC GTG CCT AGC GTG ATC CTG TTT TTG TCT
AAG AGC CCA CTC GTG GAC AAG TAC GAC TTG TCT TCA CTG CGT GAA TTG TGT TGC GGT
GCC GCT CCA CTG GCT AAG GAG GTC GCT GAA GTG GCC GCC AAA CGC TTG AAT CTT CCA
GGG ATT CGT TGT GGC TTC GGC CTC ACC GAA TCT ACC AGC GCT AAC ATT CAC TCT CTC
GGG GAT GAG TTT AAG AGC GGC TCT TTG GGC CGT GTC ACT CCA CTC ATG GCT GCT AAG
ATC GCT GAT CGC GAA ACT GGT AAG GCT TTG GGC CCG AAC CAA GTG GGC GAG CTG TGT
ATC AAA GGC CCT ATG GTG AGC AAG GGT TAT GTC AAT AAC GTT GAA GCT ACC AAG GAG
GCC ATC GAC GAC GAC GGC TGG TTG CAT TCT GGT GAT TTT GGA TAT TAC GAC GAA GAT
GAG CAT TTT TAC GTC GTG GAT CGT TAC AAG GAG CTG ATC AAA TAC AAG GGT AGC CAG
GTT GCT CCA GCT GAG TTG GAG GAG ATT CTG TTG AAA AAT CCA TGC ATT CGC GAT GTC
GCT GTG GTC GGC ATT CCT GAT CTG GAG GCC GGC GAA CTG CCT TCT GCT TTC GTT GTC
AAG CAG CCT GGT AAA GAA ATT ACC GCC AAA GAA GTG TAT GAT TAC CTG GCT GAA CGT
GTG AGC CAT ACT AAG TAC TTG CGT GGC GGC GTG CGT TTT GTT GAC TCC ATC CCT CGT
AAC GTA ACA GGC AAA ATT ACC CGC AAG GAG CTG TTG AAA CAA TTG TTG GAG AAG GCC
GGC GGT TAG 3'

Pronucleus injection resulted in 12 transgenic founder mice, named C57Bl6-tg(Socs1-MGL)Uhg. This work was done by Prof. Dr. Bernd Arnold and Günter Küblbeck (DKFZ, Heidelberg, Germany) in cooperation with Frank Zimmermann (IBF, Heidelberg) and Patrick Walker. Mice were genotyped at an age of 2 weeks using ear material for PCR detecting either Socs1 wildtype (wt) and Socs1 knock-out or Socs1 MGL and β2microglobulin (β2M) (Primer sequences see section 4.1.14). Breeding, sacrificing and dissection were approved and experiments properly recorded and reported to the regional commission in Karlsruhe (Permit number: 35-9185.81/G-54/14). Socs1$^{+/-}$MGL^{tg} mice were mated with Socs1$^{+/-}$ to generate Socs1$^{-/-}$MGL^{tg} and the corresponding control mice. Using this breeding strategy, 17.6% of the offsprings were Socs1$^{-/-}$MGL^{tg}, showing no gender bias (Fig. 4).
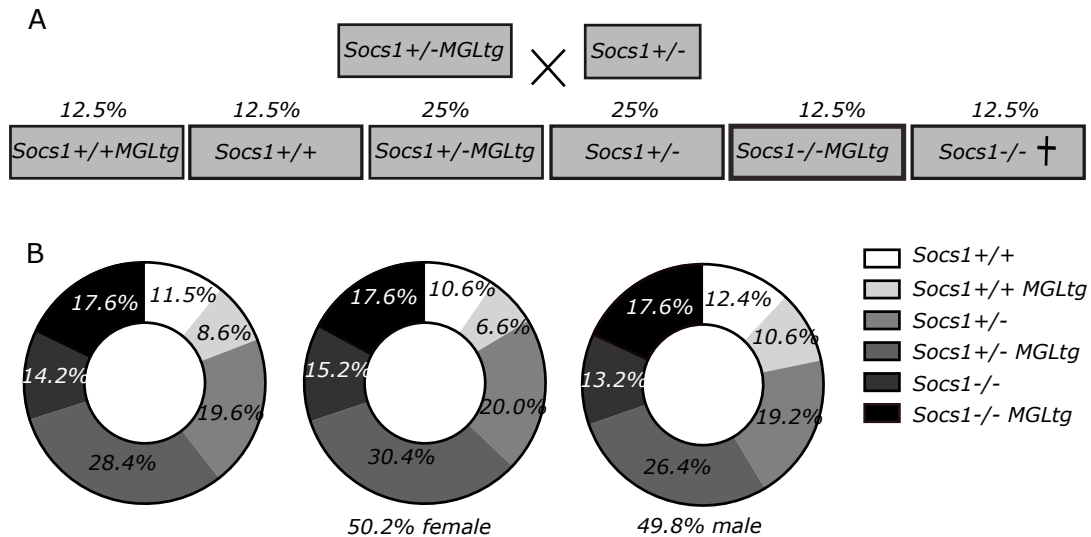
Figure 4.: Breeding strategy for Socs1$^{-/-}$MGL^{tg} mice.
(A) Socs1$^{+/-}$MGL^{tg} mice were mated with Socs1$^{+/-}$ to generate Socs1$^{-/-}$MGL^{tg} (12.5% expected) and the corresponding littermate controls. Percentages showing expected frequencies of the different genotypes. (B) Percentage of offsprings according to their genotype in all offsprings (left), female offsprings (middle) and male offsprings (right). n = 107 - 353 mice per group

Eukaryotic cells

- BEAS2B cells: BEAS2B cells were derived from normal bronchial epithelium obtained from autopsy of non-cancerous individuals and transformed by SV40 T-antigen.

- NIH3T3 cells: Mouse embryonic fibroblast cells come from a cell line isolated and initiated in 1962 at the New York University School of Medicine Department of Pathology.

- Raw264.7 cells: Macrophage cell line established from an ascites of a tumour induced in a male mouse by intraperitoneal injection of Abselon Leukaemia Virus (A-MuLV).

- BMMs: Murine bone marrow-derived macrophages, AG Dalpke (isolation protocol given below)

- pmTEC: Primary murine tracheal epithelial cells, AG Dalpke (isolation protocol given below)

- Hybridoma cells: Originated by Abmart (Shanghai) by immunizing mice against the peptide RRITRASALLDA.

Prokaryotic cells

- DH5α: Chemically competent E.coli strain for cloning. Saftey level S1.

- BL21: E.coli strain for the expression of recombinant proteins. Saftey level S1.

4.2. Methods

4.2.1. Genotyping

DNA was extracted from mouse ear tissue using the DirectPCR Lysis reagent (peqlab) according to the manufacturer's protocol. The extracted DNA was used in a PCR to check for amplification of *Socs1WT*, *Socs1KO* or *Socs1 MGL*. In brief, ear material was incubated in 180 μl DirectPCR Lysis reagent with 0.3 mg/ml Proteinase K at 55 °C overnight. After incubation at 85 °C for 45 min, 3 μl of DNA was used in a PCR using Taq Polymerase (5 U/μl). The reaction mix was composed of: 2 μl 10x buffer, 0.4 μl dNTPs, 0.2 μl primermix, 0.2 μl Taq Polymerase, 2 μl MgCl$_2$, 0.4 μl DMSO, 11.8 μl H$_2$O and 3 μl DNA template in 20 μl reaction volume. The following PCR conditions were used with 35 cycles between step 2 - 4:

1. 5 min at 95 °C

2. 1 min at 59 °C

3. 1 min at 72 °C

4. 1 min at 95 °C

5. 5 min at 72 °C

Expected bands for *Socs1WT* at 360 bp and *Socs1KO* at 160 bp or for *β2M* at 350 bp and *GFP* at 150 bp were controlled on a 2% agarose gel. Agarose gel was prepared in 1x TAE buffer and peqGREEN DNA/RNA Dye was added. Amplified DNA samples were mixed with 4 μl of 6x loading dye and loaded on the 2% agarose gel that run at 100 V for 45 min. GeneRuler DNA Ladder Mix (100-10000 bp) was used as a marker. For documentation, the gels were analyzed under UV light and imaged.

4.2.2. Cell culture and transfection of eukaryotic cells

RAW264.7 cells were cultured at 37 °C and 5% CO_2 in RPMI-1640 and Beas2B or NIH3T3 cells in DMEM, respectively. Cell culture medium was further supplemented with 10% (v/v) heat-inactivated fetal calf serum (FCS), penicillin (50 units/ml) and streptomycin (50 μg/ml) (P/S). Cells were split every 3 or 4 days when reaching approximately 80-90% confluence. After washing with PBS, Beas2B or NIH3T3 cells were trypsinized in trypsin-EDTA (0.05%) solution at 37 °C (approximately 1 min), followed by addition of corresponding culture medium to terminate trypsinization. Raw264.7 cells were split using a cell scraper. Cells were diluted 1:10 in trypan blue solution and viable cells counted with a Neubauer counting chamber. For transfection of RAW264.7 cells, the transfection reagent JetPRIME was used and for transfection of Beas2 or NIH3T3 cells, PeqFect was used and transfection was performed according to the manufacturer's protocol.

4.2.3. Cell culture of primary murine tracheal epithelial cells (pmTECs)

The procedure used for isolation of murine tracheal epithelial cells was adapted from Davidson et al. in 2000 [46]. In brief, mice were killed by CO_2 inhalation. Tracheas were removed, cut length-ways, washed in PBS and transferred to collection media (1:1 mixture of DMEM and Ham's F12 with 1% (v/v) penicillin-streptomycin). Tracheas were then incubated at 4 °C overnight in dissociation media (44 mM $NaHCO_3$, 54 mM KCl, 110 mM NaCl, 0.9 mM NaH_2PO_4, 0.25 μM FeN_3O_9, 1 μM sodium pyruvate, pH 7.5, and supplemented with 1% (v/v) penicillin-streptomycin, 0.1 mg/ml DNaseI and 1.4 mg/ml PronaseE). Enzymatic digestion was stopped by adding 20% FCS to the dissociation media. Epithelial cells were dissociated by gentle agitation followed by physical removal of the trachea skeletons. Cells were then centrifuged at 1000 x g for 10 min at RT. Cell pellets were resuspended in culture medium (1:1 mixture of DMEM and Ham's F12 with 1% penicillin-streptomycin, 5% FCS and 120 U/l Insulin) and seeded in a 10 cm cell-culture dish for 2 h at 37 °C. The supernatant containing epithelial cells was carefully collected and centrifuged at 1000 x g for 10 min at RT. Cell pellets from 2 tracheas were resuspended in 200 μl culture medium and seeded in the inner well of a transwell coated with human placenta collagen-IV. After 7 days, medium from the inner well was removed and medium from the outer well was replaced with UltroserG medium (1:1 mixture of DMEM and Ham's F12 with 1% penicillin-streptomycin, 2% UltroserG serum. After 30 days of culture, murine trachea epithelial cells were used for experiments.

4.2.4. Generation of bone-marrow derived macrophages

M-CSF derived macrophages (BMMs) were prepared as described previously [58], with minor modifications. Briefly, mice were sacrificed by CO_2 inhalation. Femurs and tibiae were removed and bone marrow was collected by flushing with supplemented DMEM using a 27 G syringe. After centrifugation of the cell suspension at 1300 rpm for 5 min, the pellet was resuspended in 48 ml of the respective medium. 12 ml of the cell suspension was placed per 145 cm^2 tissue culture plate plus 6 ml M-CSF containing cell supernatant (L929, 30%). On day 3, additional 9 ml of M-CSF containing cell supernatant were added and on day 7, adherent BMMs were harvested. For this purpose, BMM were washed with 1x PBS and detached by scraping using a cell scraper. Cells were centrifuged (1300 rpm, 5 min) and plated. For generation of BMMs from 2-week old mice, the same procedure was followed except using 29G syringes and 56.7 cm^2 dishes. 2.5×10^5 or 1×10^6 BMMs per well were cultured in 500 μl in a 24-well plate or in 2 ml in a 6-well plate. For cycloheximide chase, 1×10^6 BMMs were stimulated with IFNγ for 6 h and chased with 100 μg/ml Cycloheximide.

4.2.5. Preparation of single-cell suspensions from tissue

For analysis of lung homogenate, mice were sacrificed using xylazine and ketamine and lungs were perfused through the right ventricle with PBS. Once lungs appeared white, they were removed and sectioned. Dissected lung tissue was then incubated with 0.2 mg/ml Liberase^{TM} and 0.1 mg/ml DNaseI at 37 °C for 1 h. Digested lung tissue was gently disrupted by passage through a 19 G needle and afterwards through a 70 μm pore size nylon cell strainer. Red blood cells were lysed using red blood cell lysis buffer. CD11c$^+$ or CD4$^+$ T cells were isolated using the positive selection CD11c$^+$ beads or the negative selection CD4$^+$ T Cell Isolation Kit (Miltenyi Biotec), respectively. Magnetically labeled cells were isolated via the autoMACS Separator and purity was verified by FACS. For single cell suspension of splenocytes, spleens were dissected and treated as described above without enzymatic digestion.

4.2.6. Cell culture of prokaryotic cells

Bacteria stocks were kept at -80 °C for long term storage. For culturing of prokaryotic cells, veils were thawn on ice and used for transformation. Culture was done at 37 °C in a shaker (liquid culture) or in an incubator (agar plates). Culture volume was dependent on the copy number of the plasmid, the bacterial strain as well as the medium used.

4.2.7. Amplification of plasmids

To obtain sufficient amount of plasmids for transfection, plasmids were transformed into bacteria, amplified and purified. Chemical competent E.coli (DH5α or BL21, 50 μl per plasmid) were thawn on ice, incubated with the desired plasmid for 30 min, heat shocked for 45 sec at 42 °C and cooled down on ice for 2 min. Thereafter, 250 μl prewarmed SOC-medium was added and bacteria were incubated at 37 °C and 225 rpm for 1 h. 10% and 90% of this bacterial suspension were streaked out on two agar plates with the corresponding antibiotic and cultured at 37 °C in an incubator overnight. On the next day, one colony was picked and used for plasmid amplification in 5 ml of LB medium with the corresponding antibiotic overnight at 37 °C while shaking (ca. 250 rpm). This culture was either used for mini-prep or added to 250 ml of fresh LB medium and incubated again overnight for a maxi-prep on the next day. For harvesting, bacteria were centrifuged at 4.000 rpm at 4 °C for 20 min and further processed for plasmid isolation or stored for short term at -20 °C. For plasmid isolation, the commercially available kits from Quiagen were used according to the manufacturer's instructions either for mini-prep (for 5 ml of bacteria suspension) or for maxi-prep (for 250 ml of bacteria suspension). Eluted plasmids were stored at -20 °C.

4.2.8. Cloning

For Cloning of a part of a plasmid into another vector, different steps are necessary. First, a digest of the plasmid using restriction enzymes needs to take place. For cloning of SOCS1-WT or SOCS1ΔNLS out of the C1-GFP vector into an either PA-GFP or GST containing vector, 1 μg of vector or insert were used together with 2 μl Tango buffer, 2 μl BamHI, 1 μl EcoRI in a total volume of 20 μl and incubated at 37 °C for 1 h. Electrophoretic separation of nucleic acids was done to verify the PCR or restriction digest. Therefore, 1% agarose gels were prepared in 1x TAE buffer and peqGREEN DNA/RNA Dye (4 μl in 50 ml) was added. A DNA sample was mixed with 6x loading dye and loaded on the agarose gel and separated at 100 V for 45 min. GeneRuler DNA Ladder Mix (100-10000 bp) was used as a marker. For documentation, the gels were analyzed under UV light and imaged. Afterwards, the corresponding bands were cut out and DNA was isolated using the commercially available gelextraction kit from Quiagen according to the manufacturer's instructions. 100 ng of extracted DNA was than used in a ligation with a ratio vector to insert of 1 to 3 (amounts needed were calculated using the Ligation calculator form NEB (http://nebiocalculator.neb.com/ligation)). Ligation was performed by addition of

4 μl of T4 ligase buffer and 1 μl of T4 ligase in a total volume of 20 μl. Incubation was done at RT for 10 min. 1 - 2 μl of the ligation was used for transformation of competent E.coli (see section Amplification of plasmids) followed by amplification of the plasmid and another control digest using different enzymes. Successful cloning was verified by sequencing at GATC. Using ClustalW (http://www.ebi.ac.uk/clustalw/) or Blastn (https://blast.ncbi.nlm.nih.gov/), correct sequence was confirmed.

4.2.9. Recombinant protein expression of SOCS1

For recombinant protein expression of SOCS1 or SOCS1-GST, BL21 cells were transformed with GST-SOCS1 containing a thrombin cleavage site. 100 ml LB containing Ampicillin (100 μg/ml) were inoculated with a single colony from a freshly streaked plate and incubated at 37 °C with shaking at 250 rpm, overnight. The next morning, inoculation of 2 l LB containing Ampicillin followed that was cultured with shaking at 37 °C to an OD_{600} of 0.5-1.0. At this point, the culture was induced by the addition of 1 mM IPTG and incubated with shaking at 37 °C for 6 h. Afterwards, the cells were harvested by centrifugation at 4000 rpm at 4 °C for 20 min followed by lysis in 15 ml lysis buffer and freezing 5 ml Aliquots at -80 °C. After thawing of 5 ml of this bacterial suspension, protease inhibitors and lysozyme was added to a concentration of 2 mg/ml and the cells were incubated on ice for 30 min. After sonication for 3 times for 5 sec (on ice), centrifugation followed at 13.000 rpm at 4 °C for 30 min. The pellet was resuspended in 10 ml wash buffer containing 1% Triton X-10 and incubated at room temperature for 5 min. After another centrifugation step at 13.000 rpm at 4 °C for 30 min, the pellet was resuspended in 10 ml wash buffer without Triton and centrifuged once more. Since it has been confirmed previously, that SOCS1 is only present in the insoluble fraction, inclusion bodies were isolated. Therefore, extraction buffer and proteinase inhibitors were added to obtain a final protein concentration in the solution of 1 mg/ml (as measured by nanodrop) followed by incubation at RT for 60 min. Afterwards, the solution was diluted tenfold with extraction buffer to obtain a final protein concentration of 0.1 mg/ml, centrifuged at 13.000 rpm at 4 °C for 5 min and the supernatant was dialyzed overnight against a 100 fold volume of refolding buffer. On the next morning dialysis followed against PBS for 10 h at 4 °C. The obtained dialysate was subsequently centrifuged at 45.000 rpm at 4 °C for 30 min and the supernatant was transferred into a fresh tube. If necessary, a protein concentrator was used to concentrate the protein to obtain the concentration needed for further analysis. For removal of the GST tag, thrombin cleavage was performed using 1 U/ml thrombin per mg protein for 16 h at 4 °C in a shaker. A GST-trap column was used to get rid of cleaved GST or uncleaved GST-SOCS1 with a constant flow rate of 0.5 -1 ml per min. The column was washed with 1 ml of PBS and the flow-through containing cleaved SOCS1 only was concentrated if necessary using a protein concentrator. Small aliquots of the recombinant protein were snap frozen using liquid nitrogen and stored at -80 °C. For analysis by Western Blot, SDS loading buffer was added to the sample.

4.2.10. Generation of polyclonal SOCS1 antibodies

Generation of polyclonal SOCS1 antibodies was done by Charles River using the following immunization scheme:

- day 1: 1st injection

- day 28: 2nd injection

- day 38: 1st serum sample

- day 42: 3rd injection

- day 52: 2nd serum sample

- day 56: 4th injection

- day 70: bleeding of the rabbit

For each immunization, 0.2 mg of the antigen (rec. SOCS1-GST plus complete freud adjuvant for the 1st immunization and rec. SOCS1 plus incomplete freud adjuvant for the following immunizations) at 1 mg/ml were injected subcutaneously. Serum samples (d38 and d52) were tested by Western Blot resulting in detection of recombinant SOCS1. Bleeding of the rabbits on day 70 was done by heart puncture leading to 80 ml of serum. Serum was used for affinity purification of SOCS1 antibodies using a HYDRA protein affinity column with bound recombinant SOCS1 as an antigen resulting in 2 ml of affinity purified rabbit serum with a total antibody yield of 0.5 mg.

4.2.11. Generation of hybridoma cell supernatant containing SOCS1 antibodies

Antigen production and quality control as well as antibody production was done by Abmart (Shanghai). In brief, 8 Balb/c mice were immunized with 7 different peptides. Ascites was produced and 13 ascites samples were analyzed for detection of recombinant SOCS1, murine SOCS1 upon IFNγ stimulation or cells transfected with GFP-SOCS1. Upon decision for one ascites successfully detecting SOCS1, fusion of a B cell to a myeloma cell and subsequent subcloning of 2 - 4 rounds followed. The corresponding hybridoma cellline was both cultured for further cultivation and monoclonal antibody production. Cell culture for further cultivation was done in DMEM supplemented with 10% (v/v) heat-inactivated fetal calf serum (FCS), penicillin (50 units/ml) and streptomycin (50 μg/ml) (P/S) to reach a confluence of 60% and split 2 - 3 times a week. For collection of supernatant, hybridoma cells were cultured in DMEM supplemented with only 1% FCS and P/S until they reach a confluence of 100% and the supernatant was collected 24 h thereafter. Hybridoma cell supernatant was used in Western Blot in a 1:20 dilution.

4.2.12. Quantitative RT-PCR

Total RNA from 2.5×10^5 cells was isolated using the peqGOLD RNA Kit (peqlab) according to the manufacturer's protocol. RNA was eluted with 40 μl DNase/RNase-free water. Quality and quantity of RNA was measured by 230/260 nm and 260/280 nm absorbance ratios, acquired by the nanodrop. Afterwards, reverse transcription of 200 ng RNA into cDNA was done using the High Capacity cDNA Reverse Transcription Kit (Applied Biosystems) and the following PCR conditions: 25 °C for 10 min, 37 °C for 120 min, 85 °C for 5 min. 5 μl cDNA (diluted 1:10) was used as template in a quantitative real time PCR using SYBR Green FAST Mix (Applied Biosystems) with a total reaction volume of 15 μl. PCR conditions were as follows: initial 95°C for 20 sec and 40 cycles of 95 °C for 3 sec and 60 °C for 30 sec. Amplification and measurement was done in a StepOne Plus RT-PCR cycler (Applied Biosystems) in a 96-well format. Specificity of qPCR was controlled by non-template as well as no-RT samples and

analysis of melting curves. Each cDNA was measured in duplicates. Baseline and threshold values were manually set to the same value per gene. Detected Ct values of the endogenously expressed reference gene (ACTB) were subtracted from the determined Ct values and relative expression was calculated as $2^{-\Delta CT}$ for each target gene. qPCR for *Socs1wt* was performed with TaqMan Fast Universal PCR Master Mix (Applied Biosystems) in combination with a forward primer (P1) binding in the SH2 domain and a reverse primer (P2) binding in the SOCS Box and a FAM-labelled probe binding in the NLS of Socs1. For the detection of *Socs1ΔNLS*, SYBR green dye in combination with P1 and a reverse primer (P3) within the modified NLS region were used. For detection of total *Socs1* (both Socs1 and Socs1ΔNLS), the primers P1 and P2 were used. This qPCR strategy (Fig. 5) allows for specific detection of *Socs1*, *Socs1ΔNLS* or total *Socs1*. The amplification efficiencies for both *Socs1wt* (1.68) and *Socs1ΔNLS* (1.88) were adjusted.
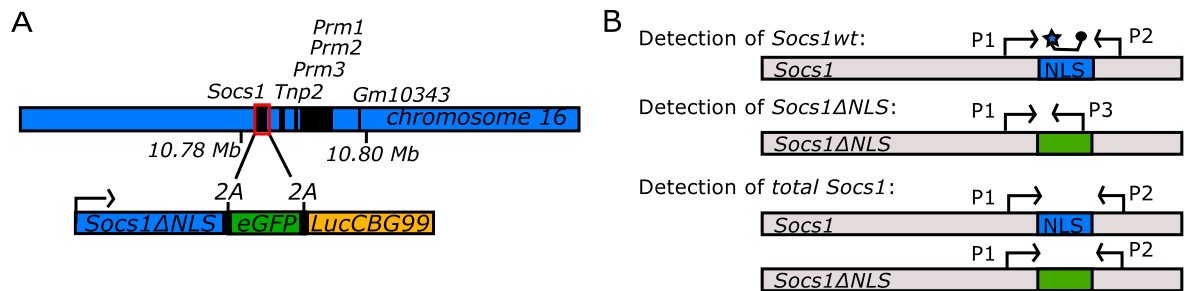
Figure 5.: Structure of the bacterial artificial chromosome and qPCR scheme to detect *Socs1WT*, *Socs1ΔNLS* and *total Socs1* mRNA.
(A) Schematic drawing of the bacterial artificial chromosome (BAC) consisting of a *m*utated SOCS1 locus containing *Socs1ΔNLS*, *eGFP* and *firefly Luciferase*. (B) qPCR strategy to specifically detect *Socs1WT* (wildtype) using the primers P1 and P2 together with a labelled probe ($\star$) binding within the NLS, *Socs1ΔNLS* using P1 and P3 (reverse primer binding in the exchanged NLS) or *total Socs1* using P1 and P2.

4.2.13. Whole-Genome Expression analysis

Total RNA from 2.5×10^5 BMMs was isolated as described above. The quality of total RNA was checked by gel analysis using the total RNA Nano chip assay on an Agilent 2100 Bioanalyzer. The laboratory work was done in the Genomics and Proteomics Core Facility at the German Cancer Research Center, Heidelberg, Germany (DKFZ). Biotin-labeled cRNA samples for hybridization on Illumina Mouse Sentrix-8 BeadChip arrays were prepared according to Illumina's recommended sample labeling procedure based on the modified Eberwine protocol [59]. In brief, 300 ng total RNA was used for cDNA synthesis, followed by an amplification/labeling step according to the Illumina Total Prep RNA Amplification Kit. The cRNA was column purified according to TotalPrep RNA Amplification Kit, and eluted in 60 μl of water and quality controlled. Hybridization was performed at 58 °C, in GEX-HCB buffer at a concentration of 100 ng cRNA/μl, unsealed in a wet chamber for 20 h. Spike-in controls for low, medium and highly abundant RNAs were added, as well as mismatch control and biotinylation control oligonucleotides. Microarrays were washed once in High Temp Wash buffer at 55 °C and then twice in E1BC buffer at room temperature for 5 minutes. After blocking for 5 min in 4 ml of 1% (wt/vol) blocker casein in phosphate buffered saline Hammarsten grade, array signals were developed by a 10 min incubation in 2 ml of 1 μg/ml Cy3-streptavidin solution and 1% blocking solution. After a final wash in E1BC, the arrays were dried and scanned. Microarray scanning was done using an iScan array scanner. Data extraction was done for all beads individually, and outliers were removed when ¿ 2.5 MAD (median absolute deviation). All remaining data points were used for the calculation of the mean average signal for a given probe, and standard deviation for

each probe was calculated. Data were processed using R, including log2 transformation of the data, significance (p≤ 0.05) and fold change (log2 ≤-1 or ≥1) filtered. Data was normalized to remove systematic variation and background subtraction. Pathway annotation was performed using the PANTHER (Protein Analysis through Evolutionary Relationships) classification system and transcription factor binding sites (TFBS) among the differentially regulated genes were analyzed using the over-representation analysis tool oPOSSUM. Microarray data is available online at ArrayExpress (accession #E-MTAB-4938).

4.2.14. Western Blotting

$1x10^6$ BMMs or RAW264.7 cells were stimulated as indicated, subsequently washed with PBS and lysed in Laemmli buffer. After incubation for 10 min at 98 °C, equal amounts of lysates were fractionated by 10% polyacrylamide gel (SDS-PAGE) and electrotransferred to Nitrocellulose membranes by a semidry blotting procedure (2.5 mA/cm^2 for 1 h 15 min). Blocking of unspecific binding was performed using 5% BSA solution in 1x TBST for at least 1 h. Membranes were stained with the corresponding primary antibodies (see table 4.1.9) or hybridoma cell supernatant for SOCS1 detection overnight at 4 °C. After three 10 min washing steps in 1x TBST at room temperature, blots were incubated with secondary antibodies for 1 h at RT (HRP-linked anti-mouse or anti-rabbit), followed by additional three 10 min washing steps in 1x TBST at room temperature. Proteins were detected using an enhanced chemiluminescence system. Gels were imaged digitally, and contrast adjustments were applied to all parts of a figure. Where indicated, membranes were stripped and reprobed. Densitometry was performed using ImageJ software (National Institutes of Health).

4.2.15. Flow cytometry

For detection of GFP present in MGL positive cells, $2.5x10^5$ BMMs were harvested in FACS buffer by centrifugation at 1300 rpm at 4 °C and analyzed by FACSCanto flowcytometer gating on GFP positive cells. For FACS staining of surface proteins, tissue was homogenized as previously described and homogenate (approx. $5x10^5$ cells) was transferred to a FACS tube. After washing the cells with 1 ml of PBS followed by centrifugation at 1300 rpm at 4 °C, cells were stained with the corresponding antibodies in 50 μl FACS buffer for 30 min at 4 °C. After an additional washing step, cells were resuspended in 200 - 500 μl of FACS buffer and analyzed by FACSCanto flowcytometer. For analysing the purity of the MACS sorted CD11c$^+$ or CD4$^+$ cells, PE Anti-Mouse CD11c (1:50) or FITC Anti-Mouse CD4 (1:100) were used. For the CD45.1 and CD45.2 staining upon bone marrow transplantation, 50 μl of blood was collected from the tail vein using a 29G syringe containing Heparin (10,000 U/ml), washed twice with ice cold PBS and resuspended in red blood cell lysis buffer for 10 minutes on ice. After washing with FACS buffer, the cells were labelled with APC-CD45.2 (1:200) and FITC-CD45.1 (1:200) for 40 min on ice, washed with FACS buffer and analyzed by FACSCanto flowcytometer.
For detection of intracellular pSTAT1 by flow cytometry, $1x10^5$ cells were stimulated for the indicated time with IFNγ (50 ng/ml), washed with PBS and transferred into a FACS tube using a cell scraper. After fixation with 4% PFA for 30 min at RT, cells were permeabilized with 90% ice-cold MeOH for 2 h at -20 °C. Cells were washed with FACS buffer and stained with anti-pSTAT1 in 50 μl FACS buffer for 90 min RT. Stained cells were washed and resuspended in 200 μl FACS buffer prior to measuring at the FACS Canto.

4.2.16. Immunofluorescence microscopy

NIH cells were grown on μ-slides (8- well, ibidi) and transfected with 0.5 μg GFP-Socs1 or GFP-Socs1ΔNLS using PeqFect. Where indicated, cells were stained with Hoechst (1 μg/ml) for 2 min or with CellMask^{TM} Plasma Membrane Stain (1:1000) for 10 min at room temperature. Coverslips were mounted and analyzed by microscopy using a Leica TCS SP5 confocal

microscope equipped with a 488- and 561-nm laser, spectrophotometer prism, tunable detectors and a HCX PL APO 63x/1.4 oil objective. All channels were recorded in a sequential order to avoid emission crosstalk. A z-stack was recorded and presented as an overlay using ImageJ (National Institutes of Health).

4.2.17. Luciferase Activity Assay

$2.5x10^5$ BMMs were lysed in Luciferase lysis buffer. After injection of Luciferase assay buffer to each well, activities in the lysates were measured using a luminometer (LUMIstar OPTIMA system). Luminescent units are presented per μg as determined by colorimetric Bradford assay using the Rotiquant reagent.

4.2.18. Measuring cytokine secretion

Supernatants of the indicated cells were harvested and analyzed for cytokines by commercially available ELISA kits for IL-6, TNFα and IL-12p40 from BD and IL-33 form R&D. The supernatant of $2.5x10^5$ cells (250 μl) was diluted 1:50, the supernatant of $1x10^5$ CD11c$^+$ cells in 200 μl was diluted 1:10 and BAL supernatant was used undiluted prior measuring murine IL-6, TNFα or IL12p40. In brief, 96-well high binding ELISA plates were incubated with a coating antibody overnight at 4 °C. After washing of the plates for 3 times, plates were blocked using 2% FCS in PBS for 2 h at RT. After 3 additional washing steps, the sample or standard was added to the plate followed by incubation for 2 h at RT. After 5 washing steps, the detection antibody was added together with the HRP-conjugate for 1 1/2 h at RT (for the IL-33 ELISA, addition of the detection antibody was done first for 1 h, followed by 3 washing steps and subsequent addition of the HRP conjugate for 20 min). After washing the plate 7 times, the substrate was added by mixing solution A with B and addition to each well until the standard turned blue. The reaction was stopped using 1 M H_2SO_4. Cytokines were detected by measuring the absorbance at 490 nm with a 650 nm reference in a photometer (Sunrise reader). Cytokine concentrations were calculated according to a standard dilution of the respective recombinant cytokines (standard) using Magellan V 5.0 software.
Upon OVA sensitization and challenge, levels of IL 4, IL-5, and IL-13 in serum were measured using an enhanced sensitivity cytometric bead array (CBA, Flex Set Kits), according to the manufacturer's guidelines.
For measurement of IgE levels in serum, 96-well high binding ELISA plates were coated with monoclonal anti-IgE antibodies overnight. Serum samples were diluted in 1% (w/v) BSA in PBS/ 0.05% (v/v) Tween 20 and incubated overnight at 4 °C. Afterwards plates were incubated with anti-IgE conjugated with HRP for 3 h at room temperature. For the colorimetric detection TMB was used as a substrate. Absorbance was measured at 450 nm with a 650 nm reference in ELISA reader and IgE concentrations calculated according to standard curve.

4.2.19. Evaluation of NFκB p65 activity

NFκB activity was measured in $1x10^6$ cells of a lung homogenate by the Trans^{AM} NFκB p65 protein assay (Active Motif), an ELISA-based method designed to specifically detect and quantify NFκB p65 subunit activation with high sensitivity and reproducibility. As a positive control Raji nuclear extract was used that was provided with the kit. Wildtype or mutant oligonucleotides were used as an internal specificity control. The assay was performed according to the manufacturer's protocol. In brief, 20 μl sample ($1x10^6$ cells from lung homogenate prepared as described in section 4.2.5 or one well of murine primary epithelial cells were resuspended in 50 μl lysis buffer) were used per well in which multiple copies of a specific double-stranded oligonucleotide have been immobilized. Either 30 μl binding buffer or 28 μl binding buffer and 2 μl wildtype or mutant oligo were added per well and incubated for 1h RT with gentle agitation (100 rpm). After 3 washing steps, 100 μl of the diluted antibody (p65, 1:1000) was added to

each well and incubated for 1 h RT without agitation. The plate was washed 3 times and 100 μl of diluted HRP conjugated antibody (1:1000) was added for 1 h at RT without agitation. After washing the plate 4 times, 100 μl developing solution was added until the optimal blue colour density developed and stopped using 100 μl stopping solution. The absorbance was read at 450 nm with a 650 nm reference in ELISA reader.

4.2.20. Macrophage phagocytosis assay

$4x10^5$ BMMs were incubated in 37 °C warm (or for the negative control in 4 °C cold) DMEM plus FCS and P/S for 30 min. 10 μl of a 1:10 dilution of Latex beads (amine-modified polystyrene, fluorescent yellow-green) were added for 1 h at 37 °C (or for the negative control on ice). After incubation with the beads, cells were washed twice with FACS buffer, resuspended in 200 μl FACS buffer and measured at the FACSCanto.

4.2.21. T cell proliferation, cell cycle analysis and differentiation

$CD4^+$ T cells were isolated from a single cell suspension as described above (section Preparation of single-cell suspensions from tissue). For proliferation analysis, $CD4^+$ T cells were stained with CFSE (5 mM) in 110 μl followed by vortexing of the cells for 5 sec. After 5 min incubation in the dark at RT, 10 ml RPMI was added and the cells were washed twice. $1x10^5$ cells were seeded per well in a 96 well plate (round bottom) with RPMI plus β-Mercaptoethanol (50 μM) and 4 μl of Dynabeads. CFSE staining was analysed on day 3.
For cell cycle analysis, $1x10^5$ $CD4^+$ T cells were fixed in 70% ethanol for 2 h to overnight. Cells were centrifuged at 13.000 rpm for 5 min at 4 °C and washed twice with PBS. Washed cells were stained with propidium iodide (50 μg/ml) with the addition of RNAse A (100 μg/ml) in 0.5 ml PBS. After incubation at 37°C for 30 min, cells were analysed by FACSCanto flowcytometer identifying PI- positive cells.
For differentiation of T cells, 1×10^5 cells per well were plated in 96-well round-bottom plate in 100 μl RPMI plus β-Mercaptoethanol (50 μM) and stimulated with 4 μl anti-CD3 and anti-CD28-coated beads plus 20 ng/ml IL-2, and either medium only or a Th2 differentiation solution consisting of 100 ng/ml IL-4, 10μg/ml anti-IFNγ and 10 μg/ml anti-IL-12. Afterwards, cells were incubated for 3 days at 37 °C. On day 4, T cells were restimulated with a cell stimulation cocktail including PMA and ionomycin for 3 h and RNA was extracted.

4.2.22. micro-CT

Micro computed tomography or micro-CT is x-ray imaging in 3D on a small scale with massively increased resolution. 6 $Socs1^{-/-}MGL^{tg}$ and 6 $Socs1^{+/-}MGL^{tg}$ mice were imaged. Mice were sacrificed using xylazine and ketamine and the lungs were infiltrated with 0.7 ml air via a tracheal cannula and closed using a silicon strand. After 4 h (rigor mortis, no further movement during the scan), the thorax of the mice was imaged with the SKYSCAN micro-CT at a resolution of 18 μm with 50 kV and 498 mA for 515 projections at a step angle of 0.7° for a total orbit of 360°. Total imaging time was approximately 21 min with an averaging of 5. No contrast agents were used. Lungs were removed, fixed using formalin and paraffin embedded for correlative histology. For scanning of paraffin embedded lungs, 9 μm with 50 kV and 498 mA and a high averaging (10 - 20) was used. CT scans were performed at AG Mall and Scans were analyzed by Dr. Willi Wagner (radiologist) in a blinded manner.

4.2.23. Bronchoalveolar lavage

Lungs were rinsed with 1 ml fresh, ice-cold PBS containing protease inhibitor via a tracheal cannula, and obtained cells were counted using a Neubauer chamber. Cytospins were prepared for each sample by centrifugation of 50 μl BAL fluid plus 150 μl of sterile PBS and subsequently stained with May Grünwald/ Giemsa. Cells were microscopically differentiated and classified

as either macrophages, neutrophils, eosinophils or lymphocytes, using standard morphologic criteria [200].

4.2.24. Histopathological Analysis

Organs were either fixed via a tracheal cannula under constant pressure of 20 cm H_2O or left uninflated using 4% (w/v) phosphate buffered paraformaldehyde overnight. Tissues were embedded in paraffin. For analysis of lung inflammation, 2 μm sections were stained with periodic acid–Schiff (PAS) or with hematoxylin and eosin (H&E), respectively.

H&E staining was performed in an automatic manner at the Institute of Pathology. In brief, sections were rinsed in distilled water and stained with the haematoxylin solution for 4 min at RT. After rinsing the sections with tap water, differentiation followed using 0.3% acid alcohol for 1-2 sec. and another washing step in tap water. Afterwards, sections were rinsed using Scott's tap water substitute, rinsed with tap water and stained with eosin for 2 min at RT. Dehydration was done using xylene followed by clearing and mounting of the sections.

PAS staining was performed of the lung sections by incubation in xylene for 20 min followed by rinsing with Ethanol of decreasing concentrations (100%, 96% and 70%) for 5 min each. After rinsing with ddH$_2$O, staining with Alcian blue followed for 30 min at RT. Afterwards, the sections were rinsed with tap water for 2 min and subsequently incubated in periodic acid (0.5% aqueous solution of periodic acid in ddH$_2$O) for 5 min. After 3 - 4 changes in ddH$_2$O, incubation in Schiff's reagent followed for 15 min. Sections were rinsed in sulfurous solution (1% HCl and 10% Sodium Metabisulfite) for 1 min and incubated in tap water for 10 min with 3 - 4 changes. Dehydration was done using xylene followed by mounting of the sections.

4.2.25. Immunohistochemistry

For immunohistochemistry, lungs were fixed overnight in 4% (v/v) formalin and embedded in paraffin. 2 μm lung sections were cut and stained for SOCS1 using the DAB staining method. After deparaffination, demasking of the antigens followed using either citrate buffer or EDTA buffer for 15–45 minutes in a steamer. Incubation with peroxidase-blocking solution and protein blocking solution was followed by incubation with the anti-SOCS1 antibody at varying concentrations (1:10–1:2000) at 4 °C overnight. The commercially available antibodies from Cell Signaling, Abcam and Santa Cruz were tested as well as hybridoma cell supernatant and a newly generated antibody against recombinant SOCS1. On the next day, incubation with serum corresponding to the species of the secondary antibody followed. Incubation with the secondary antibody (goat anti-rabbit antibody or goat anti-mouse antibody) was performed for 30 min. After washing, sections were incubated with the chromogen (liquid diaminobenzidine and peroxide buffer) until a reaction was visible. Slides were counterstained with hematoxylin to provide nuclear and morphologic detail and mounted. Lung sections of Socs1$^{-/-}$ mice were used as a negative control.

4.2.26. Measuring transepithelial resistance in primary trachea epithelial cells

Epithelial cells build up tight barriers between different compartments and are characterized by the formation of tight junctions. Tight junctions can be measured by detecting the transepithelial resistance. This was achieved by using a Ohmmeter Millicell ERS. Electrodes were disinfected with 70% ethanol and equilibrated for 15 - 30 min in the corresponding medium in the transwell. To measure the epithelial resistance the shorter end section was brought into the upper compartment, whereas the longer end section was extended into the lower compartment. A well without cells was measured as a blank. Resistance was measured twice for each transwell. The epithelial resistance was calculated by using the following formula: R_{probe}-R_{blank}=$R_{cell\ layer}$; $R_{cell\ layer}$ / Area$_{transwell}$ (0.33cm^2) = Resistance / cm^2 (Ω / cm^2)

Another method to measure transepithelial resistance is via addition of FITC-Dextran. Therefore, 1 mg/ml FITC-Dextran (4 kDa) was added to the upper chamber of the transwell and cells

were incubated at 37 °C for 2 h. Afterwards, fluorescence of FITC-Dextran was detected both in the inner and outer well by measuring the absorbance at 490 nm with a 520 nm reference in a photometer (Sunrise reader). A positive control (no cells, maximal diffusion of FITC-Dextran) and a negative control (no FITC-Dextran added) were included.

In addition, an albumin ELISA was performed with supernatant from BAL samples. Under physiological conditions, no albumin is found in lavages of lungs. In case of a leaky barrier, albumin from the blood can reach alveolar spaces and will be found in BAL samples. Albumin competitive ELISA was performed according to the manufacturer's guidelines. In brief, 25 μl BAL supernatant (undiluted) or albumin standard was added per well and immediately 25 μl of 1X biotinylated albumin was added. Incubation followed for 1 h at RT. After 5 washing steps, 50 μl of 1x SP conjugate was added to each well and incubated for 30 min at RT. After 5 washing steps, 50 μl of chromogen substrate was added per well and incubated till the optimal blue colour density developed. The reaction was stopped by the addition of 50 μl of stop solution to each well, resulting in a yellow colour. The absorbance was read at 450 nm with a 650 nm reference in ELISA reader and albumin concentrations calculated according to standard curve.

4.2.27. OVA sensitization and challenge

The OVA sensitization and challenge was performed at the Research Center Borstel by Dr. Lars Lunding and Dr. Michael Wegmann. Mice were sensitized to ovalbumin (OVA) by three i.p. injections of 10 μg OVA (OVA grade VI) adsorbed to 150 μg aluminum hydroxide on days 1, 14, and 21. Mice were exposed three times to an OVA (OVA grade V) aerosol (1% (w/v) in PBS) on days 26, 27, and 28 to induce acute allergic airway inflammation [162]. Sham sensitization and challenges were carried out using sterile PBS. On day 29, mice were anesthetized with ketamine and xylazine and sacrificed by cervical dislocation. Eight animals per group were used, if not stated otherwise. Experiments were done at the Research Center Borstel under approval of the animal ethics committee from the Department of State, Kiel, Germany (permit number: V244-7224.121.3 (108-9/14)).

4.2.28. IL-13 intratracheal (i.t.) instillation

Mice were anesthetized with isofluorane for 30 sec. and allowed to hang vertically with their mouths open, supported by a taut string placed under their canine teeth. Their tongues were gently withdrawn with a blunt forceps to keep them from swallowing, and 20 μl of PBS with or without 5 μg IL-13 was pipetted onto the base of the tongue. When the mice had aspirated the pipetted solution, they were put on their site until they woke up. This intratracheal instillation was performed on days 1,2 and 3 in KEB (IBF, Heidelberg). 5 mice per group were analyzed 24 h after the last treatment. Experiments were recorded properly under approval of the animal ethics committee in Karlsruhe (permit number: 35-9185.81/G-35/16).

4.2.29. Bone-marrow transplantation

For bone marrow isolation of donor mice, female Socs1$^{-/-}$MGL^{tg} (or CD45.1) mice were killed by CO_2 inhalation and the hind limbs removed. Bone marrow was flushed with medium from the medullary cavities of tibiae and femurs using a 27G needle. 1x10^7 marrow cells were resuspended in 100 μl of PBS and injected i.v. in lethally irradiated (2x 400 rad γ radiation with a 4 h break) CD45.1 (or Socs1$^{-/-}$MGL^{tg} and Socs1$^{+/+}$) mice with a 29G needle. Radiation was performed in the DKFZ under the supervision of Kerstin Dell. After radiation and bone marrow transplantation, mice were kept in "Maushotel" (IBF, Heidelberg) for 7 weeks until they were analyzed. Mice were weighted every day for the first two weeks and afterwards every 2 - 3 days and their health was evaluated. Mice received antibiotic treatment (2 ml CotrimK suspension in 250 ml drinking water corresponding to 125 μg Trimethoprim and 626 μg Sulfamethoxazol per animal per 24 h) for the first three weeks upon irradiation. At 10 days post transplant,

replacement of blood cells was examined by FACS staining of CD45.1 and CD45.2 using the FACS Canto (see section flow cytometry). As recipients, 10 Socs1$^{-/-}$MGL^{tg} or CD45.1 mice as well as 6 Socs1$^{+/+}$ mice were used. Experiments were recorded properly under approval of the animal ethics committee in Karlsruhe (permit number: 35-9185.81/G-35/16).

4.2.30. Statistics

All experiments were repeated three times unless stated otherwise. Data are shown as mean ±SD. Statistical significance of comparison between two groups was determined by two-tailed unpaired Student's t test (for data sets following Gaussian distribution), Wilcoxon matched pairs test (for data sets not following Gaussian distribution) or two-way ANOVA including Bonferroni post-test (for multiple comparisons). All statistical analyses were done using GraphPad Prism (GraphPad 6.05, San Diego, USA) software. Differences were considered significant at p ≤0.05 (*), p ≤0.01 (**) and p ≤0.001 (***).

5. Results

5.1. SOCS1ΔNLS is localized in the cytoplasm

It has been shown that SOCS1 is able to translocate into the cell nucleus due to a functional NLS localized between the SH2 domain and the SOCS-box (amino acids 159–173) [12, 143]. Confirming these results with murine *Socs1* constructs, NIH3T3 cells transiently transfected with murine *eGFP-Socs1* showed nuclear localization of the GFP-tagged protein. In contrast, *eGFP-Socs1ΔNLS*, in which the NLS has been replaced by the murine *Socs3* sequence, was localized more in the cytoplasm (Fig. 6A) as already described for human *eGFP-SOCS1ΔNLS* [12]. Cells transfected with *Socs1* were also stimulated with IFNγ. Upon stimulation, enhanced fluorescence in the cytoplasm could be observed, suggesting that SOCS1 is partly translocating out of the nucleus to inhibit signaling in the cytoplasm (Fig. 6B). Whereas untreated cells showed a ratio of cytoplasmic versus total fluorescence of 0.2 ± 0.07, indicating higher fluorescence in the cell nucleus, already 1 h upon IFNγ stimulation, cells showed a ratio of 0.5 ± 0.09 suggesting equal distribution of the fluorescently labelled SOCS1. To confirm fast shuttling of SOCS1 across the nuclear membrane, photoactivatable (PAGFP-tagged) *Socs1* plasmids were used. NIH3T3 cells were transfected with *PAGFP-Socs1* and a small region of interest (ROI) outside the nucleus was activated using UV light. Fast shuttling of SOCS1 into the nucleus already 200 ms after activation was observed (Fig. 6C). In contrast, activation of SOCS1ΔNLS in the cytoplasm did not result in fluorescence in the cell nucleus, but in the activated ROI in the cytoplasm. Of note, unlike SOCS1 that was highly mobile in the cell nucleus, SOCS1ΔNLS remained at the activated spot in the cytoplasm for the time monitored (1 min). This indicates that SOCS1ΔNLS was localized in the cytoplasm, less mobile and did not shuttle into the cell nucleus.

To verify that SOCS1ΔNLS is still functional in the cytoplasm, inhibition of IFNγ signaling at the receptor level was analyzed by Western Blotting. Therefore, the murine macrophage cell line Raw264.7 was transiently transfected with *eGFP*, *eGFP-Socs1* or *eGFP-Socs1ΔNLS*. Tyrosine phosphorylation of STAT1 was examined upon treatment with IFNγ 1-6 h post-stimulation. Already 1 h after IFNγ treatment, *eGFP-Socs1* or *eGFP-Socs1ΔNLS* transfected cells showed lower levels of phosphorylated STAT1 ($55 \pm 8\%$ or $53 \pm 7\%$ relative pY-STAT1 levels as compared to eGFP transfected cells 1 h after IFNγ stimulation) (Fig. 7). After 6 h of stimulation, the signal decreased to $34 \pm 10\%$ or $32 \pm 6\%$ for cells transfected with *eGFP-Socs1* or *eGFP-Socs1ΔNLS*, respectively. Cells expressing eGFP showed higher levels of pSTAT1 ($97 \pm 5\%$) at 6 h after IFNγ stimulation as compared to 1 h. Importantly, no differences in phosphorylated STAT1 levels between *eGFP-Socs1* and *eGFP-Socs1ΔNLS* transfected cells were observed. Although SOCS1ΔNLS seemed to be less mobile, data suggests that both SOCS1 and SOCS1ΔNLS were effectively inhibiting IFNγ induced STAT1 tyrosine phosphorylation.
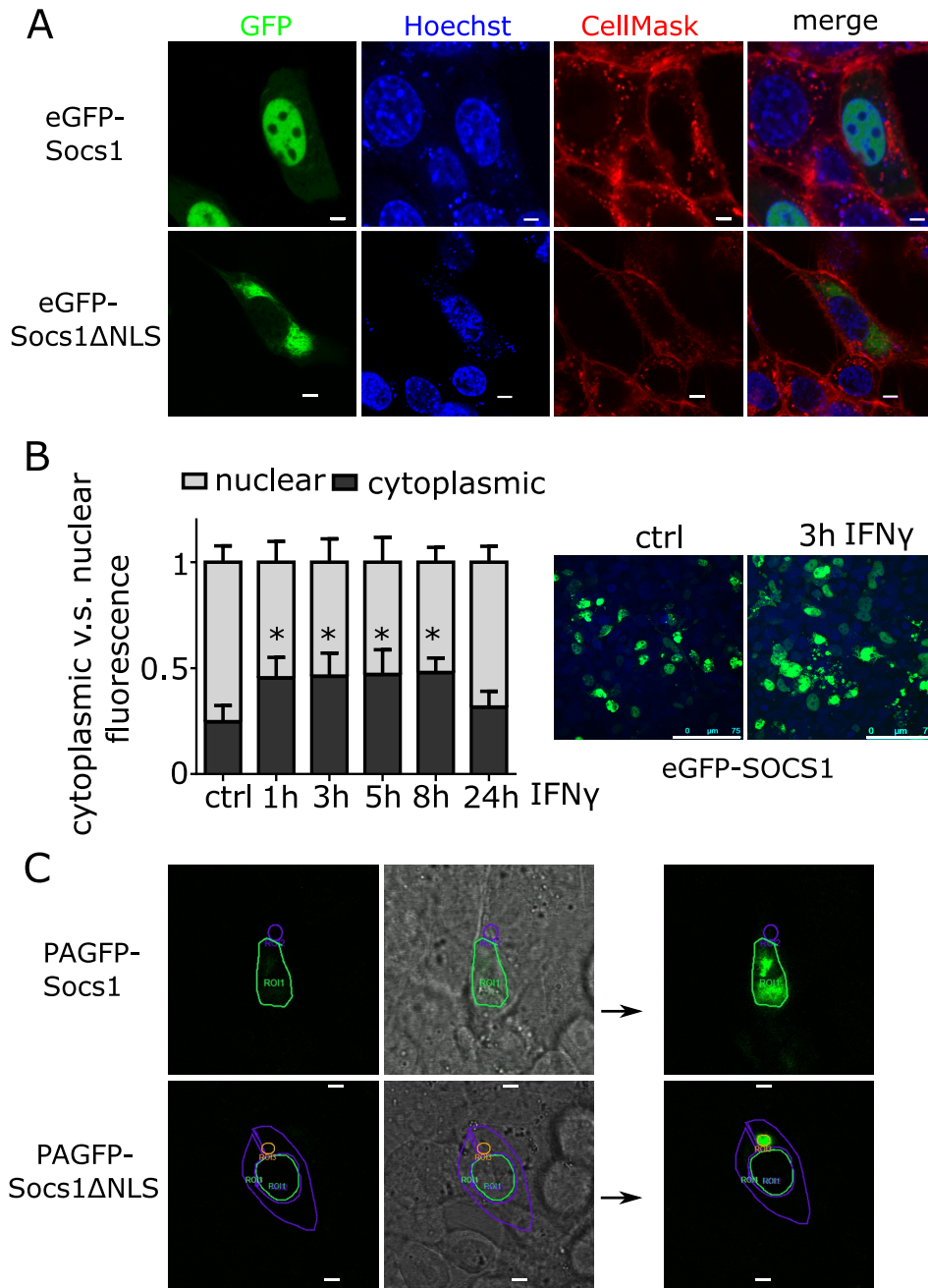
Figure 6.: Cytoplasmic expression of SOCS1ΔNLS.
(A) Living NIH3T3 cells were transfected with the indicated eGFP-tagged plasmid and visualized by confocal microscopy. Nuclei were counterstained with Hoechst and membranes were stained with CellMask™ dye. Scale bar 5 μm. (B) NIH3T3 cells were transfected with *eGFP-Socs1* and stimulated with IFNγ (50 ng/ml) as indicated. Scale bar 25 μm. A z-stack was recorded and the fluorescence in the cytoplasm (black) versus the fluorescence in the nucleus (grey) was measured using ImageJ (n = 3, each time 20-50 cells, mean +SD, Two-way ANOVA including Bonferroni post test). (C) Living NIH3T3 cells were transfected as described above using photoactivatable plasmids (PAGFP). Photoactivation was done using 100% UV laser intensity in a small ROI in the cytoplasm in close proximity to the cell nucleus (for *PA-GFP-Socs1* the purple circle and for *PA-GFP-Socs1ΔNLS* the orange circle). Using confocal microscopy, images were taken directly before photoactivation (left) and after 10 sec of photoactivation (right) and localization of SOCS1 was analyzed.
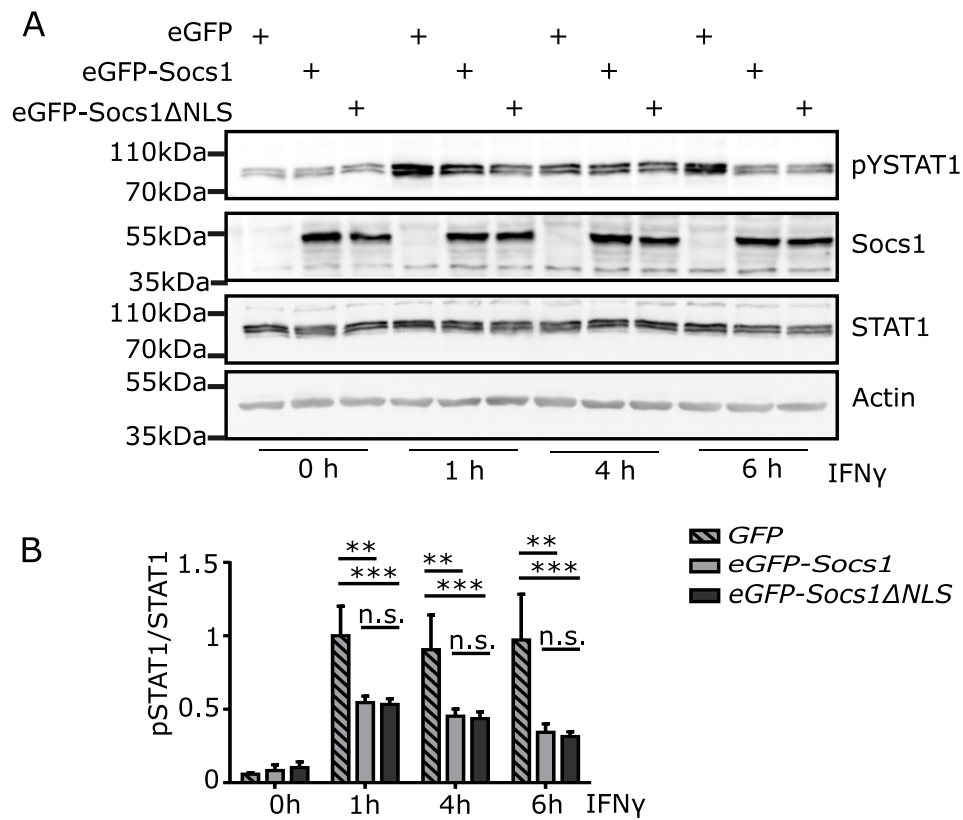
Figure 7.: Cytoplasmic SOCS1ΔNLS is able to inhibit IFNγ signaling.
(A) Western Blot analysis of tyrosine phosphorylated STAT1. Raw264.7 cells were transfected with *eGFP*, *eGFP-Socs1* or *eGFP-Socs1ΔNLS* and stimulated with IFNγ (50 ng/ml) as indicated. Protein extracts were stained for pY-STAT1 (Tyr701), SOCS1 (using hybridoma cell supernatant as described in Section 5.2), STAT1 and β-Actin. Quantification using ImageJ is shown in (B) (n = 3, mean +SD, Two-way ANOVA including Bonferroni post test).

5.2. Generation of antibodies for SOCS1 detection

Since there is no commercially available antibody specifically detecting endogenous murine SOCS1, a new antibody has to be generated for this purpose. First, a monoclonal antibody secreted by hybridoma cells was tested. Antigen production and quality control as well as antibody production were done by the company Abmart (Shanghai). Mice were immunized with the peptide (RRITRASALLDA) and ascites was produced. Upon decision for one ascites successfully detecting SOCS1, fusion of B cells to myeloma cells and subsequent subcloning followed.
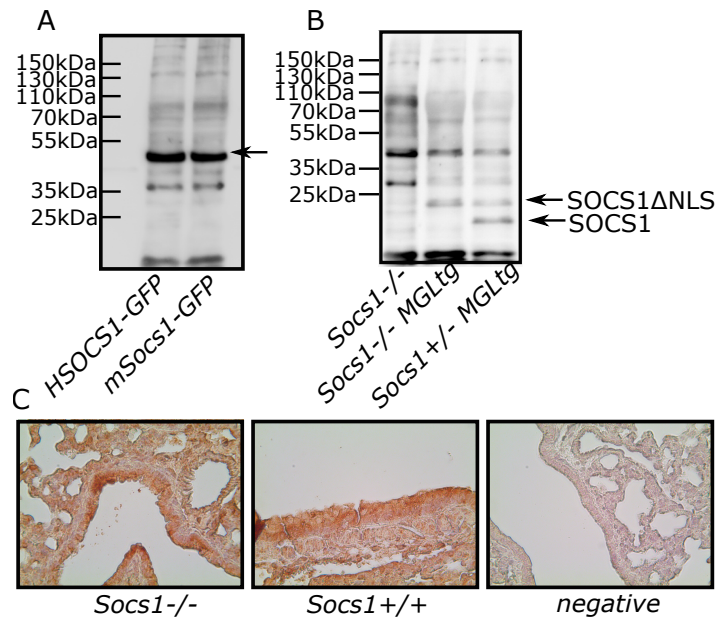
Figure 8.: Generation of SOCS1 specific antibodies using hybridoma cells. (A) Beas2B cells or NIH3T3 cells were transfected using eGFP tagged human *SOCS1* (HSOCS1) or murine *Socs1* (mSocs1), respectively. Hybridoma cell supernatant (1:20) was used to detect GFP-SOCS1 (50 kDa) in both cell lysates. Arrow indicates SOCS1-GFP. (B) Hybridoma cell supernatant (1:20) was used to detect SOCS1 (21 kDa) or SOCS1ΔNLS in lysates of BMMs stimulated with IFNγ (50 ng/ml) for 6 h. Arrows indicates either SOCS1 or SOCS1ΔNLS. (C) Unspecific staining of lung sections by hybridoma cell supernatant (1:10). Socs1$^{-/-}$ and isotype controls were included as negative controls. 200x magnification

The corresponding hybridoma cell supernatant was used in Western Blot in a 1:20 dilution for detection of SOCS1 in cells transfected with either human *GFP-SOCS1* or murine *GFP-Socs1* (Fig. 8A) and in BMMs upon IFNγ stimulation (Fig. 8B), resulting in a band at a molecular weight of 50 kDa for GFP tagged proteins and below 25 kDa for untagged SOCS1 (molecular weight of 21 kDa). Although there were unspecific bands as well, one specific band for SOCS1 could be detected in mice containing only wildtype SOCS1 (Socs1$^{+/-}$) at 20 kDa and one band for SOCS1ΔNLS in mice only expressing SOCS1ΔNLS (Socs1$^{-/-}$MGL^{tg}) at 23 kDa. Those mice were generated using a bacterial artificial chromosome (BAC) containing a <u>m</u>utated Socs1 locus with non-nuclear *Socs1ΔNLS*, <u>G</u>FP and firefly <u>L</u>uciferase (termed MGL) and crossed onto an otherwise SOCS1 deficient background. This mouse model will be discussed in more detail in section 5.3.1. The difference in the molecular weight might be due to the remaining 21 amino acids on the C-term of *Socs1ΔNLS* upon cleavage of the 2A sequence between *Socs1ΔNLS* and *eGFP* (see Fig. 5A). Although the hybridoma cell supernatant was specifically detecting SOCS1 by Western Blot, detection of SOCS1 on lung sections using immunohistochemistry was not possible due to unspecific staining of the negative control (Socs1$^{-/-}$ mice) (Fig. 8C). Despite using various concentrations from 1:10 to 1:2000 and different buffers, unspecific staining of lung sections from Socs1$^{-/-}$ mice was observed, arguing against the use of hybridoma cell supernatant for immunohistochemistry.

Therefore, a polyclonal antibody was produced against recombinant SOCS1. *Socs1* was cloned into the vector pGex containing a GST tag and a thrombin cleavage site. Recombinant protein expression was carried out in BL21 codon optimized *E.coli*. Recombinant Socs1-GST was expressed in inclusion bodies, protein purification of inclusion bodies was performed followed by refolding during dialysis. Using thrombin, the GST tag was cleaved-off, resulting in recombinant SOCS1 that was analyzed by Western Blot using hybridoma cell supernatant (Fig. 9A). Immunization of rabbits was performed at Charles River by injecting GST-SOCS1 for primary

immunization and SOCS1 (untagged) for the following 3 booster immunizations. Serum samples were tested and antibodies were purified using recombinant SOCS1 as an antigen. The resulting antibodies were tested for the detection of SOCS1 in cells transfected with murine *GFP-Socs1* resulting in high background and unspecific bands. There was one band at a molecular weight of 50 kDa increased in lysates of cells expressing eGFP-SOCS1 that could correspond to SOCS1 (Fig. 9B). However, as observed previously for hybridoma cell supernatant, detection of SOCS1 on lung sections by the new polyclonal antibody using immunohistochemistry was not possible due to unspecific staining of lung sections from Socs1$^{-/-}$ mice (Fig. 9C). In summary, a monoclonal antibody (secreted by hybridoma cells) was established detecting SOCS1 by Western Blot, however, no antibody was found specifically detecting SOCS1 by immunohistochemistry.
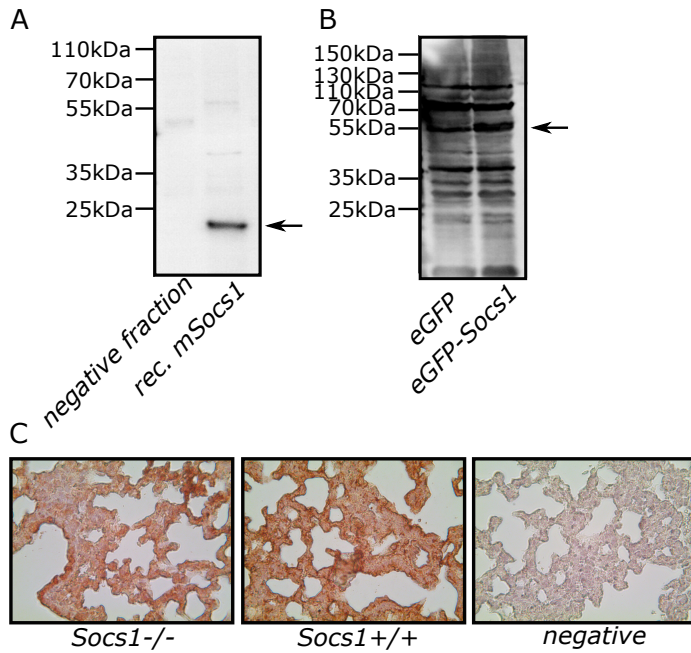
Figure 9.: Generation of antibodies against recombinant SOCS1.
(A) Protein purification of recombinant murine SOCS1. Lysates of recombinantly expressed murine SOCS1 (arrow, 21 kDa) was analyzed by Western Blot using hybridoma cell supernatant (1:20). (B) Anti-Socs1 antibody was obtained from Charles River by immunization of rabbits with recombinant murine SOCS1. This antibody was used to detect SOCS1 in lysates of NIH3T3 cells transfected with *eGFP-Socs1* (arrow, 50 kDa) using 1:500 dilution of the antibody. (C) Unspecific staining of lung sections by the anti-Socs1 antibody (1:10) from Charles River. Socs1$^{-/-}$ and isotype controls were included as negative controls. 200x magnification

5.3. Generation of mice lacking nuclear Socs1

5.3.1. Characterization of Socs1$^{+/+}$MGL^{tg} founder mice

To analyze the function of Socs1 in the cell nucleus *in vivo*, a transgenic mouse model was established using a bacterial artificial chromosome (BAC). This BAC contains the sequence of chromosome 16 between 10.78 and 10.8 Mb including a <u>m</u>utated Socs1 locus with non-nuclear *Socs1ΔNLS*, <u>G</u>FP and firefly <u>L</u>uciferase, termed MGL. After transcription, co-translational cleavage occurs due to 2A peptide sequences between the protein coding regions. In addition to the coding region for SOCS1, protein-coding sequences for proteins involved in spermatogenesis (PRM1, PRM2, PRM3 and TNP2) as well as a sequence for a predicted transcript Gm1034 are contained. PRM proteins are protamines that substitute for histones in the chromatin of sperms during spermatogenesis. TNP2 is a transition protein associated with the conversion of nucleosomal chromatin to the compact, non-nucleosomal form during spermatogenesis. Of note, no gender biases were detectable in MGL transgenic mice and male Socs1$^{+/-}$MGL^{tg} mice were breeding as efficiently as Socs1$^{+/-}$ mice, allowing the conclusion that other genes contained in the BAC did not influence analysis shown thereafter. 12 MGL transgenic mice were generated by pronucleus injection and three of them (founders #53, #45 and #29) were characterized (Fig. 10). As a BAC integrates randomly into the genome, stable expression and regulation of the mutated Socs1 locus was analyzed in different founder lines. Therefore, offsprings of the founders #53, #45 and #29 were analyzed according to the expression of *Socs1WT* and *Socs1ΔNLS* in BMMs after stimulation with IFNγ for 24 h. qPCR was specifically designed to distinguish between mRNA expression of *Socs1WT* and *Socs1ΔNLS* (see qPCR scheme in Fig. 5B). Indeed, mRNA expression and inducibility of *Socs1WT* and *Socs1ΔNLS* were comparable. After stimulation with IFNγ, both *Socs1WT* and *Socs1ΔNLS* were induced (Fig. 10A) with an relative expression after IFNγ stimulation of 0.02 ± 0.005 of both *Socs1WT* or *Socs1ΔNLS* for founder #53, 0.06 ± 0.004 of *Socs1WT* or 0.03 ± 0.003 of *Socs1ΔNLS* for founder #45 and 0.03 ± 0.005 of *Socs1WT* or 0.06 ± 0.004 of *Socs1ΔNLS* for founder #29, respectively. Due to reporter-functions of the mutated Socs1 locus, a luciferase assay could be performed. Therefore, BMMs were treated as above and luciferase activity was measured. BMMs treated with IFNγ for 24 h showed an increased activity at 4.3 ± 1.1x10^6, 3.4 ± 1.2x10^6 and 2.8 ± 1.3x10^6 luminescent units for the founders #53, #45 and #29, respectively (Fig. 10B). In addition, GFP positive cells were analyzed after stimulation with IFNγ by flow cytometry. There was a similar increase in the percentage of GFP positive cells after stimulation with IFNγ for founder #53 (to 26 ± 9%), founder #45 (to 25 ± 8%) and founder #29 (to 21 ± 9%) (Fig. 10C). Taken together, all three founders showed similar expression levels of the mutated Socs1 locus, suggesting a stable regulation and integration and of the BAC into the genome. No indications for a founder specific effect were identified and therefore following experiments were performed using founder #53 if not stated otherwise.
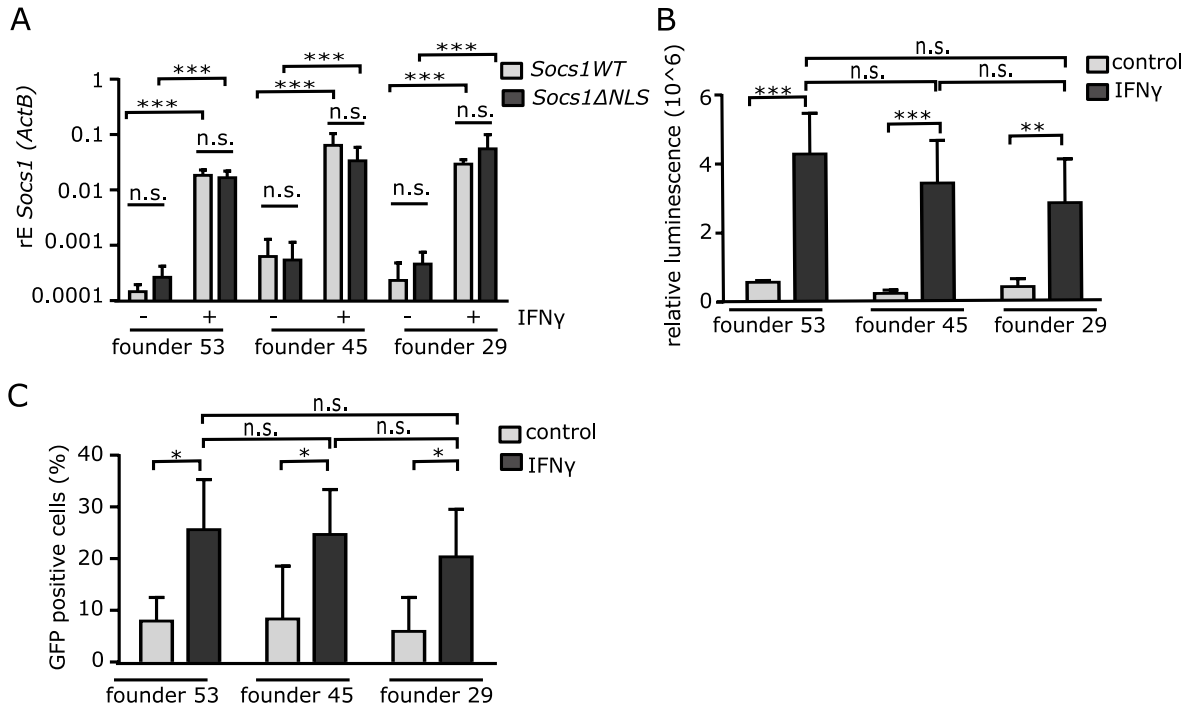
Figure 10.: Characterization of Socs1MGL[tg] founders #53, #45 and #29.
(A) BMMs of Socs1^{+/+}MGL[tg] mice from each founder were stimulated with IFNγ (50 ng/ml) for 24 h and analyzed according to mRNA expression of Socs1 wildtype (WT) and Socs1ΔNLS, (B) Luciferase activity and (C) percentage of GFP positive cells (n= 3-5, mean +SD, two-way ANOVA including Bonferroni post-test.)

5.3.2. Using Socs1^{+/+}MGL[tg] mice as reporter mice

Since *eGFP* and *Luciferase* are transcribed together with *Socs1ΔNLS* on the BAC, Socs1^{+/+} MGL[tg] mice can be used as reporter mice. Organ specific expression of *Socs1* can be measured by luciferase activity. Therefore, various organs were homogenized and luciferase activity was determined per mg tissue, revealing high activity in thymus and muscle (Fig. 11A). In addition mRNA expression of *Socs1WT*, *Socs1ΔNLS*, *eGFP* and *Luciferase* was measured in indicated organs. Again, high expression of *Socs1* was observed in thymus. Except for the liver and the pancreas (where expression of *eGFP* and *Luciferase* were higher than expression of *Socs1WT* and *Socs1ΔNLS*), expression of the BAC was in good correlation for *Socs1* expression arguing for the use of Socs1MGL[tg] mice as reporter mice. SOCS1 expression in the thymus has already been reported [256, 173, 193], confirming shown data and supporting the role of Socs1^{+/+}MGL[tg] mice as reporter mice.

5.3.3. Investigation of SOCS1 expression in Socs1MGL[tg] mice

To analyze the function of SOCS1 in the cell nucleus, Socs1[+/-]MGL[tg] mice were crossed with Socs1^{+/-} mice to generate Socs1^{-/-}MGL[tg] mice that are expressing SOCS1ΔNLS in an otherwise SOCS1 deficient background. To prove that Socs1^{-/-}MGL[tg] mice have similar expression levels of total *Socs1* (both *Socs1* and *Socs1ΔNLS*) as compared to Socs1^{+/-} and Socs1[+/-]MGL[tg] mice, BMMs were stimulated with IFNγ for 24 h and qPCR was performed to detect both, *Socs1* and *Socs1ΔNLS* indicating similar levels of total *Socs1* (Fig. 12A). Socs1[+/-]MGL[tg] mice were used as controls as they are still expressing nuclear *Socs1*, but also the *MGL* transgene which rules out a transgene specific effect. Socs1^{+/-} mice are another important control, as they only have one allele of *Socs1* as compared to Socs1[+/-]MGL[tg] mice with one allele of *Socs1*
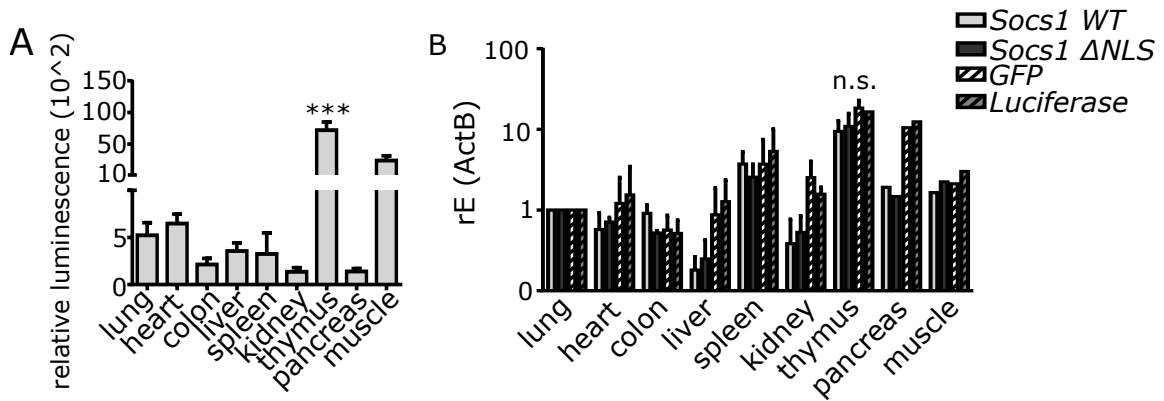
Figure 11.: Socs1$^{+/+}$MGL^{tg} mice can be used as reporter mice.
(A) Luciferase activity per mg tissue was measured in indicated organs of Socs1$^{+/+}$MGL^{tg} mice. (n= 3, mean +SD, Two-way ANOVA including Bonferroni post-test) (B) mRNA expression of *Socs1WT*, *Socs1ΔNLS*, *eGFP* and *Luciferase* was measured in indicated organs normalized to the reference genes ActB and GAPDH using the REST software (http://rest.gene-quantification.info/) and displayed in relation to their expression in lung tissue (n= 3 except for pancreas and muscle with n = 1, mean +SD, Pair Wise Fixed Reallocation Randomisation Test).

and additionally *Socs1ΔNLS*. Next, similar protein levels for SOCS1 and SOCS1ΔNLS were confirmed. Fig. 12B shows SOCS1 and SOCS1ΔNLS detection in lysates of BMMs stimulated with IFNγ for 6 h. Quantification of the Western Blot suggests equal protein levels for both SOCS1 and SOCS1ΔNLS. As previously mentioned, a band at the corresponding molecular weight for SOCS1 and a slightly higher running one for SOCS1ΔNLS were detected, the latter most likely results from the remaining 21 amino acids after cleavage of the 2A sequence.

To rule out the possibility that mutating SOCS1 alters its protein half-life, cycloheximide chase was performed. 6 h post stimulation with IFNγ, cycloheximide was added to block nascent protein synthesis. Already after 1 h of cycloheximide treatment, there was only $60 \pm 32\%$ and $50 \pm 24\%$ of the SOCS1 or SOCS1ΔNLS protein remaining and after 4 h only $6 \pm 3\%$ and $8 \pm 6\%$, respectively (Fig. 13). As a control, IκBα is shown as a protein known to be rapidly degraded. Importantly, no alteration of the mRNA expression levels, the protein levels or the protein half-life could be observed when mutating SOCS1 to SOCS1ΔNLS.
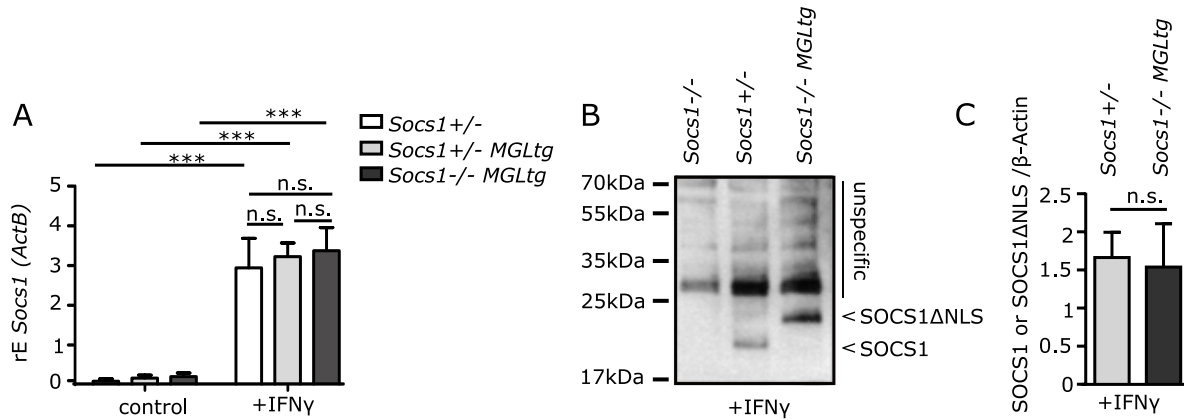
Figure 12.: Similar expression of SOCS1 and SOCS1ΔNLS in MGL transgenic mice.
(A) mRNA expression of total *Socs1* was analyzed in isolated BMMs upon stimulation with IFNγ (50 ng/ml) for 6 h (n = 4, mean +SD, two-way ANOVA including Bonferroni post-test). (B) Detection of SOCS1 by Western Blot in lysates of BMMs upon stimulation with IFNγ for 6 h. Arrows indicate band for SOCS1 (in Socs1^{+/-} mice) and SOCS1ΔNLS (in Socs1^{-/-}MGL[tg] mice) (C) Quantification of SOCS1 and SOCS1ΔNLS protein was done by densitometry using ImageJ (n = 10-13, mean +SD, Wilcoxon matched pairs test).
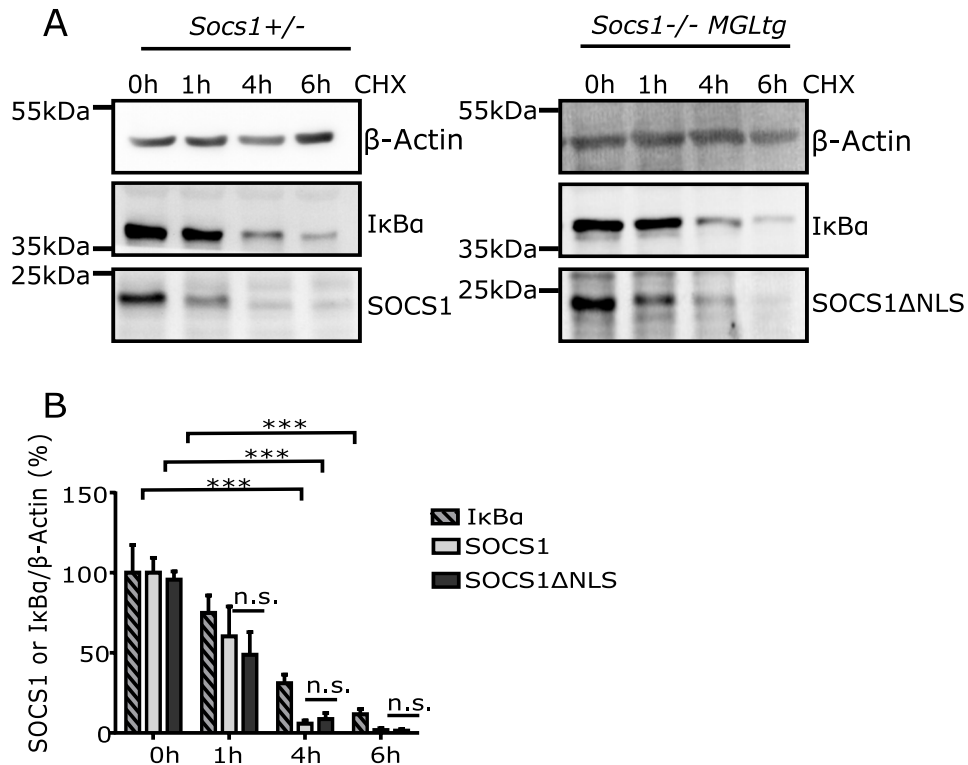
Figure 13.: Similar protein stability of SOCS1 and SOCS1ΔNLS.
(A) Cycloheximide (CHX, 100 μg/ml) was added at 6 h post-stimulation with IFNγ. BMMs were lysed at the indicated time points. (B) Following Western blotting and densitometry, SOCS1 and SOCS1ΔNLS expression was normalized to βActin in order to calculate the percentage of remaining protein relative to its expression prior to the addition of CHX. IκBα was used as a control for effective CHX treatment (n= 3-4, mean +SD, two-way ANOVA including Bonferroni post-test).

5.4. Socs1$^{-/-}$MGL^{tg} mice lack SOCS1 in the cell nucleus

In order to show that Socs1$^{-/-}$MGL^{tg} mice - only expressing non-nuclear SOCS1ΔNLS - indeed lack SOCS1 in the cell nucleus, staining of endogenous SOCS1 was performed by immunohistochemistry. However, no sufficiently specific antibody was found that did not stain sections from Socs1$^{-/-}$ mice (including newly generated antibodies described in section 5.2). Therefore, functional assays were used to identify the lack of functional SOCS1ΔNLS in Socs1$^{-/-}$MGL^{tg} mice. It has been reported that nuclear SOCS1 leads to degradation of the NFκB subunit p65 [260], therefore the hypothesis was tested whether Socs1$^{-/-}$MGL^{tg} mice show sustained NFκB signaling. In addition, SOCS1 has been reported to activate p53 in the cell nucleus suggesting an anti-proliferative role of nuclear SOCS1 [169]. For this purpose, proliferation and cell cycle were further investigated in Socs1$^{-/-}$MGL^{tg} mice.

5.4.1. Functional impairment of NFκB inhibition in Socs1$^{-/-}$MGL^{tg} mice

In order to show that Socs1$^{-/-}$MGL^{tg} mice indeed lack SOCS1 in the cell nucleus, a functional approach was used to verify non-nuclear expression of SOCS1ΔNLS. To examine whether NFκB signaling is altered in Socs1$^{-/-}$MGL^{tg} mice, CD11c$^+$ cells were isolated from lungs and stimulated *ex vivo* with TLR agonists. Stimulation of CD11c$^+$ cells from Socs1$^{-/-}$MGL^{tg} mice with CpG-DNA, LPS and pI:C for 24 h led to an increased protein expression of IL-12p40 (3748 ±142 pg/ml after LPS and 8738 ±770 pg/ml after pI:C treatment) as compared to CD11c$^+$ cells from Socs1$^{+/-}$MGL^{tg} mice (1333 ±467 pg/ml after LPS and 3430 ±791 pg/ml after pI:C treatment) (Fig. 14A). The same could be shown in CD11c$^+$ cells isolated from spleens with an increased protein expression of IL-12p40 of 4637 ±827 pg/ml after LPS and 9157 ±460 pg/ml after pI:C treatment as compared to CD11c$^+$ cells from Socs1$^{+/-}$MGL^{tg} mice with 1406 ±91 pg/ml after LPS and 3547 ±253 pg/ml after pI:C treatment (Fig. 14B). Of note, Socs1$^{-/-}$MGL^{tg} mice already showed higher (however non-significant) IL-12p40 and IL-6 protein levels without prior stimulation, suggesting pre-activation of CD11c$^+$ cells from Socs1$^{-/-}$MGL^{tg} mice. No differences were observed regarding TNFα protein levels, which is in full accordance with previous findings of Strebovsky et al. 2011 [260] showing that only a subset of NFκB dependent genes is altered in Socs1$^{-/-}$MGL^{tg} mice. In contrast to TNFα, IL-12p40 induction which needs prolonged binding of NFκB to its promoter [20] was sensitive to SOCS1 induced NFκB inhibition. Data suggest sustained NFκB activation in Socs1$^{-/-}$MGL^{tg} mice. This hypothesis was confirmed by a transcription factor activity assay for p65 (Fig. 14C,D). In this assay, the activated NFκB p65 subunit in whole-cell extracts specifically binds to a plate-bound oligonucleotide. By using an antibody that is directed against p65, the activated NFκB subunit bound to the oligonucleotide is detected. Using this Trans^{AM} approach, increased p65 activity was demonstrated in untreated complete lung homogenate (Fig. 14C) and primary murine trachea epithelial cells (pmTECs) (Fig. 14D). The results entirely phenocopy *in vitro* data using non-nuclear SOCS1ΔNLS regarding NFκB activation, suggesting that Socs1$^{-/-}$MGL^{tg} mice functionally lack SOCS1 in the cell nucleus.

5.4.2. Socs1$^{-/-}$MGL^{tg} mice have an altered cell cycle

SOCS1 expression is silenced in multiple human cancers suggesting a tumor suppressor role for this protein [39, 165, 243, 293, 125]. The anti-proliferative function of SOCS1 is thought to be dependent on its interaction with p53 within the cell nucleus, leading to activation of p53 by phosphorylation at serine15 [169]. Therefore, proliferation and cell cycle were analyzed in Socs1$^{-/-}$MGL^{tg} mice. Indeed, Socs1$^{-/-}$MGL^{tg} mice showed elevated spleen weight as well an an increased number of splenocytes as compared to Socs1$^{+/-}$MGL^{tg} mice (Fig. 15A,B), suggesting altered proliferation or cell cycle in the spleen. Proliferation of CD4$^+$ T cells was examined in an *in vitro* assay using CFSE and analysis of the cells 3 days after stimulation with anti-CD3/CD28 coated beads to induce T cell proliferation. No difference was observed comparing proliferation
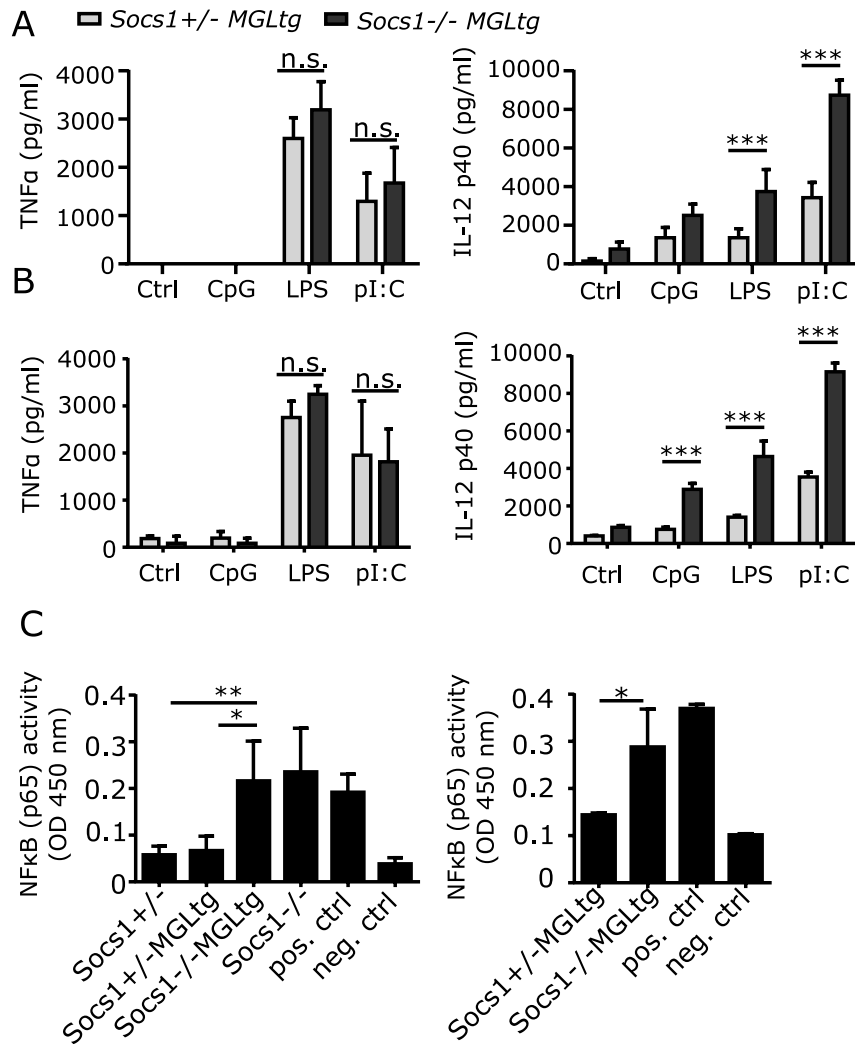
Figure 14.: Sustained NFκB signaling in Socs1$^{-/-}$MGL^{tg} mice

CD11c$^+$ cells were isolated from (A) lung homogenate or (B) spleen homogenate and stimulated with CpG-DNA (1 μM), LPS (100 ng/ml), and pI:C (10 μg/ml) for 24 h. TNFα and IL-12p40 protein levels were measured by ELISA (n = 3–5, mean +SD, two-way ANOVA including Bonferroni post-test). (C) NFκB p65 activity was examined using the Trans^{AM} DNA binding ELISA to specifically examine p65 activity in lung homogenate (left) or pmTECs (right). Raji nuclear extract was used as a positive control and a wildtype oligonucleotide was used as a competitor (negative control). (n = 4 for lung homogenate and n = 3 for pmTECs, mean +SD, One-way ANOVA including Bonferroni post test).

of CD4$^+$ T cells isolated from the spleens of Socs1$^{-/-}$MGL^{tg} or Socs1$^{+/-}$MGL^{tg} mice. On day 3, 75 ± 14% of the cells isolated from Socs1$^{+/-}$MGL^{tg} mice were proliferating and 62 ± 19% of the cells isolated from Socs1$^{-/-}$MGL^{tg} mice as compared to 10-20% of the cells that were incubated without CD3/CD28 coated beads (control) (Fig. 15C). For cell cycle analysis, CD4$^+$ T cells were isolated from spleens and stained with propidium iodide. Cell cycle analysis revealed a reduced percentage of CD4$^+$ T cells from Socs1$^{-/-}$MGL^{tg} mice in G1 phase of the cell cycle. In contrast an increased percentage of cells in the S-phase of the cell cycle was observed for CD4$^+$ T cells from Socs1$^{-/-}$MGL^{tg} mice as compared to CD4$^+$ T cells from Socs1$^{+/-}$MGL^{tg} mice (Fig. 15D), suggesting an altered cell cycle in Socs1$^{-/-}$MGL^{tg} mice. Although CD4$^+$ T cells from Socs1$^{-/-}$MGL^{tg} mice showed no difference regarding proliferation in the *in vitro* assay, data suggests alteration of the cell cycle in Socs1$^{-/-}$MGL^{tg} mice that might arise from the lack of p53 activation due to missing functional SOCS1 in the cell nucleus.
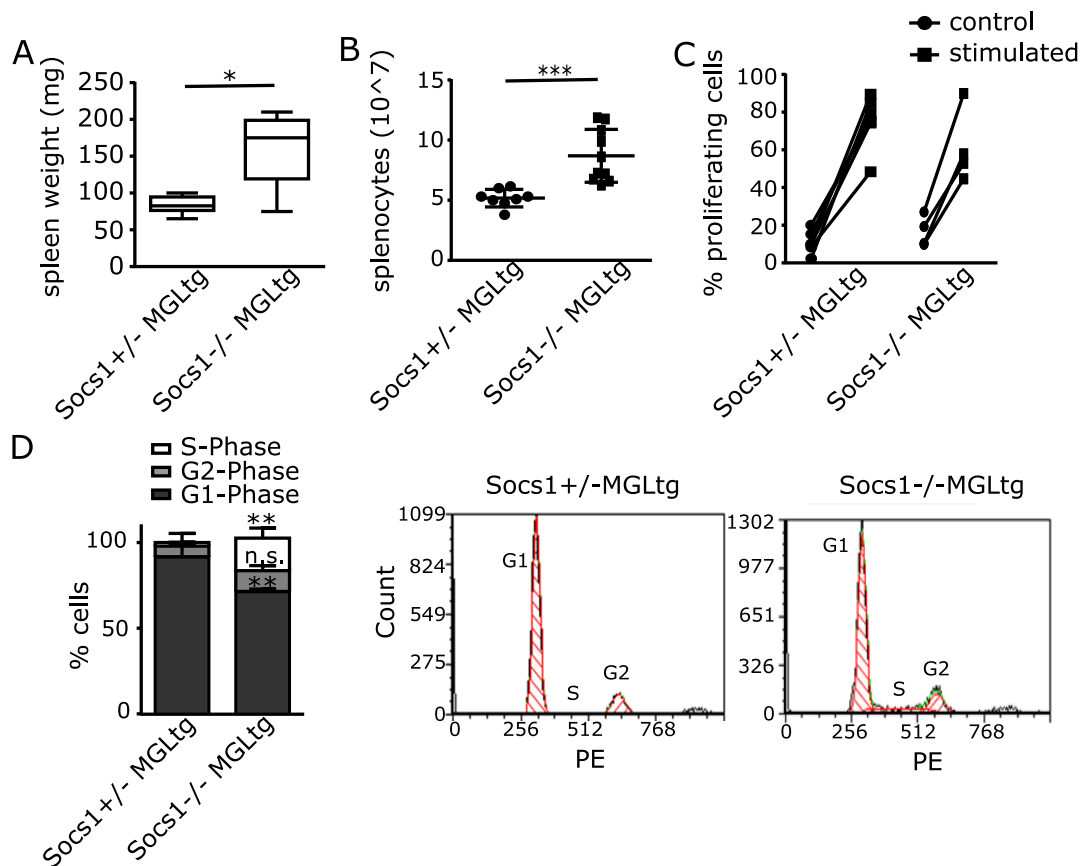
Figure 15.: Altered cell cycle in Socs1$^{-/-}$MGL^{tg} mice.
(A) Spleen weight and (B) number of splenocytes were recorded for n = 7-10 8-week-old mice (mean +SD, Wilcoxon matched pairs test) (C) CD4$^+$ T cells isolated from spleens were stained with CFSE (5 mM), stimulated with CD3/CD28 coated beads and analyzed for proliferation on day 3 using flow cytometry. Unstimulated cells (no beads added) were used as a control (n = 4-6, mean +SD, two-way ANOVA including Bonferroni post-test). (D) For cell cycle analysis, CD4$^+$ T cells were isolated from spleens and stained with propidium iodide (50 μg/ml) for 30 min. Cell cycle analysis was done using flow cytometry identifying propidium iodide stained cells in the PE channel (right) and cells in G1, S or G2 phase were identified using the DeNOVO Software (FCS Express Demo version 5) (left) (n = 3, mean +SD, two-way ANOVA including Bonferroni post-test)

5.5. Socs1$^{-/-}$MGL^{tg} mice survive the early lethal phenotype as compared to Socs1$^{-/-}$ mice due to functional regulation of IFNγ signaling

No alteration in survival was observed for Socs1$^{-/-}$MGL^{tg} mice. Fig. 16A shows the survival for Socs1$^{-/-}$MGL^{tg} mice up to 60 days unlike Socs1$^{-/-}$ mice that show stunted growth (Fig. 16C) and die within 2-3 weeks due to excessive immune signaling and fatty degeneration of the liver [173, 193, 256]. In a small cohort (n= 4) survival of Socs1$^{-/-}$MGL^{tg} mice was recorded up to 38 weeks (data not shown), showing no difference to Socs1$^{+/-}$MGL^{tg} littermates. Both female and male Socs1$^{-/-}$MGL^{tg} mice have reduced body weight as compared to Socs1$^{+/-}$MGL^{tg} littermates (Fig. 16B) with a mean of 18 ± 2.5 g and 23.5 ± 1.5 g as compared to the controls with a mean of 22 ± 1.7 g and 27 ± 1.8 g for female and male 8-week-old mice, respectively. However the observed reduction in body-weight of Socs1$^{-/-}$MGL^{tg} mice was not as severe as in Socs1$^{-/-}$ mice (Fig. 16C).
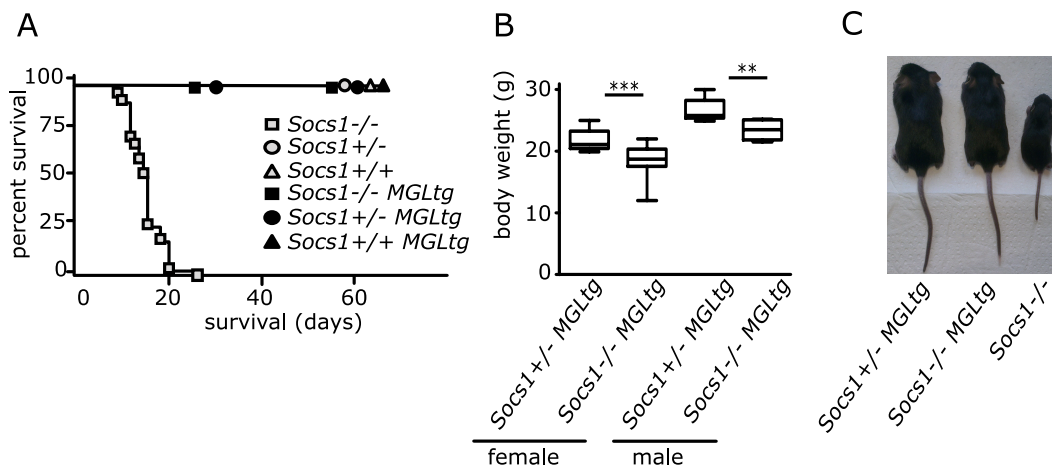
Figure 16.: Socs1$^{-/-}$ MGL^{tg} mice survive the early lethal phenotype of Socs1$^{-/-}$ mice.
(A) After mating Socs1$^{+/-}$ to Socs1$^{+/-}$MGL^{tg} mice, survival of offsprings was recorded to the age of 60 days (n = 28–92 mice per genotype). (B) Mouse body weight analysis (n = 10–15 8-week-old mice per gender and genotype, mean +SD, Wilcoxon matched pairs test). (C) Image showing 2-week-old Socs1$^{+/-}$MGL^{tg}, Socs1$^{-/-}$MGL^{tg} and Socs1$^{-/-}$ mice (left to right).

5.5.1. Functional regulation of IFNγ signaling in Socs1$^{-/-}$MGL^{tg} mice

Socs1$^{-/-}$MGL^{tg} mice are surviving the early lethal phenotype as compared to Socs1$^{-/-}$ mice. As it is known that Socs1$^{-/-}$ can be rescued by the administration of anti-IFNγ antibodies in the neonatal period or by using Socs1$^{-/-}$ IFN$\gamma^{-/-}$ mice [6, 23], the hypothesis was raised that canonical IFNγ signaling is not altered in Socs1$^{-/-}$MGL^{tg} mice. To prove this hypothesis, tyrosine phosphorylation of STAT1 was examined in BMMs upon treatment with IFNγ for 1 to 6 h. IFNγ signaling was prolonged in mice completely lacking SOCS1 as shown by the sustained levels of pY-STAT1 in Socs1$^{-/-}$ mice (60 ± 20% pY-STAT1). In contrast, there was a decline in pY-STAT1 levels for both Socs1$^{+/-}$MGL^{tg} mice (to 18 ± 7%) and Socs1$^{-/-}$MGL^{tg} mice (to 25 ± 20%) already 4 h after IFNγ stimulation (Fig. 17A,B). To confirm this result, pY-STAT1 levels were analyzed using flow cytometry. Whereas the maximal number of pY-STAT1 positive BMMs upon IFNγ treatment (22.2 - 29.1%) was reached for Socs1$^{+/+}$, Socs1$^{+/-}$, Socs1$^{+/-}$MGL^{tg} and Socs1$^{-/-}$MGL^{tg} mice after 20 min, this number was steadily increasing for Socs1$^{-/-}$ mice to 60.9 ± 15% upon 1 h of stimulation (Fig. 17B). Again, no differences could be found regarding tyrosine phosphorylation of STAT1 comparing Socs1$^{-/-}$MGL^{tg} and Socs1$^{+/-}$MGL^{tg} mice. Of

note, no gene dosage effects were detected, since levels of pY-STAT1 were comparable between Socs1$^{+/+}$ and Socs1$^{+/-}$ mice. Looking at expression levels of canonical IFNγ target genes, both *iNOS* and *Irf9* were induced upon stimulation with IFNγ. There was no difference between Socs1$^{+/-}$MGL^{tg} and Socs1$^{-/-}$MGL^{tg} mice regarding the expression of *iNOS* (relative expression after 4 h of IFNγ of 0.014 $\pm$ 0.01) or *Irf9* (relative expression after 4 h of IFNγ of 0.24 $\pm$ 0.4 for Socs1$^{+/-}$MGL^{tg} and 0.2 $\pm$ 0.2 for Socs1$^{-/-}$MGL^{tg} mice). For *Icam-1*, minor differences were observed at 6 h after stimulation with a relative expression of 0.15 $\pm$ 0.1 for Socs1$^{+/-}$MGL^{tg} and 0.67 $\pm$ 1.1 for Socs1$^{-/-}$MGL^{tg} mice (Fig. 17C).
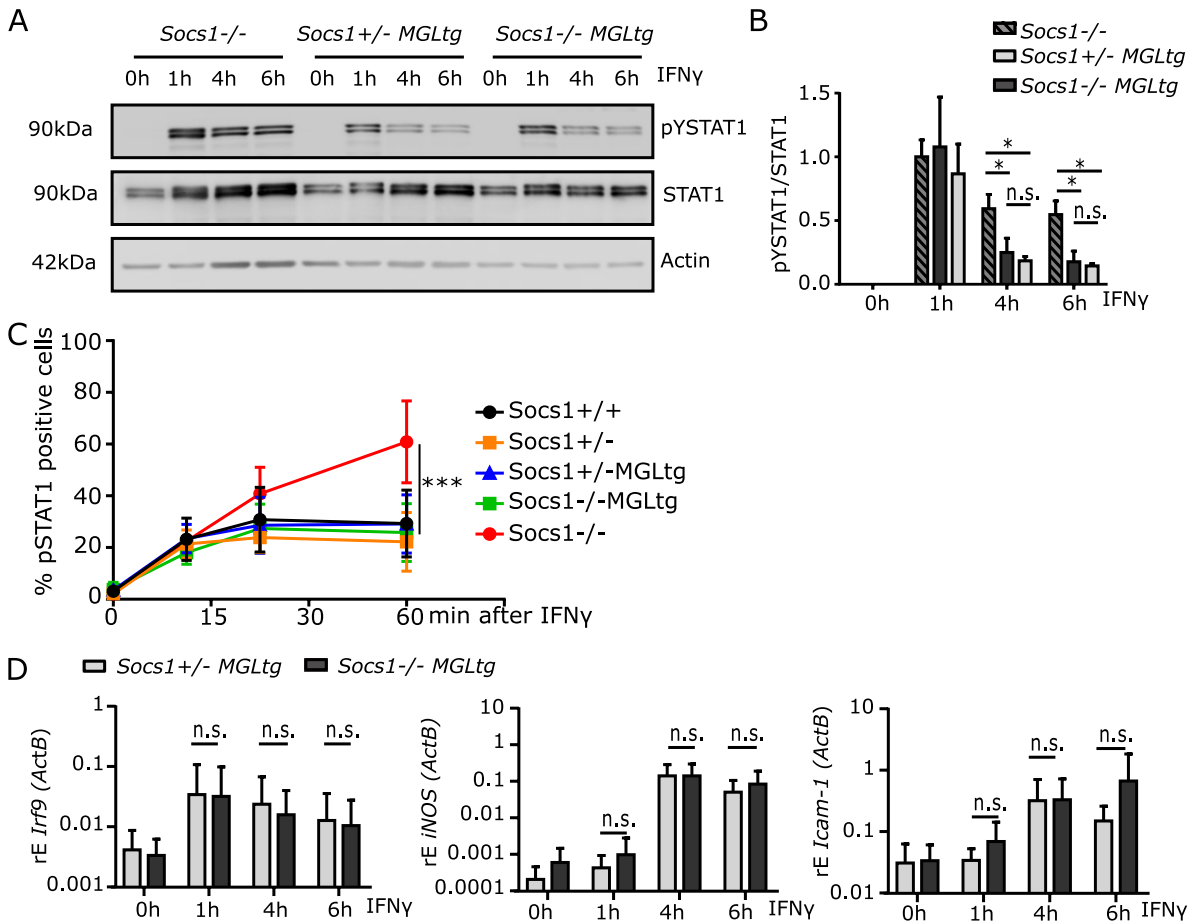
Figure 17.: IFNγ signaling is unaltered in Socs1$^{-/-}$MGL^{tg} mice.
(A) Western blot analysis of tyrosine phosphorylated STAT1 (Tyr701). STAT1 and β-Actin were used as loading controls. Protein extracts were prepared from BMMs of Socs1$^{-/-}$, Socs1$^{+/-}$MGL^{tg} and Socs1$^{-/-}$MGL^{tg} mice that were treated with IFNγ (50 ng/ml) as indicated. Quantification using ImageJ is shown in (B) (n = 4, +SD, two-way ANOVA including Bonferroni post-test). (C) Tyrosine phosphorylated STAT1 (Tyr701) was examined using flow cytometry. BMMs were stimulated with IFNγ for the indicated time and pY-STAT1 levels were examined using AlexaFluor 647 Anti-STAT1 (pY701). (n = 3, mean +SD, two-way ANOVA including Bonferroni post-test) (D) mRNA expression of interferon target genes *iNOS*, *Irf9*, and *Icam-1* are shown normalized to *Actin (ActB)* expression in BMMs treated with IFNγ (50 ng/ml) for 1–6 h (n = 4). Mean +SD is presented for each group and significance was assessed using two-way ANOVA including Bonferroni post-test.

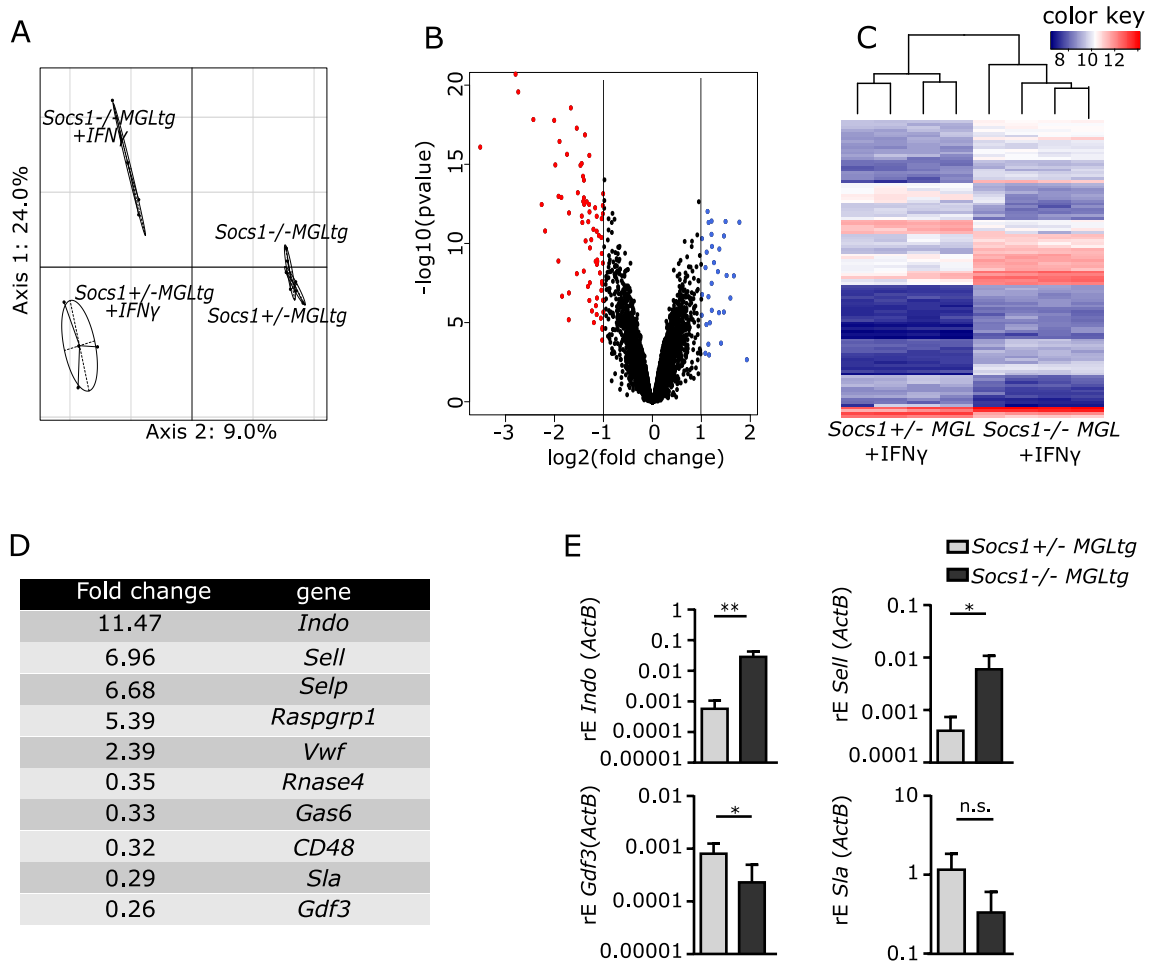### 5.5.2. Differential regulation of a subset on non-canonical IFNγ dependent genes in Socs1⁻ᐟ⁻MGLᵗᵍ mice

To confirm the hypothesis that canonical IFNγ signaling is not altered in Socs1$^{-/-}$MGL^{tg} mice, whole-genome expression analysis was performed. Therefore, BMMs were stimulated with IFNγ for 24 h, RNA was extracted and subjected to whole-genome expression analysis. Analysis was done using R looking at the significantly (p$\leq$ 0.05) and differentially (log2 change $\leq$-1 or $\geq$1) regulated genes. As a result, 1097 genes were differentially regulated between untreated and IFNγ stimulated cells, but only 86 genes were differentially regulated between Socs1$^{-/-}$MGL^{tg} and Socs1$^{+/-}$MGL^{tg} mice upon stimulation with IFNγ for 24 h (Fig. 18A-C). Principal component analysis showed that the controls (unstimulated) cluster together. Upon stimulation with IFNγ, clusters for Socs1$^{-/-}$MGL^{tg} and Socs1$^{+/-}$MGL^{tg} mice were separate suggesting differential gene regulation (Fig. 18A). According to the heat-map, most differentially regulated genes were induced rather than repressed in Socs1$^{-/-}$MGL^{tg} mice. In Fig. 18D, the top 10 differentially regulated induced and repressed genes were displayed including the genes induced in Socs1$^{-/-}$MGL^{tg} mice such as Indoleamine 2,3-Dioxygenase 1 (*Indo*, 11.47 fold) and SelectinL (*Sell*, 6.69 fold) as well as the genes repressed in Socs1$^{-/-}$MGL^{tg} mice such as Src-Like-Adaptor (*Sla*, 0.29 fold) and Growth Differentiation Factor 3 (*Gdf3*, 0.26 fold). Those genes were confirmed by qPCR to be differentially regulated in Socs1$^{-/-}$MGL^{tg} mice (Fig. 18E). As canonical IFNγ target genes were not differentially regulated in Socs1$^{-/-}$MGL^{tg} mice, the hypothesis was raised that IFNγ signaling is not altered. To confirm this hypothesis, pathway annotation was performed using the 86 differentially regulated genes (Table 3). Instead of IFNγ signaling pathway, a significant number of differentially regulated genes was annotated to TLR and TNF signaling pathways. For the TLR signaling pathway, 3 genes addressed to the signaling pathway are induced (*CD40, Cxcl10, Jun*) and 5 are repressed (*Ccl3, Ccl4, Ccl5, Tlr7, Tlr8*) in Socs1$^{-/-}$MGL^{tg} mice. For the TNF signaling pathway, 5 genes addressed to the signaling pathway were induced (*Socs3, Fas, Tnfaip3, Cxcl10, Jun*), whereas only 1 was repressed (*Ccl5*) in Socs1$^{-/-}$MGL^{tg} mice, arguing for a general induction of the pathway. Next, transcription factor binding sites (TFBS) were analyzed (Table 2). As a result, the transcription factors CTCF, IRF2 and NFκB were overrepresented among the differentially regulated genes with 21, 8 and 56 genes, respectively. STAT1 as classical transcription factor for IFNγ signaling was not overrepresented among the differentially regulated genes. The hypothesis that Socs1ΔNLS is still able to regulate cytoplasmic signaling pathways and that canonical IFNγ signaling is not altered in Socs1$^{-/-}$MGL^{tg} mice could be confirmed, since there were no differences regarding STAT1 phosphorylation or the expression of canonical IFNγ target genes *iNOS* or *Irf9*. In addition, whole genome expression analysis revealed only a small subset of genes to be differentially regulated in Socs1$^{-/-}$MGL^{tg} mice, but no canonical IFNγ target genes, suggesting that Socs1ΔNLS was still able to regulate cytoplasmic signaling pathways and that canonical IFNγ signaling was not altered in Socs1$^{-/-}$MGL^{tg} mice.

Table 2.: oPOSSUM analysis of overrepresented transcription factor binding sites.

Differentially expressed genes in Socs1$^{-/-}$MGL^{tg} mice upon IFNγ stimulation showing a log2-fold change ($\leq$-1 or $\geq$1) and p$\leq$ 0.05 were uploaded to identify overrepresented transcription factor binding sites among those genes. BG = background

TFBS	Input/ BG	class	family	z-score	Fischer score
CTCF	21/86	Zinc coordinating	$\beta\beta\alpha$ zinc finger	14.88	5.01
IRF2	8/86	Winged Helix-Turn-helix	IRF	14.343	4.42
NFκB	56/86	Ig fold	Rel	12.24	2.28

Figure 18.: Differential gene regulation of a subset of IFNγ dependent genes in Socs1^{-/-} MGL[tg] mice. BMMs were stimulated with IFNγ (50 ng/ml) for 24 h, RNA was extracted and subjected to whole-genome expression analysis (n = 4) (A) Principal component analysis (PCA). The two principal components and their fraction of the overall variability of the data (%) are shown on the x-axis and the y-axis. Clusters of experiments are circled (95% confidence interval ellipse) and annotated as ctrl for untreated samples and +IFNγ for IFNγ-stimulated samples. (B) Volcano plot showing the genes that were differentially expressed between BMMs of Socs1[+/-]MGL[tg] and Socs1^{-/-}MGL[tg] mice. Only significant values (p≤ 0.05) were considered showing a log2 fold change ≤-1 (red points) or ≥1 (blue points). (C) Heat map visualizing hierarchical clustering analysis based on the expression levels of genes that are differentially expressed between BMMs of Socs1[+/-]MGL[tg] and Socs1^{-/-}MGL[tg] mice. Red indicates higher expression and blue indicates lower expression of the corresponding gene in Socs1^{-/-}MGL[tg] mice. (D) 10 most prominently up- and downregulated genes according to their fold change. (E) Quantitative RT-PCR was performed using RNA from BMMs stimulated with IFNγ (n = 3, mean +SD, Student's t-test).

Table 3.: Pathway annotation using the protein analysis through evolutionary relationships (PANTHER) classification system.
Differentially expressed genes in Socs1$^{-/-}$MGL^{tg} mice upon IFNγ stimulation showing a log2-fold change ($\leq$-1 or $\geq$1) and p$\leq$ 0.05 were analyzed to classify and identify gene functions. BG = background

Pathway ID	Input/ BG	Induced genes	Repressed genes	p-value
TLR signaling pathway	8/101	CD40 Cxcl10 Jun	Ccl3 Ccl4 Ccl5 Tlr7 Tlr8	0.00129
TNF signaling pathway	6/109	Socs3, Fas Tnfaip3 Cxcl10 Jun	Ccl5	0.056

5.5.3. Functional differentiation of bone-marrow derived macrophages (BMMs) of Socs1$^{-/-}$MGL^{tg} mice

To control that BMMs used in this study were functionally differentiated, expression of classical macrophage markers on the surface was examined using flow cytometry. Therefore, BMMs from Socs1$^{-/-}$MGL^{tg} and Socs1$^{+/-}$MGL^{tg} mice were stimulated with IFNγ or LPS and stained for macrophage markers such as F4/80, CD86, CD11b and MHC class II. In summary, all tested surface proteins were expressed by the majority of the BMMs and in a similar ratio in Socs1$^{-/-}$MGL^{tg} mice as compared to the controls (Fig. 19A-D). Stimulation of BMMs using IFNγ or LPS led to induction of SOCS1 as shown by increased percentage of GFP^{+} cells due to expression of the BAC (30.6 $\pm$ 0.4% and 30.0 $\pm$ 0.3% in Socs1$^{+/-}$MGL^{tg} and Socs1$^{-/-}$MGL^{tg} mice) (Fig. 19E). In addition, macrophage capacity of phagocytosis was examined. Therefore, fluorescently labelled Latex beads were added to BMMs for 1 h at 37°C and uptake was measured using flow cytometry. After 1 h, 63.9 $\pm$ 3.7% of BMMs from Socs1$^{+/-}$MGL^{tg} mice and 68.4 $\pm$ 1% of the BMMs from Socs1$^{-/-}$MGL^{tg} mice took up Latex beads, suggesting functional differentiation of BMMs of both Socs1$^{+/-}$MGL^{tg} and Socs1$^{-/-}$MGL^{tg} mice.
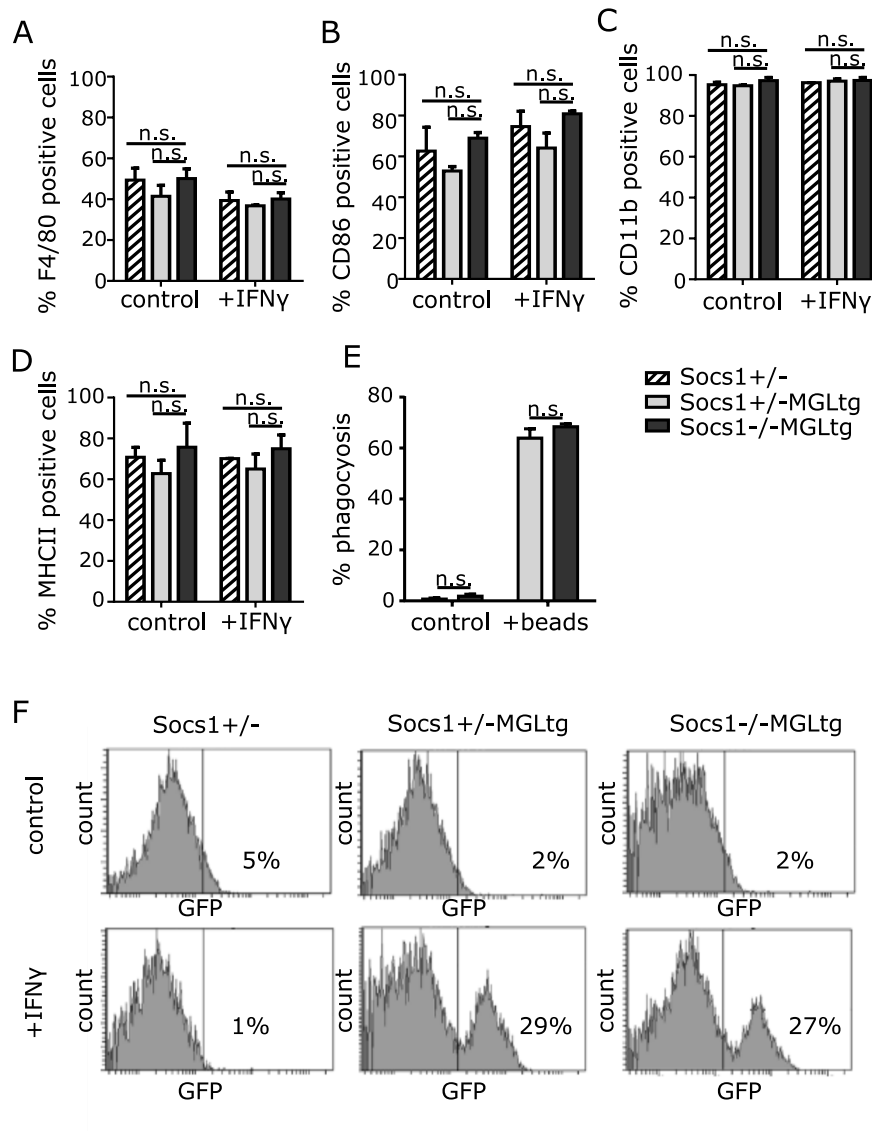
Figure 19.: Socs1$^{-/-}$MGL^{tg} mice show normal macrophage function.
BMMs were differentiated and stimulated with IFNγ (50 ng/ml) for 24 h. Expression of (A) F4/80, (B) CD86, (C) CD11b and (D) MHC class II was analyzed by flow cytometry using corresponding antibodies. (E) Phagocytosis was determined by uptake of Latex-beads (amine-modified polystyrene beads, fluorescent yellow-green) by BMMs within 1 h at 37°C (n = 2, mean +SD, two-way ANOVA including Bonferroni post-test). (F) BMMs were treated as before. Expression of the BAC was visualized by detection of GFP positive cells using flow cytometry.

5.6. Phenotypical characterization of Socs1$^{-/-}$MGL^{tg} mice

Since the cytoplasmic function of SOCS1ΔNLS seemed to be still functional in Socs1$^{-/-}$MGL^{tg} mice, it remained to be clarified whether those mice show deficiencies due to the lack of SOCS1 in the cell nucleus except for the slightly reduced body weight (Fig. 16B). Therefore, blood parameters such as white blood cell count, red blood cell count, number of granulocytes, monocytes, lymphocytes, platelets and the amount of hemoglobin were analyzed in whole blood using the Coulter Ac-T Hematology Analyzer. As a result, an increase in the number of monocytes (0.8 ± 0.2 x10^3 cells/μl in Socs1$^{+/-}$MGL^{tg} versus 1.6 ± 0.3 x10^3 cells/μl in Socs1$^{-/-}$MGL^{tg} mice) and a reduction in the number of platelets (1.2 ± 0.4 x10^6 cells/μl in Socs1$^{+/-}$MGL^{tg} versus 0.8 ± 0.3 x10^6 cells/μl in Socs1$^{-/-}$MGL^{tg} mice) was observed.
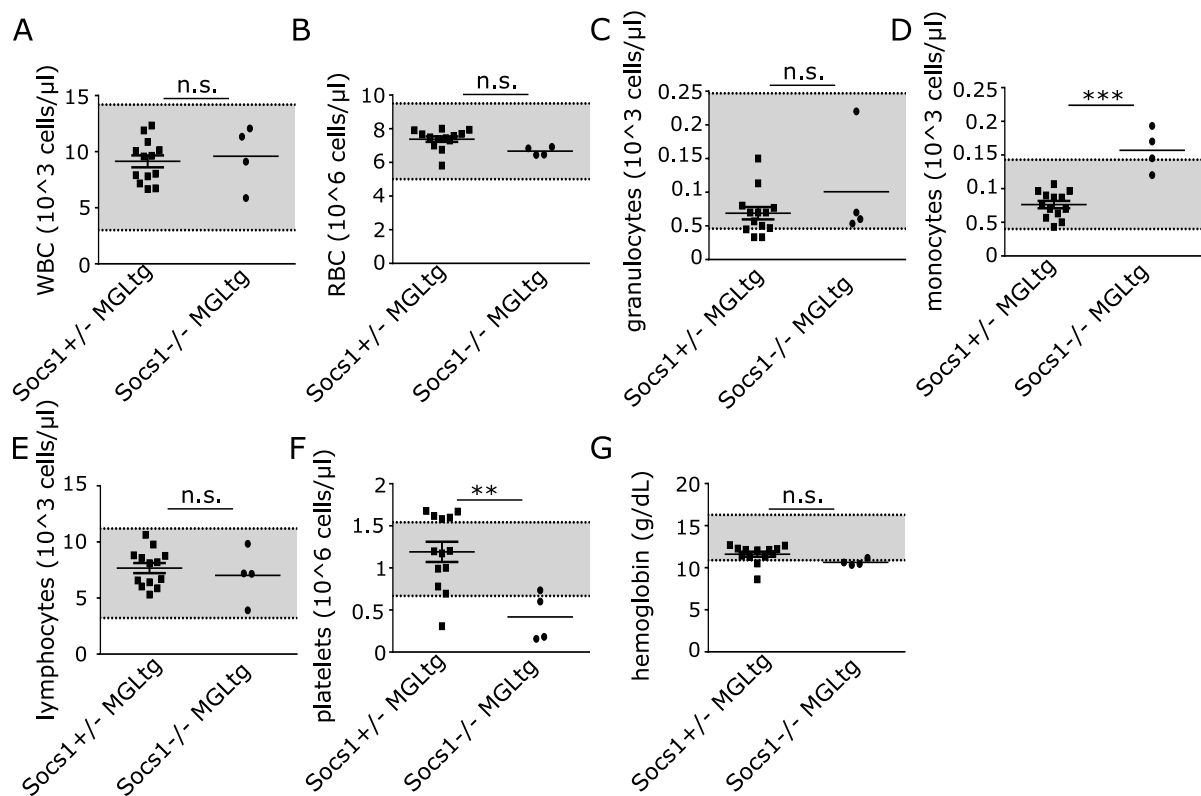
Figure 20.: Analysis of blood parameters in Socs1$^{-/-}$MGL^{tg} mice.
Numbers of (A) white blood cells (WBC), (B) red blood cells (RBC), (C) granulocytes, (D) monocytes, (E) lymphocytes, (F) platelets and (G) amount of hemoglobin was analysed from whole blood samples using the Coulter Ac-T Hematology Analyzer (n = 4-13, mean +SD, Wilcoxon matched pairs test). Grey areas indicate the physiological range (95%) according to Mouse Hematology of the C57BL/6 mouse (Charles River, www.criver.com/files/pdfs/rms/c57bl6/rm_rm_r_c57bl6_mouse_clinical_pathology_data.aspx).

In addition, histopathological analysis was performed by cutting 3 μm sections of various organs, H&E staining and evaluation by an independent pathologist in a blinded manner. This analysis revealed low-grade inflammation in lung and liver a significant number of Socs1$^{-/-}$MGL^{tg} mice (Table 4). However, low-grade inflammation in the liver could not be reproduced for the founders #29 or #45 and serum transaminase levels (ALT or AST) were in the physiological range (Fig. 21), arguing against a liver-specific phenotype in Socs1$^{-/-}$MGL^{tg} mice. Yet, 45% of Socs1$^{-/-}$MGL^{tg} mice showed infiltrations in lung tissue in all three founders. Therefore, the lung phenotype in Socs1$^{-/-}$MGL^{tg} mice was investigated in more detail.

Table 4.: Histological analysis revealing infiltrates in lungs of Socs1$^{-/-}$MGL^{tg} mice.
Organs were cut at 3 μm, H&E stained and histopathologically evaluated. n= 24 Socs1$^{-/-}$MGL^{tg} and 12
Socs1$^{+/-}$MGL^{tg} mice of the founder #53. * Fisher's exact test

Infiltrates in	Socs1$^{-/-}$MGL^{tg} (%)	Socs1$^{+/-}$MGL^{tg} (%)	p-value *	risk-factor
Lung	45	8	0.03	5.5
Liver	54	16	0.04	3.3
Esophagus	33	8	n.s.	4
Small intestine	29	0	n.s.	3
Heart	29	0	n.s.	2
Stomach	25	8	n.s.	/
Spleen	16	8	n.s.	/
Skin	12	0	n.s.	/
Kidney	8	0	n.s.	/
Muscle	4	0	n.s.	/
Brain	4	0	n.s.	/
Colon	4	0	n.s.	/
Pancreas	0	0	n.s.	/
Parotis	0	0	n.s.	/
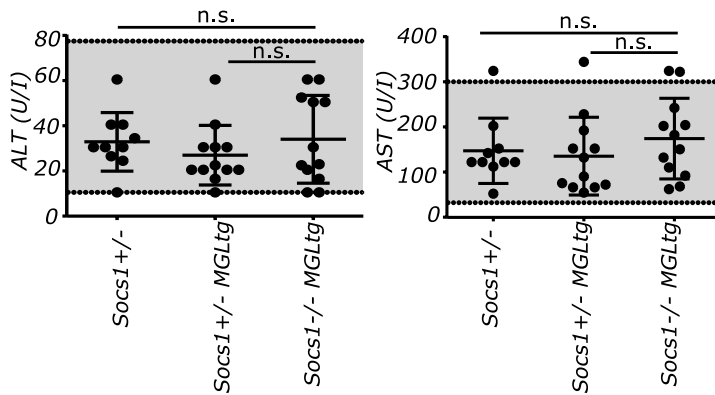
Figure 21.: Physiological ALT and AST levels in serum of Socs1$^{-/-}$MGL^{tg} mice.
Serum transaminase levels were determined at an age of 8-12 weeks in n = 10-12 mice (mean +SD, two-way ANOVA including Bonferroni post-test). Grey areas indicate the physiological range.

5.6.1. Socs1⁻ᐟ⁻MGLᵗᵍ mice spontaneously develop low-grade inflammation in the lung

Socs1$^{-/-}$MGL^{tg} mice showed infiltrates in the lungs of 45% of the analyzed mice (Fig. 22A) in all three founders. In addition, PAS staining was performed revealing a higher number of PAS positive cells in the lung of Socs1$^{-/-}$MGL^{tg} mice (Fig. 22B). To investigate the occurrence of the inflammatory aggregates observed in H&E stainings in more detail, lungs of 6 - 12 week-old Socs1$^{-/-}$MGL^{tg} mice and littermate controls were examined by micro-CT. Since previous histological analysis was performed by cutting the lung only once, irrespective which lung lobe, it was expected that micro-CT analysis gives a better overview about the frequency and location of inflammatory aggregates in Socs1$^{-/-}$MGL^{tg} mice. Optimal parameters for micro-CT scans were established first. For detection of infiltrates in inflated lungs, whole body scans were performed *post mortem* with 18 μm resolution (Fig. 22C). Afterwards, lungs were fixed using formalin and single lobes were embedded in paraffin. For detection of infiltrates in paraffin embedded lung lobes, a 9 μm scan with high averaging showed best results. Direct correlation of the CT scans from whole bodies with the scans from paraffin embedded lungs and correlative H&E stainigs was done (Fig. 22E-D). Widespread, diffuse infiltrates were found in 5 out of 6 mice, in left lobes, right upper lobes and right cardiac lobes of Socs1$^{-/-}$MGL^{tg} mice (see Table 5 and Fig. 22D). In addition, data revealed circular, local infiltrates mostly associated with smaller bronchi in 5 out of 6 Socs1$^{-/-}$MGL^{tg} mice (see Table 5, Fig. 22E). Importantly, infiltrates were distributed equally in the lung lobes and did not show a prevalence with regards to an individual lung lobe. Correlative histology confirmed the presence of infiltrates in the identified lung lobes. In littermate controls, only one infiltrate was observed in the right lower lobe, that could not be found in correlative H&E stainings. Data suggests, that more than the previously identified 45% of Socs1$^{-/-}$MGL^{tg} mice show low-grade inflammation as depicted by the presence of infiltrating immune cells.
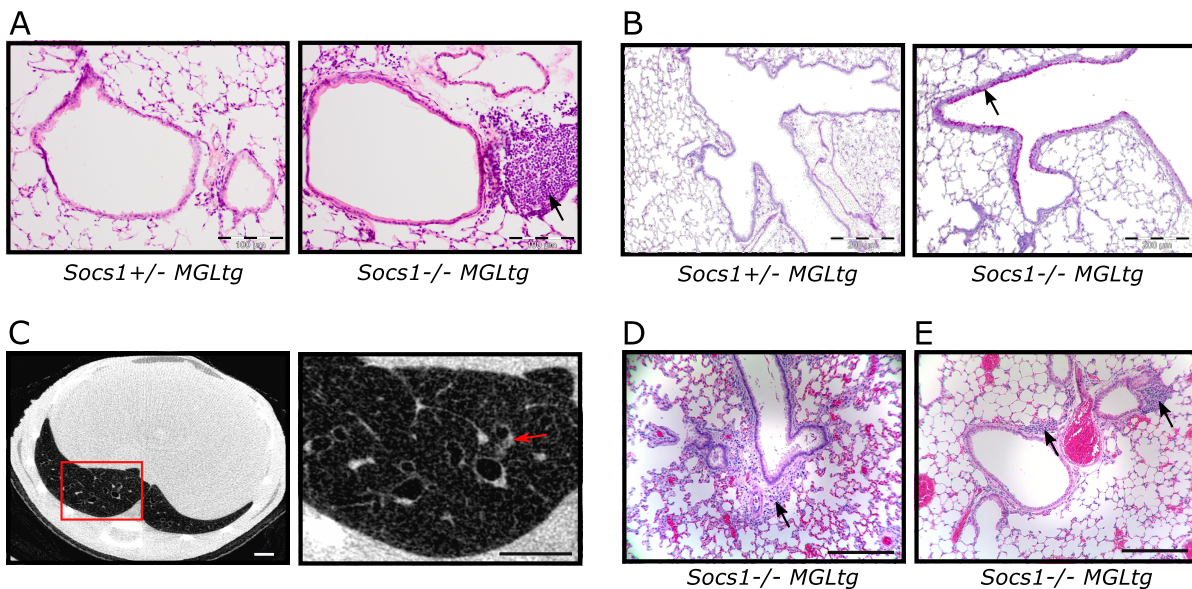
Figure 22.: Socs1$^{-/-}$MGL^{tg} mice develop low-grade inflammation in the lung.
(A) H&E-stained airway cross sections. Arrow highlighting infiltrating cells. Scale bar, 100 μm. (B) Periodic acid–Schiff (PAS) stained airway cross sections. Arrow highlights PAS positive cells. Scale bar, 200 μm. (C) Axial view of a micro-CT scan from an inflated Socs1$^{-/-}$MGL^{tg} lung post mortem showing infiltrating cells. (left) Overview. Scale bar, 2.5 mm. (right) Zoom. Arrow indicating infiltrating cells. Scale bar, 2.5 mm (D) H&E staining showing a diffuse, inflammatory aggregate identified by micro-CT in the right upper lobe of a Socs1$^{-/-}$MGL^{tg}. Arrow highlighting infiltrating cells. Scale bar, 100 μm. (E) H&E staining showing a circular, local inflammatory aggregate identified by micro-CT in the right upper lobe of a Socs1$^{-/-}$MGL^{tg}. Arrow highlighting infiltrating cells. Scale bar, 100 μm.

Table 5.: Evaluation of lung infiltrations by micro-CT.
18 μm micro-CT scans from 6 Socs1$^{-/-}$MGL^{tg} and 6 Socs1$^{+/-}$MGL^{tg} mice were evaluated for circular, local infiltrations and diffuse infiltrations in individual lung lobes by a radiologist in a blinded manner. LL = left lobe, RUL = right upper lobe, RML = right middle lobe, RLL = right lower lobe, RCL = right cardiac lobe and total = total lung.

	LL	RUL	RML	RLL	RCL	total	
Socs1$^{+/-}$MGL^{tg}	-	-	-	-	-	-	diffuse aggregate
Socs1$^{-/-}$MGL^{tg}	1/6	2/6	0/6	0/6	3/6	5/6	
Socs1$^{+/-}$MGL^{tg}	-	-	-	1/6	-	1/6	circular, local aggregate
Socs1$^{-/-}$MGL^{tg}	3/6	2/6	2/6	3/6	2/6	5/6	

5.6.2. Lack of nuclear SOCS1 leads to airway eosinophilia and a Th2-prone disease

To identify which cells were infiltrating the lung, BAL was performed. BAL cells were differentiated using May-Grünwald/ Giemsa staining, indicating elevated, however non-significant eosinophil influx in BAL (2.5 $\pm$ 2.4 x10^3 cells/ml BAL in Socs1$^{-/-}$MGL^{tg} mice as compared to 0 or 0.2 $\pm$ 0.1 x10^3 cells/ml BAL in Socs1$^{+/-}$ or Socs1$^{+/-}$MGL^{tg} mice) and to a minor extent elevated lymphocyte counts in BAL (2.5 $\pm$ 2.3 x10^3 cells/ml BAL in Socs1$^{-/-}$MGL^{tg} mice as compared to 0.35 $\pm$ 0.6 or 1.2 $\pm$ 0.4 x10^3 cells/ml BAL in Socs1$^{+/-}$ or Socs1$^{+/-}$MGL^{tg} mice) (Fig. 23A). In contrast, no differences in macrophage and neutrophil counts were observed. Socs1$^{-/-}$ MGL^{tg} mice showed 19.4 fold increased serum IgE levels (Fig. 23B), suggesting an allergic disease. Increased IgE and eosinophil influx suggest allergic predisposition and hint towards Th2 bias.
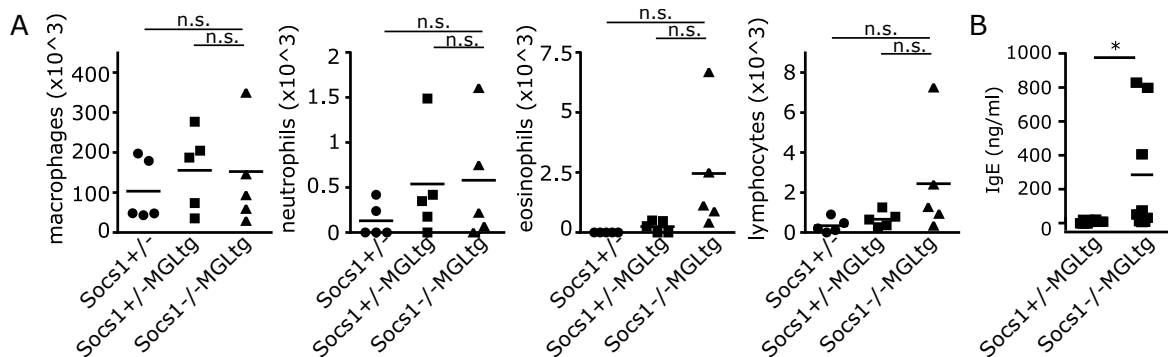
Figure 23.: Socs1$^{-/-}$MGL^{tg} mice deveopl allergic low-grade airway eosinophilia.
(A) Total numbers of macrophage, neutrophil, eosinophil and lymphocyte subpopulations in BAL are represented (n = 5, mean +SEM, two-way ANOVA including Bonferroni post-test). (B) IgE concentration in serum (n = 9, mean +SD, Wilcoxon matched pairs test).

Since SOCS1 has been shown to be important for T helper cell differentiation [194, 257, 51], it was analyzed whether Socs1$^{-/-}$MGL^{tg} mice have a T helper cell bias. Therefore, CD4$^+$ T cells were isolated from lung homogenates and transcription factors for T helper cell subsets were analyzed by qPCR. Socs1$^{-/-}$MGL^{tg} mice showed a 4.2 fold increase of Gata3$^+$ cells (indicating a higher number of Th2 cells) and a 1.2 fold, however non-significant, reduction in Rorc$^+$ cells (indicating a lower number of Th17 cells) (Fig. 24A). Using an *in vitro* differentiation assay, naïve CD4$^+$ T cells from Socs1$^{-/-}$MGL^{tg} mice tend to express more Gata3 as compared to CD4$^+$ T cells from Socs1$^{+/-}$MGL^{tg} mice, even under neutral conditions (T0, RPMI only) (Figure 24B). However, this difference was not significant. Increased mRNA expression of *IL-4, IL-5,* and *IL-13* in complete lung homogenates of Socs1$^{-/-}$MGL^{tg} mice compared to Socs1$^{+/-}$MGL^{tg} mice

confirmed this Th2 bias (Figure 24C). Notably, one population of Socs1$^{-/-}$MGL^{tg} mice was found with a strong expression of Gata3 and Th2 type cytokines in lung homogenates, and the second population showing a weaker Th2 bias, consistent with the fact that infiltrates were not observed in all Socs1$^{-/-}$MGL^{tg} mice.
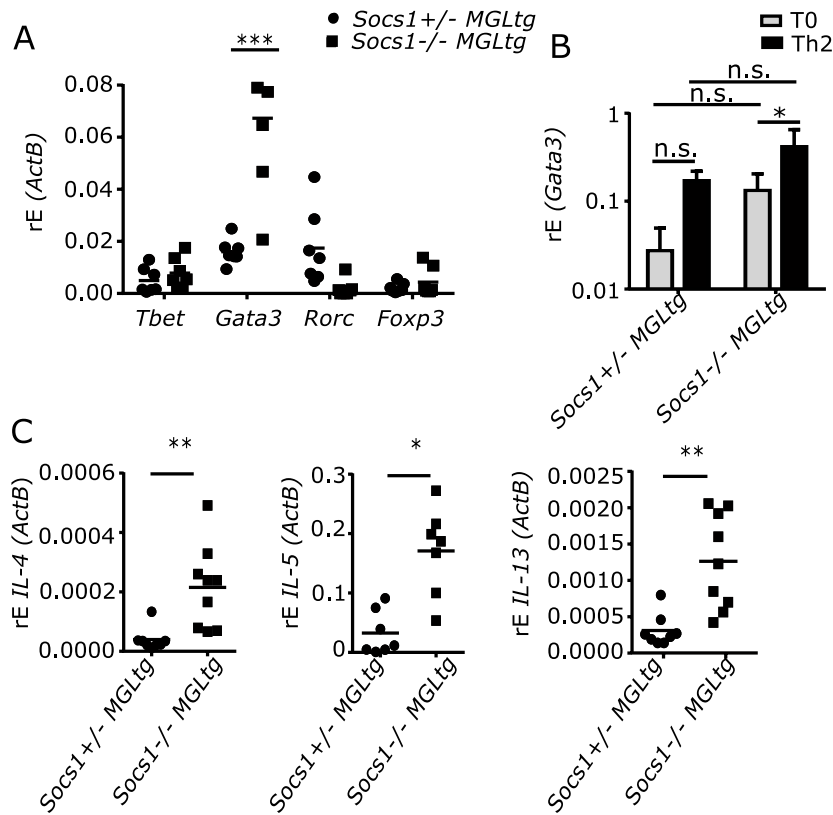
Figure 24.: Socs1$^{-/-}$MGL^{tg} mice show a Th2 bias.
(A) Expression levels of *Foxp3*, *Gata3*, *Tbet*, and *Rorc* in sorted CD4$^+$ T cells from the lung of both founder #53 and #29 (n = 7–11, mean +SD, two-way ANOVA including Bonferroni post-test). (B) Purified naïve CD4$^+$ T cells were differentiated under T0 conditions (RPMI only) or under Th2 conditions (100 ng/ml IL-4, 10 μg/ml anti-IFNγ, and 10 μg/ml anti-IL-12p40) for 3 days and restimulated using PMA and ionomycin. Expression of Gata3 was examined by qPCR (n = 4, mean +SD, two-way ANOVA including Bonferroni post-test). (C) Expression levels of *IL-4*, *IL-5*, and *IL-13* in total lung homogenates of both founder #53 and #29 (n = 7–11, mean +SD, Wilcoxon matched pairs test).

5.7. Physiological relevance of lung phenotype in Socs1$^{-/-}$MGL^{tg} mice

To analyze if the observed Th2 bias in Socs1$^{-/-}$MGL^{tg} mice is of physiological relevance, mice were challenged in a classical Th2 model using ovalbumin. In addition, Socs1$^{-/-}$MGL^{tg} mice were treated with IL-13 i.t. to provoke a Th2 response.

5.7.1. Increased airway eosinophilia in Socs1$^{-/-}$MGL^{tg} mice in an OVA experimental asthma model

To analyze if the observed Th2 bias in Socs1$^{-/-}$MGL^{tg} mice is of physiological relevance, mice were challenged in a classical Th2 model using ovalbumin. Socs1$^{-/-}$MGL^{tg} mice were subjected to a well-established protocol for the induction of experimental asthma [162, 239]. Upon OVA sensitization on days 1, 14 and 21, OVA aerosol challenge was performed on days 26, 27 and 28 and mice were analyzed on day 29 (Fig. 25A). Only minor induction upon OVA challenge and no difference with regards to nuclear SOCS1 was detectable in airway hyperresponsiveness (AHR) upon metacholine provocation (Fig. 25B). However, Socs1$^{-/-}$MGL^{tg} mice showed increased airway eosinophilia (21.5 ± 14 x10^4 cells/ml in BAL) as compared to Socs1$^{+/-}$MGL^{tg} control mice (7.3 ± 6 x10^4 cells/ml in BAL) (Fig. 25C). In contrast, macrophages and neutrophils in BAL were comparable between Socs1$^{-/-}$MGL^{tg} and Socs1$^{+/-}$MGL^{tg} mice.

In addition, IL-4 IL-5 and IL-13 levels were measured in BAL of Socs1$^{-/-}$MGL^{tg} mice upon OVA sensitization and challenge as compared to Socs1$^{+/-}$MGL^{tg} mice. Upon OVA challenge, levels of all measured Th2 cytokines increased in BAL. Increased IL-4 and IL-13 levels were detectable in BAL of Socs1$^{-/-}$MGL^{tg} mice as compared to the controls. IL-5 levels upon challenge were induced, yet showed no difference comparing Socs1$^{+/-}$MGL^{tg} and Socs1$^{-/-}$MGL^{tg} mice (Fig. 26). As a result, increased airway eosinophilia and Th2 cytokines were detected in Socs1$^{-/-}$MGL^{tg} in an classical Th2 model using ovalbumin.

5.7.2. Increased airway eosinophilia in Socs1$^{-/-}$MGL^{tg} mice upon IL-13 instillation

Since IL-13 has been shown to induce eosinophil recruitment to the lung, Socs1$^{-/-}$MGL^{tg} and control mice were treated with IL-13 intratracheally (i.t.). This model was used as a second Th2 model to trigger airway eosinophilia. Mice were treated with IL-13 i.t. on three consecutive days and analyzed on day 4. IL-13 treated mice of all genotypes developed neutrophilia in the lung (Fig. 27). Socs1$^{-/-}$MGL^{tg} mice additionally showed enhanced influx of lymphocytes (116.7 ± 37 x10^3 cells/ml BAL in Socs1$^{-/-}$MGL^{tg} mice as compared to 5.4 ± 1.4 x10^3 or 10.8 ± 3.9 x10^3 cells/ml BAL in the controls) and eosinophils (182.3 ± 79 x10^3 cells/ml BAL in Socs1$^{-/-}$MGL^{tg} mice as compared to 22.5 ± 4.4 x10^3 or 31.2 ± 7.9 x10^3 cells/ml BAL in the controls) (Fig. 27). No differences were observed for macrophages or neutrophils comparing IL-13 treated groups. In addition, Th2 cytokines were measured in complete lung homogenate. Socs1$^{-/-}$MGL^{tg} mice showed increased mRNA expression of *IL-4*, *IL-5* and *IL-13*, which was even more pronounced upon IL-13 treatment (Fig. 28A). H&E staining revealed increased infiltrations upon IL-13 treatment, most pronounced in Socs1$^{-/-}$MGL^{tg} mice (Fig. 27). As a result, both upon OVA sensitization and challenge and upon IL-13 treatment, Socs1$^{-/-}$MGL^{tg} mice responded with enhanced airway eosinophilia and an exaggerated Th2-prone lung disease.
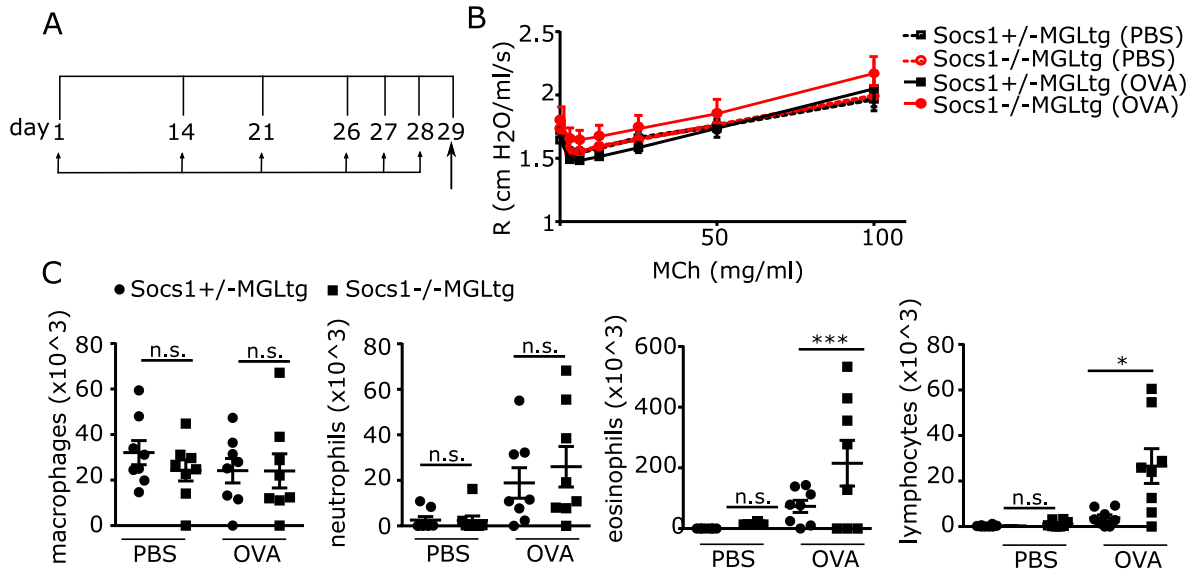
Figure 25.: Socs1^{-/-}MGL[tg] mice show increased airway eosinophilia in an experimental asthma model. (A) Mice were sensitized with OVA/Alum or PBS i.p. on days 1, 14, and 21, followed by a challenge with 1% OVA aerosol or PBS on days 26, 27, and 28. Analysis was performed on day 29 (n = 6-8) (B) Lung function was assessed in mice that were exposed to OVA or PBS. Airway mechanics were assessed after inhalation of nebulized saline and increasing concentrations of methacholine (MCh, 0 - 100 mg/ml) (mean +SEM, two-way ANOVA including Bonferroni post-test). (C) Total numbers macrophages, neutrophils, eosinophils and lymphocytes in BAL are represented (mean +SEM, two-way ANOVA including Bonferroni post-test).
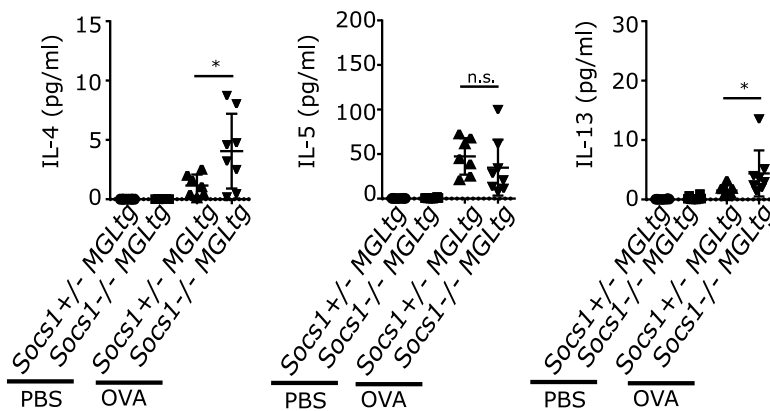
Figure 26.: Socs1^{-/-}MGL[tg] mice show enhanced expression of Th2 cytokines in an experimental asthma model. Levels of IL-4, IL-5, and IL-13 in BAL were measured by ELISA (mean +SD). Data was tested for significance using the two-way ANOVA including Bonferroni post-test.
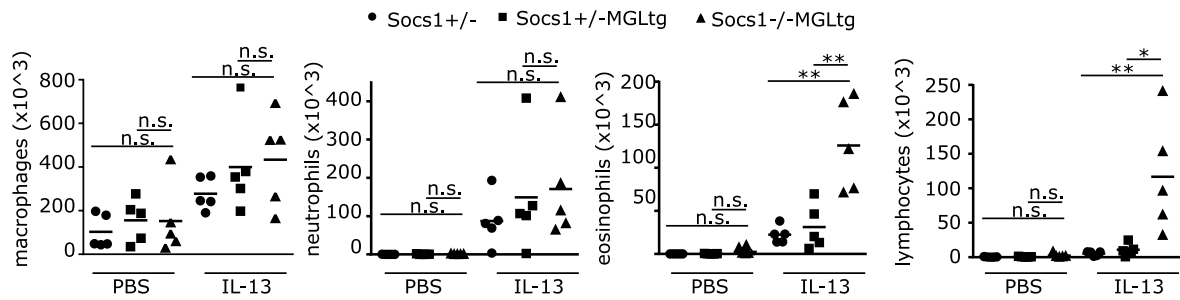
Figure 27.: Socs1$^{-/-}$MGL^{tg} mice show increased airway eosinophilia upon IL-13 instillation.
Mice were treated with IL-13 (5 μg in 20 μl PBS) intratracheally (i.t.) on day 1, 2 and 3. Analysis was performed on day 4 (n = 5). Total numbers of macrophage, neutrophil, eosinophil and lymphocyte subpopulations in BAL are represented (mean +SEM, two-way ANOVA including Bonferroni post-test.)
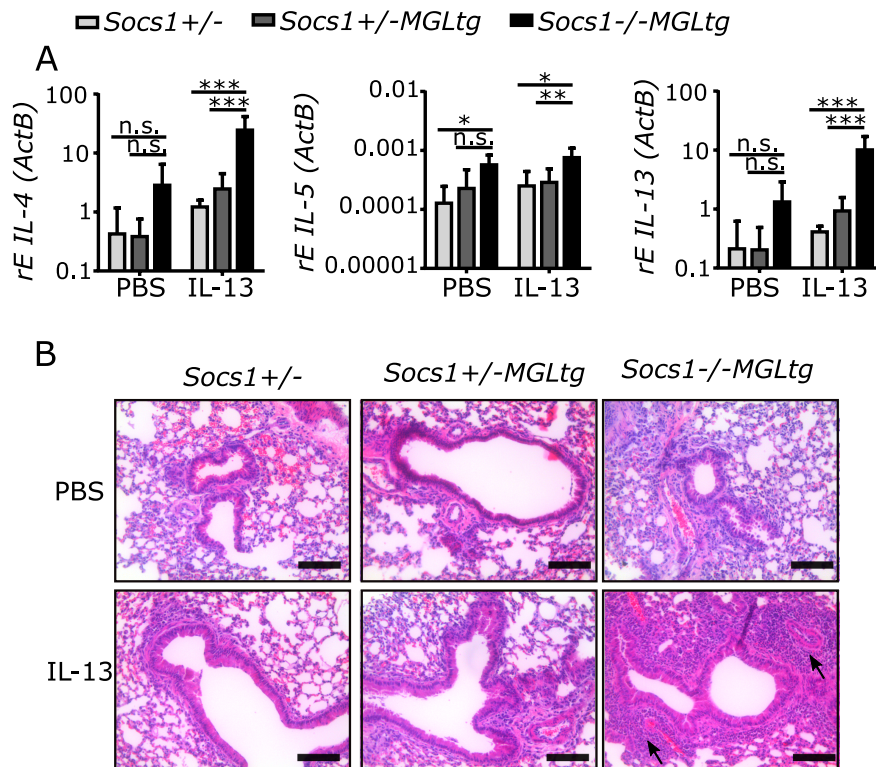
Figure 28.: Socs1$^{-/-}$MGL^{tg} mice show increased expression of Th2 cytokines upon IL-13 treatment.
Mice were treated with IL-13 (5 μg in 20 μl PBS) intratracheally (i.t.) on day 1, 2 and 3 as described previously. Analysis was performed on day 4 (n = 5) (A) mRNA levels of *IL-4*, *IL-5*, and *IL-13* in lung homogenate were measured by qPCR (mean +SD). (B) H&E-stained airway cross sections. Arrows highlight infiltrating cells. Scale bar, 200 μm. Data was tested for significance using the two-way ANOVA including Bonferroni post-test.

5.8. The role of SOCS1 in epithelial cells

To identify the cells responsible for the observed Th2 prone lung disease and airway eosinophilia in Socs1$^{-/-}$MGL^{tg} mice, bone-marrow transplantation was performed. In addition, pmTEC cultures were analyzed with respect to transepithelial resistance.

5.8.1. Radiation-resistant cells are responsible for the observed lung phenotype in Socs1$^{-/-}$MGL^{tg} mice

It was shown that Socs1$^{-/-}$ mice can be rescued on a Rag2 deficient background (Socs1$^{-/-}$Rag2$^{-/-}$ mice), arguing for an important role of SOCS1 in hematopoietic cells such as T cells. To identify the cells responsible for the observed Th2 prone lung disease and airway eosinophilia in Socs1$^{-/-}$MGL^{tg} mice, bone-marrow transplantation was performed. Using this approach, one can distinguish between radiation-sensitive cells (hematopoietic cells such as T cells) and radiation-resistant cells (structural cells such as epithelial cells). To distinguish between donor and recipient cells, bone-marrow from wildtype mice (CD45.1) was transplanted into lethally irradiated Socs1$^{-/-}$MGL^{tg} mice (CD45.2). The latter still contain radiation-resistant cells lacking nuclear SOCS1, but are replaced with wildtype hematopoietic cells. Vice versa, CD45.1 mice were lethally irradiated and replaced with bone-marrow from Socs1$^{-/-}$MGL^{tg} mice. In those mice, radiation-sensitive cells are lacking nuclear SOCS1, but the structural cells (e.g. epithelial cells) still do contain nuclear SOCS1 (see transplantation scheme Fig. 29A). As a control, bone-marrow from wildtype mice (CD45.1) was transplanted into lethally irradiated wildtype mice (CD45.2). As a result 75 - 90% of the blood cells were replaced by the donor at day 7 post transplantation (Fig. 29A). BAL was performed 6 weeks post transplantation, showing elevated number of eosinophils only in lethally irradiated Socs1$^{-/-}$MGL^{tg} replaced by donor bone-marrow from CD45.1 mice (44 $\pm$ 27 x10^3 cells/ml BAL as compared to 2.5 $\pm$ 0.7 x10^3 cells/ml BAL for lethally irradiated CD45.1 mice replaced by donor bone-marrow from Socs1$^{-/-}$MGL^{tg} mice) (Fig. 29B).

Although hematopoietic cells were replaced by wildtype donor cells in lethally irradiated Socs1$^{-/-}$MGL^{tg}, not only cytokines produced by epithelial cells, but also Th2 cytokines were elevated. Those mice showed a minor (non-significant) increase in mRNA expression of *IL-4*, *IL-5* and and a significant increase of *IL-13* (3.3 fold) (Fig. 30A). Increased expression of *IL-33* (2.7 fold) and *Ccl26* (4.7 fold) which are known to play a role in the recruitment of eosinophils [223] was observed (Fig. 30B). Elevated IL-6 protein levels of 15.8 $\pm$ 9.6 pg/ml were detectable in BAL of Socs1$^{-/-}$MGL^{tg} mice as compared to 0.1 $\pm$ 0.4 pg/ml for CD45.1 mice (Fig. 30C). Data suggest that radiation-resistant cells such as epithelial cells are responsible for the spontaneous low-grade inflammation in the lungs of Socs1$^{-/-}$MGL^{tg} mice. In addition, small infiltrates were found only in H&E stainings of lung sections from lethally irradiated Socs1$^{-/-}$MGL^{tg} mice (Fig. 30D) comparable to the ones characterized in Fig 22. As a conclusion, the lung phenotype of Socs1$^{-/-}$MGL^{tg} mice including elevated Th2 cytokines, infiltrates in lung tissue and airway eosinophilia was only observed in lethally irradiated Socs1$^{-/-}$MGL^{tg} mice replaced with wildtype bone-marrow. In contrast, transplantation of bone marrow from Socs1$^{-/-}$MGL^{tg} mice did not induce this phenotype. This suggests that nuclear SOCS1 plays a major role in structural cells such as epithelial cells.

5.8.2. Disrupted epithelial integrity in Socs1$^{-/-}$MGL^{tg} mice

Since bone-marrow transplantation revealed a critical role of radiation-resistant cells such as epithelial cells in Socs1$^{-/-}$MGL^{tg} mice, airway epithelium was analyzed in more detail. Cytokines produced by epithelial cells such as *IL-25*, *IL-33* and *Tslp* were measured in complete lung tissue. Those cytokines have been shown to contribute to control Th2 immunity [70, 121, 18, 141]. Interestingly, increased expression of *IL-25* (12.8 fold), *IL-33* (2.3 fold) and *Tslp* (5.7 fold) was observed in the lung homogenate of Socs1$^{-/-}$MGL^{tg} mice (Fig. 31). To analyze the airway
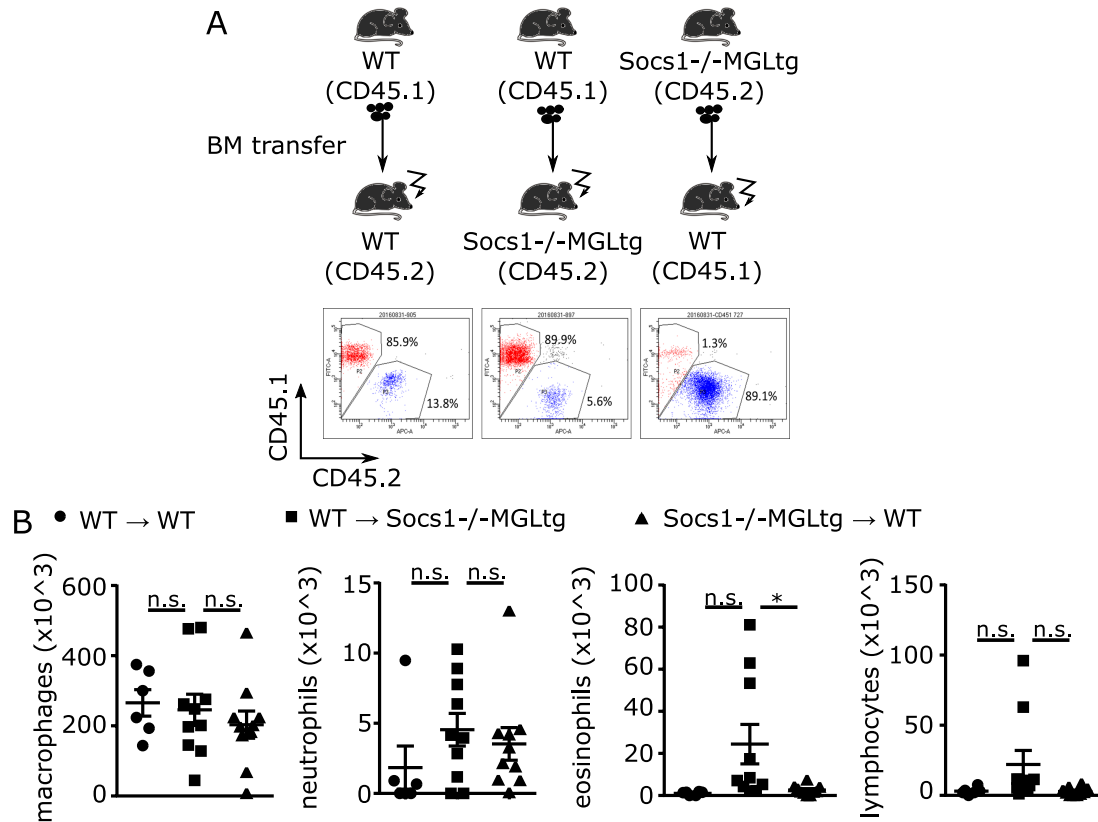
Figure 29.: The lung phenotype of Socs1$^{-/-}$MGL$^{\text{tg}}$ mice is dependent on radiation-resistant cells. (A) 8-10 week-old mice were lethally irradiated and transplanted with 1x10^7 total bone-marrow. Socs1$^{-/-}$MGL$^{\text{tg}}$ (CD45.2) mice were transplanted with bone-marrow from wildtype (CD45.1) mice and vice versa (n = 10). Wildtype (CD45.2) mice were transplanted with bone-marrow from wildtype (CD45.1) mice as a control. Flow cytometry showing the percentage of CD45.1 or CD45.2 positive cells in blood on day 7. (B) Total numbers of macrophages, neutrophils, leukocytes and eosinophils in BAL are represented (mean +SEM, two-way ANOVA including Bonferroni post-test).
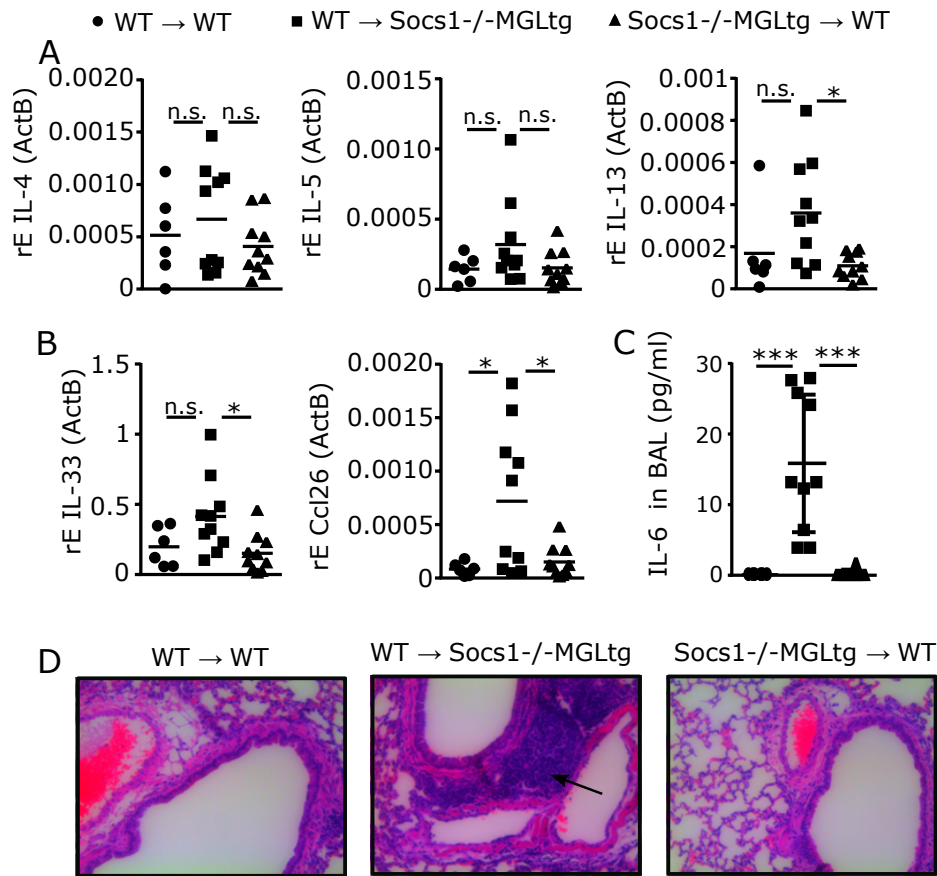
Figure 30.: Th2 bias of Socs1^{-/-}MGL[tg] mice is dependent on radiation-resistant cells.
Levels of (A) Th2 cytokines *IL-4*, *IL-5* and *IL-13*, (B) epithelial cell cytokines *IL-33* and *Ccl26* in total lung homogenate (mean +SD, two-way ANOVA including Bonferroni post-test). (C) IL-6 levels in BAL were determined by ELISA (mean +SD, two-way ANOVA including Bonferroni post-test). (D) H&E-stained airway cross sections. Arrow highlight infiltrating cells. Scale bar, 200 μm.
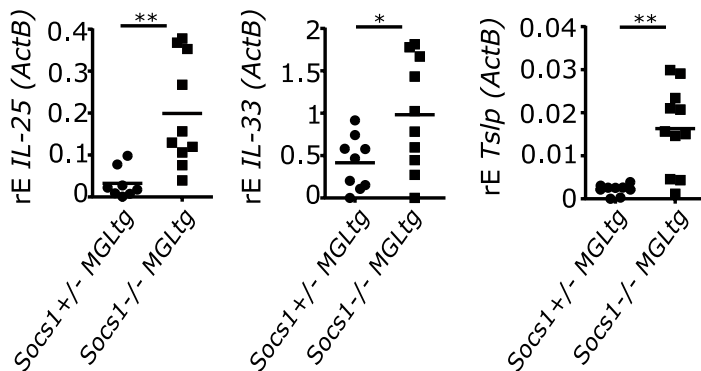
Figure 31.: Socs1^{-/-}MGL[tg] mice show enhanced expression of IL-25, IL-33 and Tslp.
IL-25, *IL-33*, and *Tslp* mRNA levels in total lung homogenates of both founders #53 and #29 (n= 9-11, mean +SD, Wilcoxon matched pairs test).

epithelium in more detail, tracheas were isolated and primary murine trachea epithelial cells (pmTECs) were differentiated in air-liquid interface (ALI) culture using transwells. Increased *IL-33* expression (4.3 fold as compared to Socs1$^{+/-}$MGL^{tg} mice and 3.2 fold as compared to Socs1$^{+/-}$ mice) could be verified in isolated pmTECs from Socs1$^{-/-}$MGL^{tg} mice. In addition, *Ccl26* expression was examined since it is known to play a role in the recruitment of eosinophils [223]. pmTECs from Socs1$^{-/-}$MGL^{tg} mice expressed significantly more *Ccl26* (3.8 fold as compared to Socs1$^{+/-}$MGL^{tg} mice and 2.2 fold as compared to Socs1$^{+/-}$ mice) (Fig. 32A). Expression of *IL-25* and *Tslp* were slightly elevated, however non-significant. Although pmTECs of control mice built tight barriers in the transwell, decreased transepithelial electrical resistance (TER) was observed in pmTECs from Socs1$^{-/-}$MGL^{tg} mice (357 ± 91 Ohm/cm$^{2)}$) as compared to cells from Socs1$^{+/-}$ (2475 ± 726 Ohm/cm$^{2)}$) and Socs1$^{+/-}$MGL^{tg} mice (2302 ± 522 Ohm/cm$^{2)}$) (Fig. 32B). To confirm the observation of a disrupted epithelial barrier *in vitro*, FITC-Dextran (4 kDa) was added to the inner well and diffusion into the outer well was determined after 2 h of incubation at 37°C. There was a significant reduction in the fluorescence in the inner well containing pmTECs from Socs1$^{-/-}$MGL^{tg} mice as compared to pmTECs from Socs1$^{+/-}$ or Socs1$^{+/-}$MGL^{tg} mice (Fig. 32C). Another *ex vivo* assay to determine disrupted barrier function is shown in Fig. 32D. Albumin was determined in BAL samples of Socs1$^{-/-}$MGL^{tg} and Socs1$^{+/-}$MGL^{tg} mice. If the epithelial barrier is intact, albumin in the blood cannot cross the barrier. If the epithelial barrier is disrupted, albumin can pass and is found in BAL. Indeed, Socs1$^{-/-}$MGL^{tg} mice showed elevated levels of albumin in BAL (180 ± 40 μg/ml as compared to 90 ± 25 μg albumin /ml BAL) (Fig. 32E), arguing for a disrupted epithelial cell barrier that could explain low-grade inflammation observed in the lungs of Socs1$^{-/-}$MGL^{tg} mice.

To investigate the mechanism of reduced epithelial cell barrier integrity, E-Cadherin expression and localization was analyzed. E-Cadherin is known to be a part of desmosomes and adherens junctions and therefore plays a major role in cell barrier function, especially in epithelial cells. Figure 33A shows staining of E-Cadherin in pmTECs of Socs1$^{+/-}$MGL^{tg} and Socs1$^{-/-}$MGL^{tg} mice. E-Cadherin is localized mainly at the cell surface and at the border between two cells. There was no obvious different localization of E-Cadherin with respect to the expression of nuclear SOCS1. Staining with Flash^{TM} Phalloidin was used to visualize F-Actin as part of the cytoskeleton. Again, no difference was detected between the two genotypes. To confirm E-Cadherin staining, immunohistochemistry (IHC) was performed on paraffin embedded lung sections. Positive staining was detected only in epithelial cells (Fig. 33B). E-Cadherin was detected mainly at the border between two neighboring epithelial cells and to a minor extend within the cell cytoplasm. IHC confirmed no different expression or localization of E-Cadherin with regards to expression of nuclear SOCS1. To investigate protein levels of E-Cadherin in pmTECs of Socs1$^{+/-}$MGL^{tg} and Socs1$^{-/-}$MGL^{tg} mice, Western Blot was performed. Lysates of three transwells were analyzed for expression of E-Cadherin and Histon3 as a loading control. No difference in protein amounts were detectable comparing pmTECs of Socs1$^{+/-}$MGL^{tg} and Socs1$^{-/-}$MGL^{tg} mice. Taken together, data suggest similar protein amounts and localization of E-Cadherin in epithelial cells of Socs1$^{-/-}$MGL^{tg} mice as compared to the controls. Therefore, the mechanism for reduced epithelial cell barrier integrity remains to be examined.
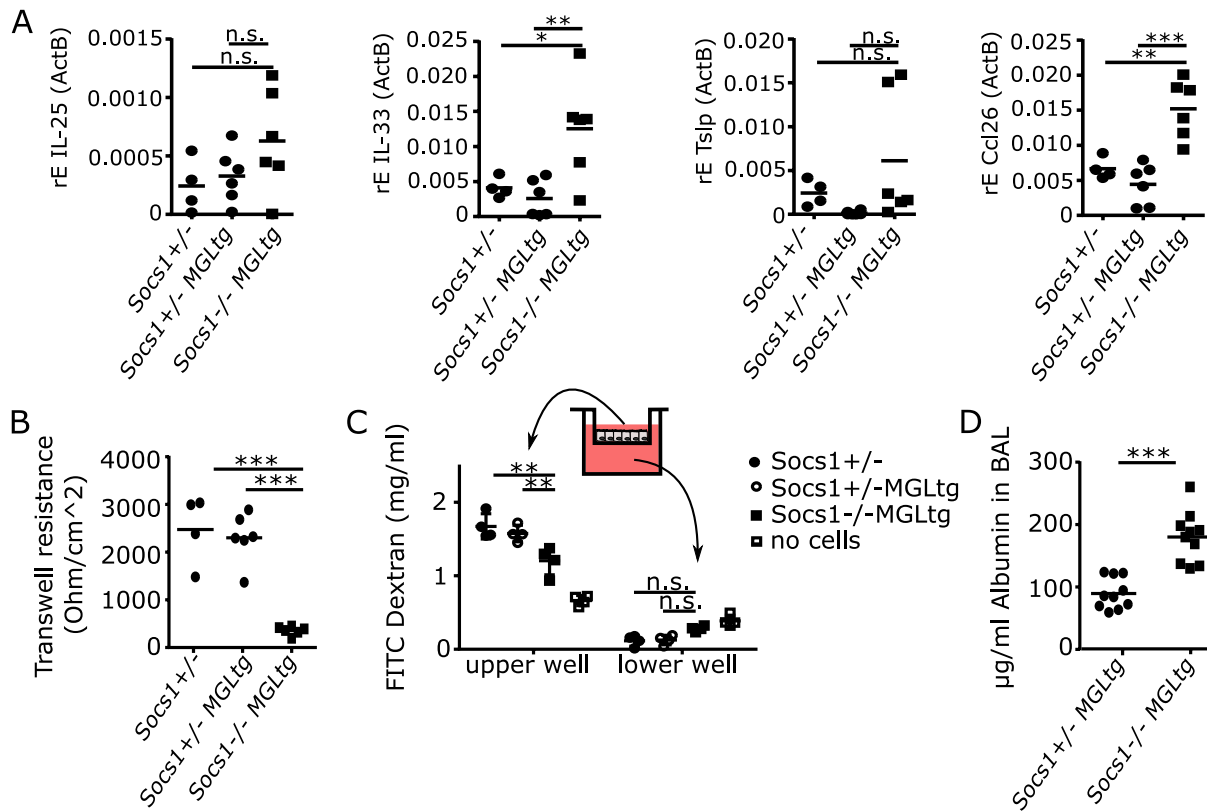
Figure 32.: Socs1$^{-/-}$MGL^{tg} mice show reduced airway resistance.

(A) m-RNA expression of *IL-25, IL-33, Tslp* and *Ccl26* in primary murine trachea epithelial cells (pmTECs) (n = 4-6). (B) Resistance in the transwell was measured using the Millicell electrical resistance system (n = 4-6). (C) FITC-Dextran (4 kDa) diffusion from the inner well to the outer well in 2 h at 37°C was detected by measuring the absorbance at 490 nm (n = 3). (D) Albumin in BAL of n = 10 Socs1$^{+/-}$MGL^{tg} and Socs1$^{-/-}$MGL^{tg} mice was determined using ELISA. Data is shown as mean +SD and significance was assessed using the two-way ANOVA including Bonferroni post-test.
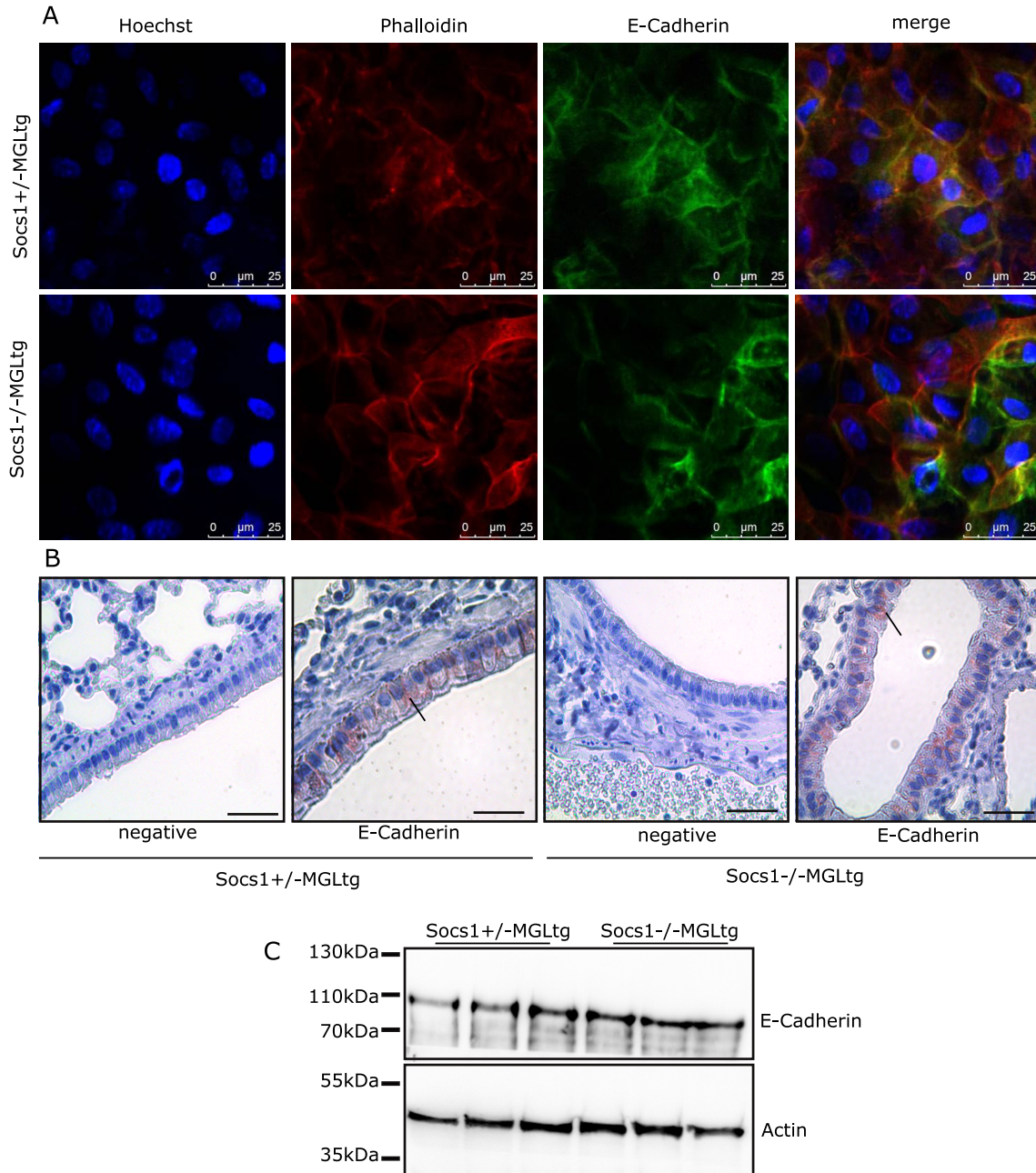
Figure 33.: Socs1$^{-/-}$MGL^{tg} mice show no difference in localization or expression of E-Cadherin. (A) Confocal microscopy images show staining of primary murine trachea epithelial cells (pmTECs) for Actin (using Flash^{TM} Phalloidin, red) and E-Cadherin (green). Nuclei were visualized using Hoechst. Scale bar, 25 μm. n = 2 (B) Immunohistochemical expression of E-Cadherin in epithelial cells was detected using paraffin-embedded lung sections of Socs1$^{+/-}$MGL^{tg} and Socs1$^{-/-}$MGL^{tg} mice. Scale bar, 50 μm. n = 6 (C) Detection of E-Cadherin in lysates of pmTECs suggests similar protein amounts for both Socs1$^{+/-}$MGL^{tg} and Socs1$^{-/-}$MGL^{tg} mice. Histon3 (H3) was used as loading control. n = 3

6. Discussion

6.1. Generation of Socs1MGL^{tg} mice

SOCS1 is a classical negative feedback regulator of cytoplasmic JAK/ STAT signaling [62, 194, 257]. However, it has been described that SOCS1 is also localized in the cell nucleus [12, 143], yet the function of SOCS1 in the cell nucleus *in vivo* remained unclear. Baetz et al. showed in 2008 that fusion of the SOCS1-NLS to CIS - a cytoplasmic SOCS family member - resulted in nuclear localization of this protein. Vice versa, deleting the NLS of human SOCS1 or substitution of this sequence with the respective region of SOCS3 resulted in loss of nuclear localization [12]. SOCS3 was chosen since it is the closest related family member to SOCS1 [115]. These 2 proteins share the same principal structure but differ in localization, because SOCS1 possesses a functional NLS. *In vitro* data using human SOCS1 could now be reproduced for murine SOCS1 (Fig. 6). Although SOCS1ΔNLS was localized in the cytoplasm and less mobile, it was still efficient in inhibiting IFNγ signaling (Fig. 7). As reported previously, SOCS1 was expressed at low levels [257, 194, 62] and relatively short-lived [248], but could be induced by IFNγ [51] (see Fig. 12 - 13). In addition, SOCS1 can be stabilized on protein level through phosphorylation by Pim kinases [29]. The NLS of SOCS1 (RRMLGAPLRQRRVR, amino acids 159–173) resembles a bipartite NLS composed of two basic stretches. Lysine as a basic amino acid is important for the ubiquitin proteasome pathway, linking ubiquitin chains onto proteins to mark them for degradation via the proteasome [27, 83]. Therefore, the question was addressed whether exchanging the NLS with the SOCS3 counterpart might alter protein half-life by performing a cycloheximide chase (Fig. 13). Protein half-life was not altered upon exchanging the NLS corresponding part of SOCS1 with SOCS3 (SOCS1ΔNLS).

To study the role of nuclear SOCS1, transgenic mice were generated using a bacterial artificial chromosome (BAC) containing a _m_utated *Socs1* (*Socs1ΔNLS*) that fails to translocate in the cell nucleus, e_G_FP and _L_uciferaseCBG99 (MGL) by pronuclear injection of fertilized oocytes. Using BACs to create transgenic mice is still a commonly used approach [92, 120, 140, 157]. Conventional transgenes often produce unpredictable results if they are too small to recapitulate a natural gene context. BACs, however, are large insert DNA clones capable of carrying genomic fragments ranging between 150–300 kb in size [244], which is large enough to encompass the natural context of most mammalian genes. The large insert size of BACs typically includes enhancers and other regulatory elements, minimizing position-effects, such as epigenetic silencing and unexpected splicing [111]. However, BAC integration site and efficiency is difficult to determine. Another approach to generate transgenic mice could be the use of nuclease-guided genome editing methods such as ZFN, TALEN and CrispR/Cas [74]. Endonucleases are capable of inducing double stranded breaks at specific locations in the genome, enabling precise genome editing with high efficiency. Due to simplicity and easy feasibility, the previously established method of generating BAC transgenic mice was chosen.

For Socs1MGL^{tg} mice, stable regulation and expression of the BAC was demonstrated by similar gene regulation of *Socs1wt* and *Socs1ΔNLS* (Fig. 10), arguing for successful BAC integration. Other genes besides SOCS1 that are encoded on the BAC are PRM1, PRM2, PRM3 and TNP2. Those genes are involved in spermatogenesis. PRM proteins are protamines that substitute for histones in the chromatin of sperms during spermatogenesis. TNP2 is a transition protein associated with the conversion of nucleosomal chromatin to the compact, non-nucleosomal form during spermatogenesis. Since no gender biases were detectable in MGL transgenic mice and male Socs1^{+/-}MGL^{tg} mice were breeding as efficiently as Socs1^{+/-} mice,

those genes apparently did not influence analysis shown thereafter. In general, the results confirmed previously described protein and mRNA expression patterns of SOCS1, indicating that the transgene has integrated in a region accessible for transcriptional regulation and that using BAC transgenic mice is a valid approach to study the function of SOCS1 in the cell nucleus.

Due to low endogenous SOCS1 expression [257, 194, 62] and the lack of sufficiently specific antibodies for SOCS1 [31, 97], detection of SOCS1 protein without prior stimulation is difficult. Despite the generation of a monoclonal antibody secreted from hybridoma cells and a polyclonal antibody produced against recombinant SOCS1, no antibody was found specifically detecting endogenous SOCS1, especially in histology. However, Socs1MGL^{tg} mice can be used as reporter mice due to the presence of eGFP and firefly luciferase on the same BAC (Fig. 11). 2A sequences between the coding regions of *SOCS1ΔNLS*, *eGFP* and *Luciferase* result in co-translational cleavage and do not result in fusion proteins. Therefore, Socs1MGL^{tg} mice can be used as reporter mice on cellular, but not on subcellular level. Luciferase assay suggested high SOCS1 expression in the thymus as reported previously [257]. High luciferase activity in the muscle, however, could arise from regeneration of ATP from phosphocreatine through the creatine kinase and did not necessarily resemble high SOCS1 expression. The discrepancy between mRNA expression in the pancreas of *Socs1wt* or *Socs1ΔNLS* one the one hand as well as *Luciferase* or *eGFP* on the other hand could be explained by the presence of specific pancreatic ribonucleases involved in endonucleolytic cleavage starting at 3' end. Isolation of intact, high-quality RNA from pancreas remains challenging [45]. Otherwise, similar mRNA levels were observed in various organs arguing for the use of Socs1MGL^{tg} mice as reporter mice.

6.2. Socs1$^{-/-}$MGL^{tg} mice can be used to study the function of nuclear SOCS1

To study the function of nuclear SOCS1 in mice, Socs1MGL^{tg} mice were backcrossed on an SOCS1 deficient background - named Socs1$^{-/-}$MGL^{tg} - and compared to littermate Socs1$^{+/-}$MGL^{tg} or Socs1$^{+/-}$ controls. Importantly, a gene dosage effect was ruled out. In contrast to Socs1$^{-/-}$ mice, Socs1$^{+/-}$ mice lacked detectable levels of IFNγ [173] and were found to be phenotypically normal [256]. In addition, Socs1$^{+/-}$ mice showed normal survival (Fig. 16) indicating that one allele of *Socs1* is sufficient for rescue of the severe knockout phenotype. In line with this, no difference in pSTAT1 levels was observed by flowcytometry (Fig. 17), between Socs1$^{+/+}$ and Socs1$^{+/-}$ mice. The lung phenotype including elevated expression of Th2 cytokines and disrupted barrier function of epithelial cells was only observed in Socs1$^{-/-}$MGL^{tg} mice. Neither Socs1$^{+/-}$, nor Socs1$^{+/-}$MGL^{tg} mice showed this phenotype, arguing for a localization specific effect resulting in eosinophilic lung inflammation and against a gene dosage effect.

To prove that Socs1$^{-/-}$MGL^{tg} mice lack nuclear SOCS1, functional assays were used to investigate interaction of nuclear SOCS1 with either p53 or the NFκB subunit p65. Nuclear SOCS1 has been shown to interact with p53, leading to its phosphorylation at serine 15 and activation by forming a ternary complex with ATR or ATM [169] (see Fig. 34A). Activation of the tumor suppressor gene p53 results in G1 arrest and apoptosis. In G1 arrest, p53 induces the synthesis of inhibitors of cyclin-dependent kinases, such as p21/WAF1 [1, 242]. In addition, activation of the p53 pathway by SOCS1 can establish an anti-proliferative program in cells exposed to sustained or aberrant cytokine stimulation, suggesting an anti-proliferative role for SOCS1 [134, 169]. This anti-proliferative function of SOCS1 has also been shown for cervical cancer cell lines infected with HPV and for non-small-cell lung cancer celllines [134, 243]. Therefore, SOCS1 is frequently downregulated in human cancer [271]. Since nuclear SOCS1 leads to activation of p53 [169], the lack of nuclear SOCS1 should result in less active p53 and a lower percentage of cells arrested in G1. Indeed, Socs1$^{-/-}$MGL^{tg} mice showed lower percentage of splenocytes in G1 and higher percentage in S phase of the cell cycle (Fig. 15). SOCS1 is further known to activate apoptosis through p53 activation. Knock-down of SOCS1 in contrast leads to reduced phosphorylation

of p53 and apoptosis of intestinal epithelial cells [39]. Although Socs1$^{-/-}$MGL^{tg} mice showed increased spleen weight and number of splenocytes as described for Socs1$^{-/-}$IFN$^{-/-}$ mice [37], no altered proliferation was detectable. Naïve T cells are usually considered to remain in a dormant state unless awakened by foreign antigens expressed on activated APCs. Following appropriate stimulation, T lymphocytes proliferate extensively. Therefore, beads coated with anti-CD3 and anti-CD28 were used to stimulate T cells in a manner that partially mimics stimulation by antigen-presenting cells. The discrepancy between proliferation and cell cycle data might be explained by the fact that splenocytes were freshly isolated and analyzed for their cell cycle, whereas splenocytes were cultured *in vitro* under the presence of anti-CD3/CD28-coated beads for three days prior analysis of proliferation. There might be increased proliferation in Socs1$^{-/-}$MGL^{tg} that is dependent on factors secreted from other immune cells. One could test T cell proliferation with isolated DCs in the presence or absence of epithelial cell conditioned medium instead of anti-CD3 and anti-CD28 coated beads. DCs of Socs1$^{-/-}$MGL^{tg} mice might produce increased IL-2 [294] and therefore lead to increased numbers of T cells in the spleen. Those conditions would resemble more the *in vivo* situation. In addition, defects in regulation of p53 target genes such as Mdm2, Pmp22, PUMA and Gadd45a should be investigated.
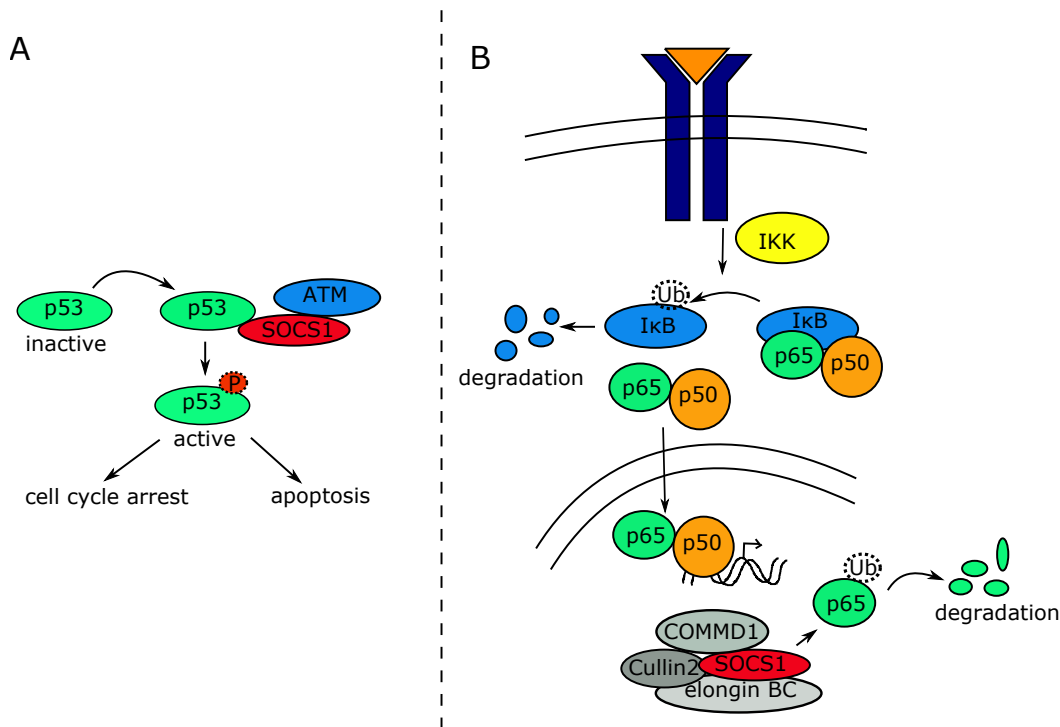
Figure 34.: Scheme summarizing the known nuclear functions of SOCS1.
(A) Nuclear SOCS1 has been shown to interact with p53, leading to its phosphorylation at serine 15 and activation by forming a ternary complex with ATM upon DNA damage [169]. Active p53 leads to cell cycle arrest via p21/WAF1 or apoptosis (B) Activation of the IKK complex leads to ubiquitination and degradation of IκB proteins. Released NFκB complexes shuttle into the cell nucleus to activate gene transcription. Nuclear SOCS1 has been shown to induce proteasomal degradation of NFκB p65 in a complex with Elongin B/C and Cullin-2 [173, 230, 260]. COMMD1 stabilizes the interaction of SOCS1 with p65 [173, 230]. Figure adapted from Ghosh and Hayden, 2008 [78].

Besides interaction between nuclear SOCS1 and p53, SOCS1 has been shown to interact with p65 in the nucleus [173, 230, 260] leading to its proteasomal degradation (see Fig. 34B). NFκB proteins are involved in the control of a large number of processes, such as immune and inflammatory responses, developmental processes and apoptosis. NFκB functions as dimeric transcription factors and consist of the subunits NFκB1 (p105/p50), NFκB2 (p100/p52), c-Rel, RelA (p65) or RelB. NFκB proteins are usually bound and inhibited by IκB inhibitors.

Activation of the IKK complex phosphorylates IκB proteins leading to their ubiquitination and proteasomal degradation and the release of NFκB complexes. Active NFκB complexes translocate into the nucleus where they induce expression of pro-inflammatory cytokines like IL-1, IL-6, IL-8, or TNFα. Nuclear SOCS1 has been shown to induce proteasomal degradation of NFκB [173, 230] by interaction with p65, thereby limiting induction of a subset of NFκB dependent genes [260]. Interaction with p65 has been shown for SOCS1, but no additional SOCS family member. The N-terminal part of the SH2 domain contributes to p65 binding, whereas the SOCS box is known to mediate E3 ubiquitin ligase activity. Therefore, a mutant lacking the SOCS-box is ineffective in p65 ubiquitination [260]. It was also suggested that SOCS1 binds to p65 depending on the ubiquitously expressed protein COMMD1. COMMD1 was found to inhibit NFκB by stabilizing the interaction of SOCS1 with p65 [168]. In mice lacking nuclear SOCS1, sustained NFκB signaling is expected. Indeed, Socs1^{-/-}MGL[tg] mice showed sustained IL-12p40 protein levels in CD11c^{+} cells of the lung and spleen as well as higher NFκB p65 activity in lung homogenate and pmTECs (Fig. 14). No differences were detected regarding TNFα protein levels. Unlike TNFα that shows fast NFκB recruitment to constitutively and immediately accessible promoters, IL-12p40 is a gene that needs a prolonged binding of NFκB to its promoter [20], suggesting that the lack of nuclear SOCS1 leads to sustained activation of NFκB that is affecting only a subset of NFκB dependent genes. Stimulation of DCs with different TLR ligands has been shown to result in striking differences in the kinetics of NFκB activation [20]. Whereas LPS induced a rapid but short-lived activation of p65, CpG-DNA stimulation resulted in prolonged p65 activity at the IL-12p40 promoter. In addition, a high number of differentially expressed genes were discovered annotated to TLR and TNF signaling, and NFκB binding sites were overrepresented among those differentially expressed genes (Table 2 and 3). Due to the lack of a sufficiently specific antibody staining endogenous SOCS1, there is no prove for the absence of SOCS1 in the nucleus of Socs1^{-/-}MGL[tg] mice. Those mice might only have reduced nuclear SOCS1 resulting in enhanced NFκB activity and altered cell cycle. Another possibility would be altered cytoplasmic concentration of SOCS1 that accounts for the phenotype of Socs1^{-/-}MGL[tg] mice, which cannot be excluded. Nevertheless, data in Socs1^{-/-}MGL[tg] mice is consistent with previously described *in vitro* data using non-nuclear SOCS1ΔNLS [260], suggesting that Socs1^{-/-}MGL[tg] mice lack functional SOCS1 in the cell nucleus.

6.3. SOCS1ΔNLS is sufficient to regulate classical IFNγ signaling, but fails to regulate a subset of non-canonical IFNγ dependent genes

SOCS1ΔNLS was sufficient to rescue Socs1^{-/-}MGL[tg] mice from the early-lethal disease described for Socs1^{-/-} mice (Fig. 16), that otherwise die within 3 weeks due to excessive immune signaling and multiorgan inflammation [173, 256, 193]. Besides neonatal death, Socs1^{-/-} mice are characterized by liver degeneration, hematopoietic infiltrations in various organs as well as accelerated apoptosis and aberrant T cell activation [173, 256, 193]. This phenotype is highly dependent on IFNγ hypersensitivity as it can be prevented in the neonatal period by the administration of anti-IFNγ antibodies or using Socs1^{-/-}IFNγ^{-/-} mice that show reduced pathology [181, 6, 23]. Although treatment of Socs1^{-/-} mice with nebulized anti-IFNγ antibodies rescued from lethal liver disease, mice showed signs of a chronic disease including T-lymphocyte infiltrations in skeletal muscle, skin, lung, pancreas, liver [23]. Also Socs1^{-/-}IFNγ^{-/-} mice developed chronic granulomas in the gut and various other organs in addition to polycystic kidneys, pneumonia and chronic skin ulcers [181]. Not only a elimination of the STAT1 gene, but also of STAT6 rescued SOCS1 deficient mice [195]. In both Socs1^{-/-}STAT1^{-/-} and Socs1^{-/-}STAT6^{-/-} mice, survival was prolonged. 50% of the mice survived until day 85. In addition, hepatomegaly was prevented and thymic atrophy was partly improved [195].

IFNγ signaling functions by binding to the IFNγ receptor complex, activating JAK1/2 and

subsequently leading to tyrosine phosphorylation of STAT1 (pY-STAT1). pY-STAT1 dimers in turn translocate into the nucleus and activate transcription of 'canonical' IFNγ-responsive genes [255]. Socs1$^{-/-}$MGL^{tg} mice showed physiological regulation of canonical IFNγ signaling by downregulating pY-STAT1 levels as well as IFNγ target gene expression upon IFNγ stimulation (Fig. 16, 17). Whole genome expression analysis revealed only 86 genes to be differentially regulated between BMMs of Socs1$^{+/-}$MGL^{tg} and Socs1$^{-/-}$MGL^{tg} mice with no canonical IFNγ target genes or overrepresented STAT1 transcription factor binding sites (Fig. 18 and Table 2), arguing that canonical IFNγ signaling was still efficiently regulated by Socs1ΔNLS. In addition to canonical signaling, a number of studies have shown that pY-STAT1-independent pathways also exist [80, 226, 251]. It was reported that STATs translocate into the nucleus in a pY-independent manner, where they activate expression of only a subset of 'non-canonical' IFNγ-induced genes [30]. Although Socs1$^{-/-}$MGL^{tg} mice showed functional regulation of canonical IFNγ signaling, a subset of non-canonical IFNγ dependent genes was differentially regulated (Fig. 18). Minor, but non-significant differences were observed in Icam-1 expression upon stimulation with IFNγ (Fig. 17D). Intercellular adhesion molecule 1 (Icam-1) is a ligand for the leukocyte adhesion protein (LFA-1), involved in trafficking and activation of T cells [144]. Regulation of T cell activation requires two signals. First, the antigen is presented on MHC molecules that interact with the T cell receptor complex. As a second signal, B7 interacts with CD28 on the T cell. In addition, a second signal can also be delivered through Icam-1 interacting with LFA-1 residing on the T cell. Not only T cell activation, but also T cell differentiation is influenced by Icam-1. Numbers of regulatory T cells (Tregs) are significantly decreased in mice lacking full-length Icam-1 [84]. Increased induction of Icam-1 in cells lacking nuclear SOCS1 is in line with literature showing that upregulation of Icam-1 by IFNγ is inhibited by SOCS1 [212] and that this inhibitory capacity depends on the functional NLS of SOCS1 [143].

In addition to Icam-1, Indoleamine 2,3-dioxygenase (Indo) was differentially regulated between BMMs of Socs1$^{-/-}$MGL^{tg} and Socs1$^{+/-}$MGL^{tg} mice (see Fig. 18). This is in line with literature, showing that SOCS1 deficient CD8$^+$ DCs express increased mRNA levels of Indo [274]. Those tolerogenic DCs have a significant role in the induction of peripheral tolerance through IL-10 and the induction of Tregs. Furthermore, Indo induction inhibits clonal expansion of T cells from TCR transgenic mice following adoptive transfer, arguing for an important role in tolerance induction [180]. Indo is an enzyme that catalyzes the first and rate-limiting step in tryptophan catabolism to N-formyl-kynurenine. Indo is involved in immune inhibition by tryptophan depletion resulting in starvation and stress of immune cells and accumulation of cytotoxic catabolites [90, 154]. In addition to immunosuppression, T cell apoptosis, proliferation and differentiation are influenced by Indo [90, 65]. Upregulation of Indo in DCs by IFNγ reduces Th1 cell responses [207, 208], whereas inhibition of Indo enhances the severity of Th1 cell-mediated diseases [150]. Odemuyiwa et al. showed that eosinophils constitutively express functional Indo that is further enhanced by IFNγ treatment. When eosinophils expressing high levels of Indo are co-cultured with either a Th1 or Th2 cells, they selectively inhibited anti-CD3 induced proliferation of Th1 but not Th2 cells [203]. Th2 bias was verified by Platten et al. showing that mice with experimental autoimmune encephalomyelitis treated with a peptide promoting Th2 response display therapeutic effects, express 70 fold higher Indo mRNA and produced increased Th2 cytokines [216]. This is in line with data from this work showing that Socs1$^{-/-}$MGL^{tg} mice expressed increased Indo levels as well as Th2 cytokines.

6.4. SOCS1 in T cell development

CD4$^+$ T cells are activated by foreign antigens presented on APC's via MHC class II and induced depending on the surrounding cytokine milieu into different Th cell subtypes. IL-12 and IFNγ lead to activation of the transcription factor Tbet via STAT4 and differentiation of naïve CD4$^+$ T cell into Th1 cells [261]. In contrast, Th2 cells are characterized by the expression of Gata3 via STAT6 in an IL-4 and IL-10 dominant milieu [8] and Th17 cells are produced upon TGFβ

and IL-6 stimulation. The latter express Rorc via STAT3 [288]. SOCS1 has been shown to be important in helper T cell differentiation [51, 194, 257]. SOCS1 is rapidly induced in response to many cytokines, including IFNγ and IL-4 and it is an important negative feedback inhibitor of both signaling pathways. When Socs1$^{-/-}$ mice are crossed with either IFN$\gamma^{-/-}$ or STAT6$^{-/-}$ mice, survival is prolonged [6, 195]. This indicates that SOCS1 regulates both IFNγ-driven Th1 and IL-4-driven Th2 responses. Supporting this finding, CD4$^+$ T cells from Socs1$^{-/-}$ mice spontaneously differentiate into Th1 and Th2 cells thereby producing IFNγ and IL-4, respectively [72, 195]. Socs1$^{-/-}$MGL^{tg} mice showed enhanced percentage of Gata3$^+$ CD4$^+$ cells and increased expression of IL-4, IL-5 and IL-13, suggesting that nuclear SOCS1 plays a role in T cell differentiation (Fig. 24). Even under neutral conditions, CD4$^+$ T cells of Socs1$^{-/-}$MGL^{tg} mice tended to differentiate into Gata3$^+$ cells, suggesting a T cell intrinsic effect for nuclear SOCS1. It has previously been shown *in vitro* that SOCS1 is a negative regulator of Th2-dependent pathways, achieved by inhibition of pSTAT6 [73]. This inhibition, however, is known to be dependent on cytoplasmic SOCS1 and no mechanism resulting Th2 skewing conditions has been found to be dependent on nuclear SOCS1 so far.

CD11c$^+$ cells from the lungs of Socs1$^{-/-}$MGL^{tg} mice showed increased NFκB p65 activity and IL-12p40 protein levels even without stimulation (see Fig. 14). It remains unclear why Socs1$^{-/-}$MGL^{tg} mice had a strong Th2 bias, although IL12p40 levels - favouring Th1 differentiation - were elevated. Th2 skewing conditions in Socs1$^{-/-}$MGL^{tg} mice seem to prevent Th1 differentiation despite the presence of IL12p40. To analyze whether the Th2 bias observed in Socs1$^{-/-}$MGL^{tg} mice is of physiological relevance, mice were challenged by IL-13. Upon IL-13 instillation, Socs1$^{-/-}$MGL^{tg} mice showed increased airway eosinophilia (Fig. 27). IL-13 induces production of CCL26 which is a chemoattractant for eosinophils, explaining airway eosinophilia upon IL-13 instillation. This IL-13 induced CCL26 production can be inhibited by SOCS1 [108]. In addition, IL-13 acts on B cells to produce IgE responsible for allergic inflammation in the lungs [49]. Recently, SOCS1 has been shown to inhibit IL-13 induced CCL26 expression in epithelial cells *in vitro* whereas reduced SOCS1 expression was correlated to enhanced airway eosinophilia [57]. The exact mechanism of Th2 skewing due to the lack of nuclear SOCS1 remains to be clarified. It might be that the increased Th2 response in the lung is due to lack of p65 degradation. There is some indirect evidence that NFκB p65 is required for aspects of Th2 responses [16]. It has been shown *in vivo* in men and mice that rhinovirus (RV) infection enhances bronchial epithelial cell NFκB p65 nuclear expression. RV-infected p65-deficient mice exhibit reduced inflammation, yet interferon induction, antiviral responses and virus loads were unaffected, indicating that NFκB p65 is required for pro-inflammatory, but not anti-viral response. In addition, IL-4 treated macrophages make Th2 chemokines MDC and TARC that seems to be partly NFκB dependent [199]. The exact mechanism of NFκB dependent Th2 skewing, however, remains elusive.

Further experiments could be performed evaluating Th2 bias in Socs1$^{-/-}$MGL^{tg} mice in more detail using infection models dependent on Th1 or Th2 responses. For example *Leishmania major* infection in mice results in a protective response in C57BL/6 mice - characterised by a Th1 cytokine pattern -, whereas BALB/c mice, that are characterised by a Th2 cytokine pattern, are susceptible [112]. There are more infection models where a Th2 response leads to worsening of the phenotype for example *Plasmodium falciparum*, *Cyptococcus neoformans* or recombinant epitope-tagged *Mycobacterium tuberculosis* infection [269, 130, 282]. Upon infection with *Plasmodium falciparum*, Th1 cytokines are upregulated and limit progression from uncomplicated malaria to severe and life-threatening complications [269]. In addition, clearance of *Cyptococcus neoformans* infection is highly dependent on the presence of Th1 cells [130]. The highly virulent *Cyptococcus neoformans* strain H99 provokes a Th2 response that results in worsening of lung function unlike the moderate virulent D55 strain that provokes a Th1 response [130]. Also infection with recombinant epitope-tagged *Mycobacterium tuberculosis* shows enhanced weight loss and lung fibrosis in mice with adoptively transferred Th2 cells as compared to mice that received

Th1 cells [282]. Therefore, it would be interesting to subject Socs1$^{-/-}$MGL^{tg} mice to the infection models described above and see whether those mice with a Th2 skewing show a worsening of the phenotype when compared to littermate controls with functional nuclear SOCS1.

Increased Th2 cytokine levels in lung homogenate of Socs1$^{-/-}$MGL^{tg} mice probably derive not only from Th2 cells that are overrepresented in those mice (see Fig. 24), but also from ILC2 cells. ILCs (innate lymphoid cells) are preferentially located at barrier surfaces and are important for protection against pathogens and maintenance of organ homeostasis [254, 53]. They consist of cytotoxic natural killer (NK) cells, and the helper subsets of ILC1s, ILC2s and ILC3s. Whereas ILC1s express the transcription factor T-bet and produce IFNγ [17], ILC3s express Rorγt and secrete IL-22 and IL-17A [36] and ILC2s express Gata3 and secrete Th2 cytokines [119]. Stimulation of ILC2s with epithelial cell derived cytokines IL-25, IL-33 and Tslp leads to the production of Th2 cytokines IL-4, IL-5 and IL-13. This has been observed also in Rag2$^{-/-}$ mice, arguing against cytokine production by Th2 cells only [70]. Also in ovalbumin-induced allergic asthma, the ILC2 population in lung and BAL fluid increases and is the major source of IL-4, IL-5 or IL-13 [287]. Recently, various groups demonstrated the presence of ILC2s in the respiratory system of mice and humans [26, 184, 185]. ILC2s play important roles in the pathogenesis of allergic lung inflammation such as asthma or allergies [202, 98]. Furthermore, ILC2s were found in nasal polyps of patients with chronic rhinitis, a classical Th2 disease [184, 183]. Interestingly, ILC3s have been shown to produce IL-22 that maintains epithelial cell integrity [228, 252]. Since Socs1$^{-/-}$MGL^{tg} mice show reduced percentage of Th17 cells, they might also have a reduced number of ILC3s that would result in reduced IL-22 levels, and explain disturbed epithelial cell integrity in Socs1$^{-/-}$MGL^{tg} mice. Therefore, presence of ILC subpopulations as well as IL-22 levels should further be examined in Socs1$^{-/-}$MGL^{tg} and control mice.

ILCs have been shown to differentially integrate signals from commensal microbes resulting in altered transcriptional and epigenetic reprogramming [96, 268]. Depletion of ILCs resulted in a changed microbiome and systemic inflammation, which could be prevented by administration of IL-22, arguing for an important role of ILC3s [252]. Commensal microbes influence the activity of the other ILC subsets as well. ILC2s for example are activated by IL-25, which is produced in a microbiota-dependent manner [236]. Therefore, it might also be of interest to compare lung microbiome between Socs1$^{+/-}$MGL^{tg} and Socs1$^{-/-}$MGL^{tg} mice.

6.5. Nuclear SOCS1 is a regulator of lung immunity

Socs1$^{-/-}$MGL^{tg} mice showed inflammation only in the lung and in no other analyzed organ. This might be due to organ specific adapted and modulated innate immunity. Unlike in sterile compartments of the body such as the blood, where every contact with a pathogen leads to activation of cells belonging to the innate immune system, the respiratory tract is colonized by commensal microbes similar to the skin or the gastrointestinal tract. Therefore, tolerance mechanisms are important to prevent from constant activation. Some tolerance mechanisms might be dependent on nuclear SOCS1 and the lack of it might lead to low-grade inflammation in the lungs of Socs1$^{-/-}$MGL^{tg} mice. However, it remains unclear why Socs1$^{-/-}$MGL^{tg} mice showed no inflammation in other organs with established tolerance mechanisms such as the gastrointestinal tract. While the gut and lungs are both mucosa-associated organs with a shared embryological origin, their anatomical features are different. This results in great variance in numbers and composition of their microbiota. Migration of microbes in the digestive tract is unidirectional and microbes must cope with extreme environments such as acidic pH of the stomach and alkaline pH of the duodenum. In contrast, migration of microbes in the oxygen-rich lung is bidirectional. Thus the microbiome of the lung is more dynamic and transient than that of the gastrointestinal tract [52]. In contrast to the lung where commensal microbes are found mainly in upper airways and only few in the lower respiratory tract [102], bacterial density

in the intestine is orders of magnitude higher [116]. In addition, the gut and lung differ their host–bacterial interactions. Whereas luminal IgA levels are higher in the gut, the lung exhibit more interactions between bacteria and host immune cells [52]. Taken together, the respiratory and the gastrointestinal tract show different environmental conditions resulting in divergent microbiota that might explain why Socs1$^{-/-}$MGL^{tg} mice showed low-grade inflammation only in the lung and not in the gut.

Socs1$^{-/-}$MGL^{tg} mice were analyzed for disease symptoms and spontaneous development of low-grade inflammation in the lung was detected (Fig. 22). Expression of SOCS1 in the lung has been reported for alveolar macrophages [56], bronchial epithelial cells [79] and eosinophils [24]. Mice deficient for SOCS1 show extensive hematopoietic infiltration in the lung [256]. This fits to the observation in Socs1$^{-/-}$MGL^{tg} mice and argues for an involvement of nuclear SOCS1 in immune regulation in the lung. NFκB p65 activation is associated with inflammation in the airways of asthmatics [103], which might explain why Socs1$^{-/-}$MGL^{tg} mice with increased NFκB p65 activity developed airway inflammation. Micro-CT analysis suggests that 5 out of 6 mice developed inflammatory aggregates in the lungs equally distributed in all lung lobes (see Table 5), mainly occurring in close proximity to smaller bronchioles or blood vessels. It remains to be analyzed of which immune cells such infiltrates consist. This could be done by immunohistochemistry staining of different markers unique for a subset of immune cells. So far, it is unclear why disease symptoms were not observed in all Socs1$^{-/-}$MGL^{tg} mice. Although genotyping confirmed that disease-free mice were indeed Socs1$^{-/-}$MGL^{tg} mice, a small percentage of analyzed mice (1 out of 6 mice according to micro-CT analysis) showed no disease symptoms regarding lung inflammation. In addition, analysis of IgE levels, Th2 cytokines or epithelial cell derived cytokines showed one population with increased expression of cytokines or IgE serum levels and a smaller population with expression levels as compared to the controls. A gender bias or age bias was ruled out. No difference in food pellets, bedding or location of the cages was observable between mice showing symptoms and mice with no disease symptoms.

The role of nuclear SOCS1 in the pathogenesis of Th2 prone diseases such as asthma was addressed upon ovalbumin (OVA) sensitization and challenge (see Fig. 25). Mouse models are commonly used to study asthma pathogenesis and to identify underlying physiological and immunological processes by OVA challenge [201]. In addition to the classical OVA sensitization and challenge model, house dust mite, cockroach extracts, or *Aspergillus fumigatus* are often used [105, 299]. There are some disadvantages using asthma models in mice. First, unlike in humans, mice exhibit only transient methacholine-induced AHR following allergen exposure. In addition, there is a lack of chronicity of the response to allergen exposure in mice. Third, early- and late-phase bronchoconstrictions are common in humans, though both are poorly defined in mice. However, observations from mouse models of allergic asthma closely resembles clinical disease symptoms of asthmatic patients such as eosinophilic lung inflammation, airway hyper-responsiveness, increased IgE, mucus hypersecretion, and airway remodeling [63, 299]. Mice challenged with ovalbumin develop a clinical syndrome that closely resembles allergic asthma. Here, OVA i.p. sensitization and OVA aerosol challenge of Socs1$^{-/-}$MGL^{tg} mice was used as a classical Th2 model, not necessarily reassembling all clinical features of asthma. Similar to IL-13 instillation, upon OVA sensitization and challenge, Socs1$^{-/-}$MGL^{tg} mice showed enhanced airway eosinophilia. Supporting this data, Socs1$^{-/-}$IFN$\gamma^{-/-}$ mice showed considerably increased serum IgE levels and infiltrating eosinophils in the lungs upon OVA-treatment as compared to IFN$\gamma^{-/-}$ and C57BL/6 controls [153].

There have been several publications linking SOCS1 expression to allergic diseases such as asthma [57, 73, 79, 101]. *Socs1* gene expression is significantly lower in the airways of severe asthmatics compared with mild/moderate asthmatics, and is inversely associated with airway eosinophilia [57, 73], suggesting that the absence of SOCS1 leads to Th2 bias. A study assessing functional variants of Socs1 within a population of adult Japanese asthma patients found a significant association between the Socs1 promoter polymorphism (-1478CA >del) and adult

asthma. It was suggested that this promoter polymorphism leads to increased SOCS1 and inhibition of interferons, leading to higher susceptibility to virus-induced asthma exacerbations [101]. In 2015, increased expression of nuclear SOCS1 in bronchial biopsies from atopic asthmatic patients was confirmed [79]. Socs1$^{-/-}$MGL^{tg} mice are on a C57BL/6 background that is known to show a Th1 bias when compared to BALB/c mice. Nevertheless, Socs1$^{-/-}$MGL^{tg} mice developed a Th2 prone disease. As compared to BALB/c mice, C57BL/6 mice show elevated eosinophil counts in BAL, but reduced airway reactivity to methacholine [93]. This might explain why Socs1$^{-/-}$MGL^{tg} and control mice showed only a weak response to metacholine exposure. Using Socs1$^{-/-}$MGL^{tg} mice, it was shown for the first time, that not only the presence of SOCS1, but also the localization is crucial for effective regulation of Th2 responses. The question remains about disease progression of Socs1$^{-/-}$MGL^{tg} mice in an asthma model for exacerbations. To study asthma exacerbations, pI:C or rhinovirus (RV) infections could be additionally used. It would be interesting to subject Socs1$^{-/-}$MGL^{tg} mice to RV-induced exacerbations upon OVA sensitization and challenge. One could expect a worse disease in Socs1$^{-/-}$MGL^{tg} mice due to Th2 skewing as observed for the OVA asthma model or IL-13 model. However, Socs1$^{-/-}$MGL^{tg} mice might also be able to clear the infection better due to possibly increased IFN responses [79, 101] as discussed in section 6.6.

6.6. Nuclear SOCS1 and IFN induction

Viral Infection with RNA viruses leads to activation of TLR3 and RIG I signaling. Both result in activation of IRF3, thereby inducing IFNβ. In turn, IFNβ is secreted and can act in an autocrine and paracrine manner to activate JAK/ STAT signaling. This broadens the set of induced genes and amplifies the signal through a positive feedback mechanism. Since SOCS1 is a negative regulator of JAK/ STAT signaling [62, 194, 257], it suppresses this feedback loop and therefore reduces the production of cytokines upon stimulation with type I and type II IFNs [12]. In addition, IRF3 is targeted by SOCS1 for proteasomal degradation that impacts the early type I IFN antiviral response [204]. In line with this, SOCS1 suppresses type I interferon induction by influenza viruses by negative regulation of JAK/ STAT signaling and downregulation of innate immune responses [219]. It would be interesting to study whether nuclear SOCS1 targets IRF3 as previously described [204]. This could be done by a pull-down assay between nuclear SOCS1 and IRF3. In Socs1$^{-/-}$MGL^{tg} mice, reduced IRF3 degradation and therefore increased interferon signaling is suggested.

In addition to type I and type II interferon signaling, also type III interferon (IFNλ) signaling leads to activation of JAK/ STAT signaling that can be inhibited by SOCS1 [283]. IFNλ consists of 3 subtypes, IFNλ1 (IL-29), IFNλ2 (IL-28a), and IFNλ3 (IL-28b) [34]. Expression of functional IFNλ receptor complexes in the lung and intestinal tract is mainly restricted to epithelial cells [187]. Due to the importance of nuclear SOCS1 in epithelial cells, INFλ signaling should be analyzed in epithelial cells of Socs1$^{-/-}$MGL^{tg} mice and compared to controls. Similar to type I interferons, IFNλ production results in antiviral, antiproliferative, and antitumor activity. IFNλ plays an important role in the defense against several human pathogens that infect the respiratory tract, such as influenza virus, respiratory syncytial virus or severe acute respiratory syndrome (SARS) coronavirus [187]. In line with that, defects in IFNλ production or signaling cause reduced innate immune responses to viral pathogens replicating in epithelia of the lung [48]. Upon infection with rhinovirus, SOCS1 levels are increased in bronchial epithelial cells which is associated with reduced levels of IFNλ. SOCS1 inhibits RV–induced IFNβ and IFNλ promoter activation [79]. Whereas SOCS1 suppression of interferon receptor signaling has been shown to be dependent on the SOCS box [215, 143], SOCS1 mediated suppression of RV-induced interferon induction is independent of the SOCS box and does not require proteasomal degradation [79]. However, it was dependent on nuclear localization because SOCS1 constructs unable to localize to the nucleus were unable to suppress rhinovirus-induced interferon promoter activation [79]. This argues for a different mechanism of nuclear SOCS1 mediated IFN suppres-

sion that needs to be further investigated. In line with this, nuclear SOCS1 levels are also increased in bronchial epithelial cells from atopic asthmatic patients suggested to be responsible for impaired IFNλ secretion. Decreased IFNλ levels in asthmatic primary bronchial epithelial cells and alveolar macrophages is highly correlated with severity of RV-induced asthma exacerbation and virus load [35]. Interestingly, recombinant IFNλ has been shown to upregulate Indo expression, whereas silencing of IFNλ decreases Indo expression during influenza infection [71]. This might hint towards higher production of IFNλ in Socs1$^{-/-}$MGL^{tg} mice, since these mice showed also increased Indo expression. It would be interesting to infect pmTECs of Socs1$^{-/-}$MGL^{tg} mice with RV and see whether their immune response differs as compared to wildtype mice. Therefore, inflammation markers OAS1 and MX1 as well as IL-6 and TNFα could be measured. In addition, production of IFNβ and IFNλ protein and mRNA as well as RV replication should be investigated. Three *in vitro* studies show that induction of IFNλ is NFκB-dependent [205, 210, 247]. However, *in vivo* it has been shown, that IFNβ and IFNλ are regulated independently of NFκB p65 [16], arguing against regulation of IFNλ by nuclear SOCS1 via p65 degradation. The exact mechanism remains to be clarified.

6.7. Nuclear SOCS1 in lung epithelial cells

To study the question whether the lack of nuclear SOCS1 in hematopoietic cells is sufficient to induce allergic lung inflammation observed in Socs1$^{-/-}$MGL^{tg} mice, bone marrow transplantation was performed. Lee et al. showed that serum IgE levels and infiltrating eosinophils were considerably increased in the lungs of OVA-treated Socs1$^{-/-}$IFN$\gamma^{-/-}$ mice [153]. They suggested that regulation of SOCS1 mainly affects hematopoietic cells, but not epithelial cells. McCormick et al. showed that reduced expression of SOCS1 prolonged IL-4-induced IRS-2 tyrosine phosphorylation and enhanced M2 differentiation [179], arguing for an important role of SOCS1 in macrophages. Increased IRS-2 in turn promoted allergic lung inflammation and remodeling [44]. In line with this, CD11c$^+$ cells from lung of Socs1$^{-/-}$MGL^{tg} mice showed increased NFκB signaling and IL12p40 production even without stimulation. In addition, SOCS1 has been described to be indispensable in T cell differentiation and activation [51, 194, 257]. Socs1$^{-/-}$MGL^{tg} mice showed an increased percentage of Th2 cells and Th2 cytokines. Therefore, the relevance of nuclear SOCS1 in the hematopoietic compartment was examined by bone marrow transplantation. Bone marrow from wildtype mice was transplanted in lethally irradiated Socs1$^{-/-}$MGL^{tg} mice and vice versa and mice were analyzed with respect to the development of lung inflammation. Interestingly, only lethally irradiated Socs1$^{-/-}$MGL^{tg} mice showed the allergic lung phenotype (see Fig. 29). This data suggests structural cells such as epithelial cells or fibroblasts to be responsible for the induction of airway inflammation in Socs1$^{-/-}$MGL^{tg} mice. In contrast, transplantation of bone marrow from Socs1$^{-/-}$MGL^{tg} mice did not induce lung inflammation, arguing against T cells, DCs or macrophages inducing airway inflammation in Socs1$^{-/-}$MGL^{tg} mice. Multiple subpopulations of macrophages exist in the lung, residing in both the alveolar and interstitial compartments [122]. Alveolar macrophages are a long-lived, self-renewing population that is efficient in removing microorganisms and particles from the lung. In contrast, interstitial macrophages function as antigen presenters and regulators of inflammation and fibrosis and are thought to be replaced by infiltrating monocytes that migrate into the lung from the circulation. Unlike interstitial macrophages, the current view is that alveolar macrophages do not origin from monocytes, but are self-renewal, radiation-resistant [104, 266, 267]. Resistance to radiation is only true, however, if lungs are shielded with lead (e.g. 2-inch lead screen [192]) instead of total body irradiation. Otherwise, loss of alveolar macrophages is observed due to irreversible radiation-induced destruction of tissue macrophages or incomplete radiation-induced suppression of tissue macrophage self-renewal [104, 192]. 3- 8 weeks after whole body irradiation, alveolar macrophage populations are markedly reduced or non-existent [91, 229, 104, 192, 198]. Both Socs1$^{-/-}$MGL^{tg} mice transplanted with bone marrow cells from wildtype mice and wildtype mice transplanted with bone marrow cells from Socs1$^{-/-}$MGL^{tg} mice were analyzed 8 weeks after

radiation and therefore should have no remaining alveolar macrophages. After bone marrow transplantation, 75 - 90% of blood cells were of donor origin (see Fig. 29). If the remaining 10 - 25% hematopoietic cells would account for the phenotype in lethally irradiated Socs1$^{-/-}$MGL^{tg} mice, we would expected to see airway inflammation in lethally irradiated wildtype mice that contain 75 - 90% of hematopoietic cells from Socs1$^{-/-}$MGL^{tg} mice as well. However, it might be possible that mice need both structural cells lacking nuclear SOCS1 and a small percentage of hematopoietic cells lacking nuclear SOCS1 to develop airway inflammation. In summary, data suggests a more important role for nuclear SOCS1 in structural, radiation-resistant cells. Therefore, epithelial cells were analyzed in more detail. In addition to epithelial cells, also endothelial cells or fibroblasts could be responsible for the observed phenotype in Socs1$^{-/-}$MGL^{tg} mice.

Epithelial cells form of a physical barrier between the outside environment and immune cells through cell-cell contacts, remove pathogens by ciliary clearance and secrete antimicrobials. To prevent from constant activation by commensal microbes, epithelial cells produce NO and prostaglandin E2 that is acting on both T cells, alveolar macrophages and DCs [133]. In addition, epithelial cells condition DCs to produce less MHC class II, CD80 and CD86 and secrete more IL-10 and TGFβ [178]. This might explain why nuclear SOCS1 deficiency only in structural radiation-resistant cells had a consecutive impact on lung immunity, leading to airway inflammation. pmTECs of Socs1$^{-/-}$MGL^{tg} mice showed increased expression of epithelial cell derived cytokines IL-25, IL-33 and Tslp. Epithelial cell derived cytokines, including IL-25, IL-33 and thymic stromal lymphopoietin (TSLP), are known to promote Th2 cell responses and allergic inflammation [128]. IL-25 is a member of the IL-17 cytokine family. It can be induced in response to allergens, particles, and helminth infection [99, 121, 70]. Main IL-25 producers are epithelial cells, eosinophils, mast cells, and basophils [55]. Administration of IL-25 was shown to induce IL-4, IL-5, IL-13 and eotaxin production, even in Rag2 deficient mice, arguing for an important role of IL-25 acting on ILC2 cells [70, 121]. In addition, IL-25-deficient mice are more susceptibile to infection with the parasitic helminthes *Nippostrongylus brasiliensis* and *Trichuris muris* due to an impaired Th2 response [211, 66]. Mice treated with IL-25 also developed epithelial cell hyperplasia, increased mucus secretion, and airway hyperreactivity [121]. Besides amplification of Th2 responses, IL-25 causes increased eosinophilic infiltration in mice [263]. This is in line with findings in Socs1$^{-/-}$MGL^{tg} mice that showed increased IL-25 levels and airway eosinophilia. Blocking IL-25 can prevent airway hyperresponsiveness in allergic asthma [13]. IL-33 belongs to the IL-1 family and binds a receptor complex consisting of the IL-1R accessory protein and ST2 that is expressed on mast cells and Th2 cells [158, 38, 238]. IL-33 functions as an alarmin that is stored within the cell and rapidly released upon cellular damage or cellular stress [25, 188]. Release of IL-33 by epithelial cells results in activation of DCs [99, 145, 214]. IL-33-activated DCs prime naïve CD4$^+$ T cells to produce the Th2 cytokines Il4, IL-5 and IL-13 [270, 18]. *In vivo*, IL-33 exposure induces DC recruitment and activation in the lung, resulting in allergic lung inflammation [18] similar to Th2 prone lung disease in Socs1$^{-/-}$MGL^{tg} mice. Epithelial expression of IL-33 is also increased in asthmatic patients [222]. Upon fungal infection with *Cryptococcus neoformans*, mice develop pulmonary cryptococcosis associated with IL-33-dependent type 2 immunity. This infection results in E-Cadherin downregulation that is dependent on IL-33 [114]. TSLP is an IL-7–like cytokine [250]. Besides promoting Th2 development, TSLP exerts a direct inhibitory effect on the development of iTregs [289]. Also Tslp is produced by epithelial cells, endothelial cells, neutrophils, macrophages, and mast cells and promotes the production of Th2 cytokines [292, 142]. In addition, it induces secretion of Th2-attracting chemokines CCL17 and CCL22 [253]. TSLP expression is increased in the lungs of mice with antigen-induced asthma, whereas TSLP receptor–deficient mice have considerably attenuated disease [297]. In addition, mice that express a lung-specific TSLP transgene develop a spontaneous and progressive asthma-like disease [107]. Taken together, published data provides a link between epithelial cell derived cytokines IL-25, IL-33 and Tslp and the development

of allergic lung diseases similar to what is observed in Socs1^{-/-}MGL[tg] mice.

pmTEC cultures were used to study the involvement of epithelial cells in allergic lung disease of Socs1^{-/-}MGL[tg] mice. These cultures have been described to differentiate into epithelial cells, expressing E-Cadherin, Pan-Cytokeratin and ZO-1 [177]. In addition, it has been shown that pmTECs consist of polarized ciliated and secretory epithelial cells with a high transepithelial resistance [47, 280]. However, it is uncertain of which epithelial cell types pmTECs consist and whether composition is altered in pmTECs of Socs1^{-/-}MGL[tg] mice. pmTECs of Socs1^{-/-}MGL[tg] showed decreased transepithelial resistance and increased FITC-Dextran flux. Confirming this observation, albumin levels in BAL of Socs1^{-/-}MGL[tg] mice were increased arguing for a leaky epithelial cell barrier in the lung of Socs1^{-/-}MGL[tg] mice (see Fig. 32). A disrupted epithelial cell barrier might explain low-grade inflammation in the lungs of Socs1^{-/-}MGL[tg] mice. Loss of barrier function in Claudin18^{-/-} mice was shown to lead to increased susceptibility of mice to infection and injury by pathogens and proteases [151]. In general, disruption of tight junctional complexes increases epithelial permeability and inflammation in both conducting airways and alveoli. This has been shown to contribute to the pathogenesis of asthma, acute respiratory distress syndrome and lung injury [151, 75, 85, 19]. Due to disrupted epithelial cell barrier in Socs1^{-/-}MGL[tg] mice, pathogens might be easier accessible for the immune cells such as DCs leading to activation and inflammation. Activation of epithelial cells by pathogens or commensal microbes leads to sustained NFκB signaling due to the lack of nuclear SOCS1. This might lead to secretion of epithelial cell derived cytokines IL-25, IL-33 and Tslp that in turn promote Th2 differentiation. Epithelial cell derived cytokines additionally activate ILC2s and stimulate further production of Th2 cytokines and differentiation of naïve CD4$^+$ T cells into Th2 cells. Th2 cells in turn secrete classical Th2 cytokines IL-4, IL-5 and IL-13. IL-5 together with CCl26 produced by epithelial cells attracts eosinophils, leading to airway eosinophilia. IL-4 and IL-13 acts on B cells to stimulate the production of IgE antibodies. IL-13 itself acts on the epithelial cells leading to increased expression of IL-25, IL-33 and Tslp and amplification of the signal (Fig. 35).

Further experiments proving the role of nuclear SOCS1 in epithelial cells could be done using conditional knock-out mice lacking nuclear SOCS1 only in epithelial cells. Therefore, a Sonic hedgehog promoter line can be used, which has been used to study trachea and lung development [273]. However, it is not possible to distinguish between alveolar type I or type II cells. Further optional epithelium-specific transgenic strains are the surfactant protein C promoter strains, specific for alveolar type II cells [284], or Aquaporin 5 promoter strains specific for alveolar type I cells [69]. In addition, type I and type II alveolar epithelial cells should be isolated by FACS [77] from Socs1^{-/-}MGL[tg] and control mice and cultured to test for transepithelial resistance. An interesting *in vitro* approach to test the influence of nuclear SOCS1 in human cells would be using CrispR/Cas to genetically modify human bronchial epithelial cell cultures. This would allow to generate human bronchial epithelial cells lacking nuclear SOCS1 and re-performing experiments to analyze epithelial cell barrier integrity in a human system.

6.8. Possible mechanism for disrupted epithelial cell barrier in the lungs of Socs1^{-/-}MGL[tg] mice

So far, it remains unclear which factor is responsible for disrupted barrier integrity. One explanation for disrupted epithelial cell barrier would be apoptosis. TNFα for example induces apoptosis of intestinal epithelial cells and causes a large gap between adjacent intestinal epithelial cells [82]. However, this hypothesis is unlikely, because healthy adjacent cells rapidly stretch out and maintain epithelial barrier function [166, 186]. In addition, no cell death was observed in pmTEC cultures. Nevertheless, an apoptosis assay should be performed since SOCS1 has
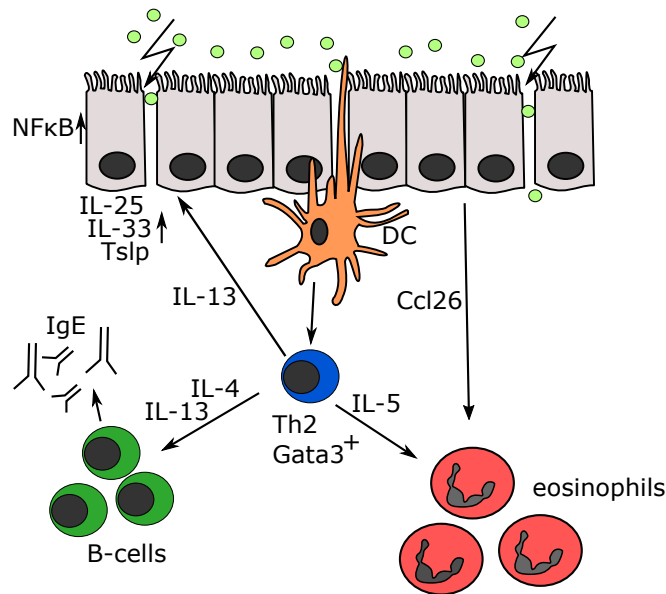
Figure 35.: Schematic view summarizing the important nuclear functions of SOCS1 in lung immunity
In mice lacking nuclear SOCS1, epithelial cell integrity is disturbed that might facilitate pathogens (green) to cross epithelial barrier. Pathogens might be easier detected by cells of the innate immune system such as DCs (orange). Activation of epithelial cells by pathogens might lead to sustained NFκB signaling due to the lack of nuclear SOCS1. This leads to increased production of IL-25, IL-33 and Tslp that favours differentiation of naïve CD4$^+$ T cells into Th2 cells (blue) producing classical Th2 cytokines IL-4, IL-5 and IL-13. IL-5 together with CCl26 produced by epithelial cells attracts eosinophils (red), explaining airway eosinophilia. IL-4 and IL-13 act on B cells (green) and stimulate the production of IgE antibodies. IL-13 itself can act on the epithelial cells leading to increased expression of IL-25, IL-33 and Tslp and amplification of the signal.

been shown to promote apoptosis of intestinal epithelial cells by activating p53 [39].

Increased expression of the epithelial cell derived cytokine IL-33 was observed in pmTEC cultures of Socs1$^{-/-}$MGL^{tg} mice (Fig. 32). Since it has been shown previously [114], that IL-33 has an impact on epithelial integrity, higher IL-33 levels in Socs1$^{-/-}$MGL^{tg} mice might result in epithelial barrier disruption. Recently, it was shown that IL-33 is constitutively expressed in the cell nucleus in epithelial cells [188] where direct interaction between SOCS1 and IL-33 might be possible. Although IL-33 mRNA levels were elevated in Socs1$^{-/-}$MGL^{tg} mice, no difference was observed on protein level (preliminary data not shown).

Moreover, Th2 cytokines shown to result in reduced transepithelial resistance. Since elevated Th2 cytokine mRNA and protein levels have been observed in Socs1$^{-/-}$MGL^{tg} mice, this might explain disrupted epithelial cell barrier integrity in those mice. IL-4 caused an increase in epithelial permeability in various cell types [286]. IL-4 treatment of intestinal T84 monolayers for 24 h led to a 60% decrease in transepithelial resistance. Also in animal models, intraperitoneal IL-4 caused a decrease in mouse intestinal tissue transepithelial resistance [146], whereas STAT6$^{-/-}$ mice were protected from this effect [167]. In addition to IL-4, IL-13 was shown to downregulate junctional components including E-Cadherin in bronchial epithelial cells leading to disruptive effects on airway epithelial barrier function [231]. IL-13 also caused a decrease in transepithelial resistance in HT-29 cells [113, 235]. However, no difference in E-Cadherin expression or localization could be found in Socs1$^{-/-}$MGL^{tg} mice. Since decreased transepithelial resistance was also observed in pmTEC cultures without the presence of IL-4 or IL-13 producing cells, there seem to be an additional mechanism for disrupted epithelial cell barrier in Socs1$^{-/-}$MGL^{tg} mice. Increased Th2 cytokines might, however, have an additional effect on epithelial cell barrier integrity *in vivo*.

Not only Th2 cytokines, but also Th1 cytokines were found to alter transepithelial resistance. IFN-γ induced an uptake of Occludin from junctional complexes into early endosomes through macropinocytosis leading to a leaky barrier [22, 166, 286]. Besides, TNFα was shown to cause a decrease in transepithelial resistance in renal epithelial cell line [191], retina [10] and intestinal epithelial cells [172, 164] by downregulation of ZO-1 and Claudin-5 mRNA and altering their subcellular localization to the cytoplasm. This effect was mediated via myosin light-chain kinase (MLCK) and by activation of nuclear transcription factor NFκB [163, 291]. Activated NFκB translocates to the nucleus and activates the MLCK gene transcription. The increase in MLCK protein results in MLCK-triggered opening of the TJ barrier. Other groups reported that epithelial NFκB protein leads to internalization of tight junction proteins Occludin, Claudin-1 and ZO-1 [265, 164]. In esophagus cells, NFκB was suggested to bind to Claudin-4 promotor [28]. Although there are different cell adhesion proteins reported to be regulated by NFκB in different celltypes, published data is convincing that increased NFκB signaling leads to a decrease in transepithelial resistance. Since pmTECs and lung homogenate of Socs1$^{-/-}$MGL^{tg} mice showed increased NFκB p65 activity (Fig. 14) due to limited degradation of p65 by nuclear SOCS1, this is likely to be responsible for decreased epithelial cell barrier function in Socs1$^{-/-}$MGL^{tg} mice. This hypothesis could be further investigated by adding NFκB inhibitors such as curcumin or triptolide to pmTEC culture of Socs1$^{-/-}$MGL^{tg} mice and see if transepithelial resistance increases. In addition, siRNA knockdown of p65 and an IκB or the pharmacological IKKβ inhibitors could be used im pmTEC cultures of wildtype mice.

The exact mechanism how increased NFκB leads to increased epithelial cell permeability, however, remains to be solved. Therefore, cell junction proteins should be investigated in more detail. In particular, adherens junctions (built from Cadherins and Catenins), tight junctions (built from Claudins), gap junctions (built from Connexins) and desmosomes (built from Cadherins) should be analyzed. First, E-Cadherin was picked as a protein important to built adherens junctions and analyzed regarding its protein expression by Western Blot and localization by immunofluorescence and immunohistochemistry (see Fig. 33). Cadherins are the major

cell adhesion molecules responsible for Ca2$^+$-dependent cell-cell adhesion in vertebrate tissues with E-Cadherin mainly expressed in epithelial cells. However, no difference in protein levels or localization of E-Cadherin was observable in epithelial cells of Socs1$^{-/-}$MGL^{tg} mice (see Fig. 33). Next, tight junctions should be investigated regarding the expression and localization of Occludin, ZO-1, Claudin-1 and Claudin-4, since those tight junction proteins have been shown to be downregulated upon enhanced NFκB signaling [28, 265, 164]. In addition, MLCK protein should be analyzed.

6.9. Summary

Taken together, cytoplasmic localization of murine SOCS1ΔNLS was shown as well as functional regulation of cytoplasmic IFNγ signaling by SOCS1ΔNLS. Therefore, a BAC transgenic mouse model was established including a <u>m</u>utated Socs1 (Socs1ΔNLS) that fails to translocate in the cell nucleus, e<u>G</u>FP and <u>L</u>uciferase, termed MGL. Three MGL transgenic founders were compared with respect to their SOCS1 expression and regulation. Since no differences were observed between the individual founders and both expression and regulation of SOCS1ΔNLS was comparable with SOCS1, stable integration of the BAC was assumed. Socs1$^{-/-}$MGL^{tg} mice, expressing non-nuclear SOCS1ΔNLS on an otherwise SOCS1 deficient background, showed sustained NFκB signaling and an altered cell cycle, arguing for a lack of functional SOCS1 in the cell nucleus. Unlike Socs1$^{-/-}$ mice that die due to excessive IFNγ upon 2-3 weeks after birth, SOCS1ΔNLS was able to rescue this lethal phenotype of Socs1$^{-/-}$MGL^{tg} mice. Functional IFNγ signaling in Socs1$^{-/-}$MGL^{tg} mice was confirmed by unaltered regulation of pY-STAT1 levels, classical IFNγ target genes and whole genome-expression analysis. However, Socs1$^{-/-}$MGL^{tg} mice showed a slightly reduced weight and differential regulation of a subset of non-canonical IFNγ target genes including Indo. Socs1$^{-/-}$MGL^{tg} mice spontaneously developed low-grade inflammation in the lung with a Th2 bias. Airway eosinophilia and Th2 type cytokines were even more pronounced in an experimental asthma model using ovalbumin and upon IL-13 treatment. Bone marrow transplantation revealed a critical role for radiation-resistant cells in development of this phenotype. Interestingly, it was found that airway epithelial cells of Socs1$^{-/-}$MGL^{tg} mice showed disrupted epithelial cell integrity as well as sustained NFκB activation. However, E-Cadherin protein levels and subcellular localization remained unaltered. Therefore, the exact mechanism of epithelial cell barrier disruption needs to be further examined. Taken together, the findings allow the conclusion that Socs1$^{-/-}$MGL^{tg} mice can be used as reporter mice and to study the function of nuclear SOCS1 *in vivo*. The lack of functional SOCS1 in the cell nucleus was suggested to be involved in development of low-grade airway inflammation and Th2 skewing conditions. Moreover, data suggests that nuclear SOCS1 plays an important role in epithelial cells that is so far underestimated.

Literature

[1] M. L. Agarwal, A. Agarwal, W. R. Taylor, and G. R. Stark. p53 controls both the g2/m and the g1 cell cycle checkpoints and mediates reversible growth arrest in human fibroblasts. *PNAS*, 92(18):8493–8497, 1995.

[2] P. Ahmad-Nejad, H. Häcker, M. Rutz, S. Bauer, R. M. Vabulas, and H. Wagner. Bacterial CpG-DNA and lipopolysaccharides activate toll-like receptors at distinct cellular compartments. *J. Immunol.*, 32(7):1958–1968, 2002.

[3] C. M. Ahmed, E. N. Noon-Song, K. Kemppainen, M. P. Pascalli, and H. M. Johnson. Type I IFN receptor controls activated TYK2 in the nucleus: Implications for EAE therapy. *J. Neuro Immunol.*, 254(1-2):101–109, 2013.

[4] S. Akira, S. Uematsu, and O. Takeuchi. Pathogen Recognition and Innate Immunity. *Cell*, 124(4):783–801, 2006.

[5] W. S. Alexander. Suppressors of cytokine signalling (SOCS) in the immune system. *Nature Rev.*, 2(6):410–416, 2002.

[6] W. S. Alexander, R. Starr, J. E. Fenner, C. L. Scott, E. Handman, N. S. Sprigg, J. E. Corbin, A. L. Cornish, R. Darwiche, C. M. Owczarek, T. W. H. Kay, N. Nicola, P. J. Hertzog, D. Metcalf, and D. J. Hilton. SOCS1 is a critical inhibitor of interferonγ signaling and prevents the potentially fatal neonatal actions of this cytokine. *Cell*, 98:597–608, 1999.

[7] L. Alexopoulou, A. C. Holt, R. Medzhitov, and R. A. Flavell. Recognition of double-stranded RNA and activation of NF-kappaB by Toll-like receptor 3. *Nature*, 413(6857):732–8, 2001.

[8] D. Amsen, A. Antov, and R. Flavell. The different faces of Notch in T-helper-cell differentiation. *Nature Rev.*, 9(2):116–124, 2009.

[9] L. Armstrong, A. R. L. Medford, K. M. Uppington, J. Robertson, I. R. Witherden, T. D. Tetley, and A. B. Millar. Expression of functional toll-like receptor-2 and -4 on alveolar epithelial cells. *Am. J. Resp. Cell Mol. Biol.*, 31(2 I):241–245, 2004.

[10] A. Aveleira, C.-M. Lin, S. F. Abcouwer, and F. Ambro. TNF-a Signals Through PKCz/NF-kB to Alter the Tight junction complex and increase retinal endothelial cell permeability. *Diabetes*, 59:2872–2882, 2010.

[11] A. Baetz, M. Frey, K. Heeg, and A. H. Dalpke. Suppressor of cytokine signaling (SOCS) proteins indirectly regulate toll-like receptor signaling in innate immune cells. *J. Biol. Chem.*, 279(52):54708–15, 2004.

[12] A. Baetz, C. Koelsche, J. Strebovsky, K. Heeg, and A. H. Dalpke. Identification of a nuclear localization signal in suppressor of cytokine signaling 1. *FASEB J.*, 22(12):4296–4305, 2008.

[13] S. J. Ballantyne, J. L. Barlow, H. E. Jolin, P. Nath, A. S. Williams, K. F. Chung, G. Sturton, S. H. Wong, and A. N. J. McKenzie. Blocking IL-25 prevents airway hyperresponsiveness in allergic asthma. *J. Allergy Clin. Immunol.*, 120(6):1324–1331, 2007.

[14] R. Bals and P. S. Hiemstra. Innate immunity in the lung: How epithelial cells fight against respiratory pathogens. *European Resp. Journal*, 23(2):327–333, 2004.

[15] A. M. Barral, H. E. Thomas, E. M. Ling, R. Darwiche, E. Rodrigo, U. Christen, M. Ejrnaes, T. Wolfe, T. W. Kay, and M. G. von Herrath. SOCS-1 protects from virally-induced CD8 T cell mediated type 1 diabetes. *J. Autoimmun.*, 27(3):166–173, 2006.

[16] N. W. Bartlett, L. Slater, N. Glanville, J. J. Haas, G. Caramori, P. Casolari, D. L. Clarke, S. D. Message, J. Aniscenko, T. Kebadze, J. Zhu, P. Mallia, J. P. Mizgerd, M. Belvisi, A. Papi, S. V. Kotenko, S. L. Johnston, and M. R. Edwards. Defining critical roles for NF-κB p65 and type I interferon in innate immunity to rhinovirus. *EMBO Mol. Med.*, 4(12):1244–1260, 2012.

[17] J. H. Bernink, C. P. Peters, M. Munneke, A. A. te Velde, S. L. Meijer, K. Weijer, H. S. Hreggvidsdottir, S. E. Heinsbroek, N. Legrand, C. J. Buskens, W. A. Bemelman, J. M. Mjosberg, and H. Spits. Human type 1 innate lymphoid cells accumulate in inflamed mucosal tissues. *Nat. Immunol.*, 14(3):221–229, 2013.

[18] A.-G. Besnard, D. Togbe, N. Guillou, F. Erard, V. Quesniaux, and B. Ryffel. IL-33-activated dendritic cells are critical for allergic airway inflammation. *J. Immunol.*, 41(6):1675–1686, 2011.

[19] J. Bhattacharya and M. A. Matthay. Regulation and repair of the alveolar-capillary barrier in acute lung injury. *Annu. Rev. Physiol*, 75:593–615, 2013.

[20] K. Bode, F. Schmitz, L. Vargas, K. Heeg, and A. H. Dalpke. Kinetic of RelA activation controls magnitude of TLR-mediated IL-12p40 induction. *J. Immunol.*, 182(4):2176–2184, 2009.

[21] S. W. Brubaker, K. S. Bonham, I. Zanoni, and J. C. Kagan. Innate immune pattern recognition: A cell biological perspective. *Annu. Rev. Immunol.*, 33, 2015.

[22] M. Bruewer, M. Utech, A. I. Ivanov, A. M. Hopkins, C. A. Parkos, and A. Nusrat. Interferon-gamma induces internalization of epithelial tight junction proteins via a macropinocytosis-like process. *FASEB*, 19(8):923–933, 2005.

[23] D. V. Bullen, R. Darwiche, D. Metcalf, E. Handman, and W. S. Alexander. Neutralization of interferon-gamma in neonatal SOCS1-/- mice prevents fatty degeneration of the liver but not subsequent fatal inflammatory disease. *Immunology*, 104(1):92–98, 2001.

[24] M. E. Burnham, C. J. Koziol-White, S. Esnault, M. E. Bates, M. D. Evans, P. J. Bertics, and L. C. Denlinger. Human airway eosinophils exhibit preferential reduction in STAT signaling capacity and increased CISH expression. *J. Immunol.*, 191(6):2900–2906, 2013.

[25] C. Cayrol and J. P. Girard. IL-33: An alarmin cytokine with crucial roles in innate immunity, inflammation and allergy. *Curr. Opin. Immunol.*, 31:31–37, 2014.

[26] Y.-J. Chang, H. Y. Kim, L. A. Albacker, N. Baumgarth, A. N. J. McKenzie, D. E. Smith, R. H. Dekruyff, and D. T. Umetsu. Innate lymphoid cells mediate influenza-induced airway hyperreactivity independently of adaptive immunity. *Nat. Immunol.*, 12(7):631–638, 2011.

[27] V. Chau, J. W. Tobias, A. Bachmair, D. Marriotr, D. J. Ecker, D. K. Gonda, and A. Varshavsky. A multiubiquitin chain is confined to specific lysine in a targeted short-lived protein. *Science*, 243(1982):1576–1583, 1989.

[28] J. Chen and Z. J. Chen. Regulation of NF-κB by Ubiquitination. *Curr. Opin. Immunol.*, 25(1):4–12, 2013.

[29] X. P. Chen, J. A. Losman, S. Cowan, E. Donahue, S. Fay, B. Q. Vuong, M. C. Nawijn, D. Capece, V. L. Cohan, and P. Rothman. Pim serine/threonine kinases regulate the stability of Socs-1 protein. *PNAS*, 99(4):2175–2180, 2002.

[30] H. Cheon and G. R. Stark. Unphosphorylated STAT1 prolongs the expression of interferon-induced immune regulatory genes. *PNAS*, 106(23):9373–9378, 2009.

[31] M. Chevrier, D. Bobbala, A. Villalobos-Hernandez, M. Gulam, M. Khan, S. Ramanathan, C. Saucier, G. Ferbeyre, S. Geha, and S. Ilangumaran. Expression of SOCS1 and the downstream targets of its putative tumor suppressor functions in prostate cancer. *BMC Cancer*, 17:1–14, 2017.

[32] J. M. Ciencewicki, L. E. Brighton, and I. Jaspers. Localization of Type I Interferon Receptor Limits Interferon-Induced TLR3 in Epithelial Cells. *J. Interferon & Cytokine Res.*, 29(5):289–297, 2009.

[33] C. Coban, Y. Igari, M. Yagi, T. Reimer, S. Koyama, T. Aoshi, K. Ohata, T. Tsukui, F. Takeshita, K. Sakurai, T. Ikegami, A. Nakagawa, T. Horii, G. Nuñez, K. J. Ishii, and S. Akira. Immunogenicity of Whole-Parasite Vaccines against Plasmodium falciparum Involves Malarial Hemozoin and Host TLR9. *Cell Host Microbe*, 7(1):50–61, 2010.

[34] S. Commins, J. W. Steinke, and L. Borish. The extended IL-10 superfamily: IL-10, IL-19, IL-20, IL-22, IL-24, IL-26, IL-28, and IL-29. *J. Allergy Clin. Immunol.*, 121(5):1108–1111, 2008.

[35] M. Contoli, S. D. Message, V. Laza-Stanca, M. R. Edwards, P. A. B. Wark, N. W. Bartlett, T. Kebadze, P. Mallia, L. A. Stanciu, H. L. Parker, L. Slater, A. Lewis-Antes, O. M. Kon, S. T. Holgate, D. E. Davies, S. V. Kotenko, A. Papi, and S. L. Johnston. Role of deficient type III interferon-λ production in asthma exacerbations TL - 12. *Nat. Med.*, 12(9):1023–1026, 2006.

[36] S. Cording, J. Medvedovic, M. Cherrier, and G. Eberl. Development and regulation of RORγt+ innate lymphoid cells. *FEBS Lett.*, 588(22):4176–4181, 2014.

[37] A. L. Cornish, G. M. Davey, D. Metcalf, J. F. Purton, Corbin J. E., C. J. Greenhalgh, R. Darwiche, L. Wu, N. A. Nicola, D. I. Godfrey, W. Heath, D. J. Hilton, W. S. Alexander, and R. Starr. Suppressor of cytokine signaling-1 has IFN-γ-independent actions in T cell homeostasis. *J. Immunol.*, 170(2), 2003.

[38] A. J. Coyle, C. Lloyd, J. Tian, T. Nguyen, C. Erikkson, L. Wang, P. Ottoson, P. Persson, T. Delaney, S. Lehar, S. Lin, L. Poisson, C. Meisel, T. Kamradt, T. Bjerke, D. Levinson, and J. C. Gutierrez-Ramos. Crucial role of the interleukin 1 receptor family member T1/ST2 in T helper cell type 2-mediated lung mucosal immune responses. *J. Exp. Med.*, 190(7):895–902, 1999.

[39] X. Cui, X. Shan, J. Qian, Q. Ji, L. Wang, X. Wang, M. Li, H. Ding, Q. Liu, L. Chen, D. Zhang, and R. Ni. The suppressor of cytokine signaling SOCS1 promotes apoptosis of intestinal epithelial cells via p53 signaling in Crohn's Disease. *Exp. Mol. Path.*, 101(1):1–11, 2016.

[40] A. H. Dalpke, S. Eckerle, M. Frey, and K. Heeg. Triggering of toll-like receptors modulates IFN signalling: Involvement of serine 727 STAT1 phosphorylation and suppressors of cytokine signaling. *J. Immunol.*, 33(7):1776–1787, 2003.

[41] A. H. Dalpke, S. Opper, S. Zimmermann, and K. Heeg. Suppressors of cytokine signaling (SOCS)-1 and SOCS-3 are induced by CpG-DNA and modulate cytokine responses in APCs. *J. Immunol.*, 166(12):7082–9, 2001.

[42] J. E. Darnell. STATs and gene regulation. *Science*, 277(5332):1630–1635, 1997.

[43] J. E. Jr. Darnell, I. M. Kerr, and G. R. Stark. Jak-STAT pathways and transcriptional activation in response to IFNs and other extracellular signaling proteins. *Science*, 264(5164):1415–1421, 1994.

[44] P. Dasgupta, N. Dorsey, J. Li, X. Qi, E. Smith, K. Yamaji-Kegan, and A. Keegan. The adaptor protein insulin receptor substrate 2 inhibits alternative macrophage activation and allergic lung inflammation. *Science*, 9(433):63, 216.

[45] S. Dastgheib, C. Irajie, R. Assaei, F. Koohpeima, and P. Mokarram. Optimization of RNA Extraction from Rat Pancreatic Tissue. *J. Med. Sci.*, 39(3):282–288, 2014.

[46] D. Davidson, F. Kilanowski, S. Randall, D. Sheppard, and J. Dorin. A primary culture model of differentiated murine tracheal epithelium. *Am. J. Physiol.*, 279:766 – 778, 2000.

[47] D. J. Davidson, M. A. Gray, F. M. Kilanowski, R. Tarran, S. H. Randell, D. N. Sheppard, B. E. Argent, and J. R. Dorin. Murine epithelial cells: Isolation and culture. *J. Cyst. Fibros.*, 3(2):59–62, 2004.

[48] T. Decker and P. Kovarik. Serine phosphorylation of STATs. *Oncogene*, 19(21):2628–37, 2000.

[49] S. S. Deo, K. J. Mistry, A. M. Kakade, and P. V. Niphadkar. Role played by Th2 type cytokines in IgE mediated allergy and asthma. *Lung*, 27(2):66–71, 2010.

[50] G. Diamond, D. Legarda, and L. K. Ryan. The innate immune response of the respiratory epithelium. *Immunology Rev*, 173:27–38, 2000.

[51] H. Dickensheets, N. Vazquez, F. Sheikh, S. Gingras, P. J. Murray, J. J. Ryan, and R. P. Donnelly. Suppressor of cytokine signaling-1 is an IL-4-inducible gene in macrophages and feedback inhibits IL-4 signaling. *Genes and Immunity*, 8(1):21–27, 2007.

[52] R. P. Dickson and G. B. Huffnagle. The Lung Microbiome: New Principles for Respiratory Bacteriology in Health and Disease. *PLOS Pathog.*, 11(7):e1004923, 2015.

[53] A. Diefenbach, M. Colonna, and S. Koyasu. Development, differentiation, and diversity of innate lymphoid cells. *Immunity*, 41(3):354–365, 2014.

[54] S. Diehl, J. Anguita, A. Hoffmeyer, T. Zapton, J. N. Ihle, E. Fikrig, and M. Rincón. Inhibition of Th1 differentiation by IL-6 is mediated by SOCS1. *Immunity*, 13(6):805–815, 2000.

[55] V. Dolgachev, B. C. Petersen, A. L. Budelsky, A. A. Berlin, and N. W. Lukacs. Pulmonary IL-17E (IL-25) production and IL-17RB+ myeloid cell-derived Th2 cytokine production are dependent upon stem cell factor-induced responses during chronic allergic pulmonary disease. *J. Immunol.*, 183(9):5705–5715, 2009.

[56] R. Dong, L. Xie, K. Zhao, Q. Zhang, M. Zhou, and P. He. Cigarette smoke-induced lung inflammation in COPD mediated via LTB4 / BLT1 / SOCS1 pathway. *Int. J. COPD*, 11:31–41, 2016.

[57] E. Doran, D. F. Choy, A. Shikotra, C. A. Butler, D. M. O'Rourke, J. A. Johnston, A. Kissenpfennig, P. Bradding, J. R. Arron, and L. G. Heaney. Reduced epithelial suppressor of cytokine signalling 1 in severe eosinophilic asthma. *Eur. Respir. J.*, 3(48):715–25, 2016.

[58] M. E. Eberle and A. H. Dalpke. Dectin-1 Stimulation Induces Suppressor of Cytokine Signaling 1, Thereby Modulating TLR Signaling and T Cell Responses. *J Immunology*, 188(11):5644–5654, 2012.

[59] J. Eberwine, H. Yeh, K. Miyashiro, Y. Cao, S. Nair, R. Finnell, M. Zettel, and P. Coleman. Analysis of gene expression in single live neurons. *PNAS*, 89(7):3010–3014, 1992.

[60] P. J. Egan, K. E. Lawlor, W. S. Alexander, and I. P. Wicks. Suppressor of cytokine signaling-1 regulates acute inflammatory arthritis and t cell activation. *J. Clinical Investigation*, 111(6):915–924, 2003.

[61] C. E. Egwuagu, C.-R. Yu, M. Zhang, R. M. Mahdi, S. J. Kim, and I. Gery. Suppressors of cytokine signaling proteins are differentially expressed in Th1 and Th2 cells: implications for Th cell lineage commitment and maintenance. *J Immunology*, 168(7):3181–3187, 2002.

[62] T. Endo, M. Masuhara, M. Yokouchi, R. Suzuki, H. Sakamoto, K. Mitsui, A. Matsumoto, S. Tanimura, M. Ohtsubo, H. Misawa, T. Miyazaki, N. Leonor, T. Taniguchi, T. Fujita, Y. Kanakura, S. Komiya, and A. Yoshimura. A new protein containing an SH2 domain that inhibits JAK kinases. *Nature*, 387(6636):921–924, 1997.

[63] M. M. Epstein. Do Mouse Models of Allergic Asthma Mimic Clinical Disease? *Int. Arch. Allergy Immunol.*, 133(1):84–100, 2004.

[64] J. L. Eyles, D. Metcalf, M. J. Grusby, D. J. Hilton, and R. Starr. Negative regulation of interleukin-12 signaling by suppressor of cytokine signaling-1. *J. Biol. Chem.*, 277(46):43735–43740, 2002.

[65] F. Fallarino, U. Grohmann, C. Vacca, R. Bianchi, C. Orabona, A. Spreca, M. C. Fioretti, and P. Puccetti. T cell apoptosis by tryptophan catabolism. *Cell Death Differ.*, 9(10):1069–1077, 2002.

[66] P. G. Fallon, S. J. Ballantyne, N. E. Mangan, J. L. Barlow, A. Dasvarma, D. R. Hewett, A. McIlgorm, H. E. Jolin, and A. N. J. McKenzie. Identification of an interleukin (IL)-25-dependent cell population that provides IL-4, IL-5, and IL-13 at the onset of helminth expulsion. *J. Exp. Med.*, 203(4):1105–1116, 2006.

[67] M. Federici, M. L. Giustizieri, C. Scarponi, G. Girolomoni, and C. Albanesi. Impaired IFN-γ-dependent inflammatory responses in human keratinocytes overexpressing the suppressor of cytokine signaling 1. *J. Immunol.*, 169(1):434–442, 2002.

[68] J. E. Fenner, R. Starr, A. L. Cornish, J.-G. Zhang, D. Metcalf, R. D. Schreiber, K. Sheehan, D. J. Hilton, W. S. Alexander, and P. J. Hertzog. Suppressor of cytokine signaling 1 regulates the immune response to infection by a unique inhibition of type i interferon activity. *Nature Immunology*, 7(1):33–39, 2006.

[69] P. Flodby, Z. Borok, A. Banfalvi, B. Zhou, D. Gao, P. Minoo, D. K. Ann, E. E. Morrisey, and E. D. Crandall. Directed expression of Cre in alveolar epithelial type 1 cells. *Am. J. Respir. Cell Mol. Biol.*, 43(2):173–178, 2010.

[70] M. M. Fort, J. Cheung, D. Yen, J. Li, S. M. Zurawski, S. Lo, S. Menon, T. Clifford, B. Hunte, R. Lesley, T. Muchamuel, S. D. Hurst, G. Zurawski, M. W. Leach, Daniel M. Gorman, and Donna M. Rennick. IL-25 Induces IL-4, IL-5, and IL-13 and Th2-associated pathologies in vivo. *Immunity*, 15(6):985–995, 2001.

[71] J. M. Fox, J. M. Crabtree, L. K. Sage, S. M. Tompkins, and R. A. Tripp. Interferon Lambda Upregulates IDO1 Expression in Respiratory Epithelial Cells After Influenza Virus Infection. *J. Interf. Cytokine Res.*, 35(7):554–562, 2015.

[72] M. Fujimoto, H. Tsutsui, S. Yumikura-Futatsugi, H. Ueda, O. Xingshou, T. Abe, I. Kawase, K. Nakanishi, T. Kishimoto, and T. Naka. A regulatory role for suppressor of cytokine signaling-1 in T(h) polarization in vivo. *Immunology*, 14(11):1343–50, 2002.

[73] S. Fukuyama, T. Nakano, T. Matsumoto, B. G. G. Oliver, J. K. Burgess, A. Moriwaki, K. Tanaka, M. Kubo, T. Hoshino, H. Tanaka, A. N. J. McKenzie, K. Matsumoto, H. Aizawa, Y. Nakanishi, A. Yoshimura, J. L. Black, and H. Inoue. Pulmonary Suppressor of Cytokine Signaling-1 Induced by IL-13 Regulates Allergic Asthma Phenotype. *Am. J. Respir. Crit. Care Med.*, 179(11):992–998, 2009.

[74] T. Gaj, C. A. Gersbach, and C. F. Barbas. ZFN, TALEN and CRISPR/Cas-based methods for genome engineering. *Trends Biotechnol.*, 31(7):397–405, 2013.

[75] S. N. Georas and F. Rezaee. Epithelial barrier function: at the front line of asthma immunology and allergic airway inflammation. *J. Allergy Clin. Immunol.*, 134(3):509–520, 2014.

[76] C. X. George, S. Das, and C. E. Samuel. Organization of the mouse RNA-specific adenosine deaminase Adar1 gene 5'-region and demonstration of STAT1-independent, STAT2-dependent transcriptional activation by interferon. *Virology*, 380(2):338–343, 2008.

[77] M. Gereke, A. Autengruber, L. Gröbe, A. Jeron, D. Bruder, and S. Stegemann-Koniszewski. Flow cytometric isolation of primary murine type II alveolar epithelial cells for functional and molecular studies. *J. Vis. Exp.*, 70:4322, 2012.

[78] S. Ghosh and M. S. Hayden. New regulators of NF-kappaB in inflammation. *Nat. Rev. Immunol.*, 8(11):837–848, 2008.

[79] V. Gielen, A. Sykes, J. Zhu, B. Chan, J. Macintyre, N. Regamey, E. Kieninger, A. Gupta, A. Shoemark, C. Bossley, J. Davies, S. Saglani, P. Walker, S. E. Nicholson, A. H. Dalpke, O.-M. Kon, A. Bush, S. L. Johnston, and M. R. Edwards. Increased nuclear suppressor of cytokine signaling 1 in asthmatic bronchial epithelium suppresses rhinovirus induction of innate interferons. *J. Allergy Clin. Immunol.*, 136(1):177–188, 2015.

[80] M. P. Gil, E. Bohn, A. K. O'Guin, C. V. Ramana, B. Levine, G. R. Stark, H. W. Virgin, and R. D. Schreiber. Biologic consequences of Stat1-independent IFN signaling. *PNAS*, 98(12):6680–5, 2001.

[81] F. Giordanetto and R. T. Kroemer. A three-dimensional model of Suppressor Of Cytokine Signalling 1 (SOCS-1). *Protein engineering*, 16(2):115–24, 2003.

[82] A. H. Gitter, K. Bendfeldt, J. D. Schulzke, and M. Fromm. Leaks in the epithelial barrier caused by spontaneous and TNF-alpha-induced single-cell apoptosis. *FASEB*, 14(12):1749–1753, 2000.

[83] M. H. Glickman and A. Ciechanover. The Ubiquitin-Proteasome Proteolytic Pathway: Destruction for the Sake of Construction. *Physiol. Rev*, 82(2):373–428, 2002.

[84] G. Gottrand, T. Courau, V. Thomas-Vaslin, N. Prevel, T. Vazquez, M. G. Ruocco, B. Lambrecht, B. Bellier, B. M. Colombo, and D. Klatzmann. Regulatory T-cell development and function are impaired in mice lacking membrane expression of full length intercellular adhesion molecule-1. *Immunology*, 146(4):657–670, 2015.

[85] C. L. Grainge and D. E. Davies. Epithelial injury and repair in airways diseases. *Chest*, 144(6):1906–1912, 2013.

[86] Catherine M Greene and Noel G Mcelvaney. Toll-like receptor expression and function in airway epithelial cells. *Archiv Immunol. Exp. Therapy*, 53:418–427, 2005.

[87] C. J. Greenhalgh and D. J. Hilton. Negative regulation of cytokine signaling. *J. Leuko. Biol.*, 70(3):348–356, 2001.

[88] A. C. Greenlund, M. A. Farrar, B. L. Viviano, and R. D. Schreiber. Ligand-induced IFN-γ receptor tyrosine phosphorylation couples the receptor to its signal transduction system (p91). *EMBO J.*, 1(1):591–1600, 1994.

[89] A. Gregorieff, S. Pyronnet, N. Sonenberg, and A. Veillette. Regulation of SOCS-1 expression by translational repression. *J biological chemistry*, 275(28):21596–21604, 2000.

[90] U. Grohmann, F. Fallarino, and P. Puccetti. Tolerance, DCs and tryptophan: Much ado about IDO. *Trends Immunol.*, 24(5):242–248, 2003.

[91] A. M. Groves, C. J. Johnston, R. S. Misra, J. P. Williams, and J. N. Finkelstein. Whole-Lung Irradiation Results in Pulmonary Macrophage Alterations that are Subpopulation and Strain Specific. *Radiation Res.*, 184(6):639–649, 2015.

[92] X. Gu, J. P. Cantle, E. R. Greiner, C. Y. D. Lee, A. M. Barth, F. Gao, C. S. Park, Z. Zhang, S. Sandoval-Miller, R. L. Zhang, M. Diamond, I. Mody, G. Coppola, and X. W. Yang. N17 Modifies Mutant Huntingtin Nuclear Pathogenesis and Severity of Disease in HD BAC Transgenic Mice. *Neuron*, 85(4):726–741, 2015.

[93] M. M. Gueders, G. Paulissen, C. Crahay, F. Quesada-Calvo, J. Hacha, C. Van Hove, K. Tournoy, R. Louis, J. M. Foidart, A. Noël, and D. D. Cataldo. Mouse models of asthma: A comparison between C57BL/6 and BALB/c strains regarding bronchial responsiveness, inflammation, and cytokine production. *Inflamm. Res.*, 58(12):845–854, 2009.

[94] C. Guiducci, M. Gong, A. Cepika, Z. Xu, C. Tripodo, L. Bennett, C. Crain, P. Quartier, J. J. Cush, V. Pascual, R. L. Coffman, and F. J. Barrat. RNA recognition by human TLR8 can lead to autoimmune inflammation. *J. Exp. Med.*, 210(13):2903–19, 2013.

[95] L. Guillott, S. Medjane, K. Le-Barillec, V. Balloy, C. Danel, M. Chignard, and M. Si-Tahar. Response of human pulmonary epithelial cells to lipopolysaccharide involves toll-like receptor 4 (TLR4)-dependent signaling pathways: Evidence for an intracellular compartmentalization of TLR4. *J. Biol. Chem.*, 279(4):2712–2718, 2004.

[96] M. Gury-BenAri, C. A. Thaiss, N. Serafini, D. R. Winter, A. Giladi, D. Lara-Astiaso, M. Levy, T. M. Salame, A. Weiner, E. David, H. Shapiro, M. Dori-Bachash, M. Pevsner-Fischer, E. Lorenzo-Vivas, H. Keren-Shaul, F. Paul, A. Harmelin, G. Eberl, S. Itzkovitz, A. Tanay, J. P. Di Santo, E. Elinav, and I. Amit. The Spectrum and Regulatory Landscape of Intestinal Innate Lymphoid Cells Are Shaped by the Microbiome. *Cell*, 166(5):1231–1246.e13, 2016.

[97] M. C. Haffner, A. Jurgeit, C. Berlato, S. Geley, N. Parajuli, A. Yoshimura, and W. Doppler. Interaction and functional interference of glucocorticoid receptor and SOCS1. *J. Biol. Chem.*, 283(32):22089–22096, 2008.

[98] T. Y. F. Halim, C. A. Steer, L. Mathä, M. J. Gold, I. Martinez-Gonzalez, K. M. McNagny, A. N. J. McKenzie, and F. Takei. Group 2 innate lymphoid cells are critical for the initiation of adaptive T helper 2 cell-mediated allergic lung inflammation. *Immunity*, 40(3):425–435, 2014.

[99] H. Hammad, M. Chieppa, F. Perros, M. A. Willart, R. N. Germain, and B. N. Lambrecht. House dust mite allergen induces asthma via TLR4 triggering of airway structural cells. *Nature Med.*, 15(4):410–416, 2009.

[100] T. Hanada, H. Yoshida, S. Kato, K. Tanaka, K. Masutani, J. Tsukada, Y. Nomura, H. Mimata, M. Kubo, and A. Yoshimura. Suppressor of cytokine signaling-1 is essential for suppressing dendritic cell activation and systemic autoimmunity. *Immunity*, 19(3):437–450, 2003.

[101] M. Harada, K. Nakashima, T. Hirota, M. Shimizu, S. Doi, K. Fujita, T. Shirakawa, T. Enomoto, M. Yoshikawa, H. Moriyama, K. Matsumoto, H. Saito, Y. Suzuki, Y. Nakamura, and M. Tamari. Functional polymorphism in the suppressor of cytokine signaling 1 gene associated with adult asthma. *Am. J. Resp. Cell Mol. Biol.*, 36(4):491–496, 2007.

[102] J. K. Harris, M. A. De Groote, S. D. Sagel, E. T. Zemanick, R. Kapsner, C. Penvari, H. Kaess, R. R. Deterding, F. J. Accurso, and N. R. Pace. Molecular identification of bacteria in bronchoalveolar lavage fluid from children with cystic fibrosis. *PNAS*, 104(51):20529–33, 2007.

[103] L. A. Hart, V. L. Krishnan, I. M. Adcock, P. J. Barnes, and K. F. Chung. Activation and localization of transcription factor, nuclear factor-kappaB, in asthma. *Am. J. Respir. Crit. Care Med.*, 158(5):1585–1592, 1998.

[104] D. Hashimoto, C. Chow, A.and Noizat, P. Teo, M. Beth, M. Leboeuf, C. D. Becker, P. See, J. Price, D. Lucas, M. Greter, A. Mortha, S. W. Boyer, and E Camilla. Adult Life With Minimal Contribution From Circulating Monocytes. *Tissue*, 38(4), 2014.

[105] E. Haspeslagh, N. Debeuf, H. Hammad, and B. N. Lambrecht. Murine Models of Allergic Asthma. *Methods Mol. Biol.*, 1559:121–136, 2017.

[106] Y. He, W. Zhang, R. Zhang, H. Zhang, and W. Min. SOCS1 inhibits tumor necrosis factor-induced activation of ASK1-JNK inflammatory signaling by mediating ASK1 degradation. *J. Biol. Chem.*, 281(9):5559–5566, 2006.

[107] M. B. Headley, B. Zhou, W. X. Shih, T. Aye, M. R. Comeau, and S. F. Ziegler. TSLP conditions the lung immune environment for the generation of pathogenic innate and antigen-specific adaptive immune responses. *J. Immunol.*, 182(3):1641–7, 2009.

[108] D. Hebenstreit, P. Luft, A. Schmiedlechner, A. Duschl, and J. Horejs-Hoeck. SOCS-1 and SOCS-3 inhibit IL-4 and IL-13 induced activation of Eotaxin-3/CCL26 gene expression in HEK293 cells. *Mol. Immunol.*, 42(3):295–303, 2005.

[109] F. Heil, P. Ahmad-Nejad, H. Hemmi, H. Hochrein, F. Ampenberger, T. Gellert, H. Dietrich, G. Lipford, K. Takeda, S. Akira, H. Wagner, and S. Bauer. The Toll-like receptor 7 (TLR7)-specific stimulus loxoribine uncovers a strong relationship within the TLR7, 8 and 9 subfamily. *J. Immunol.*, 33(11):2987–2997, 2003.

[110] M. H. Heim, D. Moradpour, and H. E. Blum. Expression of hepatitis C virus proteins inhibits signal transduction through the Jak-STAT pathway. *J.Virol.*, 73:8469–8475, 1999.

[111] N. Heintz. BAC to the future: the use of bac transgenic mice for neuroscience research. *Nat. Rev.*, 2(12):861–870, 2001.

[112] F. P. Heinzel, M. D. Sadick, B. J. Holaday, R. L. Coffman, and R. M. Locksley. Reciprocal expression of interferon gamma or interleukin 4 during the resolution or progression of murine leishmaniasis. Evidence for expansion of distinct helper T cell subsets. *J. Exp. Med.*, 169(1):59–72, 1989.

[113] F. Heller, P. Florian, C. Bojarski, J. Richter, M. Christ, B. Hillenbrand, J. Mankertz, A. H. Gitter, N. Burgel, M. Fromm, M. Zeitz, I. Fuss, W. Strober, and J. D. Schulzke. Interleukin-13 is the key effector Th2 cytokine in ulcerative colitis that affects epithelial tight junctions, apoptosis, and cell restitution. *Gastroenterology*, 129(2):550–564, 2005.

[114] L. Heyen, U. Müller, S. Siegemund, B. Schulze, M. Protschka, G. Alber, and D. Piehler. Lung epithelium is the major source of IL-33 and is regulated by IL-33-dependent and IL-33-independent mechanisms in pulmonary cryptococcosis. *Pathog. Dis.*, 74(7):ftw086, 2016.

[115] D. J. Hilton, R. T. Richardson, W. S. Alexander, E. M. Viney, T. A. Willson, N. S. Sprigg, R. Starr, S. E. Nicholson, D. Metcalf, and N. A. Nicola. Twenty proteins containing a C-terminal SOCS box form five structural classes. *PNAS*, 95(1):114–119, 1998.

[116] M. Hilty, C. Burke, H. Pedro, P. Cardenas, A. Bush, C. Bossley, J. Davies, A. Ervine, L. Poulter, L. Pachter, M. F. Moffatt, and W. O. C. Cookson. Disordered microbial communities in asthmatic airways. *PLoS One*, 5(1):e8578, 2010.

[117] J. Horino, M. Fujimoto, F. Terabe, S. Serada, T. Takahashi, Y. Soma, K. Tanaka, T. Chinen, A. Yoshimura, S. Nomura, I. Kawase, N. Hayashi, T. Kishimoto, and T. Naka. Suppressor of cytokine signaling-1 ameliorates dextran sulfate sodium-induced colitis in mice. *Immunology*, 20(6):753–762, 2008.

[118] C. M. Horvath. STAT proteins and transcriptional responses to extracellular signals. *Trends Biochem. Sci.*, 25(10):496–502, 2000.

[119] T. Hoyler, C. S. N. Klose, A. Souabni, A. Turqueti-Neves, D. Pfeifer, E. L. Rawlins, D. Voehringer, M. Busslinger, and A. Diefenbach. The transcription factor GATA3 controls cell fate and maintenance of type 2 innate lymphoid cells. *Immunity*, 37(4):634–648, 2012.

[120] M. Huang, W. Zhang, J. Guo, X. Wei, K. Phiwpan, and J. Zhang. Improved Transgenic Mouse Model for Studying HLA Class I Antigen Presentation. *Nature*, pages 1–12, 2016.

[121] S. D. Hurst, T. Muchamuel, D. M. Gorman, J. M. Gilbert, T. Clifford, S. Kwan, S. Menon, B. Seymour, C. Jackson, T. T. Kung, J. K. Brieland, S. M. Zurawski, R. W. Chapman, G. Zurawski, and R. L. Coffman. New IL-17 Family Members Promote Th1 or Th2 Responses in the Lung: In Vivo Function of the Novel Cytokine IL-25. *J. Immunol.*, 169(1):443–453, 2002.

[122] T. Hussell and T. J. Bell. Alveolar macrophages: plasticity in a tissue-specific context. *Nature Rev.*, 14(2):81–93, 2014.

[123] K. I. Igarashi, G. Garotta, L. Ozmen, A. Ziemiecki, A. F. Wilks, A. G. Harpur, A. C. Larner, and D. S. Finbloom. Interferon-gamma induces tyrosine phosphorylation of interferon-ganna receptor and regulated association of protein tyrosine kinases, Jak1 and Jak2, with its receptor. *J. Biol. Chem.*, 260(20):14333–6, 1994.

[124] J. N. Ihle. The Janus Kinase Family and Signaling Through Members of the Cytokine Receptor Superfamily. *Exp. Biol. Med.*, 206(3):268–272, 1994.

[125] K. Inagaki-Ohara, T. Kondo, M. Ito, and A. Yoshimura. SOCS, inflammation, and cancer. *Jak-Stat*, 2(3):e24053, 2013.

[126] K. Inagaki-Ohara, a. Sasaki, G. Matsuzaki, T. Ikeda, M. Hotokezaka, K. Chijiiwa, M. Kubo, H. Yoshida, Y. Nawa, and a. Yoshimura. Suppressor of cytokine signalling 1 in lymphocytes regulates the development of intestinal inflammation in mice. *Gut*, 55(2):212–9, 2006.

[127] I. Ioannidis, F. Ye, B. McNally, M. Willette, and E. Flaño. Toll-like receptor expression and induction of type I and type III interferons in primary airway epithelial cells. *J. Virol.*, 87(6):3261–70, 2013.

[128] S. A. Islam and A. D. Luster. T cell homing to epithelial barriers in allergic disease. *Nat. Med.*, 18(5):705–715, 2012.

[129] S. H. Jackson, C. Yu, R. M. Mahdi, S. Ebong, and C. E. Egwuagu. Dendritic cell maturation requires STAT1 and is under feedback regulation by suppressors of cytokine signaling. *J. Immunol.*, 172:2307–2315, 2004.

[130] A. V. Jain, Y. Zhang, W. B. Fields, D. A. McNamara, M. Y. Choe, G. H. Chen, J. Erb-Downward, J. J. Osterholzer, G. B. Toews, G. B. Huffnagle, and M. A. Olszewski. Th2 but not th1 immune bias results in altered lung functions in a murine model of pulmonary cryptococcus neoformans infection. *Infect. Immun.*, 77(12):5389–5399, 2009.

[131] S. Joshi, S. Kaur, B. Kroczynska, and L. C. Platanias. Mechanisms of mRNA translation of interferon stimulated genes. *Cytokine*, 52(1-2):123–127, 2010.

[132] Abbas A. K., Lichtman A. H. H., and Pillai S. *Cellular and Molecular Immunology*. Elsevier, 8th edition, 2014.

[133] P. Kalinski. Regulation of Immune Responses by Prostaglandin E(2). *J. Immunol.*, 188(1):21–28, jan 2012.

[134] M. Kamio, T. Yoshida, H. Ogata, T. Douchi, Y. Nagata, M. Inoue, M. Hasegawa, Y. Yonemitsu, and A. Yoshimura. SOCS1 inhibits HPV-E7-mediated transformation by inducing degradation of E7 protein. *Oncogene*, 23(17):3107–3115, 2004.

[135] T. Kamura, K. Maenaka, S. Kotoshiba, and M. Matsumoto. VHL-box and SOCS-box domains determine binding specificity for Cul2 – Rbx1 and Cul5 – Rbx2 modules of ubiquitin ligases. *Genes & Development*, 2:3055–3065, 2004.

[136] T. Kamura, S. Sato, D. Haque, L. Liu, W. G. Jr. Kaelin, R. C. Conaway, and J. W. Conaway. The Elongin BC complex interacts with the conserved SOCS-box motif present in members of the SOCS, ras, WD-40 repeat, and ankyrin repeat families. *Genes & Development*, 12(24):3872–3881, 1998.

[137] E. Keil, D. Finkenstadt, C. Wufka, M. Trilling, P. Liebfried, B. Strobl, M. Muller, and K. Pfeffer. Important scaffold function of the Janus kinase 2 uncovered by a novel mouse model harboring a Jak2 activation-loop mutation. *Blood*, 123(4):520–529, 2014.

[138] B.T. Kile, B. Schulman, W. S. Alexander, N. Nicola, H. M. E. Martin, and D. J. Hilton. The SOCS box: A tale of destruction and degradation. *Trends Biochem. Sci.*, 27(5):235–241, 2002.

[139] I. Kinjyo, T. Hanada, K. Inagaki-Ohara, H. Mori, D. Aki, M. Ohishi, H. Yoshida, M. Kubo, and A. Yoshimura. SOCS1/JAB is a negative regulator of LPS-induced macrophage activation. *Immunity*, 17(5):583–591, 2002.

[140] S. Kiryu-Seo, H. Tamada, Y. Kato, K. Yasuda, N. Ishihara, K. Nomura, M.and Mihara, H. Kiyama, Y. Cho, R. Sloutsky, K. M. Naegle, V. Cavalli, S. Kiryu-Seo, S. Nakagomi, Y. Suzuki, K. Namikawa, S. Kiryu-Seo, H. Kiyama, K. Namikawa, S. Patodia, G. Raivich, G. Raivich, M. Makwana, S. Kiryu-Seo, K. Gamo, T. Tachibana, K. Tanaka, H. Kiyama, S. Kiryu-Seo, T. Hirayama, R. Kato..., and Y. Xie. Mitochondrial fission is an acute and adaptive response in injured motor neurons. *Scientific Reports*, 6:28331, 2016.

[141] M. Kitajima, H.-C. Lee, T. Nakayama, and S. F. Ziegler. TSLP enhances the function of helper type2 cells. *J. Immunol.*, 41(7):1862 – 1871, 2011.

[142] M. Kitajima, H.-C. Lee, and S. Ziegler. TSLP enhances the function of helper type2 cells. *J. Immunol.*, 41(7):1862 – 1871, 2011.

[143] C. Koelsche, J. Strebovsky, A. Baetz, and A. H. Dalpke. Alveolar macrophage in the driver's seat. *Mol. Immunol.*, 24, 2006.

[144] J. E. Kohlmeier, M. A. Chan, and S. H. Benedict. Costimulation of naive human CD4+ T cells through intercellular adhesion molecule-1 promotes differentiation to a memory phenotype that is not strictly the result of multiple rounds of cell division. *Immunology*, 118(4):549–558, 2006.

[145] M. Kool, M. A. M. Willart, M. van Nimwegen, I. Bergen, P. Pouliot, J. C. Virchow, N. Rogers, F. Osorio, C. Reis e Sousa, H. Hammad, and B. N. Lambrecht. An Unexpected Role for Uric Acid as an Inducer of T Helper 2 Cell Immunity to Inhaled Antigens and Inflammatory Mediator of Allergic Asthma. *Immunity*, 34(4):527–540, 2011.

[146] K. Kotowicz, R. E. Callard, N. J. Klein, and M. G. Jacobs. Interleukin-4 increases the permeability of human endothelial cells in culture. *Clin. Exp. Allergy*, 34(3):445–449, 2004.

[147] P. Kovarik, M. Mangold, K. Ramsauer, H. Heidari, R. Steinborn, A. Zotter, D. E. Levy, M. Müller, and T. Decker. Specificity of signaling by STAT1 depends on SH2 and C-terminal domains that regulate Ser727 phosphorylation, differentially affecting specific target gene expression. *EMBO J.*, 20(1-2), 2001.

[148] M. Kubo. Therapeutic hope for psoriasis offered by SOCS (suppressor of cytokine signaling) mimetic peptide. *Eur. J. Immunol.*, 43(7):1702–1705, 2013.

[149] J. A. Kummer, R. Broekhuizen, H. Everett, L. Agostini, L. Kuijk, F. Martinon, R. van Bruggen, and J. Tschopp. Inflammasome Components NALP 1 and 3 Show Distinct but Separate Expression Profiles in Human Tissues, Suggesting a Site-specific Role in the Inflammatory Response. *J. Histochem. Cytochem.*, 55(5):443–52, 2006.

[150] E. Kwidzinski, J. Bunse, O. Aktas, D. Richter, L. Mutlu, F. Zipp, R. Nitsch, and I. Bechmann. Indolamine 2,3-dioxygenase is expressed in the CNS and down-regulates autoimmune inflammation. *FASEB J.*, 19(10):1347–1349, 2005.

[151] M. J. LaFemina, K. M. Sutherland, T. Bentley, L. W. Gonzales, L. Allen, C. J. Chapin, D. Rokkam, K. A. Sweerus, L. G. Dobbs, P. L. Ballard, and J. A. Frank. Claudin-18 deficiency results in alveolar barrier dysfunction and impaired alveologenesis in mice. *Am. J. Respir. Cell Mol. Biol.*, 51(4):550–558, 2014.

[152] J. Larkin, C. M. Ahmed, T. D. Wilson, and H. M. Johnson. Regulation of Interferon Gamma Signaling by Suppressors of Cytokine Signaling and Regulatory T Cells. *Front. Immunol.*, 4:469, 2013.

[153] C. Lee, T. B. Kolesnik, I. Caminschi, A. Chakravorty, W. Carter, W. S. Alexander, J. Jones, G. P. Anderson, and S. E. Nicholson. Suppressor of cytokine signalling 1 (SOCS1) is a physiological regulator of the asthma response. *Clin. Exp. Allergy*, 39(6):897–907, 2009.

[154] G. K. Lee, H. J. Park, M. MacLeod, P. Chandler, D. H. Munn, and A. L. Mellor. Tryptophan deprivation sensitizes activated T cells to apoptosis prior to cell division. *Immunology*, 107(4):452–460, 2002.

[155] W. J. Leonard and J. J. O'Shea. JAKS AND STATS: Biological Implications. *Annu. Rev. Immunol.*, 16(1):293–322, 1998.

[156] C. P. Lim and X. Cao. Structure, function, and regulation of STAT proteins. *Mol. BioSystems*, 2(11):536–550, 2006.

[157] Y. Liu, A. Pattamatta, T. Zu, T. Reid, O. Bardhi, D. R. Borchelt, A. T. Yachnis, and L. P. W. Ranum. BAC Mouse Model with Motor Deficits and Neurodegenerative Features of ALS/FTD. *Neuron*, 90(3):521–534, 2016.

[158] M. Lohning, A. Stroehmann, A. J. Coyle, J. L. Grogan, S. Lin, J. C. Gutierrez-Ramos, D. Levinson, A. Radbruch, and T. Kamradt. T1/ST2 is preferentially expressed on murine Th2 cells, independent of interleukin 4, interleukin 5, and interleukin 10, and important for Th2 effector function. *PNAS*, 95(12):6930–6935, 1998.

[159] N. Lopez-Souza, G. Dolganov, R. Dubin, L. Sachs, L. Sassina, H. Sporer, S. Yagi, D. Schnurr, H. Boushey, and J. H. Widdicombe. Resistance of differentiated human airway epithelium to infection by rhinovirus. *Am. J. Physiology.*, 286(2):L373–L381, 2004.

[160] L.-F. Lu, M.P. Boldin, A. Chaudhry, L.-L. Lin, K. D. Taganov, T. Hanada, A. Yoshimura, D. Baltimore, and A. Y. Rudensky. Function of miR-146a in controlling Treg cell-mediated regulation of Th1 responses. *Cell*, 142(6):914–929, 2010.

[161] L. F. Lu, T. H. Thai, D. P. Calado, A. Chaudhry, M. Kubo, K. Tanaka, G. B. Loeb, H. Lee, A. Yoshimura, K. Rajewsky, and A. Y. Rudensky. Foxp3-Dependent MicroRNA155 Confers Competitive Fitness to Regulatory T Cells by Targeting SOCS1 Protein. *Immunity*, 30(1):80–91, 2009.

[162] L. P. Lunding, S. Webering, C. Vock, C. Wagner, C. Hölscher, and M. Wegmann. Poly(inosinic-cytidylic) Acid Triggered Exacerbation of Experimental Asthma Depends on IL-17A Produced by NK Cells. *J. Immunol.*, 194(12):5615–25, 2015.

[163] T. Y. Ma, M. A. Boivin, D. Ye, A. Pedram, and H. M. Said. Mechanism of TNFα modulation of Caco-2 intestinal epithelial tight junction barrier: role of myosin light-chain kinase protein expression. *Am. J. Physiology.*, 288(3):G422–30, 2005.

[164] T. Y. Ma, G. K. Iwamoto, N. T. Hoa, V. Akotia, A. Pedram, M. A. Boivin, and H. M. Said. TNF-alpha-induced increase in intestinal epithelial tight junction permeability requires NF-kappa B activation. *Am. J. Physiology.*, 286(3):G367–76, 2004.

[165] S. Madar, E. Harel, I. Goldstein, Y. Stein, I. Kogan-Sakin, I. Kamer, H. Solomon, E. Dekel, P. Tal, N. Goldfinger, G. Friedlander, and V. Rotter. Mutant p53 Attenuates the Anti-Tumorigenic Activity of Fibroblasts-Secreted Interferon Beta. *PLoS ONE*, 8(4):e61353, 2013.

[166] J. L. Madara. Epithelial cells develop membrane wounds-and recover! *Gastroenterology*, 96(5):1360–1361, 1989.

[167] K. B. Madden, L. Whitman, C. Sullivan, W. C. Gause, J. F. Jr. Urban, I. M. Katona, F. D. Finkelman, and T. Shea-Donohue. Role of STAT6 and mast cells in IL-4- and IL-13-induced alterations in murine intestinal epithelial cell function. *J. Immunol.*, 169(8):4417–4422, 2002.

[168] G. N. Maine, X. Mao, C. M. Komarck, and E. Burstein. COMMD1 promotes the ubiquitination of NF-κB subunits through a Cullin-containing ubiquitin ligase. *EMBO J.*, 26(2):436–447, 2007.

[169] F. A. Mallette, V. Calabrese, S. Ilangumaran, and G. Ferbeyre. SOCS1, a novel interaction partner of p53 controlling oncogene-induced senescence. *Aging*, 2(7):445–452, jul 2010.

[170] G. Mancuso, M. Gambuzza, A. Midiri, C. Biondo, S. Papasergi, S. Akira, G. Teti, and C. Beninati. Bacterial recognition by TLR7 in the lysosomes of conventional dendritic cells. *Nature*, 10(6):587–594, 2009.

[171] A. Mansell, R. Smith, S. L. Doyle, P. Gray, J. E. Fenner, P. J. Crack, S. E. Nicholson, D. J. Hilton, L. A. J. O'Neill, and P. J. Hertzog. Suppressor of cytokine signaling 1 negatively regulates Toll-like receptor signaling by mediating Mal degradation. *Nature*, 7(2):148–155, 2006.

[172] C. W. Marano, S. A. Lewis, L. A. Garulacan, A. P. Soler, and J. M. Mullin. Tumor necrosis factor-alpha increases sodium and chloride conductance across the tight junction of CACO-2 BBE, a human intestinal epithelial cell line. *J. Membrane Biol.*, 161(3):263–274, 1998.

[173] J. C. Marine, D. J. Topham, C. McKay, D. Wang, E. Parganas, D. Stravopodis, A. Yoshimura, and J. N. Ihle. SOCS1 deficiency causes a lymphocyte-dependent perinatal lethality. *Cell*, 98(5):609–616, 1999.

[174] T. R. Martin and C. W Frevert. Innate immunity in the lungs. *Proc. Am. Thorac. Soc.*, 2(5):403–11, 2005.

[175] R. J. Mason. Biology of alveolar type II cells. *Respirology*, 11:1–5, 2006.

[176] M. Matsumoto, K. Funami, M. Tanabe, H. Oshiumi, M. Shingai, Y. Seto, A. Yamamoto, and T. Seya. Subcellular Localization of Toll-Like Receptor 3 in Human Dendritic Cells. *J. Immunol.*, 171(6):3154–3162, 2003.

[177] A. Mayer. *Basale immunmechanisms of airway epithelial cells.* Heidelberg, Univ., Diss., 2007.

[178] A. K. Mayer, J. Muehmer, M.and Mages, K. Gueinzius, C. Hess, K. Heeg, R. Bals, R. Lang, and A. H. Dalpke. Differential recognition of TLR-dependent microbial ligands in human bronchial epithelial cells. *J. Immunol.*, 178(5):3134–3142, 2007.

[179] S. M. McCormick, N. Gowda, J. X. Fang, and N. M. Heller. Suppressor of Cytokine Signaling (SOCS)1 Regulates IL-4-Activated Insulin Receptor Substrate (IRS)-2 Tyrosine Phosphorylation in Monocytes and Macrophages via the Proteasome. *J. Biol. Chem.*, pages 746–64, 2016.

[180] A. L. Mellor, B. Baban, P. Chandler, B. Marshall, K. Jhaver, A. Hansen, P. A. Koni, M. Iwashima, and D. H. Munn. Cutting edge: induced indoleamine 2,3 dioxygenase expression in dendritic cell subsets suppresses T cell clonal expansion. *J. Immunol.*, 171(4):1652–1655, 2003.

[181] D. Metcalf, S. Mifsud, L. Di Rago, N. Nicola, D. J. Hilton, and W. S. Alexander. Polycystic kidneys and chronic inflammatory lesions are the delayed consequences of loss of the suppressor of cytokine signaling-1 (socs-1). *PNAS*, 99(2):943–948, 2002.

[182] T. Meyer, A. Begitt, I. Lodige, M. van Rossum, and U. Vinkemeier. Constitutive and IFN-γ-induced nuclear import of STAT1 proceed through independent pathways. *EMBO J.*, 21(3):344–54, 2002.

[183] D. Miljkovic, A. Bassiouni, C. Cooksley, J. Ou, E. Hauben, P. J. Wormald, and S. Vreugde. Association between group 2 innate lymphoid cells enrichment, nasal polyps and allergy in chronic rhinosinusitis. *Eur. J. Allergy*, 69(9):1154–1161, 2014.

[184] J. M. Mjosberg, S. Trifari, N. K. Crellin, C. P. Peters, C. M. van Drunen, B. Piet, W. J. Fokkens, T. Cupedo, and H. Spits. Human IL-25- and IL-33-responsive type 2 innate lymphoid cells are defined by expression of CRTH2 and CD161. *Nat. Immunol.*, 12(11):1055–1062, 2011.

[185] L. A. Monticelli, G. F. Sonnenberg, M. C. Abt, T. Alenghat, C. G. Ziegler, T. A. Doering, J. M. Angelosanto, B. J. Laidlaw, C. Y. Yang, T. Sathaliyawala, M. Kubota, D. Turner, J. M. Diamond, A. W Goldrath, D. L. Farber, R. G. Collman, E. J. Wherry, and D. Artis. Innate lymphoid cells promote lung-tissue homeostasis after infection with influenza virus. *Nat. Immunol.*, 12(11):1045–1054, 2011.

[186] R. Moore, S. Carlson, and J. L. Madara. Rapid barrier restitution in an in vitro model of intestinal epithelial injury. *Laboratory investigation*, 60(2):237–244, 1989.

[187] M. Mordstein, E. Neugebauer, V. Ditt, B. Jessen, T. Rieger, V. Falcone, F. Sorgeloos, S. Ehl, D. Mayer, G. Kochs, M. Schwemmle, S. Günther, C. Drosten, T. Michiels, and P. Staeheli. Lambda interferon renders epithelial cells of the respiratory and gastrointestinal tracts resistant to viral infections. *J. Virol.*, 84(11):5670–5677, 2010.

[188] C. Moussion, N. Ortega, and J. Girard. The IL-1-like cytokine IL-33 is constitutively expressed in the nucleus of endothelial cells and epithelial cells in vivo: A novel 'Alarmin'? *PLoS One*, 3(10):1–8, 2008.

[189] A. Muir, G. Soong, S. Sokol, B. Reddy, M. I. Gomez, A. Van Heeckeren, and A. Prince. Toll-like receptors in normal and cystic fibrosis airway epithelial cells. *Am. J. Resp. Cell Mol. Biol.*, 30(6):777–783, 2004.

[190] M. G. Mujtaba, L. O. Flowers, C. B. Patel, R. A. Patel, M. I. Haider, and H. M. Johnson. Treatment of mice with the suppressor of cytokine signaling-1 mimetic peptide, tyrosine kinase inhibitor peptide, prevents development of the acute form of experimental allergic encephalomyelitis and induces stable remission in the chronic relapsing/remit. *J. Immunol.*, 175(8):5077–86, 2005.

[191] J. M. Mullin, K. V. Laughlin, C. W. Marano, L. M. Russo, and A. P. Soler. Modulation of tumor necrosis factor-induced increase in renal (LLC-PK1) transepithelial permeability. *Am. J. physiology*, 263(5):F915–24, 1992.

[192] J. Murphy, R. Summer, A. A. Wilson, D. N. Kotton, and A. Fine. The prolonged life-span of alveolar macrophages. *Am. J. Resp. Cell Mol. Biol.*, 38(4):380–385, 2008.

[193] T. Naka, T. Matsumoto, M. Narazaki, M. Fujimoto, Y. Morita, Y. Ohsawa, H. Saito, T. Nagasawa, Y. Uchiyama, and T. Kishimoto. Accelerated apoptosis of lymphocytes by augmented induction of Bax in SSI-1 (STAT-induced STAT inhibitor-1) deficient mice. *PNAS*, 95(26):15577–15582, 1998.

[194] T. Naka, M. Narazaki, M. Hirata, T. Matsumoto, S. Minamoto, A. Aono, N. Nishimoto, T. Kajita, T. Taga, K. Yoshizaki, S. Akira, and T. Kishimoto. Structure and function of a new STAT-induced STAT inhibitor. *Nature*, 387(6636):924–929, 1997.

[195] T. Naka, H. Tsutsui, M. Fujimoto, Y. Kawazoe, H. Kohzaki, Y. Morita, R. Nakagawa, M. Narazaki, K. Adachi, T. Yoshimoto, K. Nakanishi, and T. Kishimoto. SOCS-1/SSI-1-deficient NKT cells participate in severe hepatitis through dysregulated cross-talk inhibition of IFN-γ and IL-4 signaling in vivo. *Immunity*, 14(5):535–45, 2001.

[196] R. Nakagawa, T. Naka, H. Tsutsui, M. Fujimoto, A. Kimura, T. Abe, E. Seki, S. Sato, O. Takeuchi, K. Takeda, S. Akira, K. Yamanishi, I. Kawase, K. Nakanishi, and T. Kishimoto. Socs-1 participates in negative regulation of lps responses. *Immunity*, 17(5):677–687, 2002.

[197] T. Nakashima, A. Yokoyama, Y. Onari, H. Shoda, Y. Haruta, N. Hattori, T. Naka, and N. Kohno. Suppressor of cytokine signaling 1 inhibits pulmonary inflammation and fibrosis. *J. Allergy Clin. Immunol.*, 121(5):1269–1276, 2008.

[198] K. Nakata, H. Gotoh, J. Watanabe, T. Uetake, I. Komuro, K. Yuasa, S. Watanabe, R. Ieki, H. Sakamaki, H. Akiyama, S. Kudoh, M. Naitoh, H. Satoh, and K. Shimada. Augmented proliferation of human alveolar macrophages after allogeneic bone marrow transplantation. *Blood*, 93(2):667–673, 1999.

[199] T. Nakayama, K. Hieshima, D. Nagakubo, E. Sato, M. Nakayama, K. Kawa, and O. Yoshie. Selective induction of Th2-attracting chemokines CCL17 and CCL22 in human B cells by latent membrane protein 1 of Epstein-Barr virus. *J. Virol.*, 78(4):1665–74, 2004.

[200] U. Neuhaus-Steinmetz, T. Glaab, A. Daser, A. Braun, M. Lommatzsch, U. Herz, J. Kips, Y. Alarie, and H. Renz. Sequential development of airway hyperresponsiveness and acute airway obstruction in a mouse model of allergic inflammation. *Int. Arch. Allergy Immunol.*, 121(1):57–67, 2000.

[201] A. T. Nials and S. Uddin. Mouse models of allergic asthma: acute and chronic allergen challenge. *Dis. Model. Mech.*, 1(4-5):213–20, 2012.

[202] J. C. Nussbaum, S. J. Van Dyken, J. von Moltke, L. E. Cheng, A. Mohapatra, A. B. Molofsky, E. E. Thornton, M. F. Krummel, A. Chawla, H. Liang, and R. M. Locksley. Type 2 innate lymphoid cells control eosinophil homeostasis. *Nature*, 502(7470):245–248, 2013.

[203] S. O. Odemuyiwa, A. Ghahary, Y. Li, L. Puttagunta, J. E. Lee, S. Musat-Marcu, and R. Moqbel. Cutting edge: human eosinophils regulate T cell subset selection through indoleamine 2,3-dioxygenase. *J. Immunol.*, 173(10):5909–5913, 2004.

[204] S. Oliere, E. Hernandez, A. Lezin, M. Arguello, R. Douville, T. L. Nguyen, S. Olindo, G. Panelatti, M. Kazanji, P. Wilkinson, R.-P. Sekaly, R. Cesaire, and J. Hiscott. HTLV-1 evades type I interferon antiviral signaling by inducing the suppressor of cytokine signaling 1 (SOCS1). *PLoS Pathog.*, 6(11):e1001177, 2010.

[205] K. Onoguchi, M. Yoneyama, A. Takemura, S. Akira, T. Taniguchi, H. Namiki, and T. Fujita. Viral infections activate types I and III interferon genes through a common mechanism. *J. Biol. Chem.*, 282(10):7576–7581, 2007.

[206] B. Opitz, A. Rejaibi, B. Dauber, J. Eckhard, M. Vinzing, B. Schmeck, S. Hippenstiel, N. Suttorp, and T. Wolff. IFN induction by influenza A virus is mediated by RIG-I which is regulated by the viral NS1 protein. *Cellular Microbiology*, 9(4):930–938, 2007.

[207] C. Orabona, P. Puccetti, C. Vacca, S. Bicciato, A. Luchini, F. Fallarino, R. Bianchi, E. Velardi, K. Perruccio, A. Velardi, V. Bronte, M. C. Fioretti, and U. Grohmann. Toward the identification of a tolerogenic signature in IDO-competent dendritic cells. *Blood*, 107(7):2846–2854, 2006.

[208] C. Orabona, E. Tomasello, F. Fallarino, R. Bianchi, C. Volpi, S. Bellocchio, L. Romani, M. C. Fioretti, E. Vivier, P. Puccetti, and U. Grohmann. Enhanced tryptophan catabolism in the absence of the molecular adapter DAP12. *J. Immunol.*, 35(11):3111–3118, 2005.

[209] J. J. OShea, M. Gadina, and R. D. Schreiber. Cytokine signaling in 2002: New surprises in the Jak/Stat pathway. *Cell*, 109(2):121–131, 2002.

[210] P. I. Osterlund, T. E. Pietila, V. Veckman, S. V. Kotenko, and I. Julkunen. IFN regulatory factor family members differentially regulate the expression of type III IFN (IFN-lambda) genes. *J. Immunol.*, 179(6):3434–3442, 2007.

[211] A. M. Owyang, C. Zaph, E. H. Wilson, K. J. Guild, T. McClanahan, H. R. P. Miller, D. J. Cua, M. Goldschmidt, C. A. Hunter, R. A. Kastelein, and D. Artis. Interleukin 25 regulates type 2 cytokine-dependent immunity and limits chronic inflammation in the gastrointestinal tract. *J. Exp. Med.*, 203(4):843–849, 2006.

[212] E. S. Park, H. Kim, J. M. Suh, S. J. Park, O. Y. Kwon, Y. K. Kim, H. K. Ro, B. Y. Cho, J. Chung, and M. Shong. Thyrotropin induces SOCS-1 (suppressor of cytokine signaling-1) and SOCS-3 in FRTL-5 thyroid cells. *Mol. Endocrinol.*, 14(3):440–8, 2000.

[213] G. H. Patterson and J. Lippincott-Schwartz. A Photoactivatable GFP for Selective Photolabeling of Proteins and Cells. *Science*, 297(5588):1873, 2002.

Literature

[214] S. Phipps, E. L. Chuan, G. E. Kaiko, Y. F. Shen, A. Collison, J. Mattes, J. Barry, S. Davidson, K. Oreo, L. Smith, A. Mansell, K. I. Matthaei, and P. S. Foster. Toll/IL-1 signaling is critical for house dust mite-specific Th1 and Th2 responses. *Am. J. Respir. Crit. Care Med.*, 179(10):883–893, 2009.

[215] R. A. R. Piganis, N. A. De Weerd, J. A. Gould, C. W. Schindler, A. Mansell, S. E. Nicholson, and P. J. Hertzog. Suppressor of cytokine signaling (SOCS) 1 inhibits type I interferon (IFN) signaling via the interferon alpha receptor (IFNAR1)-associated tyrosine kinase Tyk2. *J. Biol. Chem.*, 286(39):33811–33818, 2011.

[216] M Platten, P. P. Ho, S. Youssef, P. Fontoura, H. Garren, E. M. Hur, R. Gupta, L. Y. Lee, B. A. Kidd, W. H. Robinson, R. A. Sobel, M. L. Selley, and L Steinman. Treatment of autoimmune neuroinflammation with a synthetic tryptophan metabolite. *Science*, 311, 2005.

[217] J. Platz, C. Beisswenger, A. H. Dalpke, R. Koczulla, O. Pinkenburg, C. Vogelmeier, and R. Bals. Microbial DNA induces a host defense reaction of human respiratory epithelial cells. *J. Immunol.*, 173(2):1219–1223, 2004.

[218] A. Poltorak, X. He, I. Smirnova, M. Liu, C. V. Huffel, X. Du, D. Birdwell, E. Alejos, M. Silva, C. Galanos, M. Freudenberg, P. Ricciardi-castagnoli, B. Layton, and B. Beutler. Defective LPS Signaling in C3H / HeJ and C57BL / 10ScCr Mice : Mutations in Tlr4 Gene. *Science*, 282(5396):2085–2088, 1998.

[219] J. Pothlichet, M. Chignard, and M. Si-Tahar. Cutting Edge: Innate Immune Response Triggered by Influenza A Virus Is Negatively Regulated by SOCS1 and SOCS3 through a RIG-I/IFNAR1-Dependent Pathway. *J. Immunol.*, 180(4):2034 LP – 2038, 2008.

[220] A. L. Pranada, S. Metz, A. Herrmann, P. C. Heinrich, and G. Mueller-Newen. Real Time Analysis of STAT3 Nucleocytoplasmic Shuttling. *J. Biol. Chem.*, 279(15):15114–15123, 2004.

[221] M. Prchal-Murphy, C. Semper, C. Lassnig, B. Wallner, C. Gausterer, I. Teppner-Klymiuk, J. Kobolak, S. Müller, T. Kolbe, M. Karaghiosoff, A. Dinnyés, T. Rülicke, N. R. Leitner, B. Strobl, and M. Müller. TYK2 Kinase Activity Is Required for Functional Type I Interferon Responses In Vivo. *PLoS One*, 7(6):e39141, jun 2012.

[222] D. Prefontaine, J. Nadigel, F. Chouiali, S. Audusseau, A. Semlali, J. Chakir, J. G. Martin, and Q. Hamid. Increased IL-33 expression by epithelial cells in bronchial asthma., 2010.

[223] V. Provost, M. Larose, A. Langlois, M. Rola-Pleszczynski, N. Flamand, and M. Laviolette. CCL26/eotaxin-3 is more effective to induce the migration of eosinophils of asthmatics than CCL11/eotaxin-1 and CCL24/eotaxin-2. *J. Leuko. Biol.*, 94(2):213–22, 2013.

[224] Y. Qing. Role of Tyrosine 441 of Interferon- Receptor Subunit 1 in SOCS-1-mediated Attenuation of STAT1 Activation. *J. Biol. Chem.*, 280(3):1849–1853, 2004.

[225] F. W. Quelle, W. Thierfelder, B. Witthuhn, and B. Tang. Phosphorylation and activation of the DNA binding activity of purified Stat1 by the Janus protein-tyrosine kinases and the epidermal growth factor receptor. *J. Biol. Chem.*, 270(35):20775–20780, 1995.

[226] C. V. Ramana, M. P. Gil, Y. Han, R. M. Ransohoff, R. D. Schreiber, and G. R. Stark. Stat1-independent regulation of gene expression in response to IFN-γ. *PNAS*, 98(12):6674–6679, 2001.

[227] C. Recio, A. Oguiza, I. Lazaro, B. Mallavia, J. Egido, and C.n Gomez-Guerrero. Suppressor of cytokine signaling 1-derived peptide inhibits janus kinase/signal transducers and activators of transcription pathway and improves inflammation and atherosclerosis in diabetic mice. *Arterioscler. Thromb. Vasc. Biol.*, 34(9):1953–1960, 2014.

[228] J. L. Rendon, X. Li, S. Akhtar, and M. A. Choudhry. IL-22 modulates gut epithelial and immune barrier functions following acute alcohol exposure and burn injury. *Shock*, 39(1):11–18, 2013.

[229] P. Rubin, C. J. Johnston, J. P. Williams, S. McDonald, and J. N. Finkelstein. A perpetual cascade of cytokines postirradiation leads to pulmonary fibrosis. *Int. J. Radiat.*, 33(1):99–109, 1995.

[230] A. Ryo, F. Suizu, Y. Yoshida, K. Perrem, Y. C. Liou, G. Wulf, R. Rottapel, S. Yamaoka, and K. P. Lu. Regulation of NF-kB Signaling by Pin1-Dependent Prolyl Isomerization and Ubiquitin-Mediated Proteolysis of p65/RelA. *Molecular Cell*, 12(6):1413–1426, 2003.

[231] B. Saatian, F. Rezaee, S. Desando, J. Emo, T. Chapman, S. Knowlden, and S. N. Georas. Interleukin-4 and interleukin-13 cause barrier dysfunction in human airway epithelial cells tl - 1. *Tissue Barriers*, 1(2):1–5, 2013.

[232] S. Saccani, I. Marazzi, A. A. Beg, and G. Natoli. Degradation of promoter-bound p65/RelA is essential for the prompt termination of the nuclear factor kappaB response. *J. Exp. Med.*, 200(1):107–13, 2004.

[233] H. Saito, Y. Morita, M. Fujimoto, M. Narazaki, T. Naka, and T. Kishimoto. IFN regulatory factor-1-mediated transcriptional activation of mouse STAT-induced STAT inhibitor-1 gene promoter by IFN-γ. *J. Immunol.*, 164(11):5833–5843, 2000.

[234] C. E. Samuel. Antiviral Actions of Interferons. *Clin. Microbiol. Rev.*, 14(4):778–809, 2001.

[235] S. E. Sanders, J. L. Madara, D. K. McGuirk, D. S. Gelman, and S. P. Colgan. Assessment of inflammatory events in epithelial permeability: a rapid screening method using fluorescein dextrans. *Epithelial Cell. Biol.*, 4(1):25–34, 1995.

[236] S. Sawa, M. Lochner, N. Satoh-Takayama, S. Dulauroy, M. Berard, M. Kleinschek, D. Cua, J. P. Di Santo, and G. Eberl. RORgammat+ innate lymphoid cells regulate intestinal homeostasis by integrating negative signals from the symbiotic microbiota. *Nat. Immunol.*, 12(4):320–326, 2011.

[237] G. Schluter, D. Boinska, and S. C. Nieman-Seyde. Evidence for translational repression of the SOCS-1 major open reading frame by an upstream open reading frame. *Biochem. Biophys. Res. Commun.*, 268(2):255–261, 2000.

[238] Jochen Schmitz, Alexander Owyang, Elizabeth Oldham, Yaoli Song, Erin Murphy, Terril K. Mc-Clanahan, Gerard Zurawski, Mehrdad Moshrefi, Jinzhong Qin, Xiaoxia Li, Daniel M. Gorman, J. Fernando Bazan, and Robert A. Kastelein. IL-33, an Interleukin-1-like Cytokine that Signals via the IL-1 Receptor-Related Protein ST2 and Induces T Helper Type 2-Associated Cytokines. *Immunity*, 23(5):479–490, 2005.

[239] S. Sel, M. Wegmann, T. Dicke, S. Sel, W. Henke, A. O. Yildirim, H. Renz, and H. Garn. Effective prevention and therapy of experimental allergic asthma using a GATA-3-specific DNAzyme. *J. Allergy Clin. Immuno.*, 121(4):910–916.e5, 2008.

[240] M. E. Selsted and A. J. Ouellette. Mammalian defensins in the antimicrobial immune response. *Nature*, 6(6):551–557, 2005.

[241] Q. Sha, A. Q. Truong-Tran, J. R. Plitt, L. A. Beck, and R. P. Schleimer. Activation of airway epithelial cells by toll-like receptor agonists. *Am. J. Resp. Cell Mol. Biol.*, 31(3):358–364, 2004.

[242] P. Shaw, J. Freeman, R. Bovey, and R. Iggo. Regulation of specific dna binding by p53: evidence for a role for o-glycosylation and charged residues at the carboxy-terminus. *Oncogene*, 12(4):921–930, 1996.

[243] K. Shimada, S. Serada, M. Fujimoto, S. Nomura, R. Nakatsuka, E. Harada, K. Iwahori, I. Tachibana, T. Takahashi, A. Kumanogoh, T. Kishimoto, and T. Naka. Molecular mechanism underlying the antiproliferative effect of suppressor of cytokine signaling-1 in non-small-cell lung cancer cells. *Cancer Science*, 104(11):1483–1491, 2013.

[244] H. Shizuya and H. Kouros-Mehr. The development and applications of the bacterial artificial chromosome cloning system. *J. Med.*, 50(1):26–30, 2001.

[245] S. Shresta, K. L. Sharar, D. M. Prigozhin, H. M. Snider, P. R. Beatty, and E. Harris. Critical roles for both STAT1-dependent and STAT1-independent pathways in the control of primary dengue virus infection in mice. *J. Immunol.*, 175(6):3946–3954, 2005.

[246] K. Shuai and B. Liu. Regulation of JAK–STAT signalling in the immune system. *Nature Rev*, 3(11):900–911, nov 2003.

[247] R. Siegel, J. Eskdale, and G. Gallagher. Regulation of IFN-lambda1 promoter activity (IFN-lambda1/IL-29) in human airway epithelial cells. *J. Immunol.*, 187(11):5636–5644, 2011.

[248] E. Siewert, W. Müller-Esterl, R. Starr, P. C. Heinrich, and F. Schaper. Different protein turnover of interleukin-6-type cytokine signalling components. *Europ. J. Biochem.*, 265(1):251–257, 1999.

[249] P. D. Simoncic, A. Lee-Loy, D. L. Barber, M. L. Tremblay, and C. J. McGlade. The T cell protein tyrosine phosphatase is a negative regulator of janus family kinases 1 and 3. *Curr. Biol.*, 12(6):446–453, 2002.

[250] J. E. Sims, D. E. Williams, P. J. Morrissey, K. Garka, D. Foxworthe, V. Price, S. L. Friend, A. Farr, M. A. Bedell, N. A. Jenkins, N. G. Copeland, K. Grabstein, and R. J. Paxton. Molecular cloning and biological characterization of a novel murine lymphoid growth factor. *J. Exp. Med.*, 192(5):671–680, 2000.

[251] C. Soler, A. Felipe, J. García-Manteiga, M. Serra, E. Guillén-Gómez, F. J. Casado, C. MacLeod, M. Modolell, M. Pastor-Anglada, and A. Celada. Interferon-gamma regulates nucleoside transport systems in macrophages through signal transduction and activator of transduction factor 1 (STAT1)-dependent and -independent signalling pathways. *The Biochem. J.*, 375(3):777–783, 2003.

[252] G. F. Sonnenberg, L. A. Fouser, and D. Artis. Functional biology of the IL-22-IL-22R pathway in regulating immunity and inflammation at barrier surfaces. *Adv. Immunol.*, 107:1–29, 2010.

[253] V. Soumelis, P. A. Reche, H. Kanzler, W. Yuan, G. Edward, B. Homey, M. Gilliet, S. Ho, S. Antonenko, A. Lauerma, K. Smith, D. Gorman, S. Zurawski, J. Abrams, S. Menon, T. McClanahan, R. de Waal-Malefyt, F. Bazan, R. A. Kastelein, and Y. Liu. Human epithelial cells trigger dendritic cell mediated allergic inflammation by producing TSLP. *Nat. Immunol.*, 3(7):673–680, 2002.

[254] H. Spits and J. P. Di Santo. The expanding family of innate lymphoid cells: regulators and effectors of immunity and tissue remodeling. *Nat. Immunol.*, 12(1):21–27, 2011.

[255] G. R. Stark, I. M. Kerr, B. R. Williams, R. H. Silverman, and R. D. Schreiber. How cells respond to interferons. *Ann. Rev. Biochem.*, 67:227–64, 1998.

[256] R. Starr, D. Metcalf, a. G. Elefanty, M. Brysha, T. Willson, N. Nicola, D. J. Hilton, and W. S. Alexander. Liver degeneration and lymphoid deficiencies in mice lacking suppressor of cytokine signaling-1. *PNAS*, 95(24):14395–14399, 1998.

[257] R. Starr, T. a. Willson, E. M. Viney, L. J. Murray, J. R. Rayner, B. J. Jenkins, T. J. Gonda, W. S. Alexander, D. Metcalf, N. Nicola, and D. J. Hilton. A family of cytokine-inducible inhibitors of signalling. *Nature*, 387(6636):917–921, 1997.

[258] D. Stoiber, P. Kovarik, S. Cohney, J. A. Johnston, P. Steinlein, and T. Decker. Lipopolysaccharide induces in macrophages the synthesis of the suppressor of cytokine signaling 3 and suppresses signal transduction in response to the activating factor IFN-γ. *J. Immunol.*, 163(5):2640–7, 1999.

[259] K. C. Stone, R. R. Mercer, P. Gehr, B. Stockstill, and J. D. Crapo. Allometric relationships of cell numbers and size in the mammalian lung. *Am. J. Resp. Cell. Mol. Biol.*, 6(2):235–243, 1992.

[260] J. Strebovsky, P. Walker, R. Lang, and A. H. Dalpke. Suppressor of cytokine signaling 1 (SOCS1) limits NFkappaB signaling by decreasing p65 stability within the cell nucleus. *FASEB J.*, 25(3):863–874, 2011.

[261] S. J. Szabo, S. T. Kim, G. L. Costa, X. Zhang, C. G. Fathman, and L. H. Glimcher. A novel transcription factor, T-bet, directs Th1 lineage commitment. *Cell*, 100(6):655–669, 2000.

[262] O. K. T. Takeuchi, H. Sanjo, H. Takada, T. Ogawa, K. Takeda, S. Akira, and K. Hoshino. Differential roles of TLR2 and TLR4 in recognition of gram-negative and grampositive bacterial cell wall components. *Immunity*, 11:443–451, 1999.

[263] T. Tamachi, Y. Maezawa, K. Ikeda, S.-I. Kagami, M. Hatano, Y. Seto, A. Suto, K. Suzuki, N. Watanabe, Y. Saito, T. Tokuhisa, I. Iwamoto, and H. Nakajima. Il-25 enhances allergic airway inflammation by amplifying a th2 cell-dependent pathway in mice. *J. Allergy Clin. Immunol.*, 118(3):606–614, 2006.

[264] K. Tanaka, K. Ichiyama, M. Hashimoto, H. Yoshida, T. Takimoto, G. Takaesu, T. Torisu, T. Hanada, H. Yasukawa, S. Fukuyama, H. Inoue, Y. Nakanishi, T. Kobayashi, and A. Yoshimura. Loss of suppressor of cytokine signaling 1 in helper T cells leads to defective Th17 differentiation by enhancing antagonistic effects of IFN-γ on STAT3 and Smads. *J. Immunol.*, 180(6):3746–3756, 2008.

[265] Y. Tang, D. R. Clayburgh, N. Mittal, T. Goretsky, R. Dirisina, Z. Zhang, M. Kron, D. Ivancic, R. B. Katzman, G. Grimm, G. Lee, J. Fryer, A. Nusrat, J. R. Turner, and T. A. Barrett. Epithelial NF-kappaB enhances transmucosal fluid movement by altering tight junction protein composition after T cell activation. *Am. J. pathology*, 176(1):158–167, 2010.

[266] J. D. Tarling and J. E. Coggle. Evidence for the pulmonary origin of alveolar macrophages. *Cell*, 15(6):577–584, 1982.

[267] J. D. Tarling, H. S. Lin, and S. Hsu. Self-renewal of pulmonary alveolar macrophages: evidence from radiation chimera studies. *J. Leukoc. Biol.*, 42(5):443–446, 1987.

[268] C. A. Thaiss, N. Zmora, M. Levy, and E. Elinav. The microbiome and innate immunity. *Nature*, 535(7610):65–74, 2016.

[269] D. Torre, F. Speranza, M. Giola, A. Matteelli, R. Tambini, and G. Biondi. Role of Th1 and Th2 cytokines in immune response to uncomplicated Plasmodium falciparum malaria. *Clin. Diagn. Lab. Immunol.*, 9(2):348–51, 2002.

[270] M. Townsend, P. G. Fallon, D. J. Matthews, H. E. Jolin, and A. N. J. McKenzie. T1/St2-Deficient Mice Demonstrate the Importance of T1/St2 in Developing Primary T Helper Cell Type 2 Responses. *J. Exp. Med.*, 191(6):1069–1076, 2000.

[271] M. C. Trengove and A. C. Ward. SOCS proteins in development and disease. *Am. J. Clin. Exp. Immunol.*, 2(1):1–29, 2013.

[272] S. Trop, P. Sepulveda, J. C. Zuniga-pflucker, and R. Rottapel. Overexpression of suppressor of cytokine signaling-1 impairs pre-t-cell receptor- induced proliferation but not differentiation of immature thymocytes. *Cycle*, 97(8):2269–2277, 2012.

[273] P.-N. Tsao, M. Vasconcelos, K. I. Izvolsky, J. Qian, J. Lu, and W. V. Cardoso. Notch signaling controls the balance of ciliated and secretory cell fates in developing airways. *Development*, 136(13):2297–2307, 2009.

[274] J. Tsukada, A. Ozaki, T. Hanada, T. Chinen, R. Abe, A. Yoshimura, and M Kubo. The role of suppressor of cytokine signaling 1 as a negative regulator for aberrant expansion of CD8??+ dendritic cell subset. *Immunology*, 17(9):1167–1178, 2005.

[275] A. Uehara, Y. Fujimoto, K. Fukase, and H. Takada. Various human epithelial cells express functional toll-like receptors, nod1 and nod2 to produce anti-microbial peptides, but not proinflammatory cytokines. *Molecular Immunology*, 44(12):3100–3111, 2007.

[276] K. Ueki, T. Kondo, and C. R. Kahn. Suppressor of cytokine signaling 1 (SOCS-1) and SOCS-3 cause insulin resistance through inhibition of tyrosine phosphorylation of insulin receptor substrate proteins by discrete mechanisms. *Mol. Cell. Biol.*, 24(12):5434–46, 2004.

[277] K. Ueno, T. Koga, K. Kato, D. T. Golenbock, S. J. Gendler, H. Kai, and K. C. Kim. MUC1 mucin is a negative regulator of toll-like receptor signaling. *Am. J. Resp. Cell Mol. Biol.*, 38(3):263–268, 2008.

[278] T. C. Van der Pouw Kraan. Prostaglandin-E2 is a potent inhibitor of human interleukin 12 production. *J. Exp. Med.*, 181(2):775–779, 1995.

[279] E. Vassiliou, H Jing, and D. Ganea. Prostaglandin E2 inhibits TNF production in murine bone marrow-derived dendritic cells. *Cell. Immunol.*, 223(2):120–132, 2003.

[280] E. K. Vladar and S. L. Brody. Analysis of ciliogenesis in primary culture mouse tracheal epithelial cells. *Methods Enzymol.*, 525:285–309, 2013.

[281] B. Q. Vuong, T. L. Arenzana, B. M. Showalter, J. Losman, X. P. Chen, J. Mostecki, S. Alexander, A. Limnander, N. Fernandez, B. Paul, A. S. Banks, and P. B. Rothman. SOCS-1 Localizes to the Microtubule Proteasome SOCS-1 Localizes to the Microtubule Organizing Complex-Associated 20S Proteasome. *Mol. Cell. Biol.*, 24(20):9092–9101, 2004.

[282] A. Wangoo, T. Sparer, I. N. Brown, V. A. Snewin, R. Janssen, J. Thole, H. T. Cook, R. J. Shaw, and D. B. Young. Contribution of Th1 and Th2 Cells to Protection and Pathology in Experimental Models of Granulomatous Lung Disease. *J. Immunol.*, 166:3432–3439, 2001.

[283] H. Wei, S. Wang, Q. Chen, Y. Chen, X. Chi, L. Zhang, S. Huang, G. F. Gao, and J. Chen. Suppression of interferon lambda signaling by SOCS-1 results in their excessive production during influenza virus infection. *PLoS Pathog.*, 10(1):e1003845, 2014.

[284] S. E. Wert, S. W. Glasser, T. R. Korfhagen, and J. A. Whitsett. Transcriptional elements from the human sp-c gene direct expression in the primordial respiratory epithelium of transgenic mice. *Dev. Biol.*, 156:426–443, 1993.

[285] J. A. Whitsett and T. Alenghat. Respiratory epithelial cells orchestrate pulmonary innate immunity. *Nat. Immunol.*, 16(1):27–35, 2015.

[286] D. M. Wisner, L. R. Harris, C. L. Green, and L. S. Poritz. Opposing regulation of the tight junction protein claudin-2 by interferon-gamma and interleukin-4. *J. Surgical Research*, 144(1):1–7, 2008.

[287] R. G. J. K. Wolterink, A. Kleinjan, M. van Nimwegen, I. Bergen, M. de Bruijn, Y. Levani, and R. W. Hendriks. Pulmonary innate lymphoid cells are major producers of IL-5 and IL-13 in murine models of allergic asthma. *Eur. J. Immunol.*, 42(5):1106–1116, 2012.

[288] X. O. Yang, B. Pappu, R. Nurieva, A. Akimzhanov, H. S. Kang, Y. Chung, L. Ma, B. Shah, A. D. Panopoulos, K. Schluns, S. S. Watowich, Q. Tian, A. M. Jetten, and C. Dong. TH17 lineage differentiation is programmed by orphan nuclear receptors ROR and RORg. *Immunity*, 28(1):29–39, 2008.

[289] L.L. Yanlu Zhang, W. Y. Zhang, M. H. Kaplan, and B. Zhou. TSLP Interferes with Airway Tolerance by Suppressing the Generation of Antigen-specific Regulatory T cells. *J. Immunol.*, 186(4):2254 – 2261, 2011.

[290] H. Yasukawa, H. Misawa, H. Sakamoto, M. Masuhara, A. Sasaki, T. Wakioka, S. Ohtsuka, T. Imaizumi, T. Matsuda, J. N. Ihle, and A. Yoshimura. The JAK-binding protein JAB inhibits Janus tyrosine kinase activity through binding in the activation loop. *EMBO J.*, 18(5):1309–1320, 1999.

[291] D. Ye, I. Ma, and T. Y. Ma. Molecular mechanism of tumor necrosis factor-alpha modulation of intestinal epithelial tight junction barrier. *Am. J. Physiology.*, 290(3):G496–504, 2006.

[292] S. Ying, B. O'Connor, J. Ratoff, Q. Meng, K. Mallett, D. Cousins, D. Robinson, G. Zhang, J. Zhao, T. H. Lee, and C. Corrigan. Thymic Stromal Lymphopoietin Expression Is Increased in Asthmatic Airways and Correlates with Expression of Th2-Attracting Chemokines and Disease Severity. *J. Immunol.*, 174(12):8183–8190, 2005.

[293] H. Yoshikawa, K. Matsubara, G. S. Qian, P. Jackson, J. D. Groopman, J. E. Manning, C. C. Harris, and J. G. Herman. SOCS-1, a negative regulator of the JAK/STAT pathway, is silenced by methylation in human hepatocellular carcinoma and shows growth-suppression activity. *Nature*, 28(1):29–35, 2001.

[294] T. Zelante, J. Fric, A. Y. W. Wong, and P. Ricciardi-Castagnoli. Interleukin-2 Production by Dendritic Cells and its Immuno-Regulatory Functions. *Front. Immunol.*, 3:161, 2012.

[295] J. G. Zhang, A. Farley, S. E. Nicholson, T. a. Willson, L. M. Zugaro, R. J. Simpson, R. L. Moritz, D. Cary, R. Richardson, G. Hausmann, B. J. Kile, S. B. Kent, W. S. Alexander, D. Metcalf, D. J. Hilton, N. a. Nicola, and M. Baca. The conserved SOCS box motif in suppressors of cytokine signaling binds to elongins B and C and may couple bound proteins to proteasomal degradation. *PNAS*, 96(5):2071–2076, 1999.

[296] J.-G. Zhang, D. Metcalf, S. Rakar, M. Asimakis, C. J. Greenhalgh, T. A. Willson, R. Starr, S. E. Nicholson, W. Carter, and W. S. Alexander. The SOCS box of suppressor of cytokine signaling-1 is important for inhibition of cytokine action in vivo. *PNAS*, 98(23):13261–13265, 2001.

[297] B. Zhou, M. R. Comeau, T. De Smedt, H. D. Liggitt, M. E. Dahl, D. B. Lewis, D. Gyarmati, T. Aye, D. J. Campbell, and S. F. Ziegler. Thymic stromal lymphopoietin as a key initiator of allergic airway inflammation in mice. *Nat. Immunol.*, 6(10):1047–1053, 2005.

[298] X. Zhou, L. T. Jeker, B. T. Fife, S. Zhu, M. S. Anderson, M. T. McManus, and J. A. Bluestone. Selective miRNA disruption in T reg cells leads to uncontrolled autoimmunity. *J. Exp. Med.*, 205(9):1983–91, 2008.

[299] G. R. Zosky, A. N. Larcombe, O. J. White, J. T. Burchell, T. Z. Janosi, Z. Hantos, P. G. Holt, P. D. Sly, and D. J. Turner. Ovalbumin-sensitized mice are good models for airway hyperresponsiveness but not acute physiological responses to allergen inhalation. *Clin. Exp. Allergy*, 38(5):829–838, 2008.

A. Acknowledgement

Mein besonderer Dank gilt Prof. Dr. Alexander Dalpke für die Möglichkeit meine Doktorarbeit in seiner Arbeitsgruppe zu schreiben, sowie für seine herausragende wissenschaftliche Betreuung in dieser Zeit. Ich danke ihm für alle hilfreichen Diskussionen, wertvollen Ratschläge und dafür dass er sich immer Zeit für meine Anliegen genommen hat. Weiterhin möchte ich mich herzlich für die Möglichkeit bedanken an Kongressen und Fortbildungen teilzunehmen.

Herrn Prof. Dr. Ralf Bartenschlager danke ich für die Begutachtung meiner Arbeit, sowie seine Funktion als Erstgutachter. An Prof. Dr. Steve Boulant und Prof. Dr. Ursula Klingmüller geht herzlicher Dank für ihre Funktion als Prüfer im Rahmen meiner Disputation und an Prof. Dr. Frauke Melchior, für Ihre Funktion als Mitglied meines TAC Komitees.

Weiterhin möchte ich mich bei dem HBIGS-Team bedanken, die mich im Rahmen einen Stipendiums unterstützt haben und mir die Möglichkeit gegeben haben, mich durch individuelle Kurse weiterzubilden.

Bei Dr. Michael Weitnauer bedanke ich mich für seine gute wissenschaftliche Betreuung und hilfreichen Diskussionen. Dank gilt auch Dr. Sébastien Boutin, der immer äußerst hilfsbereit war und vor allem bei statistischen Fragen immer eine Antwort parat hatte.

Bei Dr. Felix Lasitschka, Jutta Scheurer und Bettina Walter aus dem Pathologischen Institut möchte ich mich für die Möglichkeit der histologischen Aufbereitung aller Proben, der technischen Hilfe hierbei und der histologischen Färbungen bedanken. Prof. Dr. Bernd Arnold, Günter Küblbeck aus dem DKFZ sowie Frank Zimmermann aus dem IBF und Patrick Walker möchte ich für die Generierung der transgenen Mäuse danken. Weiterhin möchte ich mich bei Frau Hillesheim bedanken, die als Tierpflegerin im IBF einzigartiges leistet. Sie war immer äußerst kooperativ.

Für die gute wissenschaftliche Kooperation im Rahmen des OVA Asthma Models möchte ich vor allem bei Dr. Michael Wegmann und Dr. Lars Lunding aus dem Forschungszentrum Borstel bedanken. Außerdem danke ich den Kooperationpartnern aus der AG Mall, Julia Dürr und Martin Finke, sowie aus der Radiologie, Willi Wagner für Ihre Mithilfe und die Auswertung der micro-CT Scans.

Ich danke Sabrina Thiele, Simon Huck sowie Rebekka Weber, die durch ihre Masterarbeit und Laborpraktika ebenfalls zum Gelingen dieser Arbeit beigetragen haben.

Außerdem möchte ich mich bei allen Mitarbeitern der Abteilung Hygiene und Medizinische Mikrobiologie für die wunderbare Atmosphäre bedanken. Mein Dank geht hier insbesondere an die Doktoranden der AG Dalpke Vedrana, Volker und Isabelle, die mir immer mit Rat und Tat zur Seite standen, sich meine Probleme angehört haben und auch einfach mal zum Reden da waren.

Mein ganz persönlicher Dank geht an meine Eltern und meine Brüder Jannik und Luca, die mir dies ermöglicht haben und mich immer in jeglicher Form unterstützt haben. Großer Dank geht auch an Samantha, Christina und Ann-Katrin für ihr Verständnis und Ablenkung zur richtigen Zeit. Zuletst möchte ich Sebastian für seine offene, ehrliche und stets enthusiastische Art danken. Dies hat mir mehr als nur einmal neue Motivation und Durchhaltevermögen verschafft. Ich danke euch allen fürs Zuhören und dafür, dass ihr immer für mich da seid!

B. List of Publications and Presentations

B.1. Publication

J. Zimmer, M. Weitnauer, S. Boutin, G. Küblbeck, S. Thiele, P. Walker, F. Lasitschka, L. Lunding, Z. Orinska, C. Vock, B. Arnold, M. Wegmann and A. H. Dalpke. Nuclear Localization of Suppressor of Cytokine Signaling-1 Regulates Local Immunity in the Lung. *Front. Immunol* 7(514)., 2016. (This publication was based on the main part of this thesis.)

B.2. Presentations

19.10.2016	European Mucosal Immunology Group (emig) Meeting Copenhagen, Denmark; **Posterpresentation**
25.11.2015	COST Winterschool on Evolutionary Medicine and Development of Respiratory Disease Borstel, Germany; **Posterpresentation**
14.07.2015	International Congress of Mucosal Immunology (ICMI) Berlin, Germany; **Posterpresentation**
19.03.2015	DGfI Symopsium 'Infektion und Immunabwehr' Burg Rothenfels, Germany; **Oral presentation**
17.09.2014	Annual meeting of the German Society for Immunology (DGfI) Bonn, Germany; **Posterpresentation**
9.03.2014	Spring School on Immunology Ettal, Germany; **Posterpresentation**